Università degli Studi della Basilicata

PhD in

"Applied Biology and Environmental Safeguard"

"Obtaining and selecting microalgal genotypes suitable for the bioremediation of matrices containing hydrocarbons, starting from Haematococcus pluvialis (Flotow,1844)"

Settore Scientifico-Disciplinare
"AGR_07"

PhD Coordinator
Prof. ssa Patrizia FALABELLA

PhD Student
Dott.ssa Rosa Paola RADICE

Supervisor
Prof. Giuseppe Biagio MARTELLI

Co-Supervisor
Dott.ssa Giovanna BERMANO

Ciclo XXXIV

La felicità si può trovare anche negli attimi più tenebrosi,

se solo uno si ricorda di accendere la luce.

A.S

SUMMARY

LIST OF FIGURES

III

IV

LIST OF TABLE

ABSTRACT

L'economia mondiale, ancora oggi, si basa sull'utilizzo di combustibili fossili per ricavare energia e nello specifico carbone e petrolio. Il consumo di petrolio nel 2020 è aumentato di 0.9 milioni di barili al giorno mentre la domanda di combustibili liquidi ha raggiunto massimi storici arrivando a 100 milioni di barili al giorno. L'utilizzo del petrolio governa borse e mercati mondiali, infatti pochi e specifici cartelli ne determinano il prezzo di vendita mantenendo una sorta di monopolio economico. Proprio per questo, l'estrazione e la raffinazione del greggio rimane ancora un'attività estremamente intensa. La Basilicata, regione del sud Italia, in particolare, rappresenta il sito onshore più grande del continente europeo, contribuendo da solo al 63% della produzione di greggio italiana. Il processo di estrazione, di raffinazione e di trasporto, tuttavia, costituiscono dei punti nevralgici per l'inquinamento ambientale di suolo, aria e acqua. Durante questo elaborato di tesi ci si è soffermati sull'inquinamento delle acque, causato sia dal trasporto (navi e/o condutture sottomarine) soggetto a numerosi incidenti, sia dall'estrazione, durante la quale acque di lavorazione vengono in contatto con idrocarburi tossici e nocivi. Il petrolio è costituito principalmente da idrocarburi alifatici e non, oltre che da altri elementi, principalmente eteroatomi come zolfo e azoto. Gli idrocarburi, inoltre, possono essere altamente tossici: gli idrocarburi volatili (VOCs) come il benzene, il toluene, l'etil-benzene e lo xilene (BTEX), o gli idrocarburi policiclici aromatici (PAHs) rappresentano la causa dell'insorgenza di diverse patologie neurologiche, respiratorie e tumorali. Risulta evidente, quindi, come tutto il processo industriale vada regolamentato per evitare contatti con questi composti e che, qualora avvengano, fuoriuscite accidentali, queste debbano essere immediatamente confinate e trattate. Le metodologie utilizzate a tal scopo comprendono processi fisico-chimici che rompono le molecole del greggio, rendendolo più sensibile agli attacchi degli agenti atmosferici e naturali. Tra queste l'evaporazione delle molecole a basso peso molecolare, l'emulsione della frazione oleosa con l'acqua, la solubilizzazione e la sedimentazione contribuiscono in parte, alla rimozione del greggio, ma vi è un grande contributo anche da parte del mondo microbiologico, soprattutto procariotico, il quale tramite processi di bioremediation degrada e rimuove molti composti tossici. I limiti di queste tecnologie risiedono nell'utilizzo di composti chimici che risultano essere più dannosi del petrolio stesso per l'ecosistema e la saturazione dei microrganismi che riescono ad agire solo su determinati composti. Proprio in virtù della necessità di trovare una metodologia

che possa costituire una soluzione innovativa alle problematiche sopracitate, si è pensato alle microalghe. Le microalghe sono organismi unicellulari, microscopici, fotosintetici e fotoautotrofi in grado di rimuovere anidride carbonica dall'atmosfera, utilizzandola nel processo di fotosintesi per produrre energia e rilasciare ossigeno. Esistono diverse classi di microalghe collocabili anche in diversi domini (procarioti ed eucarioti), con caratteristiche e fisiologie diverse, ma l'oggetto del nostro studio sono state le microalghe verdi, eucariotiche e fotoautotrofe. La loro capacità di utilizzare il carbonio organico, modificando il loro metabolismo, divenendo così mixotrofici, le ha rese ottime candidate per il loro impiego nel mondo della bioremediation. Diversi studi si sono concentrati sul loro utilizzo per la bioremediation, ad esempio alcune microalghe sono state in grado di rimuovere solfato, e nitrati in percentuali significative. La microalga più investigata in questo ambito è stata *Cholrella spp.* che ha rimosso dopo 5 giorni di trattamento, l'80% di petrolio emulsionato nel mezzo in uno studio del 2020, e ha ridotto in maniera efficiente i PAHs presenti in uno studio del 2013. In questo elaborato di tesi la microalga analizzata è stata *Haematococcus pluvialis*, nota all'ambiente scientifico per la sua capacità di produrre uno degli antiossidanti più potenti in natura, l'astaxantina (ASX) ma mai considerata per la bioremediation di idrocarburi di origine petrolifera. Lo scopo di questo progetto di dottorato è stato quello di ricercare una nuova e innovativa tecnologia che grazie all'impiego di microalghe possa rimuovere efficacemente gli idrocarburi petroliferi in matrici acquose, creando diversi genotipi in grado di agire in maniera più efficiente rispetto al genotipo non mutato (WT). Grazie a un processo di pressione selettiva si è indotto *H. pluvialis* a mutare e ad adattarsi ad una condizione estremamente tossica. Una volta selezionati diversi ceppi mutanti, questi sono stati seguiti nella loro crescita e nella loro capacità di produrre astaxantina, comparandoli sempre con il WT. Poiché le nostre conoscenze non permettevano di determinare se le mutazioni avvenute fossero genetiche o epigenetiche, è stata effettuata anche un'analisi genetica tramite RAPD-PCR su trascritto per evidenziare le diversità di espressione dei diversi genotipi tra di loro e con la specie non mutata, in condizioni di non stress e in generazioni successive. È stato così possibile ottenere tramite "cluster analysis" un dendrogramma che evidenziasse le distanze di espressione genetica tra essi.

Questo risultato indica che la differenza di espressione in condizioni standard è ricollegabile a modificazioni genetiche alla base. Successivamente dopo aver

provato diverse condizioni di stress e bioremediation, sono stati fatti crescere in presenza dell'1% di greggio puro in condizioni anaerobiche, per valutare l'attività di rimozione e/o degradazione. Le analisi chimiche effettuate solo dopo 10 giorni di trattamento hanno subito evidenziato come la quantità di carbonio presente nel mezzo di coltura era quasi raddoppiata mentre altri parametri come fluoruri, cloruri e solfati sono diminuiti. Dopo 40 giorni di trattamento, analisi preliminari tramite GS-MS e GC-FID hanno evidenziato come sia nel mezzo acquoso, che nella biomassa algale, vi erano idrocarburi e sostanze oleose, risultati confermati, poi, da un'analisi quantitativa a 20 e 160 giorni in cui si evidenzia, con diverse cinetiche, una diminuzione degli idrocarburi, che per il ceppo mutante PA1004 erano stati totalmente rimossi sia dal mezzo che dalla biomassa. Inoltre, dopo 120 giorni è stata ripetuta l'analisi genetica per valutare eventuali meccanismi adattativi avvenuti in seguito allo stress indotto dal petrolio. Mantenendo le stesse e identiche condizioni di amplificazione (primer, temperature e concentrazioni) il risultato della "cluster analysis" ha dimostrato come, effettivamente, ci fossero stati dei cambiamenti a livello di espressione genetica, portando a una riorganizzazione delle distanze ottenute precedentemente in condizioni ottimali. Queste distanze rispecchiano il comportamento dei genotipi in presenza dell'agente esogeno. Alcuni hanno rimosso totalmente il petrolio, altri hanno agito solo sulla frazione oleosa contribuendo a creare un particolato bituminoso raggruppandosi come da dendrogramma generato. L'assenza di idrocarburi all'interno del mezzo acquoso e della biomassa algale costituisce di per sé un risultato estremamente interessante andando a confermare gli obiettivi preposti all'inizio di questo percorso di ricerca. Non solo *H. pluvialis* è stato in grado di sopravvivere in presenza di petrolio greggio, ma anche i genotipi generati, sono risultati essere una promettente alternativa nella bioremediation degli idrocarburi. In futuro ci si predispone ad analizzare non solo le pathways coinvolte dalle mutazioni, per comprendere i meccanismi sottesi a tale processo, ma anche analizzare i sottoprodotti generati per riutilizzarli in un'ottica di economia circolare atta alla rimozione e al riutilizzo di un prodotto potenzialmente dannoso per l'uomo e l'ambiente.

PART 1: INTRODUCTION

CHAPTER 1: FOSSIL FUELS

Today humanity finds itself facing a great problem related to the massive use of non-renewable energy sources. Mankind has always tried to exploit everything that nature could provide, striving and discovering numerous sources capable of generating energy: starting from wind mills through the exploitation of coal combustion and ending with nuclear power plants. Energy sources are divided into primary sources and secondary sources. **Primary energy** sources are naturally occurring sources of energy such as wind, sun, crude oil, carbon and wood. **Secondary energy** sources, on the other hand, derive from primary ones and include, for example, electricity and hydrogen [1]. The exponential increase of the world population and the industrial revolution has pushed humanity towards the search for increasingly efficient energy sources, but, at the same time, "cleaner" too. Another classification of energy sources concerns their renewability. There are **renewable** and **non-renewable** sources of energy. The main protagonists of non-renewable sources are fossil fuels (crude oil, coal, etc.) which, by definition, derived from the transformation of organic material over the course of geological eras. **Fossil fuels** are exploited in different ways to produce energy: they can be burned directly; transformed to release thermal energy or converted into non-combustible material. In fact fossil fuels not only produce energy thanks to their combustion but nowadays, they are also used in the chemical-organic industry and in the production of many everyday materials [2]. Underlying every process, however, there is the transformation or breaking of chemical bonds. Fossil fuels are formed for the most part by carbon (C) which constitutes more than 70% of the chemical composition (except for wood, which is composed of C: 49%; hydrogen (H): 6%; oxygen (O): 45%). There is a natural cycle that guarantees the continued presence of carbon on Earth. The biogeochemical cycle of carbon causes a continuous exchange between the geosphere, the hydrosphere, the biosphere, and the earth's atmosphere. In the geosphere and more precisely in the rocks, about 65,500 billion tons of carbon are stored, which is exchanged with the other reservoirs, as mentioned above, in a continuous cycle that guarantees a very important balance for the maintenance of the Earth's temperature (**Figure 1**). The **carbon cycle** can be defined as both slow and fast. **The fast cycle** is related to the life forms that use it. All living organisms exploit the great chemical capacities of carbon.

Nucleic acids (DNA and RNA) are made up of carbon atoms, and plant organisms exploit the carbon present in the atmosphere to produce sugar thanks to photosynthesis, and return it when they break down sugars (also composed of carbon) to produce energy by closing the cycle [3]. **The slow cycle**, instead, begins with rain. Water combines with atmospheric carbon to form carbonic acid which falls on the earth's surface. At this point, being a weak acid, the carbonic acid slowly begins to dissolve the rocks, releasing various ions that reach the aquifers of the rivers that transport them to the oceans. In the oceans, calcium ions combine with bicarbonate to form calcium carbonate. This compound, however, does not derive only from this chemical reaction; many organisms such as shells, corals, and plankton after they die, settle and accumulate on the ocean floor and, over time turn into rock, storing carbon and other substances. Although the seabed makes up about 80% of the carbon-containing rocks, the remaining 20% is the result of the transformation of living organisms (organic carbon), which are incorporated into mud and through heat, and pressure, are compressed to form primary fossil fuels [4].
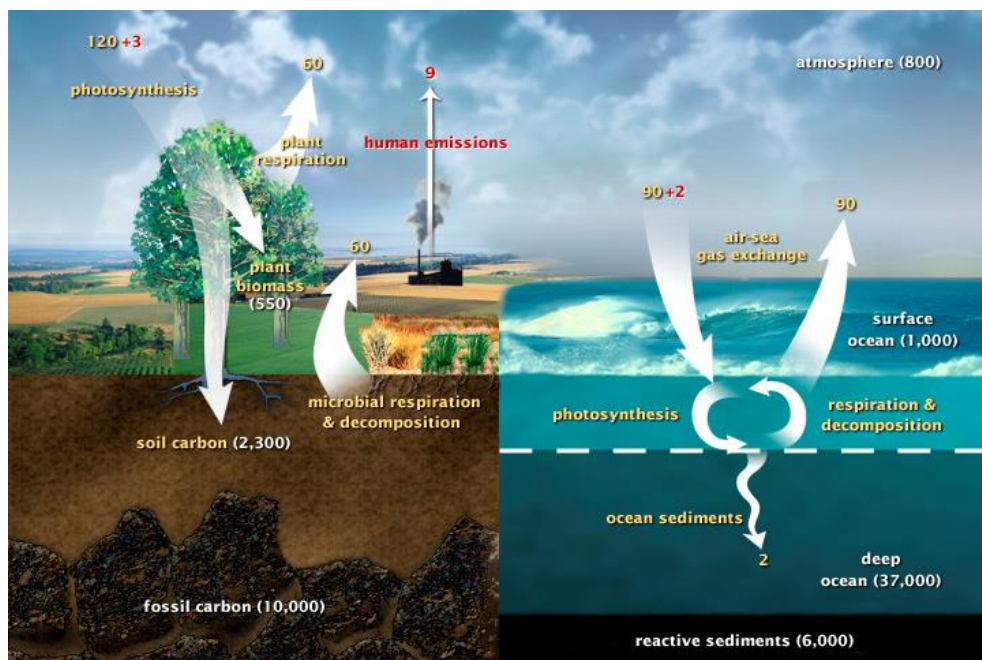
Figure 1 Carbon cycle. Adapted from [4]

The term fossil fuel implies that its formation derives from the transformation from living organisms (fossil). Some leading scientists such as Mendeleev and Berthelot, however, have hypothesized an origin of fossil fuels independent of living matter.

Mendeleev argued that the earth's high temperatures could have catalysed the reactions of carbon, thus forming metal carbides (e.g. CaC_2) which, on the crust, reacting with water, would have formed acetylene.

$$CaC_2 + 2\ H_2O \rightarrow Ca(OH)_2 + C_2H_2$$
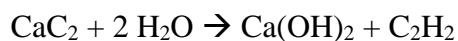
Acetylene, by trimerizing, could, in turn, generate benzene or other hydrocarbon compounds. These abiogenic theories, however, are disproved by the presence of biomarkers within fossil fuels. For example, 2,6,10,14-tetramethylpentadecane (pristane), present poorly in vegetable waxes, has been found in many crude oil samples. The formation of fossil fuels begins with the accumulation of plant material and its protection against the attack of aerobic bacteria. It is, therefore, necessary that organic matter be shielded from the air, and consequently, from oxygen. Usually, this happens thanks to the presence of mud or oxygen-free water (e.g. stagnant water). When the organic matter is about 1-meter underground, the oxygen tends to run out and, for this reason, the fermentation process of the aerobic bacteria stops whereas the action of anaerobic bacteria begins. They can use sulphates or nitrates as energy source, reducing them to hydrogen sulphide and nitrogen. Organic matter consists mostly of plant material and is mostly composed of cellulose, hemicellulose, starch, lignin, proteins, fats, oils, resins, and hydrocarbons. All these compounds at this depth can only hydrolyse, given the low temperature and pressure present. Bacterial enzymes catalyse these reactions by speeding them up, and although these bacteria work in the absence of oxygen, some oxidative processes still require oxygen. For this reason, the oxidative deamination of amino acids takes place, thus producing an immino acid capable of reacting with water to form ammonia and α-keto acid. However, fats and oils are unable to hydrolyse even under these conditions, given the presence of long hydrophobic chains that protect the ester groups. As the action of anaerobic bacteria proceeds, monosaccharides, amino acids, phenols, and aldehydes react to form fulvic acids which condense to form humic acids. At this point, the organic matter is tens of meters underground and at this level, the action of anaerobic bacteria also ceases. The remaining metabolized and non-metabolized material reacts in a little-known way to form kerogen. Three types of kerogen are known, depending on the source of the organic matter: algal kerogen, liptinitic kerogen, and humic kerogen (**Figure**

2). The formation of kerogen continues up to a depth of 1,000 meters, where temperatures begin to rise. The formation of kerogen is not only the halfway point in the formation of fossil fuels but also the end of the first step in the formation of fossil fuels and it is called "**biochemical phase of fossil fuel formation**".
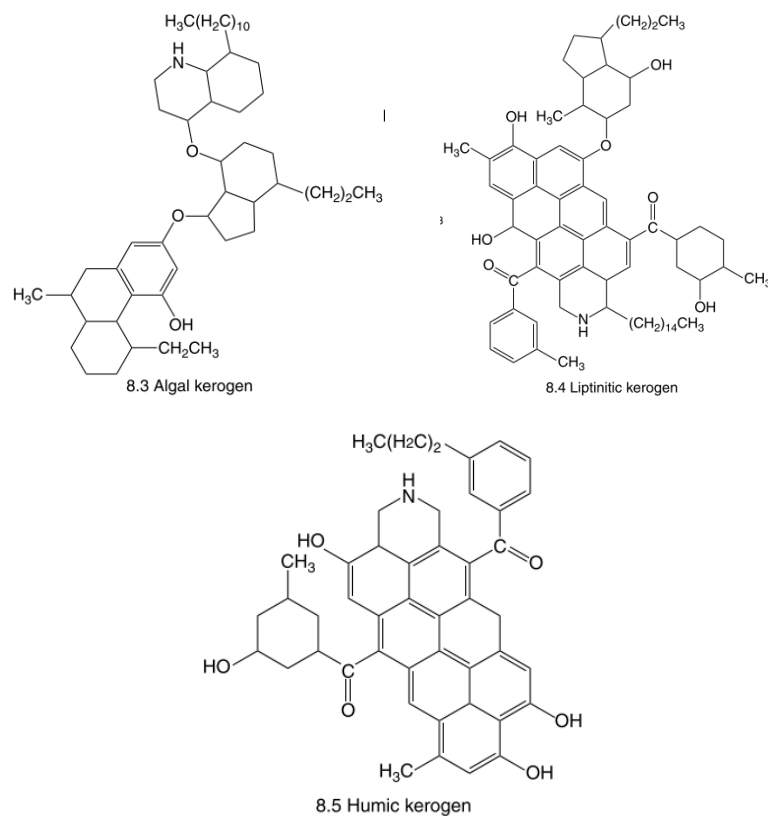
Figure 2: Different kerogen types. Adapted from [2]

The next step only takes place when the kerogen is buried even more. Its transformation depends on temperature. The close correlation between temperature and kerogen catagenesis means that this phase is called "**the geochemical phase of fossil fuel formation**". The reaction times are extremely long; they vary from thousands to millions of years because pressure must also be increased. This is important as the reactions occur mainly by structural or compositional rearrangement of the kerogen itself. Being in an environment characterized by high temperatures and in the absence of external reagents, radical processes take place that generates two types of by-product: richer in hydrogen (higher H / C) or richer in carbon (lower H / C) than the starting point. The compound richest in hydrogen and poorest in carbon is methane (CH_4) while, on the contrary, the compound poorest in hydrogen and richest in carbon is graphite which represents a

thermodynamically stable form of pure coal. The type of by-product depends on the composition of the kerogen. If the kerogen is rich in hydrogen, then the by-products will be rich in hydrogen. The three types of kerogen (**Figure 2**) have different H / C ratios. Algal and liptinitic kerogens have very high H / C ratios providing relatively hydrogen-rich by-products (such as crude oil and natural gas) while humic kerogen, being rich in carbon, can generate carbon-rich by-products such as coal [2].

1.1 Coal

The **formation of coal** dates back to about 345 million years ago thanks to a long process called coalification. The geological era to which the beginning of coal formation belongs is the Carboniferous and Permian period, following the Palaeozoic glaciation and then ending with the Permian - Triassic extinction, in which it is rare to date coal deposits [5]. The earth was presumed to be covered with dense vegetation that constitutes the starting element for the formation of coal. Once dead, it would seem that the plant material had been protected from the degradation action of moulds and bacteria that did not yet exist at the time. All this contributed to the formation of peat (a mixture of mud, acidic water, and dead plant material). Millions of years of action on peat bogs buried deep in sediments have eliminated water, methane, and carbon dioxide from the deposits, accumulating carbon. The amount of carbon and water present also determines the **type of by-product**. Mild pressure and temperatures have formed lignite, which, in turn, by losing water, forms bitumen up to the formation of anthracite (a compound with higher carbon content and higher calorific value compared to previous by-products). The last by-product is graphite [6]. **The chemical composition** of lignin starts from a monomer, the monolignol formed by a benzoic ring with a side chain of allyl alcohol. Three different monolignols can dimerize during coalification. The next step is the polymerization of the dimers in a finely controlled process that leads to lignification, in which other molecules such as carbohydrates and cellulose also participate (**Figure 3**). Lignins are racemic compounds and their assembly is regulated to control phenoxy radical coupling. Lignin is made up of 54% C, 6% H, and 49% O [7]. As described before, during coalification, lignin loses water and gain carbons. The two chemical processes: dehydration and decarboxylation lead

to the formation of bitumen. Thanks to de-dehydration, there is a loss of oxygen and hydrogen but the double bonds between the carbon molecules increase. With decarboxylation, however, only a decrease of the hydrogen atoms is obtained. Bitumen, on the other hand, also undergoes a de-methanation process which leads to a reduction in hydrogen molecules. The bituminous coal converts to anthracite undergoing further de-methanation [8]
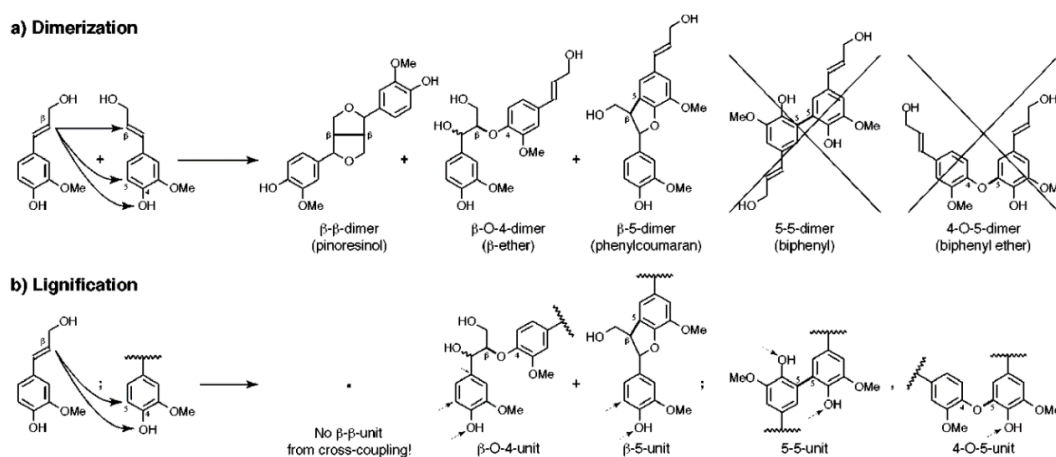
Figure 3: Coalification process [7]

The massive use of coal as an energy source begins with the **first industrial revolution**, even though coal had been used as combustible material for many centuries before. In the thirteenth century, the first form of underground mining was developed, but it was only in the eighteenth century that Great Britain began the massive extraction of coal, called "steam coal" due to its use as a fuel for locomotives and steam engines [9]. Steam coal is a variety of coal with a high degree of hydrogen which gives it a better combustion capacity, but several international standards allow coal to be classified based on the content of volatile particles that are released during combustion. The composition of coal is determined by **analytical parameters** such as humidity, volatile compounds, fixed coal, and ash; and by **chemical parameters** that identify the compounds that constitute it (e.g. carbon, hydrogen, sulphur, etc.). With the **second industrial revolution**, characterized mainly by the use of electricity and chemical compounds derived from petroleum, the use of coal, as an energy source, has changed. We have gone from steam generation to electricity generation, and then from steam coal to

thermal coal. Coal-fired power plants always use pulverized coal to produce steam but this is channelled into turbines that generate electricity with an efficiency between 25-50% [10]. More modern and efficient plants (about 94%) transform coal into synthetic-gas (**syngas**), a combustible gas synthesized through the use of high temperatures in the presence of oxygen. The gasification of coal takes place, therefore, through the oxidation of the coal which generates carbon monoxide and releases gaseous hydrogen. Syngas, in addition to being used directly within power plants, is also converted into other fuels such as diesel and gasoline. This process is called indirect coal liquefaction and follows the Fisher-Tropsch rules [11]. Since the early 2000s, many factories have closed all over the world, trying to eliminate coal as an energy source and replace it with renewable sources. Among the largest countries that are trying to become "carbon-free" are the United States of America (USA), and many countries of the European Union. In contrast, China and India have become the largest producers of coal, thanks to the numerous mines still active, and the numerous coal plants built [12]. It is estimated that China extracts almost half of the world's coal, governing the market trend. The problem of using coal as an energy source starts with extraction. During this process, the aquifers present near the extraction sites are contaminated, as well as the surrounding soils, by ash sewage which has a strong acidifying action. The combustion of coal also causes the release of sulphur dioxide into the atmosphere which, once in the atmosphere, is oxidized into sulphuric acid (H_2SO_4). The sulphur resulting from sulphuric acid is precipitated by acid rain within a few weeks, contributing to the acidification of ecosystems [13]. Furthermore, the extraction itself constitutes a physical problem for the area, because of the presence of tunnels and underground mines that affect the stability of the overlying infrastructures. However, the most catastrophic effect of using coal as an energy source is the release of carbon dioxide into the atmosphere during its combustion. In 2018, coal-fired power plants were estimated to have contributed to the release of 40% of the world's total emissions (**Figure 4**). For every megawatt-hour produced by the combustion of coal, about one ton of carbon dioxide (CO_2) is released into the atmosphere [14]. For this reason, as mentioned above, the world is trying to move towards cleaner energy sources by becoming "coal-free", but this seems to be a distant goal (**Figure 5**).

Global coal generation and CO2 emissions saw a record 3% fall in 2019
Rising capacity means fewer running hours, reduced load factors and lower profits
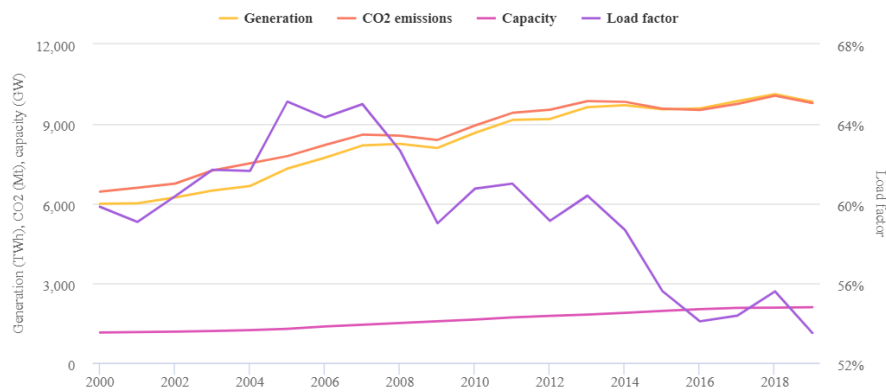
Figure 4: Global coal generation and CO$_2$ emissions [12]
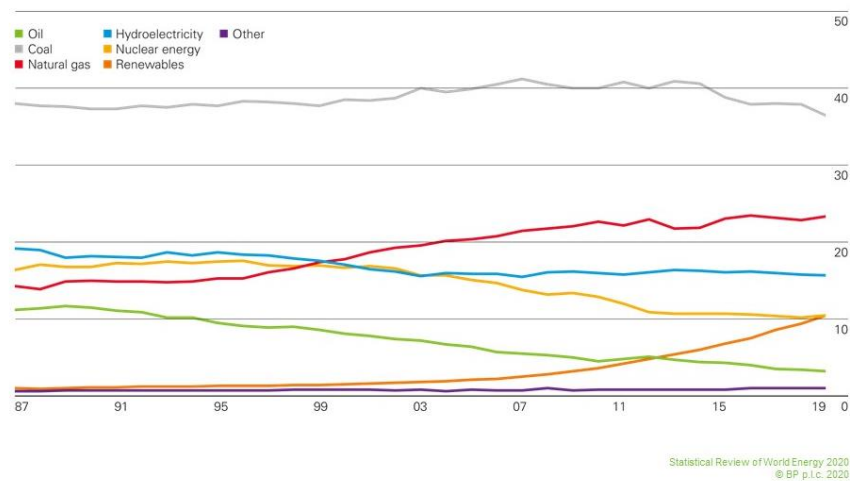
Figure 5: Share of global electricity generation by fuel (percentage) [15]

In 2018, coal production remained constant compared to 1998, to the detriment of other energy sources, which instead suffered fluctuations and decreases thanks to the advent of renewable energy sources, but at the end of 2019, coal consumption decreased by 0.6%, reaching its lowest level in the last 16 years [16]. In 2020, due to the lockdown caused by severe acute respiratory syndrome coronavirus 2 (SARS-CoV-2), the demand and production of coal suffered a further decline: 7% decrease. Despite these encouraging data, the International Energy Agency (IEA) has predicted, in its annual report that coal demand will rise by 2.6% in 2021 to reach a plateau in 2025 when the European Union and the USA will endeavour to use natural gas as a substitute for coal [17].

1.2 Natural Gas

Natural gas is a non-renewable fossil fuel. The gas we use today was mainly formed in the subsoil, millions of years ago, thanks to the decomposition of plant matter (especially diatoms) and/or animals when they were subjected to internal heat and pressure in anaerobic conditions in a process called **thermogenic**. Natural gas consists mainly of methane (CH_4), a colourless and odourless hydrocarbon. Its formation is closely linked to the absence of oxygen and it is possible that natural gas also forms on the surface, in marshes and swamps thanks to methanogenic microorganisms in a **biogenic process** [18]. Based on the extraction site, the composition of the gas also varies. Natural gas is a mixture of hydrocarbon compounds including, as mentioned above, methane, ethane (C_2H_6), propane (C_3H_8), butane (C_4H_{10}), CO_2, and nitrogen, and can be also classified according to the condensation of hydrocarbons, the presence of water and the presence of other chemical compounds. It is therefore called: **wet gas** (gas containing condensable hydrocarbons), **lean gas** (gas that does not contain condensable hydrocarbons), **dry gas** (gas with methane but without water) **sour gas** (gas containing sulphur oxide), and **sweet gas** (gas which does not contain sulphur oxide) [19]. A further classification is obtained based on the geolocation of the gas. The natural gas found in cracks or between rock layers is called **conventional gas**, while the gas that accumulates in the pores inside clayey or sedimentary formations is called **unconventional gas**. Very often, however, the gas fields coincide with those of crude oil and for this reason, the gas is called **associated** [20]. The geological composition and the source of production also help distinguish different types of gas. **Shale gas** is an unconventional gas that is trapped in shale deposits at a depth of about 3,000 meters and is either bound to kerogen (adsorbed gas) or free within natural clay fractures (free gas). The percentages vary according to the depth and temperature of the reservoir. The extraction of shale gas involves the artificial fracturing of the clayey matrix, to increase its porosity and permeability. The gas that forms during the peat carbonation process is called **coal gas**. As described in section 1.1, when the bitumen is to turn into anthracite, the hydrocarbon content breaks down into thermogenic methane, which remains partly in the coal and partly, is expelled.

However, as the coal reorganizes its structure, which is less and less humid, micropores are generated capable of adsorbing the methane, thus decreasing the expulsion of the methane itself. It is, therefore, logical to think that there is a greater quantity of natural gas in carbonaceous bituminous fields [21] (**Figure 6**).
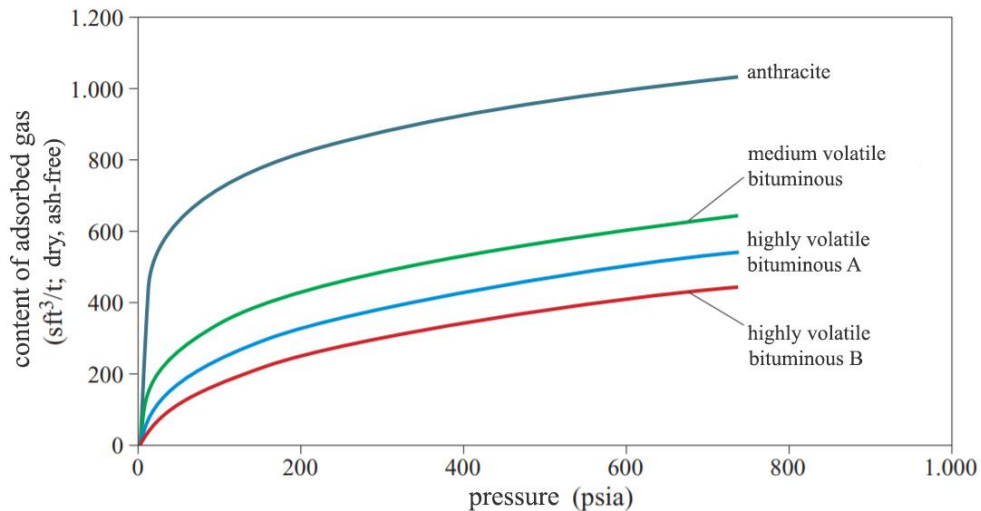
Figure 6: Gas content adsorbed by the different types of coal. Adapted from [21]

The term coal gas, however, also identifies the gas that derives from the gasification of coal and is characterized by the presence of hydrogen, carbon monoxide, methane, and other volatile hydrocarbons [22]. As previously mentioned, natural gas is also formed through the biogenic process, again through the action of methanogenic microorganisms. This type of gas is called **biogas**. Biogas can derive from landfill swamps or the decomposition of agro-food waste material and is mostly made up of methane and carbon dioxide [23]. Much colder soils, such as Siberian ones, can contain natural gas inside. It is a particular solid material, similar to water that contains methane molecules. We speak of methane hydrate, present in the continental margins of sedimentary sequences and the permafrost of polar regions. Methane hydrates are crystalline compounds that are formed when very small gas molecules meet the water at temperatures close to 0°C and high pressures. During catagenesis, the phase in which the organic material is compacted during the production of crude oil, there is a release of wet gases consisting of methane and about 40% of higher hydrocarbons.

At the end of the catagenesis, due to the thermal cracking of the crude oil, there is an increase in temperatures which leads to the formation of dry gas which, when placed at low temperatures, forms methane hydrate [18]. Natural gas was discovered by chance in China around 500 BC. The Chinese populations also managed to exploit the energy properties of natural gas by conveying them in bamboo pipes to boil water during a salt extraction process. About 1,100 years later, natural gas was also discovered and identified in America, and in Great Britain, the British used coal gas to light houses and streets. Only in the first half of the 1800s in New York, there was the creation of the first natural gas well and consequently also the creation of the first municipal-owned distribution company. Throughout the nineteenth century, natural gas has been used almost exclusively for the production of light, but with the invention of the Bunsen burner, natural gas began to be used for domestic heating, for powering kitchens up to power boilers to generate electricity [24]. During this period, most of the gas used came from crude oil production. When the extracted fluids underwent a reduction in pressure, the small carbon chains of the light gas escaped from the tank. Initially, the presence of this by-product was a problem because it constituted not only a danger for the safety of the plant but also its disposal; for this reason, the gas was vented or was burned, but with the construction of the pipelines it was possible to transfer the gas from a well to a final consumer. There are extraction sites for petroleum-associated natural gas and extraction sites for non-associated natural gas. The latter is found mainly in the Persian Gulf and Russia. In the USA, most of the extraction wells are dedicated to shale gas [25]. Generally, the search for suitable sites for natural gas extraction starts from a geological study to identify the types of geological formations most suitable for containing natural gas deposits. Seismic surveys create and analyse seismic waves in the earth to obtain information on the composition of the subsoil. Once the seismic analyses have identified a potential accumulation site, an exploration well is then installed. If positive results are obtained, and the amount of gas detected is sufficient to make a profit, then production wells are installed. Drilling can take place vertically or horizontally but, in both ways, the gas rises towards the surface where it is conveyed in collection ducts up to the transport and treatment plants [20]. The transport of methane over large distances began in 1958 when there was a transfer from Canada to the USA. Nowadays, gas pipelines or methane tankers are used on which liquefied natural gas (LNG) is loaded.

The liquefaction of the gas takes place in special plants where the gas is cooled to -162 °C, reducing its volume and facilitating its storage and transport. However, before natural gas, gaseous or liquid, can be marketed, it must be treated to remove any contaminants present. The associated gas is very often called, as previously mentioned, wet gas because it contains in addition to methane, also ethane, propane, butanes, pentanes, and water vapour, but it can also contain non-hydrocarbon compounds, such as sulphur, helium, carbon dioxide, and nitrogen. Once extracted, the associated gas is sent to purification plants where water vapour and other compounds are removed. Once purified, the gas is finally commercialized [26]. The gas is used for several purposes; Natural gas has a high calorific value and burns better than other fuels, for this reason, since its combustion produces both steam and CO_2, it is very often used to produce electricity thanks to steam turbines. The combustion of natural gas produces half of the CO_2 emitted by coal and for this reason, the generation of energy thanks to a combined cycle system (gas turbines and steam turbines), is one of the cleanest systems for producing electricity, generating 22% of the world's electricity [27]. Due to its peculiarities, natural gas continues to be used today for domestic use, generating temperatures above 1,100 °C for this reason, being odourless in nature, mercaptans substances are added that odour the gas, to make it safer for the consumer in the case of household losses [28]. The cheaper price and its lower polluting power have made methane a cleaner alternative as a fuel for cars, while not affecting energy efficiency in any way compared to petrol-powered engines. In 2014, there were over 20 million vehicles powered by methane and it is estimated that shortly even planes could be powered by methane [29]. In 2019, gas consumption increased by around 2%, although lower than the levels reached in 2018 (5.3%). Despite this regression, 24.2% of primary energy to date is produced by natural gas its production has grown by 132 billion cubic meters, exceeding the consumption growth. The natural gas trade sees Europe as the largest buyer, which has increased imports by 68% (**Figure 7**); however, as production is greater than consumption, the price of natural gas has dropped dramatically: in 2020 in the USA there was a drop of 20% [30]. The increase in the consumption of natural gas has consequently caused an increase in the emissions of methane into the atmosphere, which otherwise would not be released naturally into the atmosphere. Worldwide, methane represents 33% of anthropogenic greenhouse gases.

Methane is considered a "short-term climate forcing" as it persists in the atmosphere for only 12 years but has a global warming power, 30 times greater than CO_2 [31]. The greatest dispersion of greenhouse gases occurs during production and transport, not during the withdrawal of natural gas, and during its combustion there is a production of 30% less CO_2 than crude oil and 45% less than coal, making it a less polluting energy source. Other contaminants such as sulphur dioxide and the various nitrogen oxides produced by natural gas are also lower than other fossil fuels. A problem related to the use of natural gas is safety during its use. During extraction, hydrogen sulphide can be released, which is toxic if inhaled and the emptying of the deposits can lead to subsurface subsidence. Even transport and processing are not without dangers: the flammable potential of the gas could easily lead to explosions and fires [32]. Finally, it is expected that, as mentioned in section 1.1, in the near future natural gas could be a valid substitute for coal, leading the world to a greener perspective than in the past.
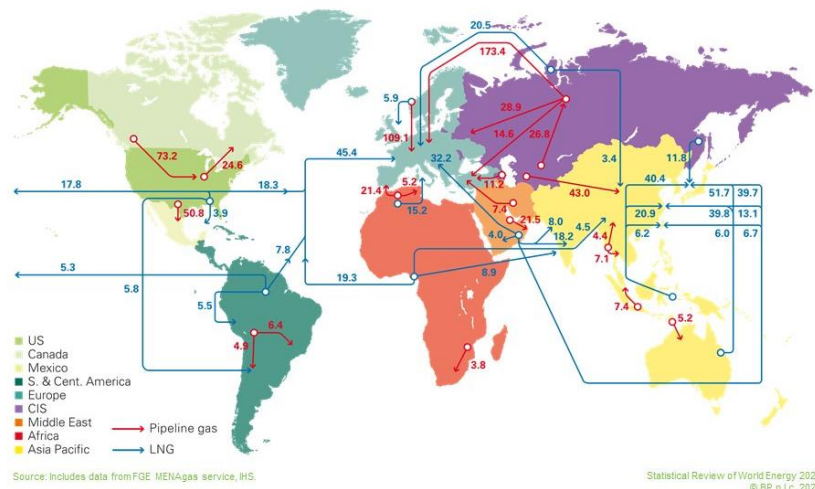
Figure 7: *Major gas trade movements 2019. Trade flows worldwide (billion cubic metres)* [30]

1.3 Petroleum

Crude oil or petroleum is a viscous and flammable liquid and, today, petroleum use represents more than 80% of global energy [33]. Its composition and its most important characteristics will be described in-depth in chapter 2.

CHAPTER 2: PETROLEUM

2.1 The History of Petroleum

The use of petroleum by humanity dates back to very ancient times. The first evidence of the use of petroleum dates back to the pre-Christian era, around 4000 BC, when the Sumerians used bitumen or asphalt in their architectural works. The origin of the words "asphalt" and "bitumen" is also archaic. H. Abraham describes, in his book, how the etymology of the word asphalt is common to different cultures and languages. For example, the Akkadian term "*sphallo*" used in those days, presumably meant to divide. Subsequently, the Greeks used the adjective "*ασφαληςες*" to indicate stability and security, and the corresponding verb "*ασφαλιζωισω*" meant to secure, to make stable. The Romans transformed the term into asphaltum. The origin of the word bitumen, on the other hand, is more difficult to trace. First traces date back to the Sanskrit language where the word *jatu* meant sticky. It is believed that the Romans used the word *gwitumen*, which however has the same root as the Anglo-Saxon term *cwidu* [34]. The study of the origin of words also helps us to understand when the use of petroleum and its derivatives dates back. The Babylonians (1500-538 BC) used bitumen to coat cisterns and pipes in the cities of Babylon, Calah, and Ur. The Persians, on the other hand, used a substance similar to paraffin which came from some crude oil deposits in the area. The Greeks dominated the Mediterranean thanks to the use of "Greek fire", a substance described as black and viscous capable of igniting once in contact with water and capable of destroying enemy ships. In China (600 BC), petroleum was discovered in salt mines and, for many years, was considered a contaminant of salt. However, the real innovation in the use of petroleum comes with the Arabs, who about 2,000 years ago developed a methodology for the distillation process. The fraction that aroused the greatest interest at the time was the kerosene used for lighting. As the years passed, in Europe around 1550, Bauer describes the separation and ownership of bituminous products that developed well before the birth of the modern crude oil industry [35]. Studies show that the use of petroleum and related materials has been observed for more than 6,000 years, but the birth of the modern oil industry begins in the mid-1800s with the discovery of petroleum wells in Pennsylvania and the related refinery processes (Table 1).

In 1855, the analyses carried out on the "black matter" extracted by the Pennsylvania Rock Oil Company, showed that 50% of the tar that made it up could be obtained through the first step of the refinery process (tar which will later be called kerosene or paraffin), whereas the remaining 40% could be distilled into material useful for lubrication and gas lighting. In 1857, the Drake Well at Oil Creek in Pennsylvania became the world's largest oil producer, taking USA oil production from 2,000 barrels in 1859 to 10,000,000 barrels in 1874.

Table 1: Process Development Since the commencement of the modern refining Era - Adapted from [36]

Year	Process Name	Purpose	By-products
1862	Atmospheric distillation	Produce kerosene	Naphtha, cracked residuum
1870	Vacuum distillation	Lubricants	Asphalt, residua
1913	Thermal cracking	Increase gasoline yield	Residua, fuel oil
1916	Sweetening	Reduce sulfur	Sulfur
1930	Thermal reforming	Improve octane number	Residua
1932	Hydrogenation	Remove sulfur	Sulfur
1932	Coking	Produce gasoline	Coke
1933	Solvent extraction	Improve lubricant viscosity index	Aromatics
1935	Solvent dewaxing	Improve pour point	Wax
1935	Catalytic polymerization	Improve octane number	Petrochemical feedstocks
1937	Catalytic cracking	Higher octane gasoline	Petrochemical feedstocks
1939	Visbreaking	Reduce viscosity	Increased distillate yield
1940	Alkylation	Increase octane number	High-octane aviation fuel
1940	Isomerization	Produce alkylation feedstock	Naphtha
1942	Fluid catalytic cracking	Increase gasoline yield	Petrochemical feedstocks
1950	Deasphalting	Increase cracker feedstock	Asphalt
1952	Catalytic reforming	Convert low-quality naphtha	Aromatics
1954	Hydrodesulfurization	Remove sulfur	Sulfur
1956	Inhibitor sweetening	Remove mercaptans	Disulfides and sulfur
1957	Catalytic isomerization	Convert to high octane products	Alkylation feedstocks
1960	Hydrocracking	Improve quality and reduce sulfur	Alkylation feedstocks
1974	Catalytic dewaxing	Improve pour point	Wax
1975	Resid hydrocracking	Increase gasoline yield	Cracked residua

The massive mining activity, throughout the USA, also allowed for the export of petroleum across the Atlantic. At the end of 1870, petroleum dominated the market also thanks to the development of new cars. Throughout the nineteenth century, USA and Russia dominated the market, but after the end of the First World War, other nations began to appear on the world market, such as Indonesia [36].

2.2 Petroleum History in Italy

Italy played an important role in the mining industry until the nineteenth century. The first crude oil wells were located east of the Apennines, in Sicily and in the Po Valley and, in 1860, Achille Donzelli built two wells in the province of Parma producing about 25 kg of petroleum daily. The low production can be linked to the depth of these wells (32 and 45 meters); for this reason, at the end of the 1800s, Guido Della Rosa built a well that reached 308 meters in depth, producing 3750 kg of petroleum per day. As in the rest of the world, in Italy, the main refining product was kerosene used for the combustion of oil lamps. The invention of the light bulb threatened the power of oil, but engines powered by petrol and gas oil, and the First World War strengthened the oil market. In fact, during the First World War, 48% of gasoline in Italy was restricted to the army. In 1926, low-decree number 556-3/4 entrusted AGIP (Azienda Generale Italiana Petroli) with the task of researching new wells in the Italian territory [37]. AGIP began to search for petroleum not only in Italy but also in its colonies in Africa and the Middle East, discovering a large petroleum field in the Po Valley, which, however, was kept hidden due to the imminent world conflict. After the Second World War, the defeat of Italy by the allies puts the existence of AGIP at risk. Enrico Mattei was commissioned by the Italian government to reorganize the company and so, in 1953, ENI (National Hydrocarbon Organization) was founded, which in the same years began an intense mining and distribution activity throughout the country [38]. Thanks to Mattei, the power of the "Consortium for Iran", also known as the "Seven Sister", was also broken. The Consortium for Iran was a cartel that dominated the production and sale of crude oil worldwide for about 40 years (1940-1973). The birth of the cartel dates back to early 1928 with the agreement between the oil companies Royal Dutch Shell, Standard Oil of New Jersey, and Anglo-Iranian Oil Company (now BP). These were joined by the Standard Oil Company of New York (later Mobil), Standard Oil Company of California (later Chevron), Gulf Oil, and Texaco. The first disagreements began in 1951 when the Iranian Prime Minister nationalized the crude oil industry, marking the total embargo of Iranian oil exports. Later, the USA formed the Consortium for Iran with which it bought crude oil from Iran as a monopoly. Enrico Mattei tried to get Italy to join the consortium but this did not happen [39].

In the first 50 years of the twentieth century, Italy extracted crude oil and gas from the Po Valley, producing 35 million cubic meters per month. Thanks to intense

exploration, AGIP had installed 27 drilling probes capable of reaching a depth of 5,500 meters [40]. At the end of the 1950s the most important deposits in Italy, as well as in the Po Valley, were also found in Sicily, in particular in Ragusa (1,500 meters deep), in Gela (3,500 meters deep), and Gagliano Castelferrato (2,000 meters deep). In 1956, the production of the Ragusa well-constituted 90% of Italian crude oil production, covering 10% of the national demand. Gela, on the other hand, was the first Italian offshore well and, throughout the 1960s and 1970s, the research led not only to the discovery of new deposits on the coasts of the peninsula but also to a better knowledge of Italian geology. The search for other offshore fields led in 1987 to the construction of Punta Cugno Augusta, the largest Italian offshore plant [41].

2.3 Petroleum in Basilicata

Basilicata is a region of Southern Italy. Always considered one of the poorest regions of the South, it has turned out to be the richest in terms of crude oil. In the Val d'Agri, there is the largest onshore crude oil field in continental Europe. The valley is intra-montane and is located at a height of about 600 meters above sea level in the centre of the southern Apennines. The valley is then surrounded by mountainous massifs that reach 1,500 meters in height. The first evidence dates back to the fifteenth century when there was talk of "torches" present on the Apennine mountains, probably attributable to natural methane leaks. The first deposits were discovered in the mid-nineteenth century, following a strong earthquake that affected the Val d'Agri. The event caused about 11,000 victims and for this reason, it attracted the attention of many geologists; precisely the study of the Lucanian subsoil allowed the development of some mines both in the Agri Valley (Tramutola and Marsico) and in the Melfese area [42]. Initially, Tramutola was the area that attracted particular attention due to natural hydrocarbon spills near a small stream, the Torrente Fossatello.

At the beginning of the 1900s, Deputy Francesco Perrone was responsible for encouraging crude oil exploration in Basilicata, leading the company "Petroli d'Italia" to stipulate a concession contract, with 87 Lucan landowners, for the

research and exploitation of crude oil resources. The first excavations were obtained with a "Canadian probe" which reached a depth of 1,000 meters but the presence of sulphurous water caused the research to be abandoned ("Fossatello" probing). In the early 1930s, thanks to new technologies for seismic analysis, led to the formation of the Tramutola 1 well (1936) on the Macchia Michelina hill, on the right bank of the Rio Cavolo. The well-reached depths of 190/270 meters turned out to be productive. Forty-seven wells were drilled between 1936 and 1943, of which 21 crude oil, 3 gas, and 6 crude oil and gas. Total production was about 3,500 barrels per year with the maximum peak reached in 1942 with 700 tons of crude oil, equal to 7% of national production. In 1960, AGIP began exploration in the Pisticci area but only at the end of the 1970s Basilicata became a centre of political interest for crude oil extraction. Thanks to more in-depth geological surveys, it was discovered that in the Lucanian subsoil there were large tectonic over thrusts that covered huge crude oil fields and this was confirmed by the first exploratory drilling that exceeded 4,000 meters deep. In 1980, the exploration continued and led to the construction of wells such as Costa Molino, Caldarossa, and Tempa Rossa 1 [43]. At the beginning of the 90s, the real crude oil business began in Basilicata. The concessions of "Grumento Nova" and "Volturino" were issued. In 1999, the "Monte Alpi Oil Center" was built in Viggiano, extracting 1,200 cubic meters of crude oil per day (7,500 barrels per day) and 300,000 cubic meters of gas per day [44].

2.3.1 Val d'Agri Oil Centre (COVA)

The Val d'Agri Oil Centre (COVA) is located in the industrial area of Viggiano, where it occupies approximately 180,000 square meters. The Val d'Agri concession is entrusted to ENI for 61% and Shell for the remaining 39%. COVA has been in operation since 2001 and the hydrocarbons extracted from the reservoir are treated inside it, separating crude oil, gas, and stratum waters. The crude oil is stored in specific tanks from which, subsequently, the crude is sent by pipeline to the Taranto refinery. COVA has a daily treatment capacity of 104,000 barrels per day which corresponds to approximately 63% of the Italian crude oil production. The extraction takes place from 24 different wells (including Monte Alpi, Monte Enoc, Cerro Falcone). The production of hydrocarbons in Basilicata comes mainly from COVA and in 2019 the fields provided 47% of the Italian ENI production [45].

2.3.2 Tempa Rossa

Tempa Rossa is an crude oil field located in the Sauro valley between the municipalities of Corleto Perticara and Gorgoglione. The field was discovered by the Belgian company FINA and then absorbed by the French company Total. In 1999, the concession for the exploitation of liquid and gaseous hydrocarbons was granted and between 2011 and 2012, Total obtained the authorizations to build the plants that were completed in 2018. In 2019, during explorative extractive tests, 10 million barrels of crude oil have been obtained, so in December 2020 the extraction activity began, to produce 50,000 barrels per day of crude oil, 230,000 cubic meters of natural gas, 240 tons of LPG, and 80 tons of sulphur [46]. The extracted hydrocarbon mixture is particular as it is heavy oil with API values from 10 to 22 and with sulphur inside [47]. Hydrocarbon is treated in the treatment centre. Working at different temperatures, it is possible to obtain crude oil, LPG, and gas. The extracted methane is sent free of charge to the Basilicata distribution network; LPG is stored in underground tanks while crude oil is transported *via* the crude oil pipeline (diameter equal to 51 cm and long 136 km) to the ENI refinery in Taranto. In November 2020, the Bank of Italy report argued that Basilicata alone contributed, through Tempa Rossa, to increase the production of crude oil by 27% compared to 2019. However, the decrease in crude oil prices caused by the Covid-19 pandemic, the increase in production did not coincide with an increase in profits. Basilicata in 2020 obtained 110 million royalties from crude oil companies, based on 2019 production (Banca di'Italia, 2020). The geographical position of Tempa Rossa and its activity has created numerous problems also at an environmental level, being in the centre between the regional park of Gallipoli Cognato and the Pollino national park. Furthermore, the investment seems to be in contrast with the rest of the world which, instead, focuses on more renewable and cleaner sources.

2.4 Economy of World and Italy petroleum

Worldwide, daily crude oil consumption in 2020 increased by 0.9 million barrels per day (b/d) while demanding liquid fuels by 1.1 million b/d exceeding the record threshold of 100 million b/d for the first time. This historic increase was achieved thanks to an increase in Chinese demand, which reached 680,000 b/d. The Organization for Economic Co-operation and Development (OECD), however, decreased its demand for the first time since 2014, following a global trend, with

China and Iran being the exceptions. The Organization of the Petroleum Exporting Countries (OPEC), founded in 1960 to balance the economic power imposed by the "Seven Sisters", had a drop in production in 2019 of about 2 million b/d, and this allowed the USA to record the largest increase in production with an increase of 1.7 million b/d. Brazil and Canada also recorded an increase, albeit to a lesser extent than in 2018. Some of the largest crude oil producers (Iran, Venezuela, and Saudi Arabia), members of OPEC, experienced severe slowdowns in production (Saudi Arabia, for example, recorded a drop of 430,000 b/d) while others including Iraq and Nigeria had a sharp increase to 150,000 b/d. However, the production of crude oil and condensate has decreased (- 580,000 b/d) while natural gas has grown substantially (+ 4.2% compared to 2019) thanks to the production strength of the United States which doubled their production, in 2018. Compared to 2019, crude oil prices have fallen slightly, averaging $ 64.21 per barrel. Crude oil is also known as black gold because it is the basis of the world economy [15]. Its production is influenced not only by economic demand and supply but also by world politics and for this reason events such as the Covid-19 pandemic have heavily influenced the market. As previously mentioned, in 2020, the price of crude oil underwent a decline, even touching minimum prices of $ 20 a barrel and this fully reflects how the price of crude oil is influenced by political, economic, and social events (**Figure 8**) [49]. The main markets in which crude oil is traded are NYMEX in New York and the International Exchange (ICE) in Atlanta. The trading model applied in NYMEX is a continuous auction model on-site, called Open Auction, while the ICE model is based on the online trading of energy products, commodities, and derivatives in markets not belonging to the official ones. The markets, however, are also influenced by the qualitative characteristics of crude oil; based on the differences found concerning the reference product, the price can increase or decrease (**Figure 9**). The characteristics considered are the density of the crude oil (heavy-light), analysed in detail in the following chapters, and the sulphur concentration (sweet-sour).
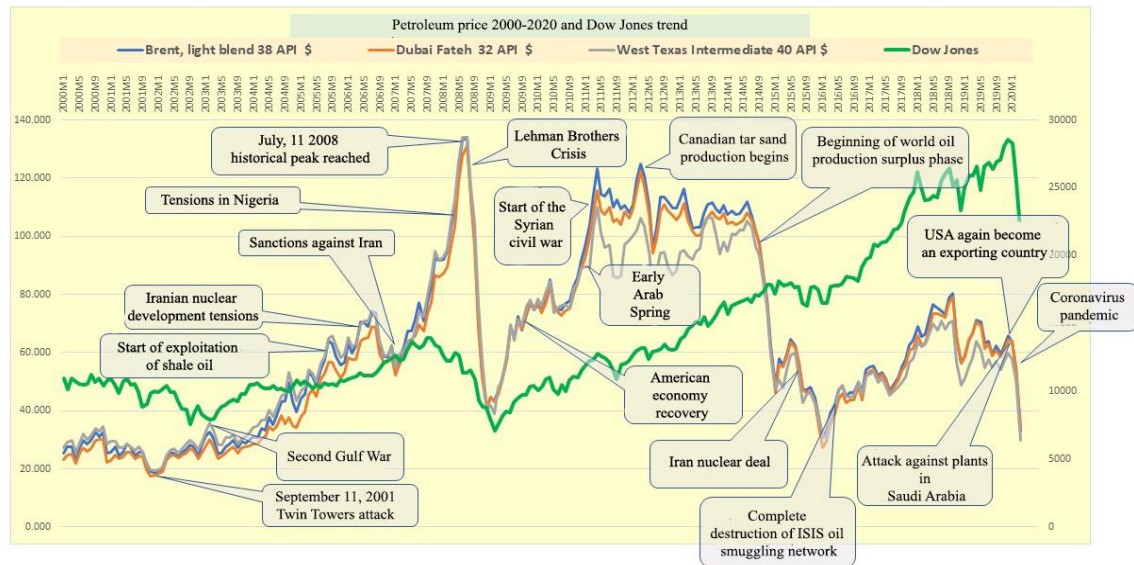
Figure 8*: Crude Oil price 2000-2020 and Dow Jones trend. Adapted from* [49]

The main qualities of crude oil are West Texas Intermediate (WTI), Brent Blend, and OPEC reference basket. **WTI** is considered the first quality of crude oil to arrive in the crude oil market and it derives from the American fields of Texas. Thanks to the exploitation of shale oil, after a difficult period, it had a great role in the global market. It went from 0.4 million barrels a year in 2007 to around 4 million in 2014, making American refineries the main competitors on the market. The WTI has undergone several fluctuations in the last decade, reaching historic lows in April 2020 reaching $ 37.63 per barrel. **The Brent Blend**, on the other hand, comes from the North Sea. It is considered less valuable than the WTI as it contains greater quantities of sulphur but is, in turn, the absolute protagonist of the crude oil market. In the last 10 years, it has reached prices of $ 120 per barrel in 2011, reaching the WTI in 2020 in its historical lows with $ 21 per barrel. **The OPEC** reference basket is a high-density crude oil and represents the production of the 13 countries belonging to the cartel itself (including Iraq, the United Arab Emirates, Venezuela, and various African states).

The price is calculated by averaging the prices of the crude oil produced by each member state. Among the three main qualities of crude oil, the OPEC Reference basket is the one that reached the lowest levels following the pandemic, reaching $ 17 per barrel (compared to $ 131 per barrel in 2008) [50].
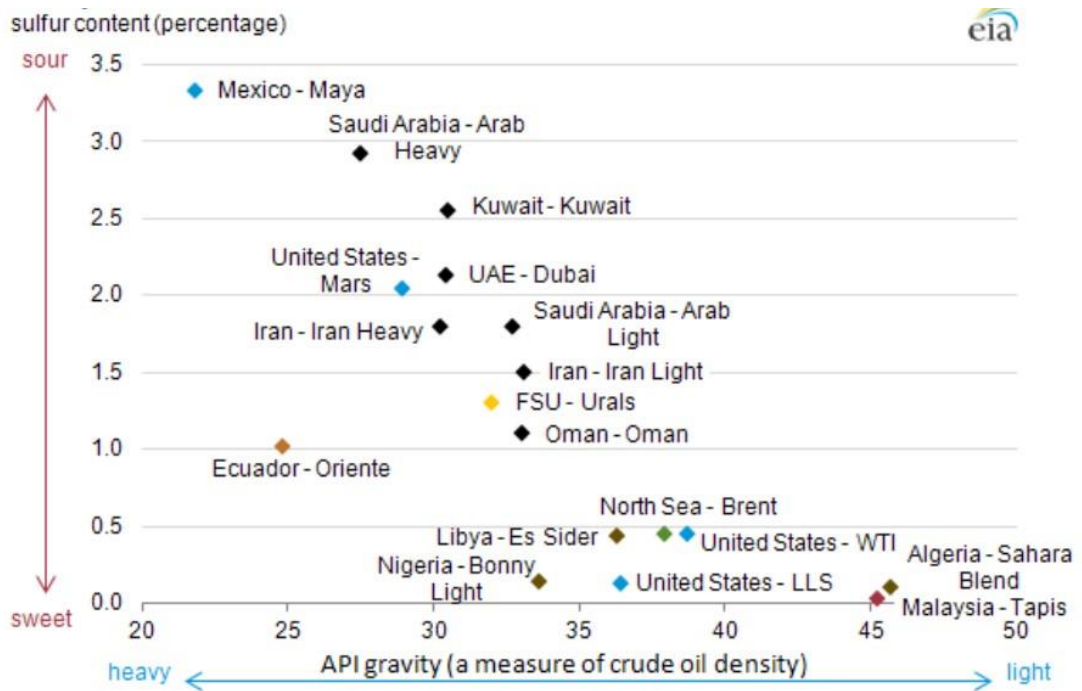
Figure 9: Density and sulphur content of selected crude oils [51]

2.5 Petroleum formation

The formation of crude oil occurred in a similar way to that of coal and natural gas; it is believed that especially during the Palaeozoic era there was an accumulation of biological material composed mainly of single-cell marine, plant and animal organisms that were submerged underground for millions of years. The first stages of crude oil formation are common to those described in section 1.2 relating to the formation of natural gas. The key process leading to crude oil formation is the transformation of kerogen into crude oil. This occurs through a thermal degradation process called cracking. Cracking can take place by catalytic or thermal route depending on the presence or absence of catalysts, but the result is the breaking of heavy hydrocarbon molecules into lighter molecules. The formation of crude oil, although it may seem simple, is supported by two opposing theories (the most important differences between the two theories are summarized in the Table 2). The **abiogenic theory** argues that petroleum originates from inorganic material such as, for example, acetylene from which the various constituents of petroleum are produced once conjugated with water [52]. Furthermore, many abiogenic

hydrocarbons were believed to arise from tectonic geological processes, such as erosion, orogenesis, rifting, and deep gas releases [53]. This theory was supported by many, especially because, according to thermodynamic experiments, *n*-alkanes cannot form spontaneously from methane through the action of pressure but geological analyses, and chemical experiments, have shown the actual biogenic formation. The **biogenic theory**, on the other hand, argues that crude oil derives from a series of processes that have contributed to transforming the organic matter deposited on the seabed (**Figure 10**). In detail, about 600 million years ago, organic material deposited on the seabed and over time was covered for about 1 meter by layers of mud and earth that prevented aerobic decomposition but allowed anaerobic decomposition by suitable bacteria to work in the absence of oxygen. The condition of anaerobiosis allowed the reduction of sulphates and nitrates in hydrogen sulphide and nitrogen which consequently caused hydrolysis reactions of the polysaccharides that generated monosaccharides which in turn generated CO_2 and methane, and of the proteins in amino-acids before and in immino-acids after. All hydrolysis processes collaborated in the creation of phenol compounds and aldehydes.
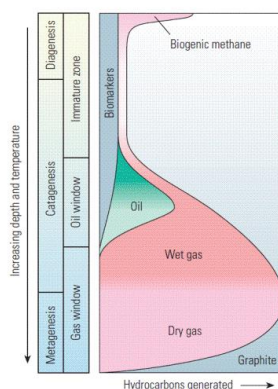
Figure 10: Formation of crude oil and gas from kerogen [54]

At a depth of about 10 meters, the bacterial action stopped to ensure that the mixture obtained could combine thanks to the action of temperature and pressure that increased, thus leading to the formation of kerogen in a key process of crude oil formation: **the diagenesis** [36]. The kerogen formation process continues up to a depth of 1,000 meters, where the temperature reaches about 50°C. At this point, radical rearrangement reactions take place via **catagenesis**. This process requires millions of years and also involves external agents, as well as taking place in a

temperature range that goes from 50 to 150°C. Through catagenesis, there is a transformation of the crude oil molecules that can generate gas molecules [55]. Catagenesis was a pyrolytic process although it occurred at low temperatures; the action of time favoured the decomposition of radioactive materials in the earth's crust. At this point, the hydrocarbons migrate through the rocks until they are trapped in porous rocks called "reservoirs".

Table 2: Difference between the abiogenic and biogenic theory. Adapted from [53]

	BIOGENIC	ABIOGENIC
Raw material	Organic matter	Deep carbon deposit derived from planet formation or subducted material
Events before conversion	Plant and animal life were buried. Sediments accumulating slowly compressed it and cover it. At several hundred meters, diagenesis and catagenesis happened.	At depths of a hundred kilometres, carbon deposits are mixed of hydrocarbons that migrate upward through the crust.
Conversion to petroleum and methane	Catagenesis occurs with the increase of sepulture. The heat and pressure break down kerogen to form petroleum.	When the material passes through temperatures, some resistant extremophile bacteria consumed and converted material into heavier hydrocarbons.
Evidence supporting theory	Abiogenic theory cannot explain the detection of various biomarkers in petroleum (such as tetracyclic diterpene, sterane, hopane and oleanane). Microorganisms exist deep underground and some that can metabolize carbon are only known so far to be created in surface plants. This confirmed that some petroleum deposits may have been in contact with ancient plant residue	Possible hydrocarbons origins: hot planet caused methane and other hydrocarbons outgassed and oxidized. Carbonaceous chondrite meteorites heated under pressure released hydrocarbon fluids and created solid carbon deposit. Unusual origins: some crude oil fields have been found in really depth granite basement rock (not possible for biogenic theory). Microbial life has been discovered 4.2 km deep in Alaska and 5.2 km in Sweden.

The subsequent reactions are highly dependent on the temperature the liquid petroleum marketed is formed at maximum temperatures between 130 and 150°C, in a range called "oil window". Once these temperatures are exceeded, **metagenesis** occurs, with the final formation of methane or dry gas through the thermal cracking process [36]. Sometimes, however, the crude oil gets trapped at very low levels producing tar sands (bitumen). However, it must be pointed out that the details on

how the formation of crude oil took place are still unclear today and would need further analysis to definitively refute one theory over the other.

2.6 Petroleum composition

Under natural conditions, the lighter hydrocarbons such as methane, ethane and propane are in a gaseous state while the heavier hydrocarbons are in a solid or liquid state. These conditions may vary according to the crude oil field and the phase diagram of the mixture [56]. Petroleum is mainly composed of 4 classes of compounds, including alkanes, cycloalkanes, aromatics and heteroatomic compounds containing one or more nitrogen, sulphur and/or oxygen atoms. **Alkanes,** also called paraffin, result from the cracking of lipids. Alkanes with less than five carbon atoms are usually found in the gaseous state under normal conditions, but alkanes with a greater number of carbon atoms are found in a liquid state, such as heptadecane $C_{17}H_{36}$. The largest alkane found in crude oil is $C_{78}H_{158}$. Some wells produce a gelatinous substance called "*petroleum jellies*", also known as petrolatum, used in cosmetics or as an ointment to protect and soften the skin. Any residues of alkadienes and alkynes are not naturally present in crude oil but derive from refining processes [57]. The **cycloalkanes**, on the other hand, all derive from cyclopentane or cyclohexanes which refer to structures present in the organic material. In principle, cyclic molecules could exist in structures containing two or more carbon atoms. From the two precursors, cyclopropane and cyclobutane are derived which are rare in nature. Petroleum also contains a variety of polycyclic naphthenes such as pregnane and dinosterane, both biomarkers that testify to the biogenic origin of crude oil as they derive from aquatic microorganisms such as dinoflagellates. **Aromatic** compounds in petroleum are found mainly in liquid form; among these are benzene, toluene, xylene and mesitylene (1,3,5-trimethyl benzene). Aromatic compounds containing condensed rings are also found in a solid-state at room temperature. The amount of aromatic compounds present in petroleum varies between 10 to 60% both in the light fraction in which they are unsubstituted and in the heavy fraction where they have one or more alkyl substituents or connected cycloalkane rings. Some aromatics derive from organic matter, in fact, some amino acids such as phenylalanine could have contributed to

the formation of kerogen. Polycyclic aromatic hydrocarbons (PAHs) contain two or more aromatic rings fused. The first compound among the PAHs is naphthalene, but anthracene, phenanthrene and pyrene are also present, which in turn are divided into soluble resins and non-soluble asphaltenes. Also present in a smaller percentage are heteroatomic compounds that are often found conjugated with nitrogen (less than 1%), sulphur and oxygen. Oxygen in petroleum is present in the form of phenols, carboxylic acids, alcohols, esters and ketones. Among the carboxylic acids, fatty acids and naphthalenic acid are also included, which are composed of both a single ring and complex structures that reach the weight of about 1,000 Da. Petroleum containing hydrogen sulphide is called sour crude, while if sulphur is present in different forms than hydrogen sulphur, then petroleum is called crude high-sulphur. Other compounds that contain sulphur are mercaptans, sulphides, and disulphides, and heterocyclic compounds derived from thiophene. Finally, petroleum also contains inorganic compounds, such as ionic ones that derive from the contact of the petroleum with the frost in the tanks. Among these is sodium chlorite which is present in excessive quantities (more than 0.06 g / l) and causes the crude oil to be desalted before being refined. Specific metal porphyrins have also been found in the composition of petroleum, which at their centre can bind nickel or vanadium. Light oils usually contain smaller amounts of vanadium and nickel than heavier oils.

2.6.1 Classification and properties of petroleum

As previously described, the crude oil market characterizes crude oil according to its composition. There are therefore parameters that allow this classification **Figure 11**).

2.6.1.1 API gravity

The API gravity (American Petroleum Institute) is a parameter that indicates how heavy or light oil is compared to water. It indicates how much a petroleum liquid is more or less dense than another and emphasizes the small differences that would not be appreciated if only gravity was taken into account. The gravity API is expressed in degrees even if it is a dimensionless number and is measured using a hydrometer. The formula for calculating API gravity is:

$$\text{API gravity} = \frac{141.5}{specific\ gravity\ (SG)} - 131.5$$

where the specific gravity of the liquid is relative to that of water at 15.6°C. This identification, therefore, provides a precise indication of the quality of the crude oil. A crude oil that has API gravity equal to 10°, will have the same density as water. API values higher than 10° characterize a light crude oil; on the contrary, lower values (<10°) characterize extra heavy oils or bitumen. Light crude oil usually has API gravity greater than 31.1° while the one that governs the economic market has API gravity between 40-45°[58].

2.6.1.2 Viscosity

Viscosity is the parameter used to measure resistance to flow. The unit of measurement is the pascal-second or the centipoises (cp). A clear line that divides crude oil and tar sands is 10,000 cp. Below this value, we talk about petroleum and heavy oil while above bitumen, which usually reaches even 50,000 cp [36].

2.6.1.3 Carbon distribution

A further parameter to classify crude oil is the *n.d.M* method (*n* = refractive index; *d* = density; *M* = molecular weight). This method allows to determine the carbon distribution and therefore the % of aromatic carbon (% C_A), of naphthene (% C_N) and carbon in paraffin structures (% C_P) [59].
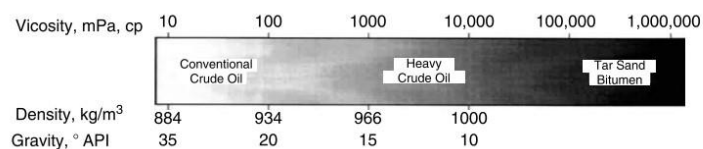
Figure 11: Petroleum classification according to viscosity, API gravity and density. Adapted from [36]

2.7 Extraction of Petroleum

Crude oil extraction requires planning. It is possible to divide the project cycle into four crucial phases: the search for hydrocarbons, the drilling of the well with any pipelines, the operation of the well and the territorial restoration. The processes described below refer to inshore crude oil extraction.

2.7.1 Search for hydrocarbons

The search for hydrocarbons begins with the location of the reservoir through seismic surveys to highlight any suitable geological structures. It starts with a reconstruction of the geological evolution of the area to understand if there are source rocks, at what depth they could be and if there are reservoir rocks that have allowed the accumulation of hydrocarbons [60]. **Traditional methods** evaluate the seismic response following underground and controlled explosions, in the vicinity of the investigated area selected through the study of surface topography and geography using technologies such as photointerpretation, remote sensing or digital cartography. The search for hydrocarbons is also supported by geophysical techniques such as **magnetotellurics prospecting** (MT), which uses low-frequency electromagnetic energy to evaluate the electrical resistivity of the soil. Through MT, it is possible to characterize the various types of rocks including reservoirs, which are highlighted by a low resistivity. The MT, therefore, allows defining the geotectonic structure of the subsoil also thanks to the generation of secondary electromagnetic fields that penetrate deeply. The result of the analysis is an association between the fluxes of the magnetic fields produced and the earth's electromagnetic field, reported in a frequency spectrum usually below 0.1 Hz called the magnetotellurics field. Finally, by carrying out series measurements, it is possible to cover a large area by detecting the rocky nature and any forming fluids based on their resistivity, discriminating intervals ranging from a few tens of meters to tens of kilometres [61]. A further methodology is a **geophysical survey,** which allows the discontinuity of the surfaces through special instruments. This occurs through the use of elastic waves and specific sensors that record how the waves propagate.

There are two types of detection, the refraction one and the reflection one, currently preferred because the quality of the images obtained is better and it is possible to obtain information not only on the localization but also on the geometry of the surfaces encountered by the elastic waves. [62].

2.7.2 Drilling of the well and construction of the adduct

Once all the information about the composition of the subsoil has been acquired, the construction of an exploratory well at the point where the geo-structural conditions highlight a potential accumulation site is carried out (**Figure 12**).

Initially, the ground on which the well will be built, is levelled, and the area is waterproofed by using a PVC sheet covered with gravel to separate and isolate the materials. Storage tanks where rainwater and plant washing waters are collected and suitable buried tanks to collect drilling muds and waste fluids are then built. In a lateral position to the well, a "torch area" is built to burn any hydrocarbons extracted, while in the centre of the identified area, the actual well is built [63]. The drilling initially involves overcoming the rock, which is crushed into small pieces and simultaneously removed, and preventing the entry of fluids present in the formations crossed inside the well. Several drilling rigs use two different drilling methods but the most used is the rotary one which uses a rotating chisel that is pushed against the rock. This technique is mainly used for low abrasive and particularly hard soils. The debris generated by drilling is removed using a muddy drilling fluid, which is circulated in a closed circuit from the bit to the surface. The sludge is produced by mixing water and specific additives that facilitate the escape of debris, creating a gelatinous substance which, however, balances the entry of fluids into the well through a hydrostatic load. Finally, if the exploration well confirms the presence of a reservoir, the installation of all the structures necessary for the extraction of the fluids from the subsoil proceed and the connection pipeline that connects the well with the nearest areas of first treatment of the crude oil (in some cases the extraction and treatment site is the same) are also installed [64].

Figure 12: _Drilling Ring_ composed by **1**= fixed side; **2**= derrick; **3**= pontist platform; **4**= mobile sides; **5**= hook; **6**= injection head; **7**= elevators; **8**= square rod or driving rod; **9**= drag bushing; **10**= broad bricks; **11**= storage hole for the square rod; **12**= storage hole for the rod to be connected; **13**= winch; **14**= battery weight indicator; **15**= workstation of piercer; **16**= booth of the perforator; **17**= hose; **18**= pressure accumulators; **19**= rod extraction corridor; **20**= slide; **21**= rod shelter rack; **22**= substructure; **23**= mud return pipe; **24**= vibrating screen; **25**= surface circuit for well control; **26**= gas-mud separator; **27**= degassers; **28**= reserve mud tank; **29**= mud tanks; **30**= sand removal equipment; **31**= silt removal equipment; **32**= mud pumps; **33**= mud delivery pipe; **34**= storage of materials used for sludge packaging; **35**=sludge preparation cabin; **36**= water tank; **37**= fuel tank; **38**= power generation plant; **39**= cable. Translated from [61]

2.7.3 Crude oil Extraction

Once the well begins its extraction, it can continue for 20 to 30 years, or until the revenues buy the costs of the operation. In the early stages, the "primary recovery phase" takes place, which involves the exploitation of natural phenomena for the crude oil spill. For example, groundwater may displace crude oil or associated gas expands and creates underground movements of crude oil that tend to rise upwards. During this phase, the recovery yield is extremely low and varies from 5 to 15%. Over time, however, the pressure from gas is created and more crude oil is not naturally pushed upwards. For this reason, the "secondary recovery phase" uses external liquids that are injected to increase the internal pressure.

Wastewater, gases and gases associated with carbon dioxide and anhydride can be reinjected [65]. From the secondary recovery, the yield increases to 30%, but with the "tertiary recovery phase" there is an improvement in the mobility of the crude oil. The thermally improved crude oil recovery techniques (TEOR) heat the crude oil reducing its viscosity and favouring its extraction. The TEORs increase efficiency by a further 15% but in some fields, the final recovery has doubled if not tripled [66]. As mentioned above, very often associated gas is also present in a crude oil field which can be economically advantageous. For the recovery of the gas there must be suitable structures which, however, are also very expensive, so if the quantities are not copious, it is disposed of differently. One solution is gas flaring, which is controlled combustion through the combustion torch on the head of oil towers. Another solution is gas venting, which involves the release of gas into the atmosphere, especially if the gas is rich in carbon dioxide and nitrogen [67].

2.7.4 Decommissioning

When the reservoir runs out, the well is closed, the permanent structures removed and the final territory restored. The closure of the well begins with the isolation of the production structures, the safety and cementation of the hole which takes place through the use of concrete plugs, the injection of mortar to close the layers crossed by the drilling, the use of mechanical plugs, the "bridge plugs", which are fixed to the lining column, and the injection of sludge to fill the free sections created between the concrete and mechanical plugs [63].

2.7.5 Territorial restoration

Following the mining closure of the well and the dismantling of the ancillary structures, surface drainage works to restore the original hydraulic conditions are put in place. The territory is also involved, in fact, in the agricultural areas the lands are brought back to the natural conditions of capacity and fertility, while green areas are restored to re-establish the composition of the original phytocoenoses [61].

2.8 Crude-Oil Refinery

A fundamental aspect to take into consideration is that crude oil, as it is, cannot be used for commercial purposes and therefore needs to be refined. The simplified refining process involves the crude oil being heated in a distillation column to vaporize and distil it into separate substances. The basic principle exploits the boiling temperature between the substances contained in the crude oil itself, in a specific crude oil distillation unit. The distillation column contains several tanks that allow the heated vapours to separate in a gradient that sees the temperature decrease towards the top of the column. This allows the different substances to condense and collect in their respective tanks. Generally proceeding from top to bottom, butane is first followed by primary distillation gasoline, naphtha, kerosene, diesel and heavy diesel. However, this process is extremely controlled to direct the distillation towards the most requested products. For example, since gasoline is one of the tops of production, there is a tendency to favour its production through the cracking process that converts heavy liquids (breaking the long hydrocarbon chains), into gasoline whose quality and quantity is regulated by a catalyst, through a series of reforming processes that reorganize the hydrocarbon bonds to obtain cleaner fuels. The crude oil, however, in addition to being distilled must also be purified from all contaminants such as sulphur, nitrogen and heavy metals that would cause problems in fuels. Through a process of hydro-treatment, the bonding of these molecules with hydrogen is favoured, which is then absorbed in special columns. However, if the entire process is analysed in more detail, refineries are large industrial complexes to which pipes, that travel even hundreds of kilometres, flow, have several distillation columns and multiple technologies are used exploiting ingenuity of professionals from different fields, such as chemistry, physics and engineering. There are several processing units in refineries that are distinguished by the methods applied. The **crude oil distillation unit** (CDU), described above in general terms, represents the first stage of the manufacturing process and provides for a first pre-heating stage during which the organic salts present are eliminated. The desalination process is very important as any residues could have a negative effect either in the subsequent distillation processes, for example by deactivating some chemical catalysts, or in the corrosion of the pipes. [68].

The CDU often consists of two distinct units: the atmospheric distillation unit (ADU), which operates at pressures slightly higher than atmospheric ones, and the

vacuum distillation unit [69] which improves separation by preventing product degradation and possibly the formation of polymers, by reducing the residence time in packed columns and not in tanks, by increasing the capacity, yield and purity of the product obtained [70]. It is of fundamental importance to keep the initial treatment temperatures under control. The crude oil must be heated to temperatures ranging between 370-380°C and that cannot be exceeded, in this phase, as otherwise the crude oil would undergo cracking and a sticky paste would form clogging the pipes and the column itself [71]. For this reason, vacuum is used to increase atmospheric pressure and the amount of vapour is increased in relation to a certain volume of distilled liquid. Subsequently the crude oil passes into a furnace where it is heated to about 400°C and enters the distillation tower. Once entered, the separation of the various by-products takes place as described above but the processes that follow this separation are multiple and simultaneous (**Figure 13**). The **hydrodesulphurisation** of the naphtha takes place in the head of the column in which the elimination of sulphur from the lighter fractions that have formed takes place. Desulphurisation is very important for the creation of naphtha by-products that are formed during **catalytic reforming** (increase in the octane number, an index of resistance to detonation) and to reduce the release into the atmosphere of sulphur dioxide which causes atmospheric contamination, acid and corrosive rains [72]. The next process is **alkylation** which uses an acid catalyst (sulfuric acid and hydrofluoric acid) to protonate alkenes, such as propane and butane. Through the formation of carbocations, isobutene is alkylated into a high octane product by the **fluid catalytic cracking** (FCC) unit, which is used to convert that fraction of crude that has a boiling point above 340°C or a medium / high molecular weight [36].
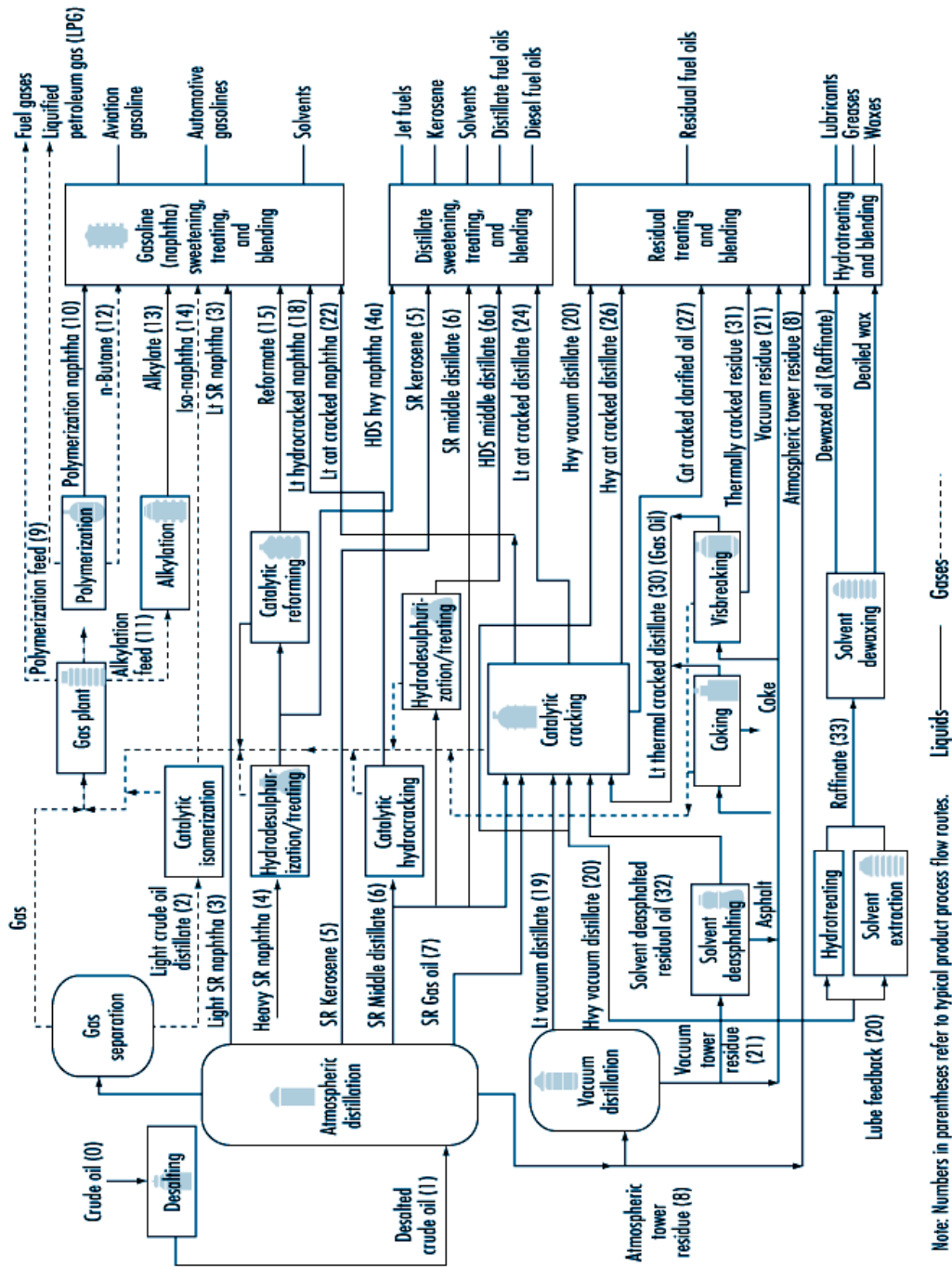
Figure 13: Schematic flow diagram of petroleum refinery [73]

When carbocations are formed, they can branch out by branched **isomerization**; furthermore, various molecules such as pentane are converted into branched molecules [74]. This step allows a refinery to reach a yield of 70% of gasoline. The heavier fractions undergo both the aforementioned fluid catalytic cracking converting them into lighter products and **hydrocracking,** which uses the presence of hydrogen to break the carbon-carbon bonds, forming saturated hydrocarbons [75].

The **visbreaker** unit reduces the amount of residual crude oil by increasing the yield of medium products such as diesel and fuel oil, thermally breaking large hydrocarbon molecules [36]. Finally, the delayed coker unit converts the residual oils into end-product petroleum coke or bitumen, bringing them to the temperature of thermal cracking in several parallel ovens [76].

2.9 Contamination, disasters and environmental impact

As described in the previous paragraphs, since its discovery, crude oil has represented not only a source of technological innovation for its application in various energy and/or industrial fields but has governed and still governs the global economy today. The race for the crude oil monopoly, however, has led not only to war conflicts but also to an increase in global pollution, which, in the last 70 years, has reached all-time highs. All the crude oil processing steps, starting from exploration to transport, release pollutants that are dispersed into the air, water and soil [77]. The crude oil composition also makes it one of the major pollutants as several molecules contained within it are capable of causing damage. Oil industries need to monitor all processes to ensure that no spills and/or leaks occur, but this is not always the case. The crude oil disasters with the greatest environmental and media impact are those that occur in the ocean due to crude oil tankers that, for any type of accident, pour tons of crude into the water, but also those that directly involve the off shore extraction sites. The first disasters date back to 1911 when the Lakeview Gusher, a drilling platform in California, in the San Joaquin Valley, spilt 9.4 million barrels for 18 months peaking at 125,000 barrels/day on American soil. [78]. Between the 50s and the 80s of 1900, there were numerous accidents all over the world, but in 1989 the Exxon Valdez, a US crude oil tanker, ran aground in an inlet of the Gulf of Alaska (Prince William Strait), dispersing at sea, only a week after the accident, 17,750 tons of crude oil [79]. In 1991, in the Mediterranean Sea, the supertanker Haven was wrecked following a serious explosion on board, in the Gulf of Genoa. The explosion, in turn, caused the fire of the fuel carried by ship itself which spilt onto the surface of the sea. The ship after days of explosion sank between Genoa and Arenzano, releasing 144,000 tons of crude oil into the water, of which 90,000 were burned.

The Haven had several sister ships which were previously used in different parts of the world, spilling more than 300,000 tons of crude oil in total. [80]. The Deepwater Horizon (DWH) was a crude oil platform that completed the drilling of the Macondo well in the Gulf of Mexico, the deepest in the world, about 10,000 meters long. On April 20, 2010, a terrible explosion on the platform resulted in the deaths of 11 people. The tragic event continued until two days after the explosion, the platform sank, breaking the safety valves of the well which allowed the crude oil to rise to the surface, pushed by the strong pressure of the field. The crude oil released was a light, sweet crude oil with a low level of sulphur and a high level in kerosene fraction [81]. Only after 86 days and 5 million barrels of crude oil spilt, British Petroleum (BP) was able to cement the leak in the well. Losses peaked at 1552 x 10^7 L/day covering a total area of 62,159 km^2 [82] (**Figure 14**), which, after 100 days, was dissolved by a tropical storm. The efforts applied to remedy the damage were varied, in fact, initially, as mentioned, submarine vehicles tried to close the safety valves, but at the same time, it was necessary to try to clean up the sea surface. This was done using floating platforms that sucked the crude oil that rose to the surface, burning 260,000 barrels *in situ*, and through the use of chemical dispersants to favour the precipitation of the crude oil [83]. It is not uncommon for natural oil losses to occur in nature, and in fact, compounds with low and medium molecular weight remain on the surface of the water, volatilize or are degraded over time, while compounds with heavier molecular weight tend to settle. Crude oil is made up of more than 17,000 compounds with different volatilization (VOCs: Volatile Organic Compounds and BTEX: Benzene, Toluene, Ethylbenzene, and xylene), density and solubility. VOCs make up about 15% of crude oil while polycyclic aromatic compounds (PAHs), present at about 10%, represent the most toxic and harmful fraction of crude oil [84]. Several studies have analysed the long-term effect of the spill in the Gulf of Mexico, highlighting, for example, how PAHs already present at low concentrations in the crude oil deriving from the Macondo well, were not found on the surface of the water but in coastal water; this was also favoured by the use of 2 million gallons of Corexit® (composed mainly with dioctyl sodium sulfosuccinate (DOSS)) which helped precipitate crude oil in the depths of the sea [85]. The use of dispersants also favoured the solubilisation of some compounds during physical transport from the accident site to the coasts, especially on the beaches of Alabama where, even after 3 years from the accident, tar balls were found.

This allowed to elaborate a sort of "fingerprint" of the crude oil extracted from the Macondo well since each crude oil, has a unique and specific set of biomarkers of hopane and sterane based on the composition of the geological conditions following which it was formed [86,87].
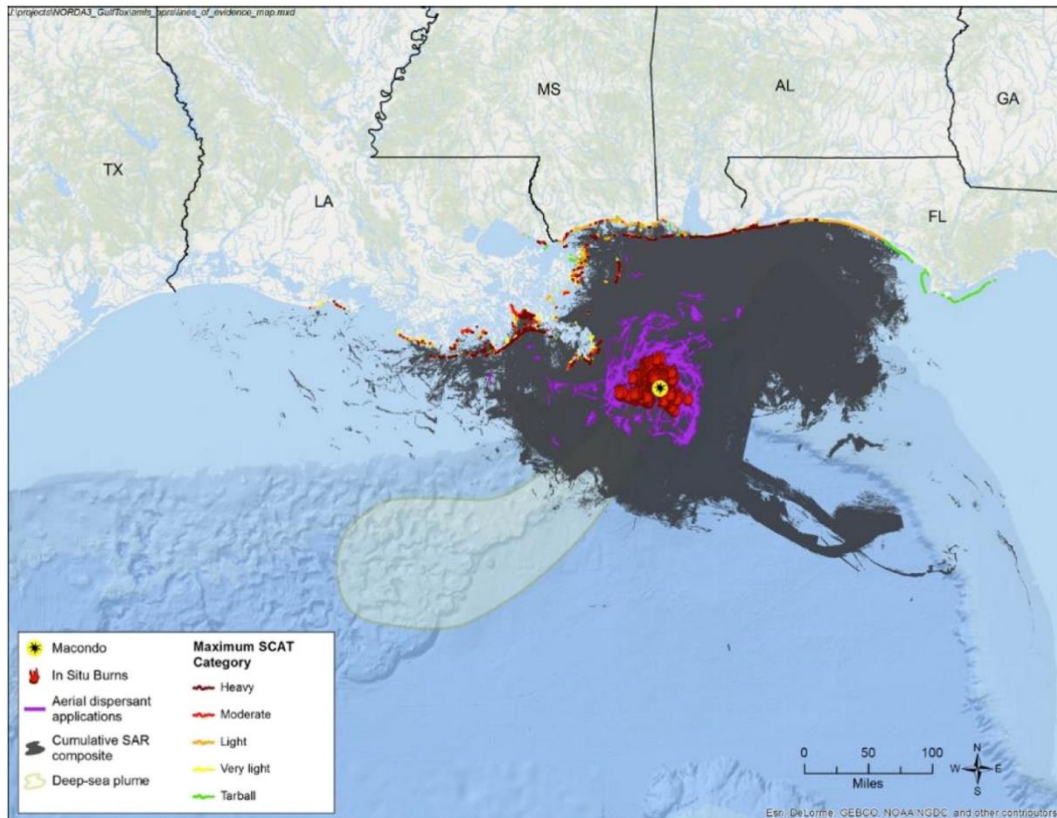
Figure 14: Maps of the DWH crude oil spill in Gulf of Mexico [81]

To analyse, in detail, the fate and, therefore, the environmental repercussions of the crude oil spill, it is necessary to consider that the nature of the crude oil itself is of fundamental importance. As previously mentioned, the crude oil extracted from Macondo is a light and sweet crude, with a lower density than saltwater. Considering the high pressure, following the accident, the crude was physically dispersed in microscopic particles causing its dispersion. The large drops rose more quickly to the surface while the smaller ones, having a neutral buoyancy, remained in the water column, even at great depths (1,200 meters) (**Figure 15**). In the plume, which extended for 13 km from the wellhead, PAHs were found at a toxic concentration for marine organisms (greater than 189 μg / L (ppb)) while 40% of the dispersants used were poured on the head of the well on the ocean floor [88].

However, this practice was not at all safe, as the concentrations of dispersants found near the wellhead exceeded 200 μg / L while the subsurface samples remained below the safety levels established by the US. EPA (40 μg / L) [89].
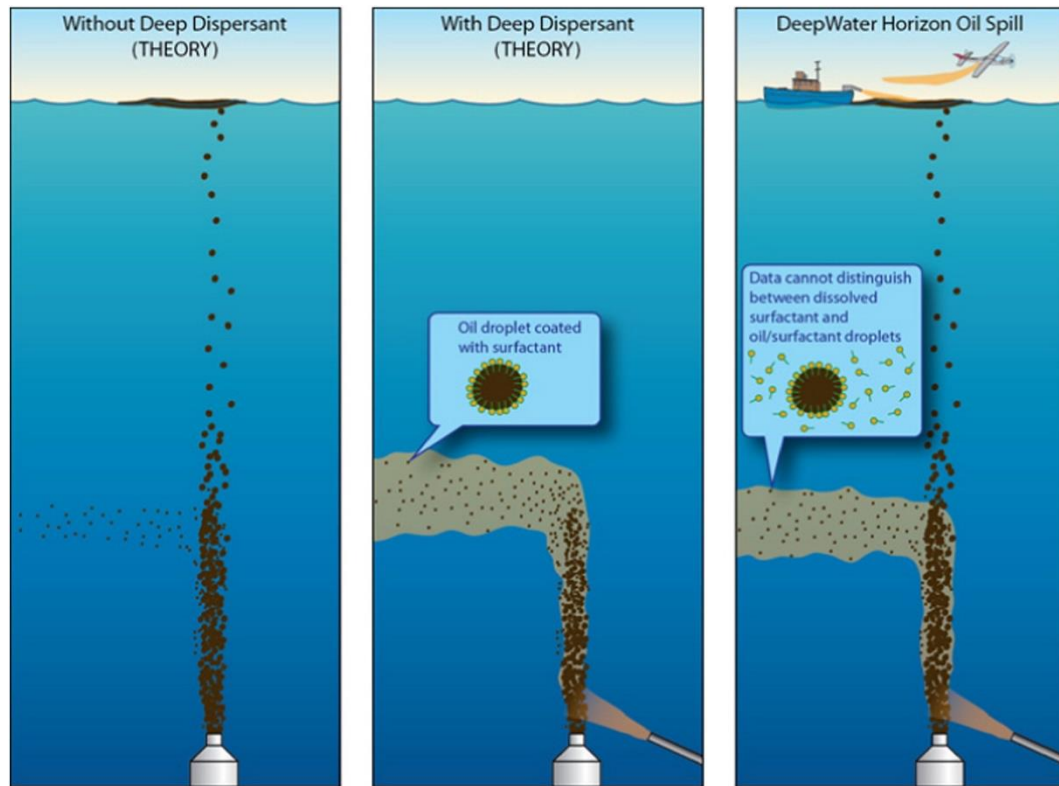
Figure 15: *Hypothetical scenarios of crude crude oil dispersion applying oil dispersant.* [81]

Less than 15% of crude oil has landed on Gulf coasts despite the high water temperature, the high depth of the leak, the massive use of dispersants, the burning of the surface crude oil, and the microbial action to remove the crude particle. The consequences have been greatest for marine flora and fauna such as plankton, invertebrates, fish [90], marine mammals and seabirds. All these organisms have shown reduced growth, the onset of various diseases, reduced reproductive capacity and high mortality, with consequent repercussions on the balance of different habitats and ecological functions. The conditions of several animals that populate the coasts of the Gulf were dramatic, including sea turtles, dolphins and various cetaceans that, immediately after the accident, were overwhelmed by the wildfire that caused physical damage. But also the compromising of the seabed and phytoplankton has had no less important long-term effects [81].

Following monitoring analyses carried out for seven years after the accident, significant damage was found in coral colonies that have lost numerous branches and will take many years to recover from the damage caused by the crude oil and the chemical compounds used to recover it [91].

2.10 Remediation techniques

As a result of a crude oil spill in water, as previously described in section 2.9, there are several procedures that involve different physical and chemical treatments, and have the objective of removing the crude oil as quickly as possible.

2.10.1 Physico-chemical processes

Initially, climatic factors trigger degradation processes, known as "weathering", which modify the composition of the crude oil thanks to the action of oxygen, water, solar radiation and naturally present microorganisms. The actions of atmospheric and natural agents are very rapid and tend to reach thermodynamic equilibrium. Usually, different phases that are not necessarily consequential to each other constitute degradation processes (**Figure 16**) [92]

2.10.1.1 Spreading

Based on the viscosity, the crude oil spot expands in an inversely proportional and non-homogeneous manner. Atmospheric conditions such as wind and surface sea currents tend to disperse and fragment the accumulation areas. The formed crude particles can create a thin layer (sheen) or strips (windrow) on the water surface that follows the air currents [93].

2.10.1.2 Evaporation

Low and medium molecular weight compounds (benzene, toluene and xylene) are very thick volatile compounds that evaporate quickly. The dispersion process of volatile compounds is influenced by temperature, wind speed, and the quantities of crude oil poured out. The concentrations are usually reduced considerably after the first six hours [94].

2.10.1.3 Emulsification

The sea currents create emulsions of crude oil in water and of water in crude oil thanks to the action of the waves. The problem related to the formation of emulsions is that these increase the volume of the polluting mass and slow down the dispersion, causing the crude to stabilize and last longer. [92].

2.10.1.4 Solubilisation, sedimentation and photoreactions

All the soluble components of petroleum are released into the water column, facilitating the dispersion process [95]. However, it happens that the crude oil can thicken and join with sand or other suspended solids, which lead it to settle on the seabed even after its deposit on the coasts. [96]. Solar radiation can act on crude oil by oxidizing it, decomposing it and polymerizing it, generating products that can vary according to the composition of the crude oil.
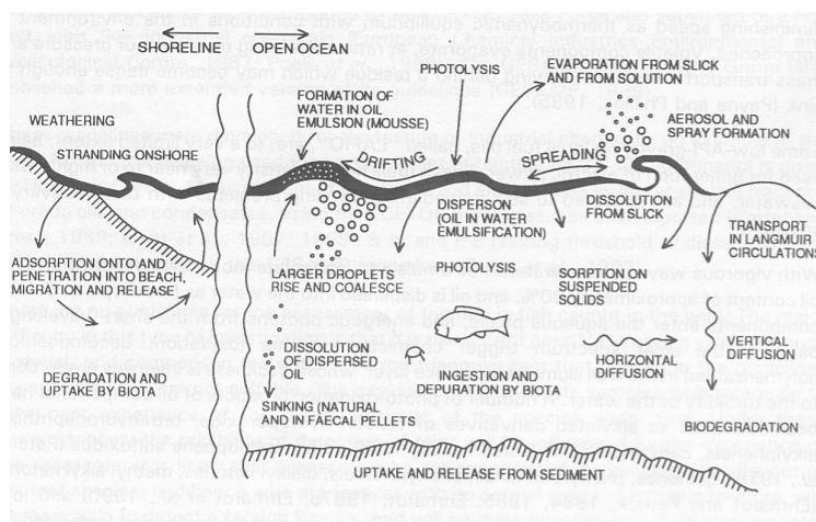
Figure 16: Physico-chemical processes [97]

2.10.2 Bioremediation

The methods, described above, blend synergistically with the action of microorganisms present in the marine environment, which can degrade the spilled hydrocarbons. Since hydrocarbons are molecules found in the environment for millions of years, evolution has led to the selection of microorganisms capable of using them as the principal source of carbon and thus energy.

There are 175 genera of bacteria, many archaea and some eukaryotic, that can grow in the presence of hydrocarbons and transform them [98]. The bioremediation process is complex; it requires numerous steps but it is a synergistic work between different species that can remove hydrocarbons. However, the remediation capacity varies according to the presence of the hydrocarbons themselves, the temperature and the nutrient concentrations. Generally, different genera intervene in the early stages of biodegradation. The *Oceanispirillales* (class gammaproteobacteria; phylum proteobacteria) order, and specifically the genre *Alcanivorax spp,* intervenes in the first phase when the quantities of n-alkanes and cycloalkanes are particularly high, degrading straight-chain and branched alkanes [99]. In this phase, various metabolic pathways are active because the *Alcanivorax spp.* almost exclusively use alkanes as an energy source, using different hydrolases (a non-haem diiron monooxygenase AlkB1 and AlkB2) and three cytochrome P450-dependent alkane monooxygenases [100]. Furthermore, having to survive even in the presence of ultraviolet light and having to search for nutrients, the gammaproteobacteria activate special monooxygenases capable of binding the flavin (AlmA), which allows them to use long-chain n-alkanes C_{22} and C_{36} [101]. *Cycloclasticus spp.,* *Colwellia* and *Pseudoalteromonas* (class gammaproteobacteria; phylum proteobacteria), instead, degrade aromatic hydrocarbons when, in a second phase, they are found in larger quantities [102,103]. Volatile hydrocarbons, such as propane, and ethane play a fundamental role as if present in the depths of the sea, they can contribute to 70% of the oxygen consumed in the fresh plume. The activation of microorganisms, in this case, stimulates the microbial populations present in the oldest plum (second phase) [104]. Even exopolymeric by-products are eliminated by heterotrophic bacteria that have a greater peptidase and hydrolytic activity than the microbial community present in uncontaminated waters; for example in the case of the Deep Water Horizon, *Halomonas* bacteria produced exopolysaccharides which increased the solubilisation of aromatic hydrocarbons, improving their biodegradation and the formation of aggregates [105]. However, the lack of nutrients decreases in proportion to the increase in bacterial biomass, and, for this reason, especially on the coasts, fertilizer (uric acid) containing sulphur is added to improve biodegradation. The growth of biomass is also an indicator of good degradation; many hydrocarbons may be converted into biomass especially in-depth where the lack of nutrients is less. However, the biodegradation process also has a negative side. The consumption of hydrocarbons by microorganisms

causes high oxygen degradation. In this way, other live organisms present in the marine habitat haven't enough oxygen to survive; methanotrophic bacteria also release methane into the atmosphere. All marine microorganisms, not just bacteria, cooperate for the degradation of hydrocarbons, both phytoplankton and zooplankton. The result of good biodegradation is the formation of agglomerates which tend to settle on the seabed. This marine "snow" is rich in crude oil and is formed thanks to the production of oily particulates and the coagulation of phytoplankton with embedded oil droplets [81]. Several studies have shown that the bacterial genes responsible for motility, chemotaxis and degradation of aliphatic hydrocarbons are more expressed near an crude oil leak. The whole biodegradation process is favoured by the marine currents which continuously mix the spilt hydrocarbons, favouring bacterial blooms and accelerating degradation [106]. Several studies carried out near the various marine environmental disasters have shown that even at low temperatures, about 10-16 °C (as opposed to DWH where temperatures were higher), the action of indigenous microorganisms plays a fundamental role. In this case, the presence of nitrogen and phosphorus supported the growth of degrading microorganisms [107].

2.11 Effect on human health

By definition, a compound is toxic when it generates an "abnormal response" in healthy organisms, which may include either a behavioural, reproductive or physiological modification; the toxic effects vary according to the type and duration of exposure [92]. Crude oil according to Regulation (EC) no. 1272/2008 and subsequent updates is classified as (**Figure 17**):

- Flammable liquid - Category 1
- Aspiration toxicity – Category 1
- Serious eye damage / eye irritation – Category 2
- Germ cell mutagenesis – Category 1B
- Carcinogenicity – Category 1B
- Specific target organ systemic toxicity (single exposure) – Category 3
- Specific systemic toxicity for some target organs (repeated exposure) – Category 2

- Chronic toxicity to the aquatic environment – Category 2

Figure 17: Labelling in accordance with Regulation (EC) no. 1272/2008

Based on the technical datasheet, it is possible to understand how the worst effects of direct contact with crude oil involve different organs. Prolonged or repeated skin contact can cause dryness or irritation but studies show no skin corrosion. Direct contact with the eyes, on the other hand, causes irritation and reversible damage. In both cases, burns can occur if the crude oil is hot or burning. Greater risks happen if inhalation occurs, and it can cause intoxication by hydrogen sulphide (H_2S) that causes olfactory paralysis and hinders its perception, leading the individual to lose consciousness up to death in the rarest cases. Finally, ingestion irritates the digestive system with the risk of central nervous system depression. Aspiration can cause pulmonary oedema and pneumonia. Benzene is a constituent of petroleum that is also carcinogenic to the skin [108]. The toxic effects of crude oil are not related only to direct contact, but they are also related to all the extraction and processing processes [109]. Both VOCs and PAHs pose a problem for human health, as they can be inhaled, ingested or come into contact with the skin. The most dangerous VOCs for human health (**Figure 18**) are the so-called BTEX (Benzene, toluene, ethylbenzene and xylene) and given their high volatility, they do not cause problems only in the vicinity of crude oil extraction and processing centres; in fact, the VOCs are one of the principal causes of global warming, producing ozone (O_3), interacting with nitrogen oxide (NOx) in the atmosphere and helping to form the tropospheric ozone [110]. As indicated by the safety data sheet, benzene is classified as carcinogenic compound, which can cause leukaemia, haematological diseases, vascular disease, and have effects on the central nervous system causing dizziness, nausea and headaches. Prolonged exposure to benzene can cause

genotoxicity, chromosomal aberrations, reproductive problems and death. The effect of exposure to benzene in Texas near a refinery caused severe haematological disorders in children in the area with a reduction in white blood cells, haemoglobin and thrombocytopenia [111]. On the other hand, ethylbenzene, considered potentially carcinogenic, causes eye and respiratory tract irritation if exposure is short; long-term exposure causes severe kidney damage. Toluene, not considered carcinogenic, causes headache and dizziness on direct contact, and effects are much more serious as it can cause permanent loss of vision, mental retardation and multi-organ disorders in the kidneys, liver and immune system if exposure is continuous. Long-term xylene can also cause kidney and liver damage [112].
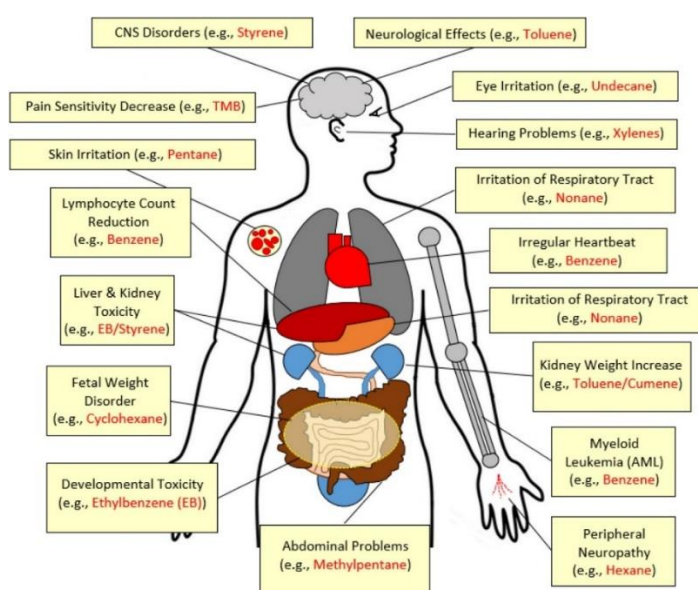
Figure 18: Effect of VOCs on human body. Adapted from [112]

CHAPTER 3: MICROALGAE

Microalgae are unicellular, microscopic, photosynthetic and photoautotrophic organisms. They produce oxygen and biomass using carbon dioxide and sunlight. As exhaustive as it may seem, this definition is extremely generic as microalgae vary in evolutionary and metabolic classification; the term "microalgae" describe a form of life and not a taxonomic unit [113]. Historically, algae and microalgae were known for their nutritional value and their hazard in relation to toxic compounds produced such as phycotoxins and spirolides (SPXs) [114]. People from Asia, Aztecs and Egyptians have reported the use of algae as functional foods, while post-

medieval documents report how algal blooms in the Caribbean created problems for the first Spanish explorers. Microalgae are a large heterogeneous group that has evolved over the last 2500 million years: they occupy different ecological niches, grow on different soils (e.g. sandy, muddy), and make up phytoplankton and photo-benthos present in aquatic, sweet, salty environments and in brackish waters (microalgae founded in watercourses at 200-300 m high) [115]. Approximately 41,000 species of microalgae are known that have been distinguished, over time, through the use of microscopy (morphological characteristics) and increasingly sophisticated molecular techniques, highlighting evolutionary differences. Microalgae can be divided mainly into two domains: eukaryote and bacteria, also including cyanobacteria [116].

3.1 Classification

The classification of microalgae is made up of four main groups. The first group includes prokaryotic algae to which only *cyanobacteria* (blue.-green algae) belong, the second (The Archaeplastida), the third, and the fourth eukaryotic group includes algae that are characterised by double chloroplastic membrane, single chloroplastic membrane and endoplasmic reticulum, or double-membrane chloroplastic and endoplasmic reticulum [117] .

3.1.1 Group one: Cyanobacteria

Cyanobacteria, also known as blue-green algae, are the only prokaryotic microalgae. They mainly contain photosynthetic pigments, chlorophyll α, phycocyanins that give them the characteristic bluish colour, phycobiliproteins, and they use glycogen as energy storage. They represent the most archaic photosynthetic organisms, the first to produce oxygen on Earth more than 3.5 billion years ago. Cyanobacteria exist as cellular organisms but can group into trichomes that, if enclosed in a sheath, take the name of filaments and can be more or less complex [118,119]. Their morphology is very varied but, there are common structures, including the cell wall made up of peptidoglycan on the outside, periplasmic space and cell membrane inside (making them similar to Gram-negative bacteria) (**Figure 19**).
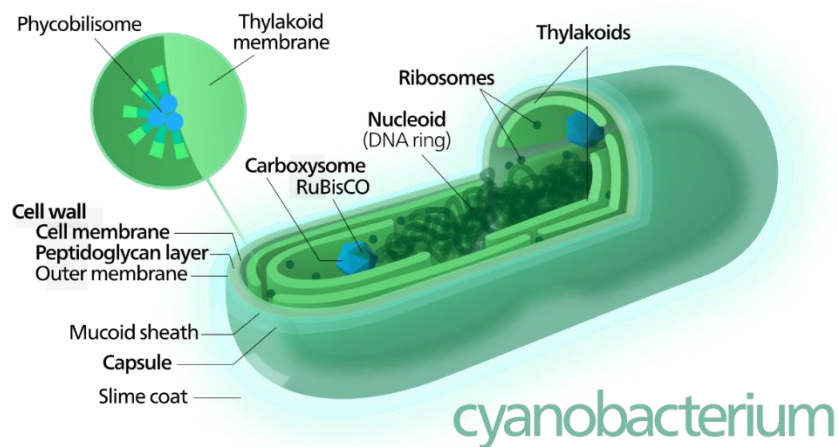
Figure 19: Cyanobacterium diagram [120]

They can have piles, of different lengths, on their surface that allows cells to move or make connections with neighbouring cells. Often in cyanobacteria, there is an extracellular polymeric sheath (EPS), formed by mucilage and, sometimes, by polysaccharides, which protects the cells from drying and allows the cyanobacteria to survive, in the most disparate territories, even in the most hostile conditions [121]. The central protoplasm contains nucleic acid, formed by circular DNA not associated with proteins. The peripheral protoplasm, on the other hand, is mainly composed of thylakoids and phycobilisomes. Ribosomes are distributed throughout the cell concentrating around the nucleoplasm.

Cyanobacteria can be nitrogen-fixing and accumulate nitrogen thanks to cyanophycin (**Figure 20**); this makes them very important in the ecosystem because they produce the combined nitrogen required by other organisms. In cyanobacteria that do not fix nitrogen, nitrogen is accumulated in the phycobilisomes. Ribulose-1,5-bisphosphate carboxylase/oxygenase (Rubisco) is an enzyme that fixes carbon dioxide within carboxysomes, which can be of two categories (α and β). α-carboxysomes are found in cyanobacteria living in carbon-rich waters, while β-carboxysomes in low-carbon waters [122].
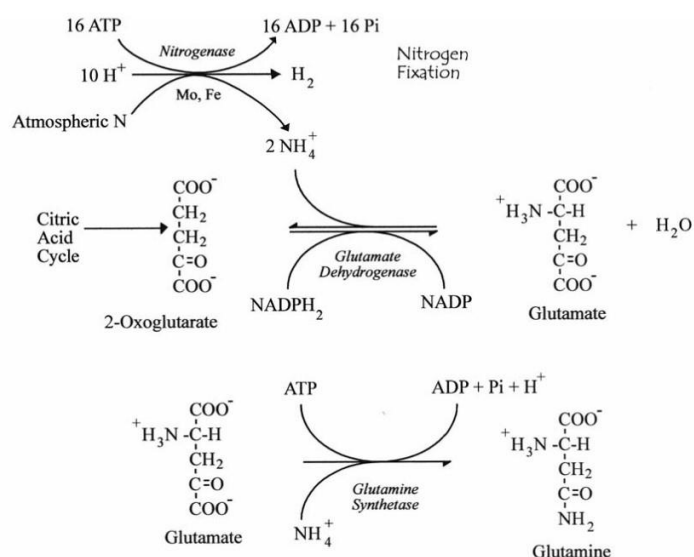
Figure 20: The chemistry of nitrogen fixation and the subsequent incorporation of the fixed nitrogen into glutamate and glutamine [117]

.

3.1.2 Group two: The Archeaplastida

Glaucophytae is an eukaryotic algae with endosymbiotic cyanobacteria in their cytoplasm, called cyanelles or cyanoplasts. Two membranes surrounded the cyanelles, one external and one internal that containing Rubisco. Glaucophyta produce oxygen through photosynthesis, contain free circular DNA, and also phycobiliproteins and chlorophyll α, the principal photosynthetic pigment [123]. They can be both non-flagellated and bi-flagellated [124]. **Rhodophytes** are known as "red algae" due to particular pigments such as biliprotein, phycoerythrin, blue phycocyanin, and chlorophyll α They are found mainly in marine aquatic environments and are for the most part macrophytes; only a few species are considered microalgae [125].

Rhodophytes have different morphological forms and are non-flagellated. Plastids have two outer membranes and contend for the characteristic pigments described above, and their thylakoids are single with phycobilisomes on the surface. Rhodophytes contain two peculiarities: a chlorophyll-binding protein α / β (CAB) similar to green algae and a particular form of starch (floridean starch) which accumulate in the cytoplasm [126]. Eight classes form the **Chlorophyta** phylum: *Brypsidophyceae*, *Pedinophyceae*, *Pleurastrophyceae*, *Trebuxiophyceae*, *Prasinophyceae, Ulvophycae, Charophyceae* and *Chlorophyceae*. In particular, the algae belonging to the *Ulvophyceae* and the *Charophycea*e are generally macro-algae that live in freshwaters. The *Prasinophyceae* class is formed by unicellular

microalgae (10-15 μm in diameter), covered with organic scales of which 120 species are known and divided into 13 genera. The *Trebuxiophyceae* class is unicellular, filamentous or lamellar microalgae, adapted to live both in fresh water and in the sea. About 746 species of this class are known, among which those of high biotechnological interest, belonging to the genus *Chlorella* [127]. The *Chlorophyceae* are the largest group, of which about 2,500 species exists and are divided into 350 genera. Most of the members of this group have unicellular and filamentous forms, live mainly in fresh water and are capable of producing useful compounds such as carotenoids (carotene or astaxanthin). Among the most known and used algae, there are *Chlamydomonas* and *Haematococcus* [128]. *Chlorophyceae* have a cell wall consisting mainly of cellulose but also other polysaccharides such as xylans or mannans. In some families, such as Volvolcaceae, the cell wall contains glycoproteins. The main pigments involved in chlorophyll photosynthesis are chlorophyll α and β, but numerous others are also present. The chloroplasts are surrounded by a double membrane not associated with the endoplasmic reticulum and, for this reason, this phylum belongs to the archeaplastids. In chloroplasts, starch (composed of amylose and amylopectin) is formed and accumulates in a pyrenoid, a protein complex involved in carbon fixation and starch formation; it is present usually one per plastid. The photosynthesis carried out by the Chlorophyceae is identical to that made by the higher plants. They contain a contractile vacuole and are flagellated (**Figure 21**) [117]. Chlorophyceae will be describe in detail in section 3.2.
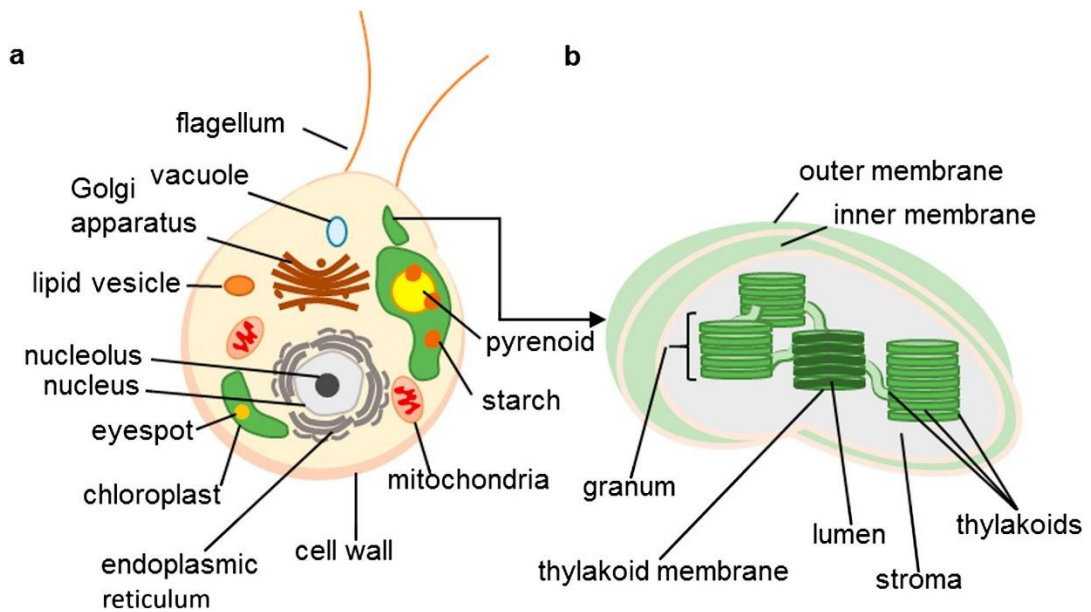
Figure 21: Chlorophyta (a) and chloroplast (b) diagram [129]

3.1.3 Group three: Euglenophyta and Dinophyta

A single membrane surrounds the chloroplasts of the endoplasmic reticulum, and characterises the third group. **Euglenoids** belong to the third group and live in salty, sweet and brackish aquatic environments. They usually contain chloroplasts, are large, fusiform, flagellated, and their metabolism can be photoautriotic, mixotrophic or heterotrophic. At the centre of their cells, there is an eyespot that characterizes them, consisting of 20-50 red/orange lipid drops containing mostly α-carotene, xanthophylls, β-carotene and derivatives [125]. Euglenoids, therefore, contain chloroplasts surrounded by a double membrane and chloroplasts of the endoplasmic reticulum surrounded by a single membrane. Chloroplasts are circular and contain thylakoids. Paramylon grains, containing β-1,3 linked glucan, surround the pyrenoid [117]. **Dinoflagellates**, or Dinophyta, include photosynthetic species and endosymbiont species of small invertebrates, cause harmful blooms and produce dangerous toxins for humans (saxitoxin or okadaic acid). Their nucleus, dinokaryon, contains chromosomes condensed throughout the cell cycle, adhered to the nuclear envelope and made up of a strange nitrogenous base, hydroxymethyluracil [130]. Dinoflagellates are single-celled organisms with two flagella, one transverse and one longitudinal. Below the cell membrane, there is a vesicular layer called amphiesma, and in addition, an external theca may be present. In order to incorporate the prey through the groove formed by the transverse flagellum, cells use plasmalemma present under the theca [125] (**Figure 22**).

Dinoflagellates also have a particular peridinin pigmented plastid surrounded by three membranes and contain a particular Rubisco much more sensitive to oxygen, which carries out photosynthesis [131]; contain chlorophyll c, in addition to chlorophyll α. Chlorophyll α and peridinin together form a water-soluble compound called peridinin-chlorophyll α-protein (PCP) [117]. Dinoflagellates are famous for marine bioluminescence and photoluminescence, caused by the presence of luciferin inside the cells, which is oxidized into tetrapyrrole by luciferase, releasing light [132].
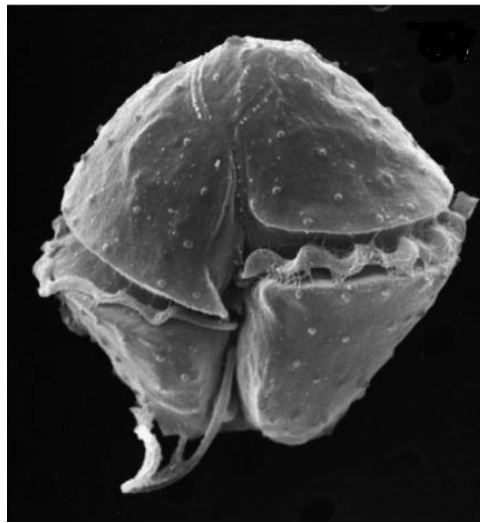
Figure 22: SEM of a cell of Dinoflagellate [125].

3.1.4 Group four: Cryptophytes

The fourth group includes all algae with chloroplasts surrounded by four membranes of chloroplast endoplasmic reticulum. In **Cryptophytes**, for example, the outermost membrane is a continuation of the endoplasmic reticulum and is connected to the outer membrane of the nuclear envelope. The plastids of the Cryptophytes show many similarities with those of the Rodophytes, but the pigments are different; the Criptophytes contain chlorophyll c2 and phycobiliproteins with different α-subunits that accumulate in the thylakoids [125]. They are flagellated organisms with a periplast composed of plates placed under the plasma membrane. Characteristic is the nucleomorph, a structure that contains paired chromosomes that code for about 30 genes.

A nucleomorph surrounded by the envelope, as mentioned previously, has pores and has an internal division that exploits structures similar to microtubules. The thylakoids contained in the chloroplast are pair, and this feature is unique to Cryptophytes. The major carotenoid is α-carotene, and the main xanthophyll is diatoxanthin. Phycobiliproteins accumulate in the intra-thylakoid space, and the presence of phycoerythrin excludes that of phycocyanin and vice versa [117].

3.2 General morphological green micro-algae composition

In this thesis, green microalgae belonging to the class of *Chlorophyceae* (see section 3.1.2 for classification) will be specifically analysed. Green microalgae have a cellular organization very similar to that of higher plant species, and biochemical and ultrastructural similarities highlight how green algae can be considered "ancestral" to land plants [131]. A **cell wall** (not always present) and a **cell membrane** enclose the cytoplasm; a **nucleus** contain genome organized in chromosomes that condense during cell division [133]. Several organelles are suspended in the cytoplasm, and are listed below. The **Golgi apparatus** re-processes and selects the products of the endoplasmic reticulum and completes the formation of cellular biomolecules. The **endoplasmic reticulum** is a system of endomembranes where the synthesis and transport of proteins and other important cellular components take place. **Mitochondria** are the place of cellular respiration to obtain ATP essential for the vital activities of the cell. **Ribosomes** are the places where protein synthesis occurs, while the **eyespot** or stigma is a photoreceptive organelle capable of perceiving the direction and intensity of light and determining phototaxis (positive or negative) by moving the cell towards optimal lighting conditions [117,134]. Others cellular structures are described in more detail below.

3.2.1 Cell Wall

Microalgae as unicellular organisms, do not need cytoskeletal structures to have support, but they need protection against osmotic variations that could occur in the aqueous environment in which they live. For this reason, some species of green microalgae have a very rigid cell wall (12-36% total cell mass) (**Figure 23**), called primary wall, which gives them rigidity and support, consists mainly of cellulose

arranged in regular layers and contains sulphated glucuronoxylorhamnans (ulvans) and other sulphated glycans [135]. In addition to the primary wall, microalgae can have one or more external envelopes characterized by different compositions. Some species do not have any structure similar to a cell wall or some species have only a glycoproteic wall [136]. The major algal wall components studied are carbohydrates, including mainly cellulose, hemicellulose and neutral sugars; the latter distribution is species-specific, and the percentage of proteins can vary between 1% and exceed 30% w / w for some species [137]. Some species during their life cycle develop an extremely resistant biopolymer placed in trilaminar sheets (TLS) called algaenan [138,139]. **Algaenan** is a non-hydrolyzable aliphatic compound, little branched and with a high carbon content [140]. The principal constituent elements of algaenan are mono or polyunsaturated C30-34 carbon chains of hydroxyl fatty acids (i.e. long chains of carbon and hydrogen atoms with one or more $C = H$ double bonds, a final carboxylic -COOH group and one hydroxyl –OH) held together by ether and ester bonds, which contribute to forming an extremely resistant structure [141].
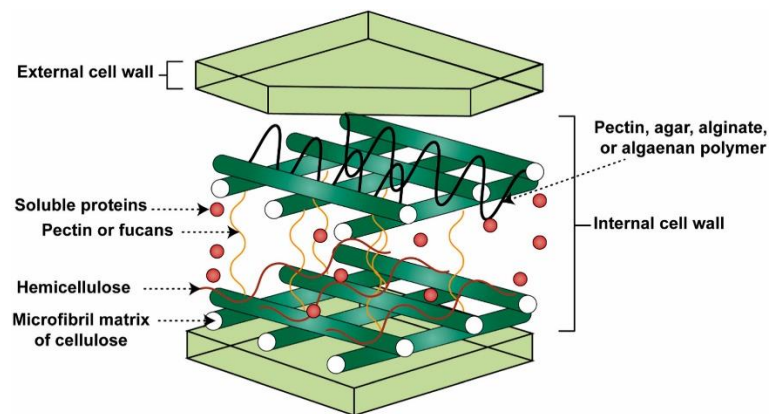
Figure 23: *Typical microalgae cell wall* [142]

3.2.2 Vacuoles

Many green algae contain non-contractile vacuoles whose function was unknown for years. Studies on *Chlamydomonas* have shown that non-contractile vacuoles guarantee turgor to cells and provide storage of cellular waste, as in higher plants. Contractile vacuoles are present and discharge their contents outside the cell.

There are also other intracellular granules called volutin or metachromic granules, which act as storage containing polyphosphate. The presence of polyphosphate requires a proton pyrophosphatase and an acid phosphatase which would have the role of degrading plastic proteins within the granules that represent a lytic compartment [143].

3.2.3 Chloroplasts and Pirenoids

Plastids are eukaryotic organelles, and they play a central role in cellular metabolism. Plastids carry out photosynthetic processes, metabolizing lipids, amino acids and assimilating nitrogen; it is possible to find them within plant cells and green microalgae following events of primary and secondary endosymbiosis [144]. Plastids can be defined as semi-autonomous organelles as they have retained a complete mechanism of protein synthesis and sufficient genetic information to encode approximately 100 of their 2,500 proteins. Furthermore, they are capable of dividing by fission before cytokinesis and are equally distributed among daughter cells. In different organisms, many plastids are present (central, lenticular, parietal, unique or variously perforated, cup or star-shaped). They can play multiple roles (Amyloplasts, Chromoplasts, etc.), and can reduce carbon by constituting the site of carbon oxidation through photorespiration, and the site of synthesis of chlorophylls, carotenoids, α-tocopherol, various vitamins (E and K), lipids (leucoplasts), amino acids and nitrogen metabolism [145]. If plastids carry out photosynthesis, they are called chloroplasts. **Chloroplasts** morphologically have a more complex organization, formed by a system of both external and internal membranes (thylakoid membranes) immersed in a stroma. The number of external membranes of the chloroplast varies from species to species, as described in the classification of microalgae, and by the probable endosymbiotic events that have occurred; the number of chloroplasts per cell is also varied and usually quite low. Chlorophytes, for example, contain only one chloroplast associated with a pyrenoid [124]. Usually, the chloroplast is considered only as an energy supplier but has its division cycle influenced by light and contains 30% of the total RNA of the cell and about 15% of the total DNA. Since microalgae can have different types of metabolisms, in the autotrophic type the chloroplast supports all the photosynthetic activity for its survival and that of the cell itself by producing energy and assimilating carbon.

The DNA of the chloroplast is contained, in part, in the nucleoid: structures placed at the border of the membrane of the chloroplast; however, the nucleus of the cell encodes most of the chloroplastic proteins and for this reason, it is necessary that the chloroplast work intensively to support its growth, in a mechanism of interdependence. This mechanism means that as cell growth increases, both the nucleoid containing plastid DNA and the amount of chloroplastic RNA in the cytoplasm increase [146]. As previously mentioned, the chloroplast is often associated with a pyrenoid. **Pyrenoids** are permeable organelles characterized by a homogeneous granular structure present in the stroma of the chloroplast. The function of the pyrenoids in the different types of algae is not yet fully known. In many species of Chlorophyceae, starch deposits are within the pyrenoid; consequently, this structure could synthesize starch within [147]. However, the pyrenoid can improve the photosynthetic activity of the Rubisco enzyme (ribulose-1,5-diphosphate carboxylase-oxidase), providing high concentrations of CO_2 to the enzyme thanks to the presence of membranes capable of separating the inorganic carbon and thanks to a dense matrix rich in Rubisco. Peripheral elements can surround the pyrenoid or not. Pyrenoids are inherited from daughter cells, and the mechanism by which the passage of generation takes place is not entirely clear and varies according to the microalgae species. Furthermore, the pyrenoid is involved in the metabolism of carotenoids, amino acids and the polymerization process of reserve sugars [148].

3.3 Metabolism

All microalgae can adopt an autotrophic metabolism and obtain the energy necessary for their sustenance from light through photosynthesis [117]. In reality, most of these microorganisms can follow different metabolic pathways because many of them are not obliged photoautotrophs and can therefore adapt to different substrates for their growth depending on the environmental conditions in which they live. This very high adaptability is possible thanks to the coexistence inside the cell of both the chloroplasts, within which the photosynthetic process takes place, and the mitochondria, where the oxidation of the organic carbon takes place, which provides the energy and the carbonaceous substrate for the later stages of

metabolism [149]. The microalgal activity was observed both in autotrophic and heterotrophic conditions and in mixotrophic conditions. **Heterotrophic metabolism** uses a source of organic carbon for growth, and it depends on the energy source used. The heterotrophic metabolism can be chemoheterotrophic when the energy needed for cell growth comes from chemical reactions or photoheterotrophic when, instead, it comes from light radiation [150]. Heterotrophic organisms produce energy only through the breading.

$$Glucose + O_2 \rightarrow CO_2 + H_2O + Energy$$

In **mixotrophic metabolism**, on the other hand, cells use both organic and inorganic carbon in a combined way, combining the autotrophic metabolism with the heterotrophic one. This way, the cells can grow faster [151]. The **autotrophic**, or photoautotrophic, metabolism, in this case, uses a source of inorganic carbon, generally CO_2 and a light source which, through **photosynthesis**, provides the energy to reduce the inorganic carbon, in a process that, therefore, involves the transformation of light energy into chemical bond energy [152]. Photosynthesis is a process that uses the light energy of the sun to promote the fusion between water and carbon dioxide molecules, to build complex organic glucose molecules. The generic formula of all photosynthesis is the following:

$$CO_2 + H_2O + 8 \text{ photons} \rightarrow \text{photosynthetic pigment} \rightarrow O^2 + 1/6 \ C_6H_{12}O_6$$
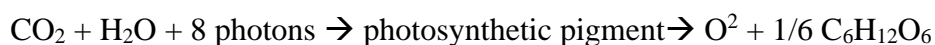
Adenosine tri phosphate (ATP) is synthesized starting from light energy; a proton gradient is created thanks to the excitation of an electron of a pigment, such as chlorophyll, which rises to a higher level of energy. When it falls back, the energy emitted serves to move protons with the ultimate purpose of phosphorylation of adenosine di-phosphate (ADP), a reaction catalysed by ATP-synthase. Photosynthesis consists of two phases, a light phase and a dark phase [153].

3.3.1 The Light reaction

The light reaction (**Figure 24**) depends on the light that occurs on the thylakoid membranes within the chloroplast and synthesizes ATP and nicotinamide adenine dinucleotide phosphate (NADPH), necessary for the synthesis of carbohydrates in the dark phase of the Calvin cycle.

The membranes of thylakoids are composed of lipid mono and digalactosylglycerol arranged in a double layer that encloses a liquid matrix. In green algae, thylakoids are grouped in two or stacks of three and within their membranes are five main complexes: light-gathering antennae, photosystem II (PS II) and photosystem I (PS I) (both containing a reaction centre), cytochrome b6 / f and ATP synthase (ATPase, which maintain photosynthetic electron transport and photophosphorylation [154]. Photosystems work following a Z-pattern in which the redox potential grows from negative to positive. The light radiation transfers two electrons from the water to the electron carriers to produce NADH2. The passage of electrons that occurs simultaneously between the stroma and the luma creates a pH gradient that activates the ATPase following the following process:

$$2NADP + 3H_2O + 2\ ADP + 2\ P_i \rightarrow \text{light energy/chlorophyll} \rightarrow 2NADPH_2 + 3ATP + O_2$$
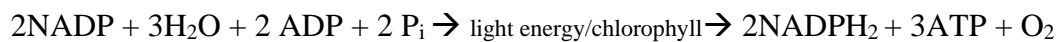
Oxidized chlorophyll stimulates the enzymatic mechanism of photosynthesis of the hydration water present in the internal lumen of the thylakoid and the further release of electrons according to the equation:

$$H_2O \rightarrow 2H^+ + 2\ e^- + 1/2\ O_2$$
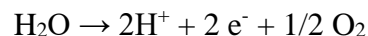
The electrons reduce the oxidized molecules of chlorophyll (which are thus available to capture light energy) and arrive at a NADP + molecule combining with the H + ions remaining in solution, and transforming into NADPH. Water, in addition to releasing electrons, acts as a donor of protons (H+). This reaction releases oxygen from the plant.
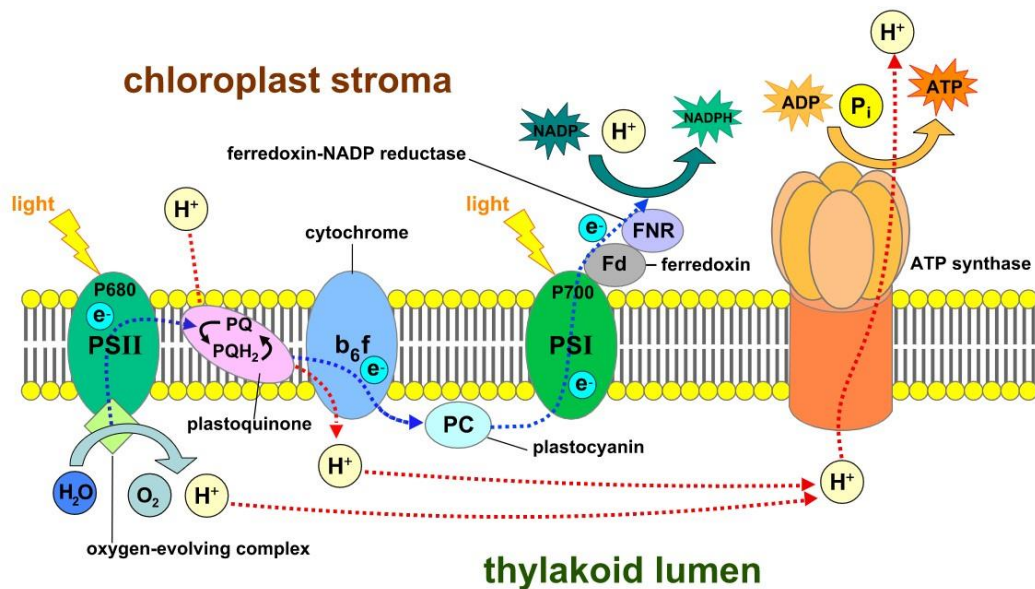
Figure 24: *Light reaction process* [155]

3.3.1.1 Antennas for light collection

These antennas collect the light, convey it to the reaction centres, and contain the pigments and proteins responsible for its capture. The principal pigments in green algae are hydrophobic pigment-protein complexes called LHC II and LHC I, which contain chlorophyll α (Chlα), chlorophyll β (Chlβ), carotenoids and xanthophylls [156].

3.3.1.2 Photosystem II (PS II)

Photosystem II (**Figure 25**a) is a protein complex contained within the thylakoid membranes. Twenty subunits of about 300 kDa makeup photosystem II dividing it into the reaction centre, oxygen-evolving complex and the internal antennas for capturing light. The intrinsic proteins CP43 and CP47, form the inner-antennas, transferring excitation energy from the outer antennae to the reaction centre. The proteins D1 and D2, with the subunits "a" and "b" of cytochrome b559, constitute, on the other hand, the reaction centre. The proteins D1 and D2 have the task of transporting the prosthetic groups, necessary for the separation and stabilization of the charge, towards the tyrosine Z, which is the first electron donor; subsequently towards the pheophytin P680 and then towards the secondary quinone acceptors QA and QB [157].

3.3.1.3 Photosystem I (PS I)

About ten proteins make up photosystem I (**Figure 25**b) which contains about 100 chlorophylls and has a molecular mass of about 360 kDa. The role of photosystem I is to generate the potential to reduce ferredoxin and thus produce NADPH2. PsaA and PsaB are two large proteins that make up the monomer centre where the prosthetic cofactors of the reaction centre are. The dimer Chl P700 initiates the separation of the primary charge, and the electrons pass to the carriers A0 (Chlα), A1 (phylloquinone) and FX (4Fe-4S). The PsaC subunit receives the generated electrons and passes them to the mobile acceptor, ferredoxin [158].
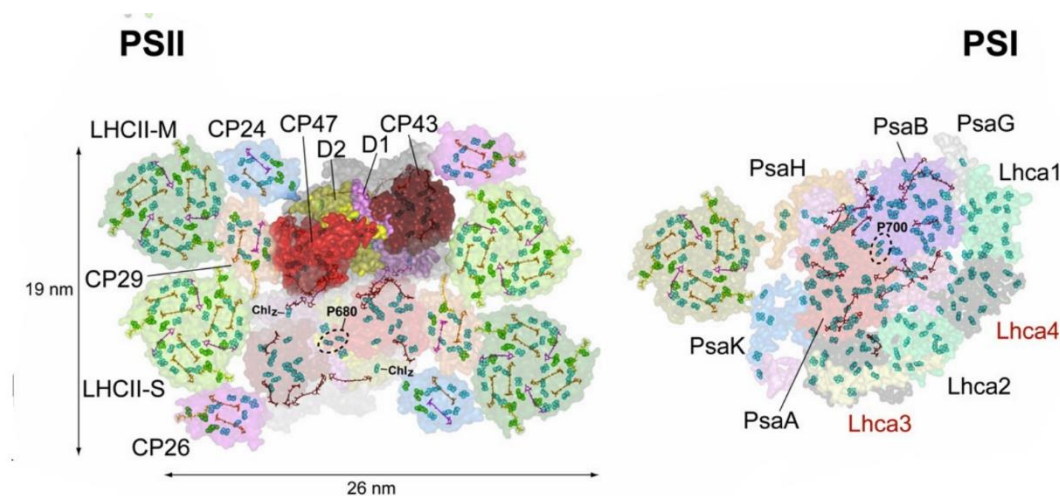
Figure 25: Comparison between a) PSII and b) PSI [158]

3.3.1.4 The cytochrome b6/f complex

Cytochrome b6/f guarantees the transport of electrons between the two photosystems thanks to two mobile carriers. Plastoquinones and plastocyanin. Plastichinones carry two electrons between PS II and cytochrome b6 / f, while plastocyanin transfers electrons between cytochrome and PS I (from stroma to lumen) [153].

3.3.1.5 ATPase

ATPase is a membrane enzyme composed of two subunits: hydrophobic CF0 that crosses the thylakoid membrane and forms a proton channel; and hydrophilic CF1 attached to CF0 on the stromal side that forms a ring structure for ATP catalysis.

As previously mentioned, the pH gradient created between the stroma and the lumen catalyses the synthesis of ATP starting from ADP + P_i [153].

3.3.2 The dark reactions

The second phase of the photosynthetic process takes place in the stroma of the chloroplast, constitutes the Calvin cycle (**Figure 26**), and does not require light radiation; for this reason, the set of reactions that compose it are called dark reactions [159]. The general reaction of this phase (contained in the formula described below) begins with the fixation of carbon through the use of $NADPH_2$ and ATP produced at the end of the light reaction [160]:

$$CO_2 + 4H^+ + 4\ e^- \rightarrow 2NADPH_2, 3ATP/enzymes \rightarrow (CH_2O) + H_2O$$
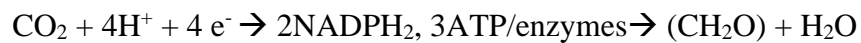
The dark reaction begins with carboxylation. In this reaction, atmospheric carbon dioxide and water combine with ribulose-1,5-diphosphate thanks to the action of the enzyme ribulose-diphosphate-carboxylase (Rubisco). The reaction forms two unstable 6-carbon compounds, 3-phosphoglycerate (Glycerate-P). After carboxylation, there is the reduction phase, which converts Glycerate-P into 1,3-diphosphoglycerate (thanks to the energy provided by ATP) which will subsequently be reduced to phosphoglyceraldehyde (Glyceraldheyde-3P), through $NADPH_2$. Two phosphoglyceraldehyde molecules join together to form a glucose molecule. The final stage of the Calvin cycle is the regeneration of ribulose to allow for the fixation of other CO_2 molecules. This occurs through the transketolase and aldolase enzymes which combine sugar phosphates with 3/4/5/6 carbon atoms to form sugars with 5 carbon atoms. The final products of photosynthesis are carbohydrates but, in different growth conditions, the fixation of CO_2 can also form fatty acids, amino acids and organic acids [161]. The energy balance of the Calvin cycle, to fix a molecule of CO_2, synthesize a molecule of glucose and reconstitute ribulose, involves the use of 18 molecules of ATP and 12 of NADPH.

$$6CO_2 + 12NADPH + 12H_2O + 18ATP \rightarrow C_6H_{12}O_6 + 12NADP^+ + 18ADP + 18P_i + 6H^+$$

As evidenced by the formula above, at the end of the cycle, the ATP and NADPH transporters exhaust their charge, transforming into ADP and $NADP^+$ and re-entering the luminous phase of photosynthesis.
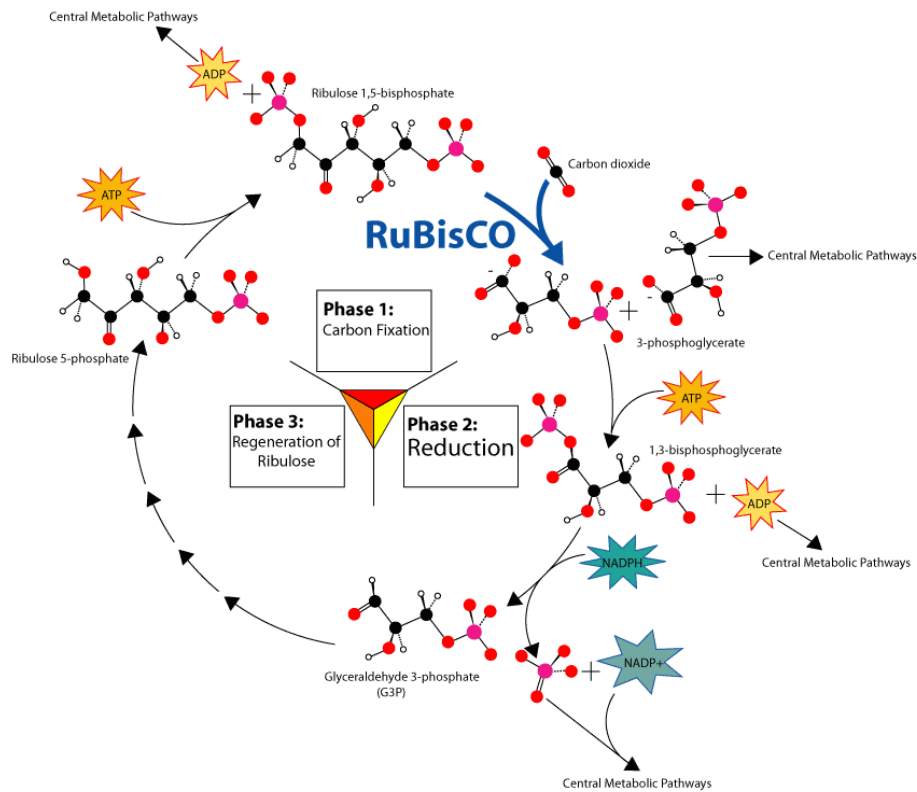
Figure 26 *Calvin cycle* [162]

3.3.2.1 Photorespiration

Microalgae, like higher plants, are capable of producing CO_2 in a reverse process to carboxylation. In this phase, Rubisco works as oxygenase and not as carboxylase, catalysing the reaction of oxygen O_2 with ribose-phosphate to create phosphoglycolate, which is dephosphorylated into glycolate. The glycolate, through several steps, produces serine, ammonia and CO_2. Photorespiration is O_2/CO_2-dependent because high concentrations of O_2 stimulate the process, while high concentrations of CO_2 stimulate carboxylation. The ability to produce CO_2 depends a lot on the species, but microalgae usually do little photorespiration [153].

3.4 Metabolites

As seen in section 3.3, microalgae are photosynthetic organisms and therefore contain pigments involved in the process. Chromophores are pigments related to photosystems. LHCs (Chlorophyll / Carotenoid Complexes) are attached directly to each thylakoid reaction centre and mainly contain α/β chlorophyll and lutein as a carotenoid. The phycobilisomes (PBS), on the other hand, present in photosystem II are formed by different phycobiliproteins, which can be phycocyanin, allophycocyanin, phycoerythrin, and phycoerythrocyanin [163].

3.4.1 Chlorophylls

Chlorophylls are pigments with a structure similar to porphyrin containing a magnesium atom in the centre and with a lateral hydrophobic structure that varies according to the absorption characteristics (**Figure 27**). There are different types of chlorophylls: chlorophyll α, the most abundant and contained in all oxygenated organisms, has an absorption peak at about 438 nm in the blue region and 670 nm in the red region. Chlα fluoresces around 677nm when excited at 440nm [164]. Chlorophyll β, present only in green algae, has a common basic structure to Chlα, but an aldehyde group is present in the lateral structure instead of methyl. Chlβ has an absorption peak around 457 nm and 645 nm [164,165]. There are also other types of chlorophylls contained in different classes and phyla. For example, chlorophyll c is present in golden-brown algae and has various functional groups in the lateral structure, as does chlorophyll d found in red algae. [163].

Chlorophyll	R_1	R_2	R_3	R_4
a	$CHCH_2$	CH_3	CH_2CH_3	Phytyl
b	$CHCH_2$	CHO	CH_2CH_3	Phytyl
c_1	$CHCH_2$	CH_3	CH_2CH_3	H
c_2	$CHCH_2$	CH_3	$CHCH_2$	H
d	CHO	CH_3	CH_2CH_3	Phytyl

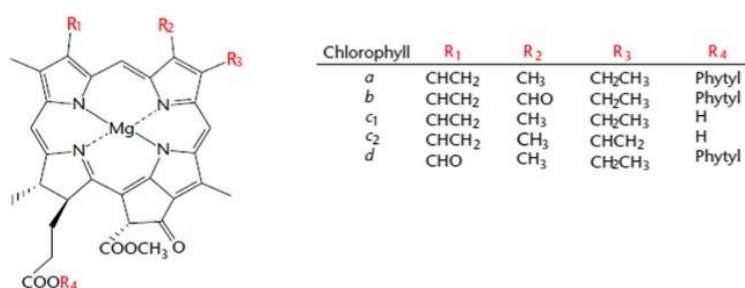***Figure 27***: *Chlorophyll structure* [165]

3.4.2 Carotenoids

Carotenoids are one of the three groups of natural pigments found in microalgae, other than chlorophylls and phycobiliproteins. In general, carotenoids have a colour ranging from red to yellow, absorb light at wavelengths of 400–550 nm thanks to the presence of paired double bonds, and are divided into two main classes. Primary carotenoids, such as β-carotene, lutein and violaxanthin, reduce the excess energy requirement produced by photosynthesis, transferring the absorbed energy to the chlorophylls, and act as complementary pigments that expand the light absorption spectrum of microalgae. Secondary carotenoids, on the other hand, such as astaxanthin and canthaxanthin, protect chlorophyll from photo-damage by forming a protective layer on microalgal cells when exposed to extreme light intensities [166]. A carotenoid generally belongs to the tetraterpenes and is formed by two small rings with six carbon atoms linked by a carbonyl chain. The carotenoids are considered lipids due to their structure. The functional characteristics of carotenoids are linked precisely to their nature; in addition to absorbing light, they can fight free radicals thanks to their antioxidant properties and act as protection against the action of high light intensities that could damage cells [167]. Based on their structure, carotenoids are also divided into carotenes and xanthophylls (**Figure 28**).

3.4.2.1 Carotenes

Carotenes are polyunsaturated hydrocarbon compounds that contain about 40 carbon atoms bonded to a variable number of hydrogen atoms. The main carotenes present in algae are β-carotene and α-carotene, hydrophobic, characterized by a typical yellow/orange colour and precursors of vitamin A. The algae synthesize β-carotene in its *cis* conformation (9-*cis*- β-carotene), which has a higher power in the removal of free radicals and the prevention of cellular oxidative damage and accumulates β-carotene in drops in the chloroplast stroma [166].

3.4.2.2 Xanthophylls

Xanthophylls are oxygenated compounds deriving from carotenes, and in fact, their structure contains a carbonyl chain linked with hydroxides or epoxides groups at the ends. Xanthophylls include a large variety of pigments, including Lutein, which

is the main pigment of green algae, Zeaxanthin, Violaxanthin and Antheraxanthin [165]. Even xanthophylls, based on their structure and functionality, are divided into two classes: primary xanthophylls are part of the photosynthetic system, especially in LHC complexes and are essential for cell viability; secondary xanthophylls, on the other hand, are synthesized by the cell only under stress conditions and serve to protect it. A xanthophyll of particular interest in this thesis work is astaxanthin, produced by the microalga *Haematococcus pluvialis*, which has the task of protecting cells in conditions of high light stress, saline or nutrient deficiency, placing itself at the limit of the cellular wall to create a physical barrier (against UV rays) and a chemical barrier against free radicals. The biosynthesis of xanthophylls starts from lycopene units and involves several enzymes that regulate the biosynthetic pathway [168]
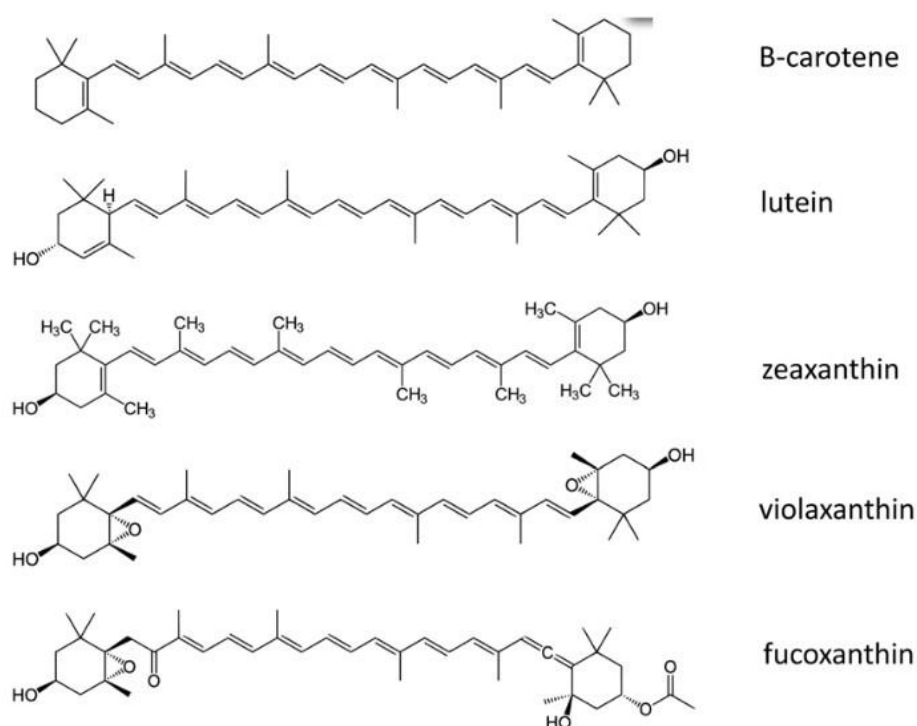

Figure 28: Chemical structures of some of the more important carotenoids [146]

3.4.3 Vitamins

Microalgae contain interesting amounts of vitamins, including Vitamin A or retinol, essential for vision and bone development; the B vitamins play a fundamental role in the normal functioning of the immune system, and among these, the main ones

are Vit. B1 (thiamine), Vit. B2 (riboflavin), Vit. B3 (niacin), Vit. B6 (pyridoxine), Vit. B9 (folic acid), Vit. B12 (cobalamin); vitamin C or L-ascorbic acid, useful as an antioxidant and in the functioning of the immune system; vitamin D, which is made up of a mixture of ergocalciferol and cholecalciferol; vitamin E or tocopherol, which fights free radicals and protects against damage caused by pollution; vitamin H or biotin, and vitamin K. Vitamins concentration produced is related to the conditions of growth and harvest [169].

3.4.4 Lipids

Lipids are heterogeneous compounds insoluble in water but soluble in non-polar solvents and are essential for normal cell function. They constitute biological membranes and act as storage sites for energy reserves. Based on their chemical/physical characteristics, lipids are divided into eight classes: fatty acyls, glycerolipids, glycerophospholipids, sphingolipids, sterol lipids, prenol lipids, saccharolipids, and polyketides [170]. The lipids most present in microalgae are neutral or non-polar lipids and polar lipids, but there are singular lipids that are found only in specific genera or species [171]. Generally, **polar lipids** such as phospholipids (PL) and glycolipids (GL) represent the average 65% of total lipids constituting membranes and intermediaries in lipid synthesis. The most identified phospholipids are phosphatidylcholine, phosphatidylethanolamine, and phosphatidylglycerol. PL are localized in extra-chloroplastic and thylakoid membranes (especially phosphatidylglycerol), giving rigidity and stability to both the cell and the photosynthetic machine. Betaines are lipid complexes that contain betaine linked to the sn-3 position of glycerol through an ethereal bond with the esterified fatty acid in positions 1 and 2, instead of phosphorus or a carbohydrate chain as a polar group. The peculiarity of betaines is their zwitterionic nature at neutral pH, and they also constitute the extra-plastidial lipids and participate in the acyl-lipid desaturation outside the chloroplast. In recent years, betaines have attracted the attention of many scholars as they replace phospholipids in their metabolic role when microalgae are in conditions of stress, such as phosphorus deprivation [172]. The synthesis of phospholipids and betaines occurs outside the plastid, in the endoplasmic reticulum. Glycolipids can contain one (monogalactosyldiacylglycerol: MGDG) or two molecules of galactose (digalactosyl diacylglycerol: DGDG) and are mainly located in the plastid

membrane (GL), in the thylakoid membrane (MGDG) and in the extra-plastid membrane (DGDG). The ratio between MGDG and DGDG in micro-glues depends on the environmental and nutritional conditions, but all GLs are synthesized starting from the DAG diacylglycerol (**Figure 29**) [172,173]. The **non-polar lipids**, most present in microalgae, are glycerolipids, sterols and fatty acids, and in Chlorophyceae, they represent the highest group. Sterols, essential for the fluidity of the membranes that contain them, have different and variegated structures also based on the algal species, but those present with a percentage greater than 30% and present in almost all species are cholest-5-en- 3β-ol (cholesterol), 24-ethylcholest-5-en-3β-ol (sitosterol and / or clionasterol), 24-ethylcholesta-5,22E-dien-3β-ol (stigmasterol and / or poriferasterol), 24-methylcholesta -5,22E-dien-3β-ol (crinosterol or brassicasterol), and 24-methylcholesta-5,24 (28) -dien-3β-ol (24-methylenecholesterol) [174]. Fatty acids (FA), for definition, are carboxylic acids with long linear or branched aliphatic chains, saturated (with no double bonds), monounsaturated (with one double bond), or polyunsaturated (two or more double bonds, called PUFA). Depending on the position of the double bond, PUFAs are called omega 3(ω3) or omega 6 (ω6) and are usually separated by a methyl group but, in microalgae, some FAs do not have this interruption, such as octadecatrienoic acid (picolinic acid, 18: 3Δ5,9,12) and octadecatetraenoic acid (coniferonic acid, 18: 4Δ5,9,12,15). The ω3 fatty acids, present in marine algae, are distinguished by being particularly resistant to oxidation. In microalgae, the percentage of unsaturated FA is 2-3 times greater than in marine algae, although it is almost always ω6, and in particular essential cis-linoleic acid (C18: 2 ω6) and gamma-linoleic acid (C18: 3 ω6), quite rare the quantity contained in some microalgae is second only to that present in breast milk [175].

Figure 29*: **a**) <u>Neutral and polar lipid synthesis pathways in microalgae</u> (AACPT, acyl-ACP thiolase; ADMS, S-adenosylmethionine synthetase; BLS, betaine lipid synthase; CDP- DAG:IPT, cytidine-5'-diacylglycerol:inositol phosphotransferase; CDPE:DAGEPT, cytidine-5'-diphosphate-ethanolamine:diacylglycerol-ethanolamine phosphotransferase; DGAT, diacylglycerol-acyltransferase; DGDGS, digalactosyl diacylglycerol synthase; GPAT, glycerol-3P acyltransferase; GPDH, glycerol-3 phosphate dehydrogenase; I3PS, inositol 3-phosphate synthase; LCACAS, long chain acyl-CoA synthase; LPAAT, lyso-phosphatidic acid acyltransferase; MGAT, monoglycerol-acyltransferase; MGDS, monogalactosyl diacylglycerol synthase; PAP, phosphatidic acid phosphatase; PDAT, phospholipid:diacylglycerol transferase; PGD1, plastid galactolipid degradation 1 protein; SLS, sulfolipid synthase) **b**) <u>Fatty acid synthesis</u> (ACCase, acetyl-coA carboxylase; Fab, fatty acid biosyn- thesis enzyme; FabD, malonyl-CoA:ACP transacylase; FabG, 3-ketoacyl-ACP reductase; FabH, β-ketoacyl-ACP synthase III; FAD, fatty acid desaturase; MUFA, monounsaturated fatty acids; PalD, palmitoyl-acyl desaturase; PUFA, polyunsaturated fatty acids; SFA, saturated fatty acids). Adapted from [172]*

The FA synthesis, in photosynthetic organisms, occurs in the mitochondrion that synthesizes FA with chains no greater than 18 carbon atoms (C18). The synthesis starts from an acetyl-CoA molecule transformed into malonyl-CoA by acetyl-CoA carboxylase. Once synthesized, malonyl-CoA is transformed into β-ketoacyl-ACP thanks to two important enzymes, malonyl-CoA: ACP transacylase (FabD) and 3-ketoacyl-ACP synthase III (FabH). From β-ketoacyl-ACP, we proceed to the synthesis of carbon chains which can arrive in the chloroplast where the galactolipids are incorporated, or in the endoplasmic reticulum to continue the synthesis of polar lipids or to synthesize FA with a longer chain than C18 (**Figure 29**) [172]. Microalgae are a source of very important PUFAs such as eicosapentaenoic acid (EPA, 20: 5, n-3) and docosahexaenoic acid (DHA, 22: 6, n-3) [176]. Glycerolipids and specifically triacylglycerols (TAGs) represent the site of energy storage in the form of lipid droplets, unlike polar lipids which instead have a structural function [177]. In glycerolipids, the positions sn-1, sn-2, and sn-3 are esterified, all or only some, to form monoacylglycerol (MAG), diacylglycerol (DAG) or triacylglycerols (TAG). They constitute important accumulation products that can be catabolized to provide energy. Growth conditions affect their biosynthesis, especially during the light reaction of photosynthesis where they accumulate in cytosolic lipid bodies exploited in the dark reaction; in fact, the PUFA-rich TAGs donate acyl groups for the synthesis of polar lipids, moreover, the TAGs are the substrate of glycerol-3 phosphate dehydrogenase (GPDH), a key enzyme in the synthesis of glycerol [178]. The synthesis of TAGs, as mentioned above, takes place in the chloroplast through the action of various enzymes that act on lipids, starting with glycerol 3-phosphate. After two steps, through two acyltransferases, the final phase of TAG synthesis takes place thanks to the phospholipids and galactolipids that donate the acyl; all regulated by phospholipid: diacylglycerol transferase (PDAT) and from acyl-CoA: diacyl-glycerol acyltransferase (DGAT) 1, identified in *P. tricorium* and involved in the last phase of synthesis by regulating the production of TAG under stress conditions such as nitrogen deficiency, which downregulates the photosynthetic activity and increases lipid synthesis [179,180].

3.4.5 Carbohydrates

Carbohydrates, including mono-, oligo- and polysaccharides, have both structural and metabolic functions. Microalgae accumulate energy products similar to glucose and starch, which are the main products of photosynthesis. Polysaccharides are produced in a variety of forms depending on the group of microalgae, but Chlorophytes synthesizes starch in the form of two glucose polymers, amylopectin and amylose [181]. Carbohydrates have different functions, both structural and metabolic, in fact, the cell walls contain hemicellulose and cellulose, a rigid and crystalline β-1,4 glucan, less soluble than hemicellulose [182].

3.4.6 Phenols

Phenolic compounds are secondary metabolites commonly found in all terrestrial plants as well as microalgae. Phenols are typically synthesized to protect cells from pathogens and UV rays and possess a wide variety of biological activities, including antioxidant ones [183]. The antioxidant activity of phenolic compounds is strongly dependent on their chemical structure, characterized by an aromatic ring bearing one or more hydroxyl substituents. Hydroxyl groups contribute to antioxidant activity through their ability to chelate metals, as well as the ability to donate electrons/hydrogen, generating intermediate radicals of greater chemical stability than the initial radicals [184]. Furthermore, the action of hydrophobic benzenoid rings and hydroxyl groups makes phenols capable of inhibiting various enzymes involved in the generation of reactive oxygen species (ROS) (lipoxygenases, cyclooxygenases and xanthine-oxidase) [185,186].

3.5 Microalgae applications

As previously described, microalgae are a natural source of different metabolites that find application in different fields: industrial, biopharmaceutical, nutraceutical and energetic. In fact, in recent years, microalgae have attracted the attention from industries as their production is renewable, sustainable and economically advantageous, considering that all components can be used and that even from a single cell culture it is possible to obtain even more industrial products. To date, large-scale microalgal crops are mainly used for aquaculture both as a nutritional

food for fish and shellfish larvae (being rich in PUFA) and as a chemical stabilizer for the culture tanks themselves [187].

3.5.1 Bioplastic

In the last half of the twentieth century, the use of plastic reached very high levels as its accumulation in natural environments, constitutes one of the major pollutants for the planet. This issue has stimulated scientific research towards the production of renewable and biodegradable plastic. In this context, algal biomass is considered an innovative eco-friendly resource for new generation bioplastics production. Germany and Italy were the first countries that published studies on bioplastics based on microalgae, underlining how microalgae solve various problems. First of all, their cultivation does not compete with agricultural products as their production can take place on non-arable land; this would also increase the global photosynthetic capacity as the microalgae are organisms capable of subtracting CO_2 from the atmosphere. Furthermore, microalgae can grow in salty and/or wastewater (as it will be described), and this is at the centre of a circular green production mechanism, together with the recycling of nutrients [188]. When microalgae are placed under stressful conditions in the culture medium, particularly in nutrient depletion (nitrogen, sulphur or phosphate), they accumulate biopolymers such as polysaccharides, including starch, lipids, proteins and other metabolites which can be extracted directly from algal biomass [189]. Another way to link algal biomass to the plastics industry is to convert the biomass into methane through a fermentation process. Methane can then be used to produce polyhydroxyalkanoates (PHA), lactic acid (precursor of polylactic acid or PLA), ethanol (precursor of bio-polyethene or bio-PE and bio-polyvinyl chloride or bio-PVC) and proteins. Polylactic acid (PLA) is a thermoplastic aliphatic polyester derived from renewable biomass and typically obtained from fermented vegetable starch such as corn, sugar cane or sugar beet pulp, which in 2010 was the second most consumed bioplastic in the world [188]. Some of the species considered for the production of bioplastics are: *Chlorella spp. Spirulina platensis, Nannocloropsis gaditana,* and *Scenedesmus almeriensis* [189].

3.5.2 Biofertilizers

Bio-fertilizers can provide cost-effective alternatives to synthetic products and renewable and eco-friendly solutions for the future of agriculture, presenting a high

potential for bio-stimulation and improvement of culture productivity and increasing soil fertility while also protecting it from abiotic stress. The global increase in population and the related increase in water consumption, correlated with the decrease in water supply in some geographic areas, the pollution of terrestrial and underground waters and climate change, are currently generating a water crisis that directs the research towards wastewater recycling and management of nutrient cycles. In this context, the environmentally friendly production of microalgae-based bio-fertilizers appears as a realistic alternative for the environmental management of wastewater, combined with the supply of nutrients for crops. Nitrogen, phosphorus and potassium (NPK) are the first three primary nutrients used as commercial fertilizers and constitute the first three nutrients studied for the growth of microalgae to produce biomass that can be, subsequently, transformed into biofuels or bio-fertilizers. Studies were also conducted to identify microalgae species that combine the best bio-remediation and bio-fertilization capabilities. For example, it has been shown that *Chlorella spp.* has high phytostimulant activities on wheat (30% increase in plant length), becoming a possible substitute for chemical fertilizers to increase soil fertility [190], and several species belonging to *Nannochloropsis* have been identified as a sustainable biofertilizers to increases the sugar and carotenoid content in tomatoes [191].

3.5.3 Nutraceutical and pharmaceutical applications

For centuries, the microalgae *Spirulina* have been used, by African populations of Lake Chad and Central America, such as those of Lake Texcoco in Mexico. The interest in microalgae and their use in the food sector manifested around the 1950s when the problem of global overpopulation began to emerge for the first time: algae, more than any other food, presented itself as a low-cost protein source. At first, given the poor results, the idea was abandoned, but in 1961 a Japanese company called "Nihon Chlorella" began to cultivate the *Chlorella* genus on a large scale for commercial purposes. [192]. In the 1980s in Asia, 46 factories were producing more than 1,000 kilos of biomass per month, mostly Chlorella [193].

So microalgae have been used as a source of nutrition for humans for hundreds of years, but today only a few GRAS (Generally Recognized as Safe) species have obtained authorization for marketing as a "food" suitable for humans. The consumption of whole dried microalgae has increased significantly in the last 20

years, and they are now considered an eco-friendly, organic, sustainable, alternative and complementary food to "classic" food, with beneficial properties for health because they contain a wide range of nutrients and bioactive compounds, including proteins, polysaccharides, lipids, pigments, polyphenols, minerals and vitamins with high nutritional value [194]. Nutraceuticals can be defined as food nutrients not only used to supplement diet, but also to prevent diseases and disorders and to improve symptoms. As seen in section 3.4.4, microalgae are a natural source of Ώ3s and PUFAs that improve human health and reduce risk of developing cardiovascular disease, cancer, type 2 diabetes, inflammatory bowel disorders, asthma, arthritis, skin disorders, depression and schizophrenia [195]. Furthermore, pigments such as carotenoids have great pharmacological activities improving fertility (astaxanthin), preventing macular degeneration (lutein and zeaxanthin), treating rheumatoid arthritis, cardiovascular diseases, neurodegenerative diseases, obesity (astaxanthin and fucoxanthin) and tumours (β-carotene, fucoxanthin, zeaxanthin, violaxanthin, lutein alloxanthin, etc.). Microalgae have also stimulated considerable interest as pro-healing extracts for wound care, extracts stimulating blood circulation, and photosensitive pigments for phototherapy [196]. Some metabolites have anti-angiogenic activity. Angiogenesis is a physiological process that leads to the development of new blood vessels and which takes on considerable importance in the development of tumours, atherosclerosis, arthritis, diabetic retinopathy and ischemic stroke [197]. Fucoxanthin, present in several microalgal species and also sifonaxantina, can inhibit the process of angiogenesis in the aortic ring of rats by suppressing the growth of micro vessels [198]. Fucoxanthin also has therapeutic effects for diabetes, induces the synthesis of arachidonic acid and DHA in mouse livers, inhibits cutaneous melanogenesis by negatively regulating the transcriptional factors involved, and protects DNA from photo-oxidation. [199]. The ability of microalgae to act on bacteria and fungi is another parameter to consider when studying their applications. Bacteria and fungi are the principal causes of different diseases in plants and animals, including humans. They reduce yields and are the main cause of food spoilage.

Widespread use of various antibiotics in recent decades has resulted in increased resistance of microbes to antibiotics, necessitating the search for new antimicrobial agents. Microalgae exhibit a wide range of bioactive natural products that are effective, in raw or purified form, as antimicrobial agents. The first antibacterial

products were found in *Chlorella*, and they were able to inhibit the growth of Gram-positive and Gram-negative bacteria. Some microalgae also produce compounds that have antifungal activity [200]. *P. lima* and *G. toxicus* produce okadaic acid and ciguatoxin, respectively, two effective antifungal agents. *Chaetoceros lauderi* produces lipid metabolites to inhibiting the growth of serval bacterial strains. *M. aeruginosa*, instead, is rich in toxic metabolites with cytotoxic and antimicrobial effects. Also, *Dunaliella salina* produces compounds that are active against various bacterial and fungal strains (for example, *Staphylococcus aureus*, *Escherichia coli*, *Candida albicans, Pseudomonas aeruginosa, Aspergillus niger*); moreover, its extract significantly inhibits the growth of *Klebsiella pneumonia* [201].

3.5.4. Cosmetics

Even in the cosmetics sector, microalgae play an important role by offering a wide range of pigments, polysaccharides and polyphenols with effective "cosmeceutical" activity, focused on the production of cosmetic products with biologically active ingredients that claim medical or pharmacological benefits. Antioxidant, anti-ageing, UV protection, immuno-protective, moisturizing and texturizing, whitening and healing properties are some of the biological activities microalgae have. Pigments have also been studied for natural dyes for beauty cosmetics: lipsticks with phycocyanin, bronzers containing canthaxanthin, eyeliner, etc. Proteins and carbohydrates have also been studied to use as ingredients and texturizing agents. Polysaccharides were mainly used as thickeners and moisturizers [202]. Several microalgal species can accumulate appreciable quantities of lipids and therefore are characterized as oilseeds. In cosmetic formulations, lipids and their derivatives are one of the main ingredients. Different classes of lipids are excellent moisturizing, emollient and softening agents, function as surfactants and emulsifiers, give texture to products, are colour and fragrance carriers, act as preservatives to maintain product integrity, and can be part of the delivery system of molecules [170].

The skincare market is mainly dominated by *Chlorella*, *Arthrospira*, *Nannochloropsis*, *Porphyridium*, *Nostoc* and *Dunaliella* for their potential to prevent skin ageing, protect against UV light damage and oxidative stress [202]. In this case, it is possible to consult a review published during the PhD work on the use of lipids extracted from microalgae in cosmetic applications (De Luca et al, 2021 – Appendix 1).

3.5.5 Biofuel

The continuous emission of carbon dioxide into the atmosphere by human activities, especially those based on fuels derived from petroleum, is changing the entire ecosystem of the planet Earth, modifying upwards the thermal balances (IPCC). Therefore, for years, scientists and researchers have searched for solutions capable of solving this problem concretely. One of the main objectives is to replace fossil fuels with others of plant origin that do not release large amounts of CO_2 into the atmosphere. The photosynthetic biomass, during its growth, absorbs the same amount of carbon dioxide emitted when it is finally combusted; however, the processes for the transformation of biomass can negatively affect the total balance. The production of biofuels obtained from edible plants (first generation) is considered an unsustainable practice for the reduction of agricultural areas that can be used for food purposes, and for the increase in the price of raw materials (e.g. water, fertilizers) necessary for the production of necessities, such as wheat, corn, rice and sugar cane. Furthermore, the currently cultivated land may not be enough to fill the food shortage for a big part of the world population. For this reason, to the focus on the use of non-edible biomass for the production of biofuels can be an alternative solution to reduce the competition that could arise between the energy and agri-food sectors. In light of this situation, areas of research have been activated in several countries aimed at developing new eco-sustainable technologies for the production of clean energy (second generation) [203]. For several years, the possibility of using microalgae to produce, in a sustainable manner, a quantity of much higher energy per unit area compared to that obtained from corn, soybean or crude oil of tropical palm has been taken into consideration, even in Italy, [204]. Microalgae are an optimal example of second-generation energy crops, capable of avoiding harmful impacts on the agri-food market and terrestrial biodiversity.

They can be cultivated on poorly productive soils otherwise unusable such as arid coastal areas and marshy areas with brackish waters or marine productions. For their growth, it is possible to use eutrophic waters rich in nutrient salts of agricultural or civil origin, thus also obtaining their purification. Microalgae can produce 30 times the equivalent in crude oil compared to the same area cultivated with terrestrial species such as corn or soy, but, to date, there are no technologies necessary to produce large-scale bioenergy at low costs [205].

CHAPTER 4: MICROALGAE AND PETROLEUM

Based on what has been described in the previous chapters, microalgae constitute a fundamental element in the treatment of water contaminated by crude oil and hydrocarbons. Several studies have focused on their use for bioremediation (section 2.10.2). Ugya et al. evaluated the ability of some microalgae grown on a biofilm to remove contaminants of petroleum origin, including PAHs and total petroleum hydrocarbon (TPH). The results showed a significant reduction of phytochemical

parameters such as sulphate -17.5%, chloride -14.65%, nitrates -33% total suspended solids (TSS) -26%, total dissolved solids (TDS) -7.9%, and chemical oxygen demand (COD) and biochemical oxygen demand (BODs) reduced by 8% and 16.7% respectively. Although not in high percentages, the removal of TPH was equal to 15% after 14 days of exposure [206]. Kuttiyathil et al., on the other hand, analysed not only the removal of crude oil by the microalga *Chlorella spp* but also how, in nature, the mechanical action of sea waves contributes to creating an emulsion of water and crude oil that could favour the removal of pollutants making them more available. Their results show that following an initial period of adaptation, the Total Organic Carbon (TOC) of the solution was drastically reduced and that, after 5 days, *Chlorella* removed 80% of the emulsified oil [207]. Water mixing and how it can alter bioremediation was also studied in 2014 by Özhan et al., which demonstrated how the bioavailability of crude oil is altered by physical mixing applied in the laboratory. The mixing of the water column containing crude oil does not significantly affect the concentration of total petroleum hydrocarbons (TPH) but increases the concentration of some alkanes and PAHs and causes the formation of colloidal micro-particles (1-70 μm), which improve the degradation of hydrocarbons. [208]. *Chlorella spp* has been the subject of several studies precisely because of its ability to survive in contaminated media. Znad et al, reported that the treatment of petroleum effluent (PE) with *Chlorella spp* completely removed phosphorus after 13 days, reduced nitrogen by 78% and reduced COD from 504 mg / L to 144 mg / L. However, treatment of petroleum effluent with *Chlorella spp* initially increased the biomass, but inhibited cell growth in the long term and was toxic, even though organic carbon usually has the opposite effect on *Chlorella spp* [209].

The nature and concentration of the crude oil, and its constituents, greatly influence the growth and removal of *Chlorella*. For example, the use of Water-Accommodated Fraction (WAF) deriving from diesel is more toxic for *Chlorella* than diesel as it is containing many low molecular weight hydrocarbons (LMW-HC), which can cause damage to cell membranes and affect the production of protective pigments, as reported by Ramadass et al. in its 2017 study [210]. Further studies carried out on *Chlorella* have confirmed its ability to remove various compounds contained in crude oil. For example, Xaaldi Kalhor et al., in both of

their studies [211,212] tested different concentrations of crude oil (10 and 20 g / L) on *Chlorella vulgaris* for two intervals (7 and 14 days). The results were encouraging, and the best removal of low compounds (LW), equal to 100%, was achieved with 10 g / L for 14 days, while at higher concentrations (20 g / L), after 14 days, the LW were reduced by 82%. The removal of heavy compounds (HW) followed the same trend as the light ones, reaching higher values for the 14-day intervals and at a concentration of 10 g / L (reduction of HW equal to approximately 78%) [211]. Hamouda et al. (2016) and El-Sheekh et al. (2013) evaluated how the addition of crude oil to the *Chlorella* culture affected its metabolism and, specifically, whether the microalgae preferred a mixotrophic and heterotrophic mechanism rather than the classic autotrophic one. Hamouda et al. tested the growth of *Chlorella* in mixotrophic conditions using 1% crude oil. His results on the hydrocarbons concentrations, present after 30 days of incubation, showed that the following aliphatic compounds: 3-methyl decane, heptadecane, octadecane, nonadecane, docosane, and tetracosane were removed, while decane, undecane, tridecane, hexadecane, tricosane were significantly reduced compared to the control [213]. El-Sheekh et al. instead, tested *Chlorella's* bioremediation capacity using up to 2% crude oil. The results obtained by gas chromatography-mass spectrometry (GC-MS) showed that, after 15 days of incubation, Indole-3-acetic acid was removed at all tested concentrations, while decane, Indole-3-acetic acid, p-Phenyltoluene, Naphthalene, 3-ethyl, Tridecane, phenanthracene, 1-methyl, Benzene, decyl, phenanthracene, 2-methyl, cyclohexane undecyl, b-pregnane and Octacosane were removed at a concentration of 2% crude oil [214]. One of the most interesting aspects concerning the El-Sheekh study is that PAHs were reduced more efficiently in heterotrophic conditions.

This supports the hypothesis that eukaryotic microalgae, such as *Chlorella*, use organic carbon, present in solution, improving their growth range and biomass using a heterotrophic metabolism that allows them to split and/or convert hydrocarbons into intermediate metabolites. Confirming this hypothesis is also the study conducted by Das et al. in 2019, which demonstrated how *Chlorella* reached the highest biomass yield (1.72 g / L) in mixotrophic conditions with the addition of pre-treated produced water (PPW) of petroleum origin and removed 92% of the total nitrogen (TN) and 73% of the TOC [215].

4.1 Mechanisms of action

From the studies analysed, it is evident that green microalgae, in particular *Chlorophyceae*, are excellent candidates to remove crude oil pollutants. The mechanism of action with which this happens is not yet completely known, but the principal hypotheses are two: either they use organic carbon deriving from hydrocarbons, or they accumulate them inside by carrying out a defence mechanism and treating them as real contaminants. Ugya et al. analysed both hypotheses, and their results show that, in the microalgae, there was a net increase of saponins after the treatment of petroleum contaminants. Saponins usually play a protective role thanks to their glycosidic-terpenic nature, lowering the surface tension and forming colloidal and foamy solutions [216]. Their amphipathic and surfactant nature increases the bioavailability of petroleum contaminants which are easier to "attack". Ugya et al., also demonstrated that the production of ROS increased, highlighting cellular stress induced by crude oil after the treatment. This is related also to the increase of alkaloids, flavonoids and carotenoids within the algae after treatment, suggesting that the ROS produced by the microalgae have degraded the hydrocarbons, protecting them from their toxic action. [206]. Ghodrati et al., instead, focused on the genetic nature underlying the bioremediation mechanism. At the basis of their study, there is the idea that PAHs could be a source of ROS, alkoxyl (RO °) and hydroxyls (OH °) inside of cells.

Starting from the knowledge on degrading bacteria [217], they hypothesized that green algae, being aerobic, could also use dioxygenases to remove and degrade PAHs, focusing specifically on lipoxygenases (LOXs) which oxidize PAHs through the insertion of two oxygen atoms which lead to the rupture of the aromatic ring through ortho-cleavages or meta-cleavages. The addition of oxygen in the hydrocarbon skeleton generates the formation of hydroperoxypes activated by becoming oxylipins. The molecular mechanism in microalgae has not yet been studied, but it would seem that lipoxygenases have both lipoxygenase and hydroperoxidase activity. Consequently, the results of Ghodrati et al. show that

exposure to 1% crude oil for 21 days induced the expression of the LOX genes, ultimately leading to the decomposition of hydrocarbons and the production of hydroperoxy acids, fats and oxylipins which are useful to the algae for growth and sustenance, as well as for the resistance to stress-induced by crude oil [218]. SureshKumar et al. hypothesized that the degradation mechanism of PAHs in microalgae could be similar to that implemented by prokaryotes, turning an eye to the bacterial world. Starting from the idea that higher plants and animals share enzymatic and genetic pathways in the removal of exogenous substances, the group of researchers carried out a non-laboratory predictive analysis, considering as a metabolizing mechanism the oxidative system of cytochrome P450 (CYP450), which intervenes in the degradation of those molecules resistant to dioxygenases. Several parameters were analysed to create a model that could simulate the link between PAHs and CYP450 of *Haematococcus pluvialis*. Thirty-eight PAHs formed from 1 to 6 benzene rings were involved in the analysis, and the results showed that hydrogen, hydrophobic, electrostatic, π-π, and Van der Waals interaction occurred in the active site of CYP450. Specifically, 18 PAHs interacted with Threonine282 (Thr282), Alanine337 (Ala337), Serine404 (Ser404) and Lisyne407 (Lys407) *via* hydrogen bonds. However, in this study, it is evident that only LMW-PAHs were able to bind CYP450, while HMW-PAHs did not [219]. Therefore, there is an antioxidant mechanism for the degradation of petroleum pollutions, in particular, hydrocarbons. It acts in a double capacity, removing the toxic agent and producing nutrients useful for cell growth. Low doses of toxins could activate mechanisms to repair not only the damage induced by the toxin but also other damages previously accumulated by the cell, according to hormesis hypothesis [220].

However, some studies show that the ability of microalgae to remove contaminants continues even after the cell is dead as the microalgae can adsorb micro-drops of crude oil on their surface and, consequently, TOC, removing it from the solution as demonstrated by Kuttiyathil et al. [207].

CHAPTER 5: SPECIES IN OBJECT

5.1 *Haematococcus pluvialis*

Haematococcus pluvialis (HP) is a unicellular green alga that grows in different geographical areas of the world and belongs to the class of *Chlorophyceae* [221]. *H. pluvialis* is extensively studied for the high production of astaxanthin (ASX), up to 7% of the wet biomass [222]. Astaxanthin (3,3′- dihydroxy-ß-carotene-4,4′-dione) is a red secondary carotenoid belonging to the xanthophyll family, and it is considered a powerful antioxidant [223,224]. ASX is ubiquitous in nature, in fact it can be produced by plants, bacteria and yeast [225]. The economic interest for ASX is linked to its use in various sectors, including aquaculture (responsible for the characteristic red/pink colour of some fish and crustaceans), pharmaceutical, nutraceutical [226] and cosmetics [227]: this makes *H. pluvialis*, consequently, an important algae for commercial purposes. *H. pluvialis* produces ASX under stressful conditions such as high salinity of the growth medium, changes in pH, temperature and a lack of specific nutrients such as phosphorus [228–230]. Furthermore, the production of ASX is also linked to the cell cycle of *H. pluvialis* [231], which rarely reproduces sexually but implements an asexual reproduction divided into four different phases [232,233]. The first phase begins with gametogenesis in which *H. pluvialis*, found in an oval and biflagellate shape called a macrozooid (8-20 μm), begins to divide by mitosis into 2-32 daughter cells, called microzooids. Following germination, the microzooids, small and biflagellate, settle and become palmelloid cells [223], called coccoids or encysts [234]. In this phase, as previously mentioned, if a stressful situation occurs, *H. pluvialis* after maturation, becomes "red non-motile astaxanthin accumulated encysted" (20 - 50 μm) (**Figure 30**) accumulating ASX in the centre of the cell inside small lipid drops that migrate to the cell surface to protect the cell from induced stress [235]. Carotenoids can neutralize free radicals and ROS, thanks to their molecular structure characterized by long terpene chains with conjugated double bonds. When the environmental or cultural conditions return to optimal, the red aplanospore germinate to form flagellated zoospores to initiate a new cycle of vegetative growth.

Most of the green stage cells of *H. pluvialis* are characterized by high protein content of 29 –45% by dry weight (dw) [236]. In red cells, the protein content decreases and is between 21% and 23% dw. Carbohydrates that allow the cell to survive during a prolonged stress, increase from 15–17% dw in the green phase to 60–74% dw in the red cyst. In the green phase, total lipid content ranges from 20% to 25% [237]. The carotenoid content increases in *H. pluvialis* cell from 0.5% dw in the green phase to 2–5% dw in the red phase. Lutein is the principal carotenoid of green cells (70-80% dw), while β-carotene (16.7% dw) represents the second pigment by quantity contained in the cell. The amounts of violaxanthin and neoxanthin are, respectively, 12.5% and 8.3% dw. The above compounds are not found in red cells or are present only in small quantities. The next pigment, mostly present in green cells, is chlorophyll, whose content is 1.5 –2% dw [223]
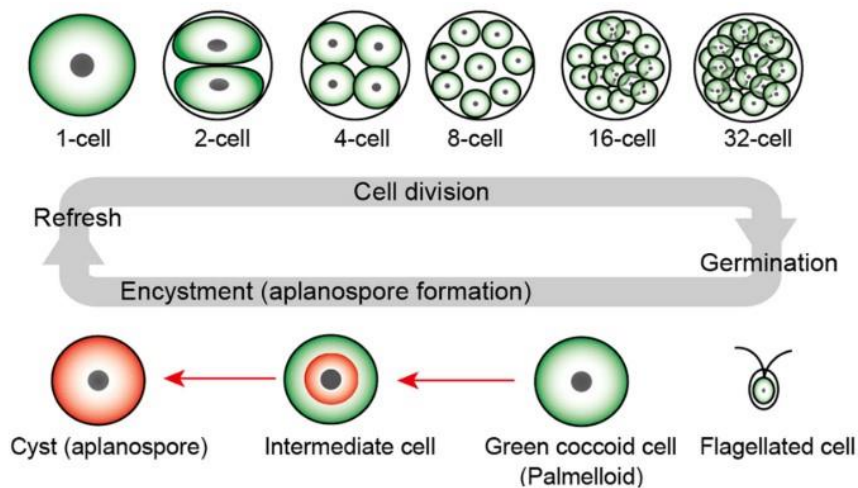
Figure 30 *Life cycle of Haematococcus pluvialis* [223]

In a recent study published by us (Radice, Fiorentino, et al., 2021), it was shown how it is possible to separate the different growth phases of *H. pluvialis* through the application of an electric field in an electrophoretic cell to optimize the production of ASX by isolating only the red non-motile encysted. This is possible thanks to the negative charge present on the cell wall. The innovation of the technique confirms the current knowledge on the conformation of the cell wall; it is known that during the encyst phase, the cell wall is rigid and thick (1.8–2.2 μm) and it consists of different layers, including trilaminar sheath (TLS), secondary wall (SW) and

tertiary wall (TW) [138]. TLS is formed by algaenan [139], an aliphatic, insoluble, resistant biopolymeric compounds [140], which could be responsible for the cell migration, having negative groups in its structure. Furthermore, the electric field separates the cell based on cell diameter at the different growth phases. For more information on the experiment conducted and results obtained, it is advisable to read section 8.1 and the attached article in Appendix 1.

5.1.1 Astaxanthin

Astaxanthin (ASX) is a carotenoid with formula $C_{40}H_{52}O_4$, with a molar mass of 596.84 g/mol, and, as previously mentioned, is a powerful antioxidant thanks to its characteristic chemical structure. The two ketone (-CO) and hydroxyl (-OH) groups at the end of the chain make the antioxidant activity, ten times higher than other carotenoids (e.g. β-carotene, lutein and zeaxanthin) and hundred times than α-tocopherol [239,240]. *H. pluvialis* is the primary source of ASX for the food industry due to the presence of the 3S, 3S 'astaxanthin isomer, which is the most effective for human application. In addition to 3S, 3S', there are also 3R, 3S' and 3R, 3R' isomers which differ in the configuration of the two hydroxyl groups on the molecule [241]. In humans, its absorption occurs in the intestinal mucosa via passive diffusion and reaches the liver via the lymphatic pathway and the circulatory system, enclosed in chylomicrons [242]. During this PhD project, we also analysed the ability of ASX to reduce obesity-associated diseases risk in animal models and discovering how the supplementation of ASX in the diet has positive effects on symptoms associated with obesity-related diseases in animals. We showed that ASX had lipid-lowering, hypo-insulin and hypoglycaemic capacity protecting organs from oxidative stress and mitigating the immune system [243]. ASX increased energy expenditure without affecting food intake and activated 5′ AMP-activated protein kinase (AMPK) in skeletal muscle, and upregulated expression of transcription factors, thus inducing mitochondrial remodelling that subsequently increased oxidative phosphorylation and β-oxidation of fatty acids [244]. ASX had a lipid-lowering effect, inducing the transcription of acyl-CoA oxidase 1 (ACOX-1), which is also responsible for the oxidation of fatty acid; ASX induced expression of the peroxisome proliferator-activated receptors (PPAR), a subfamily of nuclear receptors that control many different target genes involved in both lipid metabolism and glucose homeostasis [245], as PPAR increases the

expression of ACOX-1. ASX, by increasing the transcription of PPARα, improved transport, metabolism, and oxidation of FAs, and therefore, reducing their accumulation in adipocytes. This led to an increase in the levels of FA in the blood, especially high-density lipoprotein (HDL) [246–250]. The rise in HDL levels was due to the action of liver X receptor alpha (LXRα), which was increased by treatment with ASX whereas hepatic lipogenesis was blocked. ASX inhibited the phosphorylation of protein kinase B (Akt), inducing the expression of Insig-2α and consequently reducing sterol regulatory element-binding transcription factor 1 (SREBP1) and glycogen synthase kinase-3 (GSK3). In non-alcoholic fatty liver diseases (NAFLD), lipid accumulation is an important aspect of the pathology and ASX may reduce not only hepatic steatosis but may interfere with transforming growth factor beta 1 (TGF-β1) activity, a strong pro-fibrogenic factor [251]. For more information on the mechanism of action of astaxanthin, please refer to the attached article in Appendix 1.

5.1.2 Astaxanthin biosynthesis

The biosynthesis of ASX is a complex process up-regulated under stressful conditions during the "red" phase of *H. pluvialis* cultivation. Since astaxanthin is a secondary carotenoid, its synthesis is closely linked to the biosynthesis of primary carotenoids. At the beginning of astaxanthin biosynthesis, both higher plants and green algae share the same path until the formation of β-carotene [252]. Astaxanthin is synthesized from isoprene units (C_5H_8), which are the basic units for carotenoid synthesis (**Figure 31**) [223]. The first step for the biosynthesis of carotenoids is the sequential addition of 3 IPP molecules (isopentenyl pyrophosphate) to dimethyl allyl pyrophosphate (DMAPP) to obtain geranylgeranyl pyrophosphate C_{20} (GGPP). Isopentenyl pyrophosphate (IPP) can originate *via* two pathways: the mevalonate (MVA) pathway located in the cytosol and the non-mevalonate (MEP) located in the chloroplast. The metabolic pathway of mevalonic acid is an important pathway for the production of IPP and DMAPP, which serves for the biosynthesis of molecules involved in different processes, such as the prenylation of proteins, the maintenance of cell membranes, the biosynthesis of hormones, etc. In contrast to this pathway, plants and protozoa can use the MEP pathway to synthesize DMAPP and IPP [253].

Once GGPP has been obtained phytoene synthase (PSY) catalyses the condensation of two GGPPs to form the phytoene, while the expression of the *psy* gene is upregulated in *H. pluvialis* cells stressed with intense light (during the transformation from green to red cells).
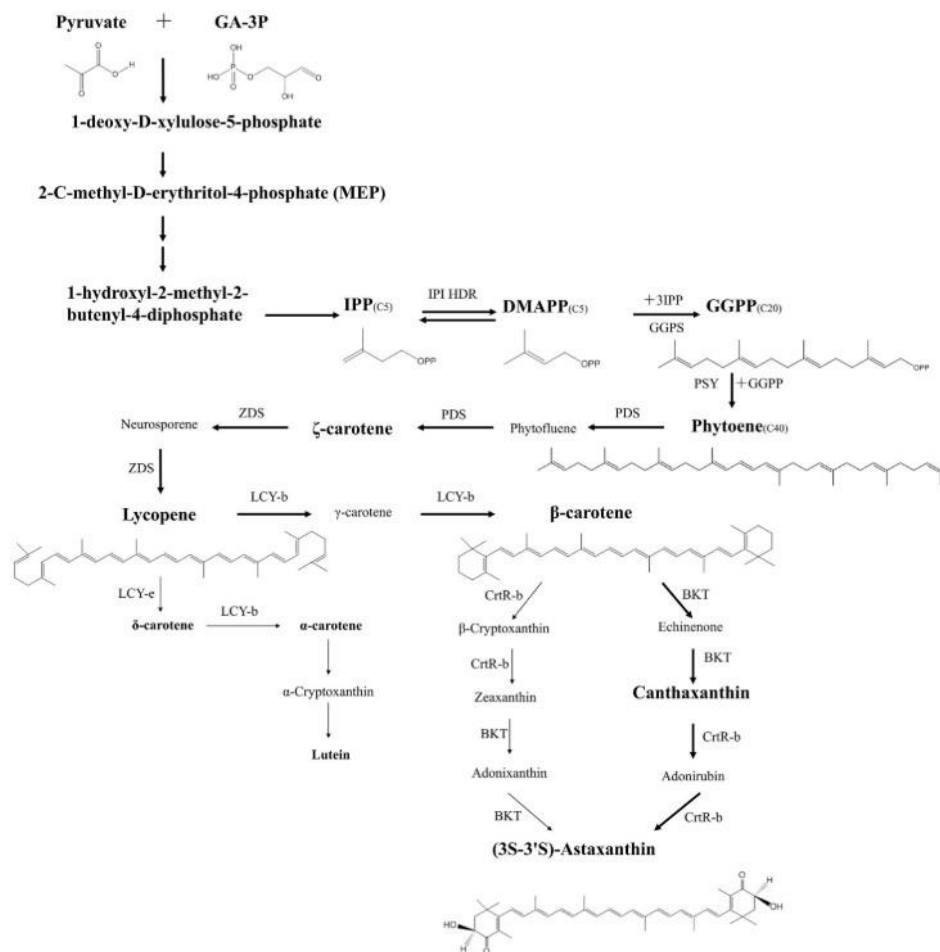

Figure 31 Pathway of (3S-3'S)-astaxanthin biosynthesis in H. pluvialis [223]

The conversion of phytoene into lycopene occurs with the following enzymes: phytoene desaturase (PDS) and carotene desaturase. Both lycopene end groups undergo cyclization catalysed by lycopene cyclase (LCY-e and LCY-b), and elevated levels of transcripts of LCY-b have also been observed under stress conditions [223]. Cyclization is the branching point of carotenoid biosynthesis in most organisms and involves the production of α-carotene (precursor of lutein) and β-carotene (precursor of other carotenoids, including astaxanthin).

Once β-carotene is formed, it can follow two pathways. In the first, β-carotene is converted into canthaxanthin through two ketolation steps catalysed by β-carotene ketolase (BKT); followed by two steps of canthaxanthin hydroxylation, catalysed by β-carotene hydroxylase (CrtR-b), leading to the formation of astaxanthin. In a second way, β-carotene hydroxylase (CHY-beta) converts β-carotene into zeaxanthin which, thanks to the action of BKT, is converted into astaxanthin [254]. There are three different bkt genes in *H. pluvialis*, *bkt1*, *bkt2* and *bkt3*. All β-carotene ketolase (*bkt*) genes are upregulated when *H. pluvialis* cells are subjected to various stressful conditions. In several studies, the transcription level of *bkt* genes in cells under normal growth conditions and "stressed" cells (treated with high light irradiation or high salt stress), was evaluated and under these conditions, high amounts of astaxanthin were produced. Therefore, the existence of multiple *bkt* genes and their upregulation under stress conditions can induce the high accumulation of astaxanthin in *H. pluvialis*.

PART 2: SPERIMENTAL SECTION

CHAPTER 6: AIM OF THE PROJECT

Nowadays, the use of fossil fuel, such as crude oil, is one of the most discussed problems around the world. The need to direct the world economy towards a "greener" and renewable formula brings to light all the problems caused by the petrochemical industry. The extraction and processing of crude oil generate air pollution, which attracts most of the media attention, and processing water, which is contaminated by hydrocarbons. The processing water constitutes a non-recyclable waste material that should be stored as a pollutant and has extremely high disposal costs. Moreover, the extraction of crude oil very often causes damage to groundwater and aquifers present near the extraction sites. With a view to environmental protection, microalgae constitute an important link between the "bio" and the industrial world, as they can be used as bio-restorers in environments and areas affected by hydrocarbon pollution. This is an aspect of particular importance in relation to the great impact that algae can achieve in terms of application and satisfaction of the principles of circular economy and, more generally, of the green economy. The aim of this project was to develop a new and innovative methodology, by using microalgae, to remove hydrocarbons of petroleum origin from aqueous matrices, in addition to create different genotypes capable of acting more efficiently than wild type (WT) microalgae. The choice of the target algal species, *Haematococcus pluvialis*, a unicellular alga belonging to the *Chloroficeae* class, derives from the high interest in this species because of the composition of secondary metabolites that can be biosynthesized. Through a selection process, high performing strains have been isolated and inoculated with matrices polluted with hydrocarbons. More specifically, liquid matrices containing crude oil were used to evaluate firstly their ability to survive in the presence of an extremely toxic contaminant, and subsequently to verify the algae's ability to use organic carbon deriving from petroleum, as a nutritional element. An additional aim of this project was to characterize the mutant strains that showed degradative activity. Specifically, differences at morphological level, in non-stress conditions, were first evaluated followed by the characterisation, on a transcriptomic basis, of the differences in expression in order to assess the degree of relationship between the different mutant strains and the WT genotype, both before and after the induction of stress-induced by crude oil.

CHAPTER 7: MATERIALS AND METHODS

7.1 Cell Growth

Culture of cells was performed in different testing media to evaluate optimal microalgae growth. The media and glass containers used for the cultures were autoclaved (VAPORMATIC 770, ASAL S.r.l.), for 20 minutes, at 1 atm and 120° C. The standard media (HC) composed by 0.3 gr of Greenhouse Special 20–20–20 (GS3X20) (BIOGARD) powder in 1 litre of distilled water, used in the initial phase is shown in **Table 3**. In 20 ml of each medium, 1 ml of *Haematococcus pluvialis* UTEX 2505 (HP), containing approximately 1.5×10^7 cells, was inoculated and cells were grown under a light intensity of 120 mmol photons m – 2s – 1 on a 16 h: 8 h light / dark cycle at 25° C.

Table 3: *GS3X20 (BIOGARD) powder composition.*

Components		Percentage Values (%)
Total nitrogen (20%)	Nitric nitrogen	6
	Ammonia nitrogen	5.2
	Urea nitrogen	8.8
Sulfur trioxide	soluble in ammonium citrate	20
	soluble in water	20
Potassium oxide	soluble in water	20
Boron	soluble in water	0.005
Cupper	soluble in water	0.001
	chelated in EDTA	0.001
Iron	soluble in water	0.2
	chelated in EDTA	0.2
Manganese	soluble in water	0.1
	chelated in EDTA	0.1
Molybdenum	soluble in water	0.005
Zinc	soluble in water	0.01
	chelated in EDTA	0.01

Cultures were not supplied with an extra source of CO_2 and were shaken by mechanical agitation (g24 environmental incubator shaker, American Laboratory Trading) at 70 rpm. Algal growth was assessed by measuring optical density at 750

nm (SPECTROstar® Nano, BMG Labtech) and cell counts by light microscopy (Zeiss Axioplan) using the Burker chamber (BLAUBRAND).

7.2 Mutagenesis and mutant strains' analysis

A new method was created to apply selective pressure and induce mutagenesis in WT algae. After finding the optimal growth conditions, 5 µl of HP were subjected to selective pressure and inoculated in 500 µl of pure crude oil. After four days, the crude oil drop was plated on fresh medium and allowed to grow for 25 days. Five different colonies were then collected (**Figure 32**) to obtain five different mutant strains called PA1001, PA1002, PA1003, PA1004, PA1005 and fresh plates with standard medium were inoculated. The mutant strains obtained were grown on fresh plates for 38 days to evaluate their adaptability, but, after seven days, one colony was isolated from each plate, and inoculated in fresh liquid media. Furthermore, mutant strains were grown in 4 different media to highlight the differences between them. In this case their growth was followed for 16 days by measuring optical density as described in section 7.1. Different media composition is shown in **Table 4**. Each media differs only for the solvent composition, in which 0.3 gr of Greenhouse Special 20–20–20 (BIOGARD) is dissolved.

STANDARD MEDIA plus CRUDE OIL

a)
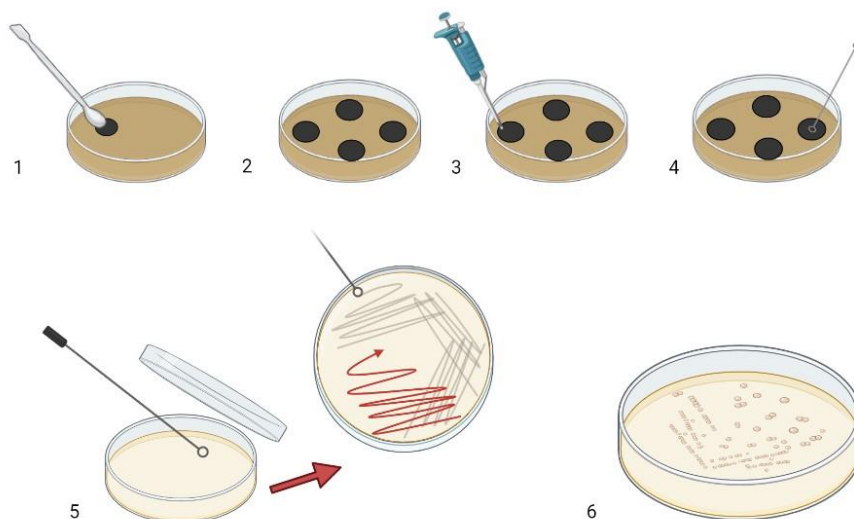
b)

Figure 32: Mutagenesis experimental scheme. a) Media for mutagenesis; b) methodology used to obtain selected colonies 1-2: wells creation; 3: microalgae injection 4: microalgae recovery; 5: microalgae plate; 6: colony isolation.

Table 4: Different growth media used.

Media	Ingredient	Solvent used
RC	0.3 gr/l of GS3X20	Water * not **autoclaved**
RCA	0.3 gr/l of GS3X20	Water * **autoclaved**
HC	0.3 gr/l of GS3X20	Distilled water **
HCS	0.3 gr/l of GS3X20 plus 0.3 g/l Magnesium sulphate (MgSO$_4$ 7H$_2$O)	Distilled water **

* **Water composition:** Water hardness (19° f); Fixed residue (271 mg/l); Arsenic (0.4 µg/l); Bicarbonates (215 mg/l); Calcium (55 mg/l); Free residual chlorine (0.9 mg/l); Chloride (15 mg/l); Total chromium (0.2 µg/l); Iron (14 µg/l); Magnesium (12 mg/l); Manganese (0.6 µg/l); Nitrate (NO2-) (1 mg/l); Lead (0.2 µg/l); Potassium (2 mg/l); Sodium (17 mg/l); Sulphate (35 mg/l); Trialomethanes (14 µg/l); Vanadium (1 µl/l). **** Distilled water composition**: No mineral salts, no gas dissolved

7.3 Bioremediation

Once optimal biomass was obtained for all mutant strains and WT in the standard media, three experiments were conducted. In Experiment 1 two different crude oil concentrations were tested (0.001 and 1%), by adding directly the crude oil in the media. In Experiment 2, instead, the same crude oil concentrations of experiment 1, have been sonicated in the media to improve microalgae degradation. In Experiment 3, subcultures of the mutant strains were carried out by inoculating 25 ml of HP in500 ml of RCA medium containing different percentages of crude oil (0.01%, 1%, 2%, 5%) in order to better evaluate the ability to remove the petroleum. The experiment was conducted in anaerobic condition and in duplicate. Growth was followed macroscopically by direct observation of the cultures. The subsequent analysis on the hydrocarbon components of Experiment 3, were carried out at the ACCREDIA accredited S.C.A Lab Service in Marconia following the standard procedures for their detection. An exploratory analysis was initially carried out after 10 days of bioremediation, analysing various parameters such as TOC, fluorides, chlorides, nitrates, sulphates and phosphates. After 40 days of treatment, analysis by gas chromatography-mass spectrometry (GC-MS) triple quadrupole (TQ) in full scan (FS), and by gas chromatography with flame ionization detection (GC-FID) were carried out to analyse hydrocarbons and oily substances present in the aqueous matrix and microalgae biomass. Subsequently, 150 ml of cell suspension from each culture after 20 and 160 days were taken. The samples were placed in a separating funnel and left to rest for five hours to separate and collect separately the three phases: microalgae biomass, aqueous phase and oily phase (**Figure 33**). A quantitative analysis was carried out on the concentrations of hydrocarbons present in the water and microalgae biomass. The protocols used at S.C.A. Lab are as follows:

- Aqueous phase extraction with hexane in a ratio of 1:10 with the quantity of water → liquid-liquid extraction in a separating funnel → filtration on packed column;
- Microalgae biomass extraction with hexane → filtration on packed column.

Each extract was filtered first on a Na_2SO_4 column for the analysis of oily substances (fats and oils + hydrocarbons), then on Na_2SO_4 and silica for the analysis of hydrocarbons.
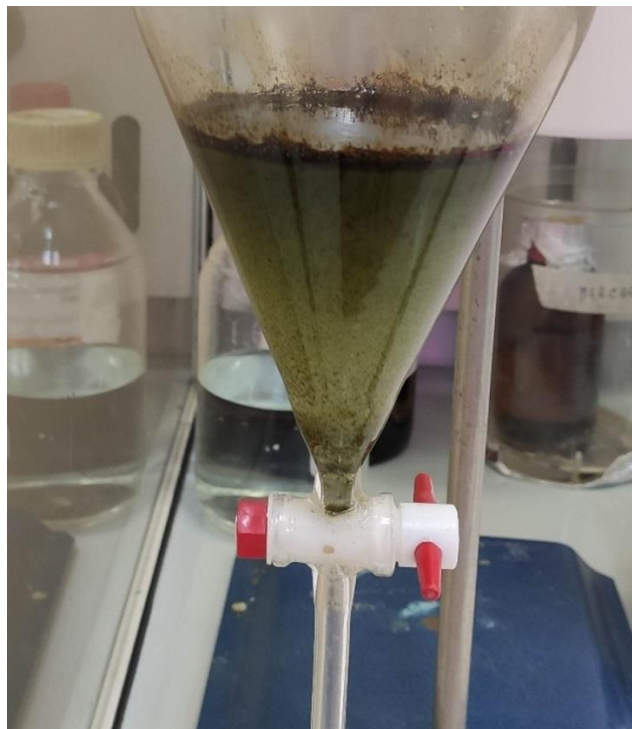
Figure 33: Separation of the three phases (biomass, aqueous phase and crude oil phase) through a separating funnel

7.4 RNA extraction and quantification

The extraction of total RNA from algal cells in suspension was carried out both on the mutant strains under optimal conditions and after 120 days of treatment with 1% petroleum, following the instructions and using the reagents contained in the NucleoZOL RNA Isolation kit (Marcherey- Nagel), which allows the extraction of the sample RNA at room temperature. The mechanical lysis of the algal cell wall took place using a sonicator (Bransonic® Ultrasonic Baths) at room temperature for 10 minutes. Subsequently, the homogenization of the sample was obtained by adding 500 µl NucleoZOL to each sample, with a cell density of about 5×10^6 cells/ml. Subsequently, 200 µl of H_2O were added to the crushed samples, and the

solution was centrifuged (with Sigma 1-15) for 15 minutes at 12000 g to allow the precipitation of the contaminants. The supernatant, containing the RNA, was removed and precipitated by adding 500 μl pure isopropanol. Generally, the precipitated RNA, obtained by centrifugation (at 12000 g for 10 minutes), appears, at a macroscopic level, as a whitish pellet deposited on the bottom of the extraction tube. After washing the pellet with 500 μl of 75% ethanol (ACS reagent, ≥99.8%, Honeywell Riedel-de HaënTM) and the subsequent centrifugation at 8000 g for 3 minutes to eliminate washing residues, the RNA was resuspended in RNase-free water (DEPC). The amount of total RNA was quantified using a spectrophotometric assay (NanoDROPTM 1000) using 1 μl of extracted RNA. Absorbance at 230 nm, 260 nm and 280 nm was measured to determine the purity of the analysed sample

• The ratio between A260 / A280 = index of contamination of the sample by proteins. The optimal values are 1.6-1.8 for DNA; 1.8-2 for RNA;

• The ratio between A260 / A230 = index of contamination of the sample by carbohydrates or solvents. The optimal values must be around 2.2 for both RNA and DNA.

7.5 Reverse transcription

Reverse transcription of RNA into cDNA was carried out to analyse the transcript. The reverse transcription was conducted using the FIREScript RT cDNA synthesis MIX with Oligo (dt) and Random primers kit (Thermo Fisher Scientific). Reverse transcriptase (1.5 μl), 2 μl of buffer containing dNTPs, polyT primers and random primers, and DEPC water were added to the RNA to reach a final volume of 20 μl. The reaction was carried out by incubation at 25 ° C for 10 minutes to guarantee the annealing of the primers, subsequently, at 37 ° C for 30 minutes to allow polymerization by the reverse transcriptase and finally at 85 ° C for 5 minutes to block the process.

7.6 RAPD-PCR

The analysis of the variability of expression of the various samples was evaluated by RAPD-PCR, which is a PCR (Polymerase Chain Reaction) reaction conducted using random primers. Random primers and 1µl of cDNA were added to a master mix (Phire Plant Direct PCR Master Mix - ThermoFisher Scientific), used to conduct the analysis, containing dNTP, Taq-polymerase, Reaction buffer and magnesium chloride. The primers used are shown below with their respective sequences (Table 4).

Table 5: *Primer sequences*

Primer	Forward	Reverse
1.1	5'-CTAGACGAGCCACCAGAT-3'	5'-TCGGCCAGACAAATGATG-3'
1.2	5'-CAGCTAGACGAGCATCTGTT-3'	5'-TCGGCCAGACCTTAAAAGTG-3'
3.4	5'-AGCTAGACGAGAACTTCTA-3'	5'-TCGGCCAGACACCATTGA-3'
4.1	5'-TAGACGAACTTCTGGTTGGA-3'	5'-TTTAATGGTGTCTGGCCGA-3'
5.1	5'-AGCTAGACGAAACACAGTTT-3'	5'-ATATTTTAAGGTCTGGCCGA-3'
6.2	5'-AGCTAGACGAGAGCAGTATA-3'	5'-AATTATGCTTGTCTGGCCGA-3'
7.1	5'-AGCTAGACGATCCTCCTCCA-3'	5'-ACATTACACAGTCTGGCCGA-3'

7.7 Gel electrophoresis

The amplification products were visualized on a 1.5% agarose gel. For the agarose gel preparation, 4.5 g of agarose (EMR010001, EuroClone S.p.a., lot no.468654) were weighed and poured into a flask containing 300 ml of 0.5 X TBE (Tris-Borate-EDTA) and 3 µl of Ethidium Bromide as intercalator. GeneRuler 1 kb DNA Ladder (Thermo Fisher Scientific) was used as a molecular weight marker. TBE (0.5 X) was used as running buffer. The gel was run, using PowerPac 3000, Biorad, at 80 V for 45 minutes. After the run, the bands obtained from the different samples were analysed to evaluate the differences between the 5 mutant strains.

7.8 Genetic distances analysis

Create dendrogram was generated using the Population Genetic Analysis program, in order to create a graphic representation for assessing the genetic distance, and therefore the differentiation process, which occurred between the mutant strains. To generate the dendrogram, it was necessary to evaluate the agarose gels obtained by using different primers. A comparison between the gels was carried out to highlight which primers on the same sample gave bands and which did not: a value of 1 was assigned if the band was present, 0 if not.

A matrix was generated (**Figure 34**) by repeating this procedure for all the samples. The samples number, total loci (bands considered), and their name were reported; by inserting the obtained the matrix into the program, it was possible to generate the dendrogram.

```
name = P1
fis = 0.0
01000100010 0000001001000 000000000000000 01010001000000001000000 000000000000000000 00001101001100010 1111011111011000000

name = P2
fis = 0.0
00000011100 0000000001000 000110010000101 00101010000000000000000 00001100100101000000 01000010100000010 0011000000000101100

name = P3
fis = 0.0
10101011100 1111110101001 111010100010011 10100110100100100101010110 1000000100011100000 1000000000000000 1001000000100010000

name = P4
fis = 0.0
00000111101 0010100001010 110101001010011 000001100100101001100110 0101100001000011000 00111001100010000 0010000000000100101

name = P5
fis = 0.0
00010110100 0000000010000 001000101011101 000000000100011110110101 0010101000101100011 00001011011101001 0000000111000011011

name = T
fis = 0.0
01010111100 0000000001011 101010010100100 0000010000101001101011101 0001000001000000111 00000011010101100 0000100000000011100
```

Figure 34: Matrix obtained following the elaboration of the amplification profile

7.9 Production of astaxanthin and extraction of carotenoids

The cultures were stressed by adding sodium chloride (NaCl) (8gr / L) to promote ASX production from *H. pluvialis*. The extraction of the carotenoids was carried out on days 0, 7 and 10 to evaluate the progress of astaxanthin production. The extraction protocol used, was developed by Wellburn et al.[255] and it is shown below.

- Take 1 ml of culture and centrifuge for 5 minutes at 14000 rpm at room temperature;

- Remove the supernatant and recover the pellet and add 1 ml of DMSO;

- Incubate for 10 minutes at 70 ° C;

- Centrifuge at 7000 rpm for 4 minutes;

- Collect the supernatant and analyse.

Once the carotenoids were extracted, absorbance at 480 nm (absorbance of carotenoids), 649 nm (absorbance of chlorophyll a), 665 nm (absorbance of chlorophyll b) were measured to evaluate the variation in the concentration of the pigments. The concentrations (μg / ml) of chlorophyll a, chlorophyll b and the total carotenoid content were calculated with the following formulas:

$Ca = 12.19 \times A665 - 3,45 \times A649$

$Cb = 21.99 \times A649 - 5.32 \times A665$

$C\ x+c = (1000 \times A480 - 2,14 \times Ca - 70.16 \times Cb) / 220$

CHAPTER 8: RESULTS AND DISCUSSIONS

8.1 *H. pluvialis* growth and astaxanthin production

The initial challenge of this PhD project was to identify the optimal growth conditions and learn how to control them for microalgae and specifically for *Haematococcus pluvialis*. Many conditions were tested, including i) the shape and material of the containers used to culture the algae and ii) the culture media with diverse nutrients and suspension solvents. However, once the optimal conditions were identified (reported in section 7.1), *H. pluvialis* growth followed the trend reported in the bibliography.
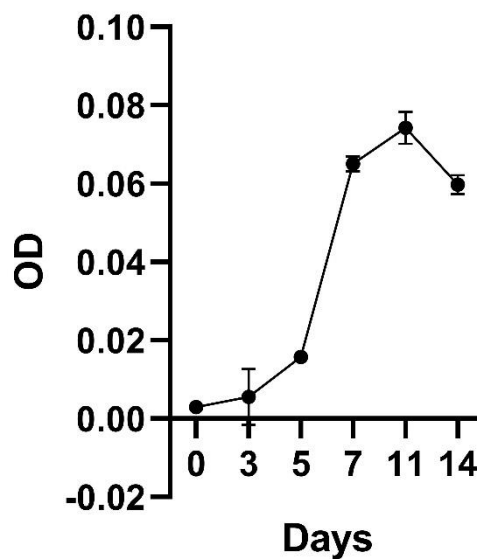
Figure 35: H. pluvialis growth. OD = 750 nm (Mean with SEM)

As shown in **Figure 35**, *H. pluvialis* growth followed a sigmoidal trend, with an adaptation or latency phase in the first three days of culture, followed by an exponential, logarithmic phase that ended in a stationary phase and finally in a decay phase around the fourteenth day. During the exponential phase, 1 ml of culture was withdrawn and re-inoculated in fresh medium to keep the culture healthy. The ability of *H. pluvialis* to produce astaxanthin, after inducing a stress

condition, was evaluated following the addition of sodium chloride. Given the peculiar morphology of *H. pluvialis* and its different growth phases, a protocol was developed to select the best growth phase capable of producing large quantities of astaxanthin. A careful literature review showed that the amount of astaxanthin produced was greater in cells in the encystic phase. Li et al., 2019 [256] showed how astaxanthin production is higher in non-motile cells than motile cells. Their results showed that the astaxanthin content in macrozooids was 1.94 times lower than in non-motile cells cultures. For this reason, through the application of an electric potential, the *H. pluvialis* cells were separated according to their size, using the negative charge present on their cell wall (**Figure 36**). The measurements showed that cells size recovered near the positive pole (C1) were 2.8 times smaller than cells recovered in the distal section (C3). In fact, cells at the positive pole have an average size of 5.7 μm in diameter. Proximal cells (C2) have an average size of 6.7 μm, whereas distal cells have an average size of 8.5 μm (**Figure 37**).
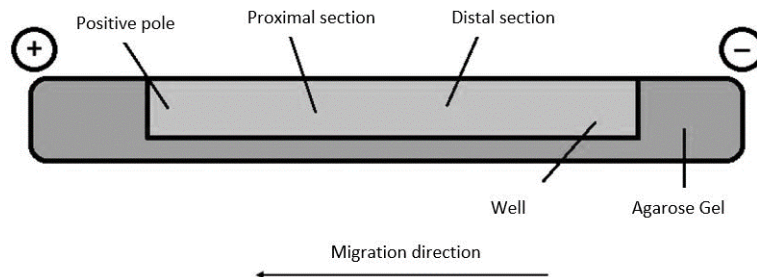
Figure 36: Schematic description of sample collection after the run
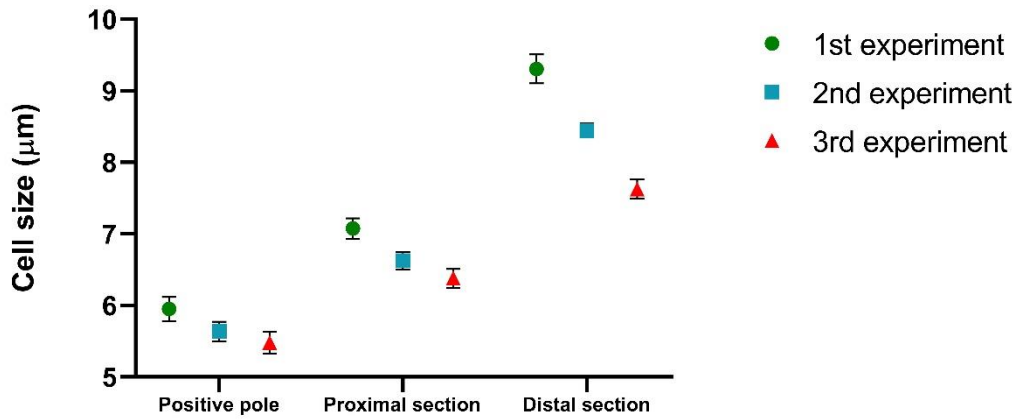
Figure 37: Cell size in a different section. Results shown cell size mean with SEM (p-value < 0.05). For each experiment, 180 cells were count (60 for each section).

Cell cultures were stressed with NaCl (1%) to evaluate if the selection of *H. pluvialis* cysts is advantageous for astaxanthin production. Chlorophyll and carotenoid content were measured every 4 days over the following 16 days using dimethyl sulfoxide (DMSO) as extraction solvent as described in section 7.9. ASX content is very low in each section at the start of salinity stress induction, but at the end, after 16 days, astaxanthin content was equal to 4.700 μg/ml−1 in C1, 5.843 μg/ml−1 in C2 and 9.081 μg/ml−1 in C3, showing that astaxanthin production is 1.93 times higher in C3 culture than C1 culture (**Figure 38**).
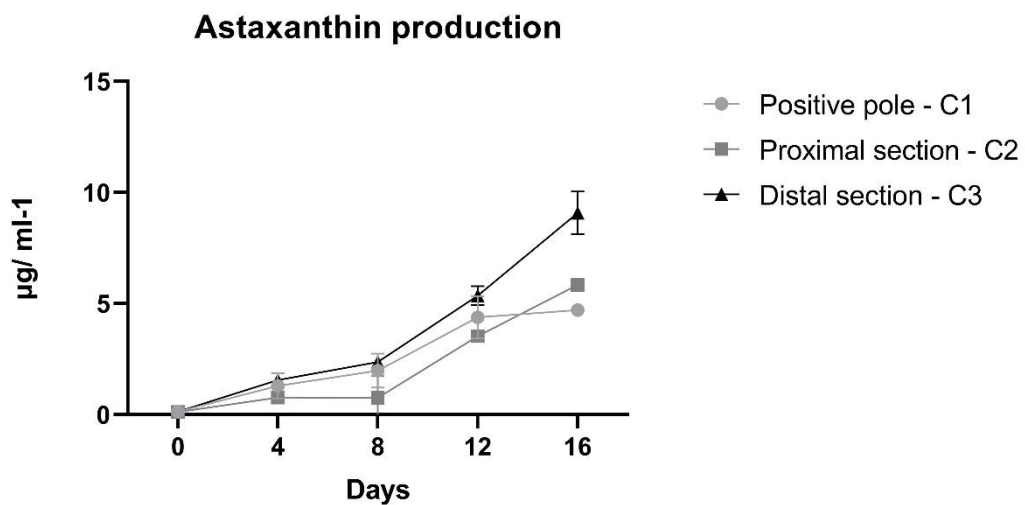
Figure 38: Concentration of astaxanthin produced in cultures after saline stress induction at 7th day of gel electrophoretic recovery (Mean with SEM)

8.2 Selective pressure and mutagenesis

Few *H. pluvialis* cells were inoculated in pure crude oil to evaluate their ability to survive at high concentrations of a toxic contaminant. Initially, the challenge was to understand how to test the microalgae survival capacity and evaluate their growth due to the difficulty of removing the crude oil from the algae. After several attempts, Petri dishes containing petroleum and in the created wells to allow the crude oil to collect have been created. As described in section 7.2, 5 µl of microalgae were inoculated into one of the wells containing approximately 500 µl of crude oil. The presence of a halo around the wells was expected to be evidence of algal growth and reduction of crude oil amount. After four days of incubation, no changes were noted inside the well, and, therefore, the wells content was placed on two fresh dishes using a loop (**Figure 32**). As shown in **Figure 39**, five colonies were isolated from the plating and were then re-plated on fresh plates.
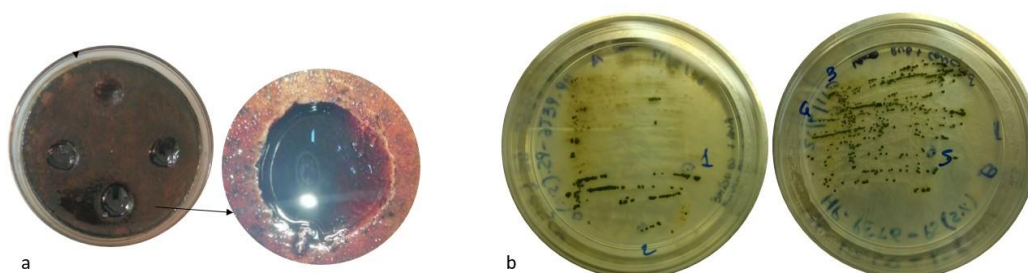
Figure 39: *a) Mutagenesis induction; b) colony selection*

Other colonies were subsequently isolated from the fresh plates and transferred to a liquid medium. The plates were left in nutrient deficiency for 38 days to evaluate astaxanthin production. The PA1004 mutant strain did not seem to produce astaxanthin, unlike the other mutant strains, which after 23 days, began to turn towards the characteristic red colour, given by the increase in astaxanthin (**Figure 40**). This first morphological analysis allowed to identify preliminary differences between genotypes. Subsequent microscopic analyses revealed structural differences in the cells. Mutant strains PA1001 and PA1003 showed a slightly different morphology than the WT. Their dimensions were smaller than the WT, and a more complex granulation within the cytoplasm was present. Cells with a

sickle-like conformation were also present in the PA1003 culture, probably caused by the different osmotic concentrations of the crude oil. This conformation disappeared in subsequent generations. The mutant strains PA1002 and PA1004, on the other hand, showed numerous vacuoles, especially PA1004, which appeared to be very sub-structured. PA1005 mutant strain was the most similar to the WT, with normal dimensions and morphologies (**Figure 41**).
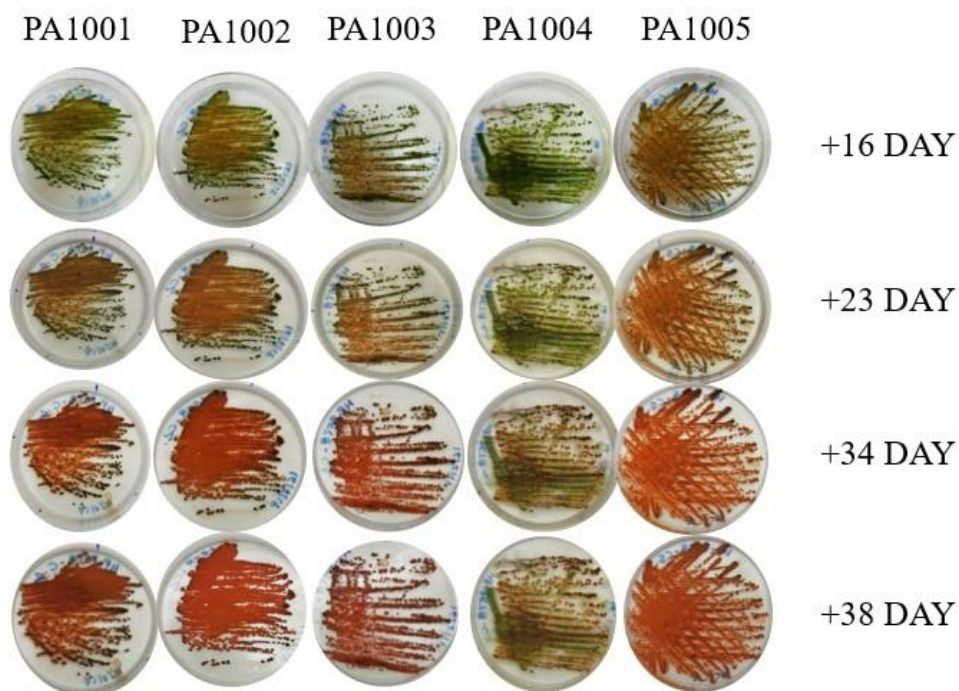
Figure 40: Astaxanthin production by mutant strains cells'
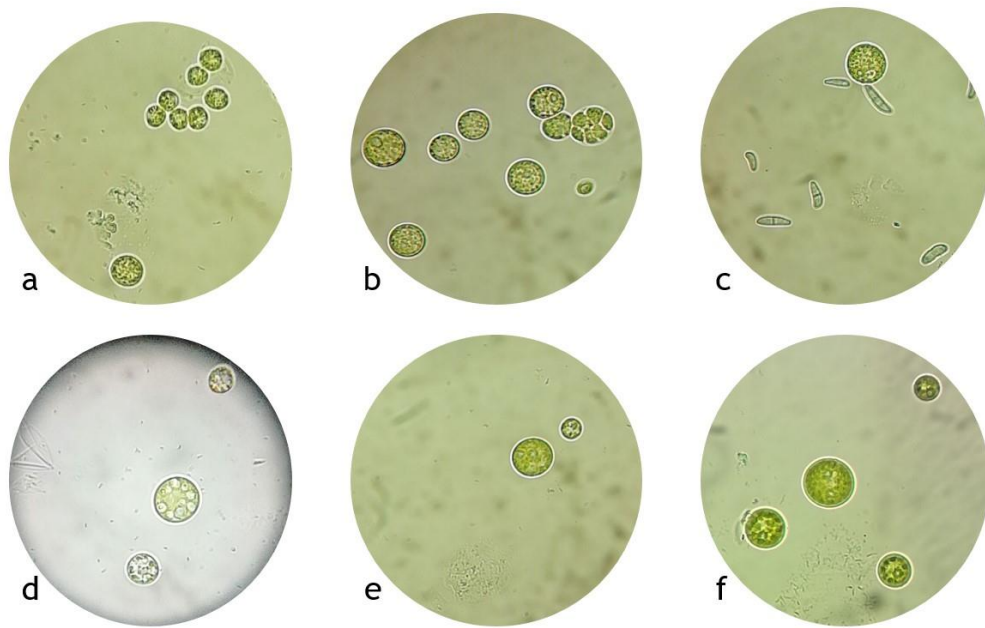
Figure 41*: Mutant strains 40x magnification. a) PA1001; b) PA1002; c) PA1003; d) PA1004; e) PA1005; f) WT*

8.3 Mutants strains

The growth of the mutants strains was assessed, after being inoculated into liquid medium, following the protocol described in section 7.1 and using the four media listed in **Table 4**. In **Figure 42**, 43 and 44, the growth curves for the mutant strains are reported. The mutant strains followed a different growth curve in the different soils, compared to the WT, which grew indistinctly in all 4 soils (**Figure 43f and Figure 44f**). Media suspended in distilled water are not very suitable for the growth of mutant strains. HC appears to be the worst terrain in which mutant strains struggled to grow. They not only took on an orange hue indicating unhealthy but also achieved extremely low growth rates compared to WT. The media containing water richer in mineral salts, RC and RCA, on the other hand, provided optimal growth conditions for the mutant strains and the growth rates also exceed the WT trend. However, these growth curves had the purpose of highlighting how mutant strains behave differently from the WT, confirming a genomic differentiation rather than highlighting possible differences between the mutant strains. If the modifications induced by the selective pressure were of an adaptive type, the mutant

strains would have had to behave like WT, once the optimal growth conditions were restored: this did not happen suggesting genetic changes occurred.
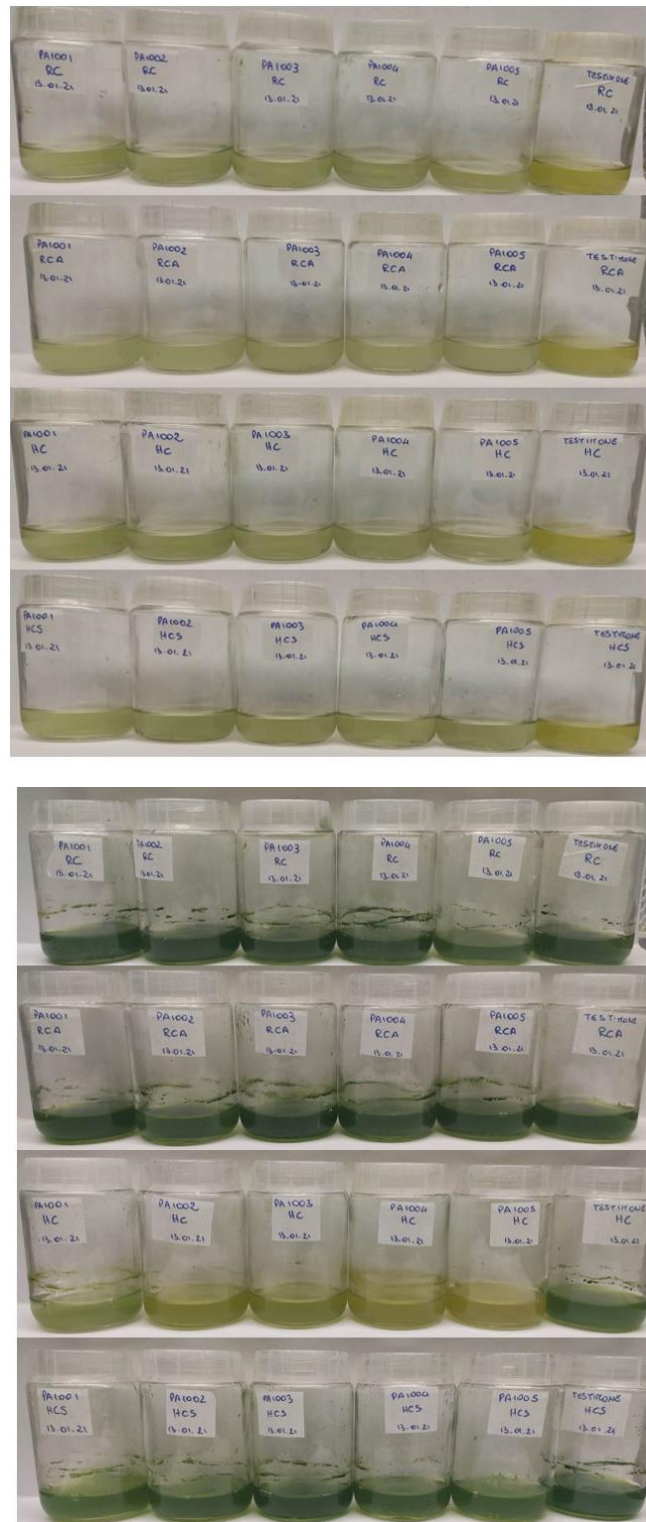
Figure 42: Mutant strains growth in different media

PA1001
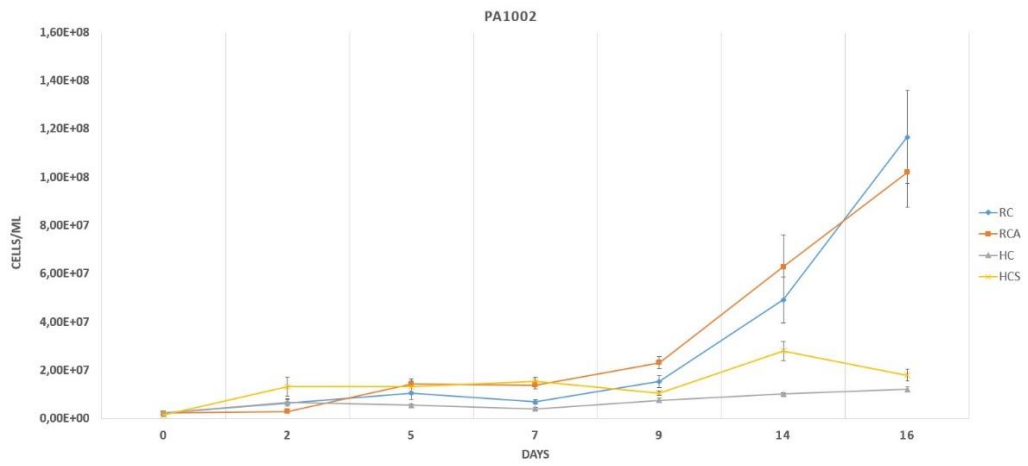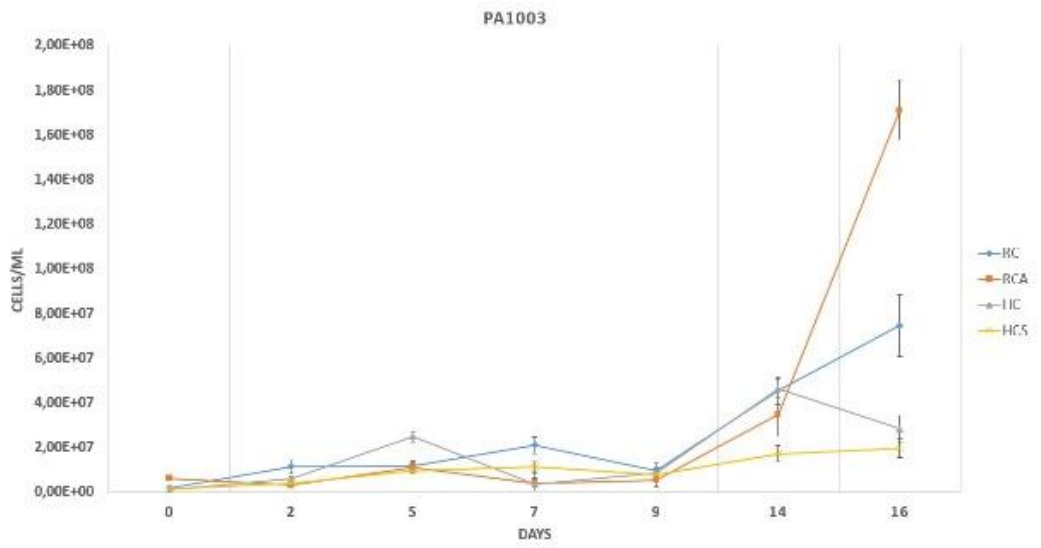
a

PA1002

b

PA1003

c

- 104 -
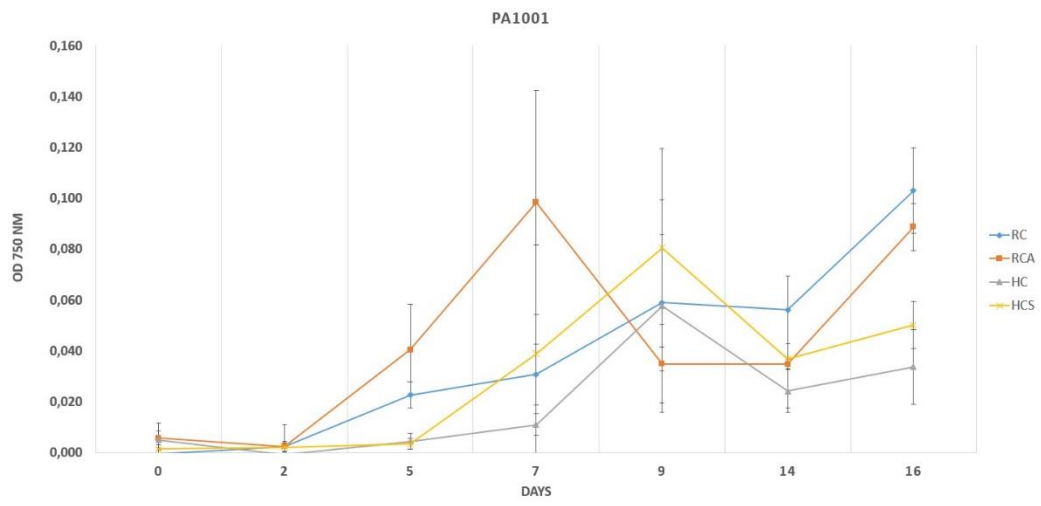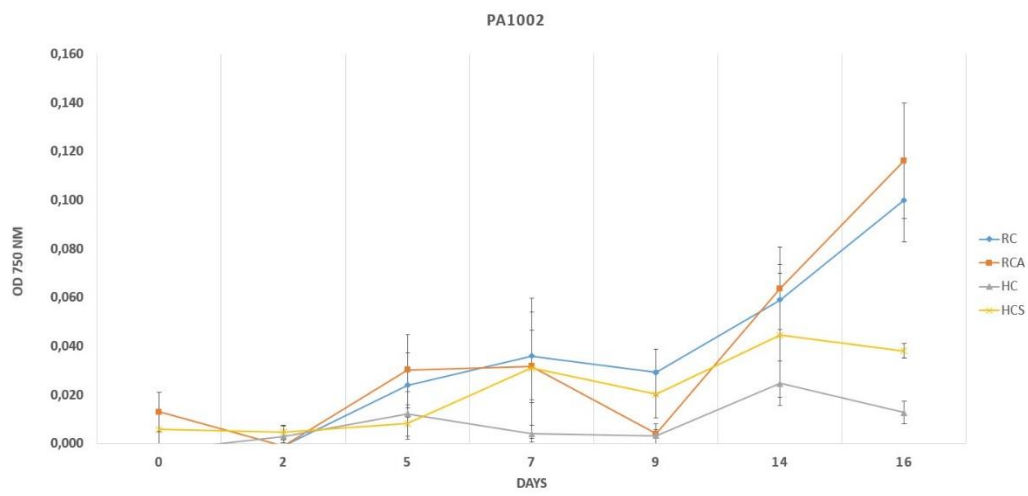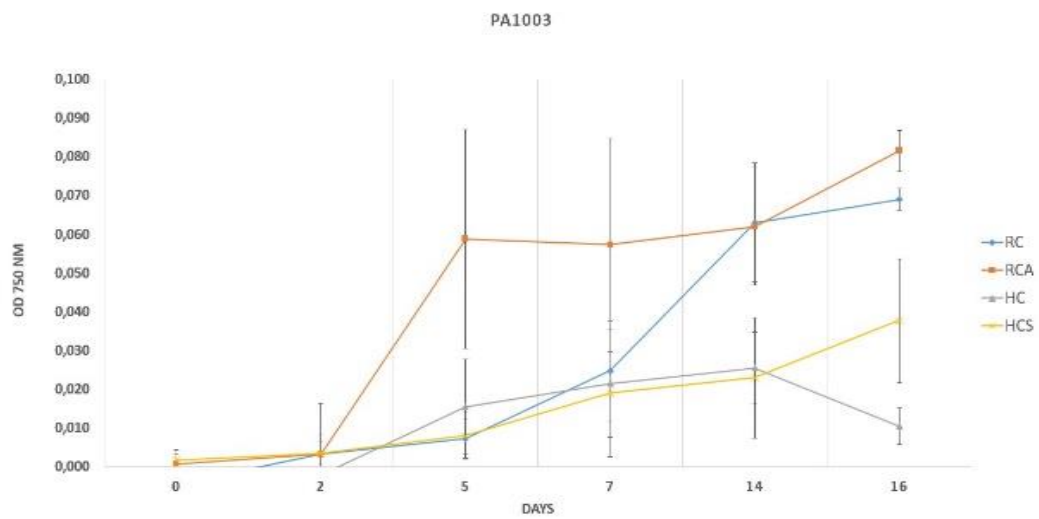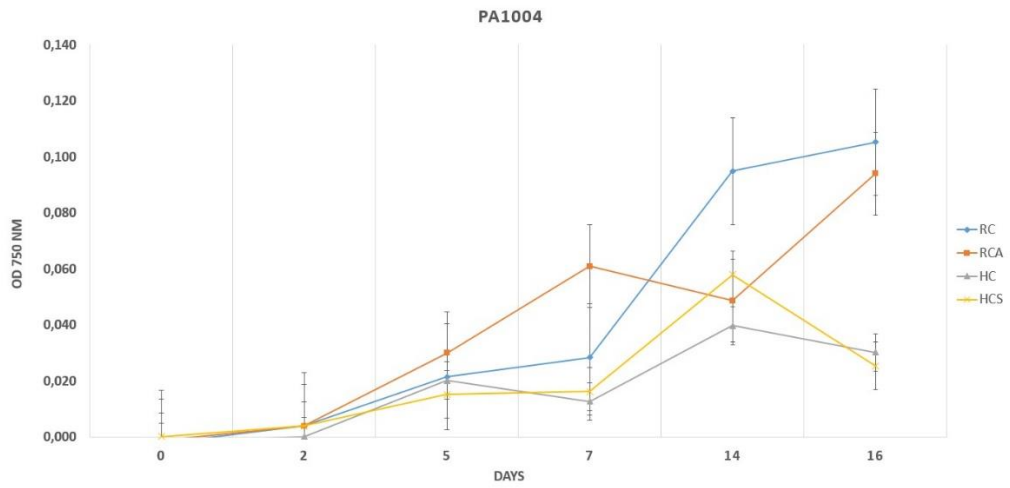
d
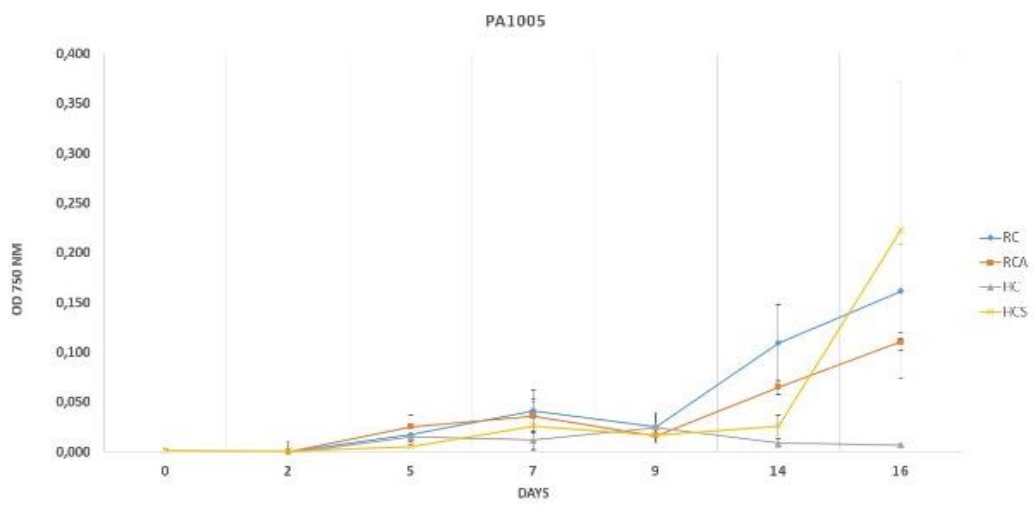
e
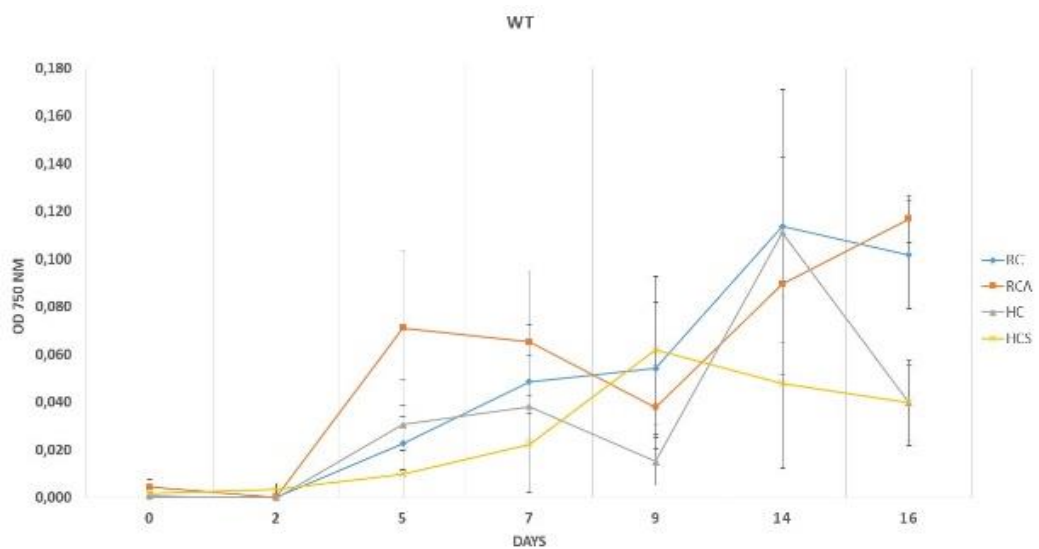
f

Figure 43: *Absorbance of each mutant strains in the different media (OD=750 nm). a) PA1001; b) PA1002; c) PA1003; d) PA1004; e) PA1005; f) WT (Mean with SEM)*
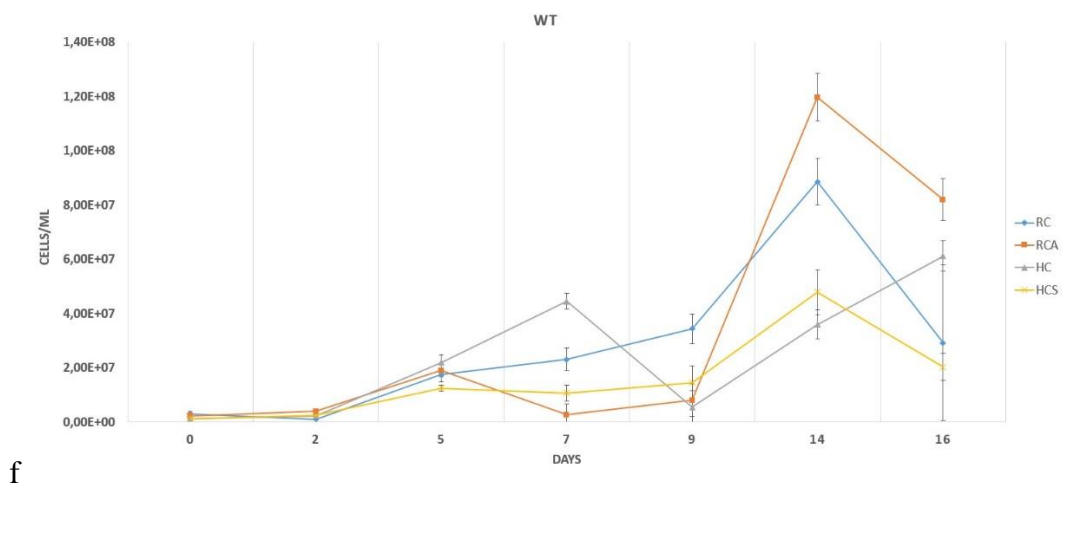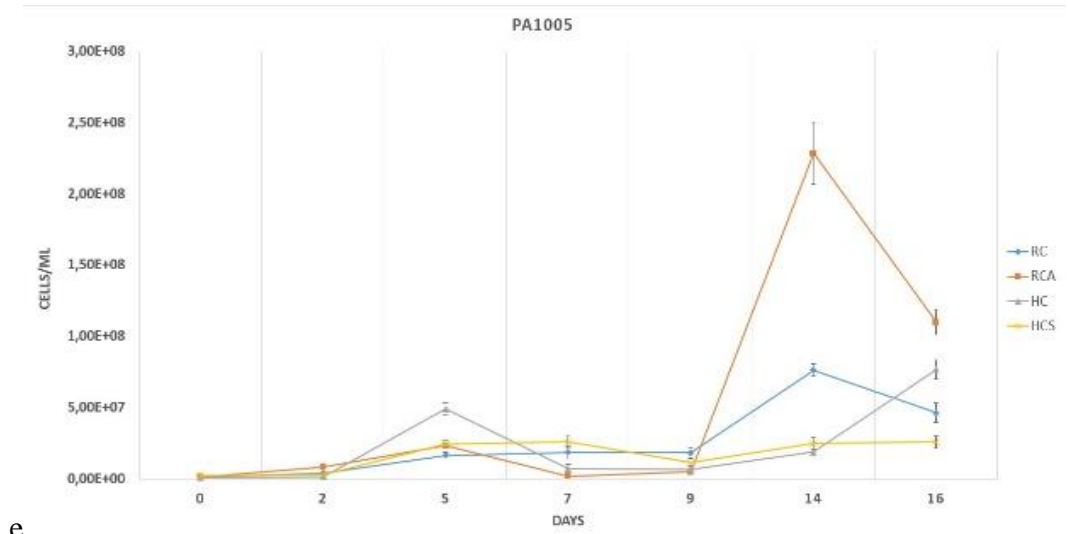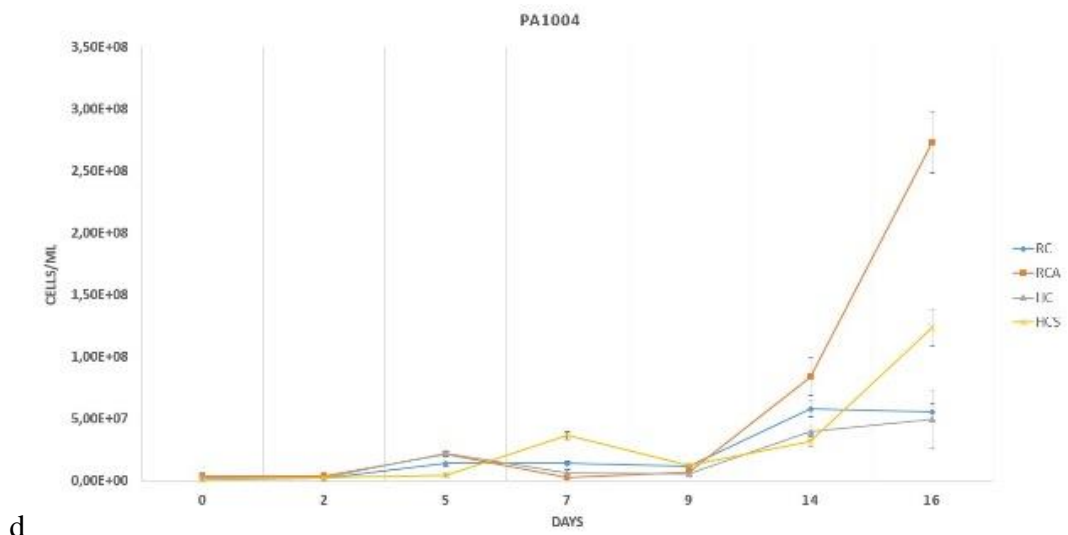
a

b

c

d

e

f
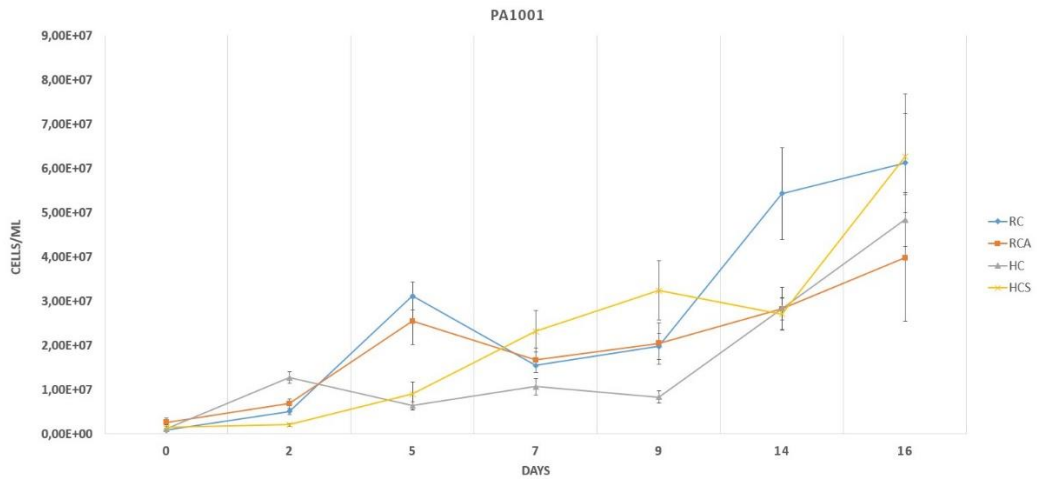
Figure 44: Cells number of each mutant strains in the different media (cells ml^{-1}). a) PA1001; b) PA1002; c) PA1003; d) PA1004; e) PA1005; f) WT (Mean with SEM)

8.4 Mutant strains astaxanthin production

The mutant strains were stressed with sodium chloride (NaCl) as described in section 7.9, and ASX production was followed for 18 days. The assay for measuring ASX was performed on day 0, 7 and 10. As it can be seen in **Figure 45**, the response of mutant strains to stress is different. The colour of mutant strains PA1001, PA1003 and PA1005 culture was different already after five days.

PA1001   PA1002   PA1003   PA1004   PA1005   WT
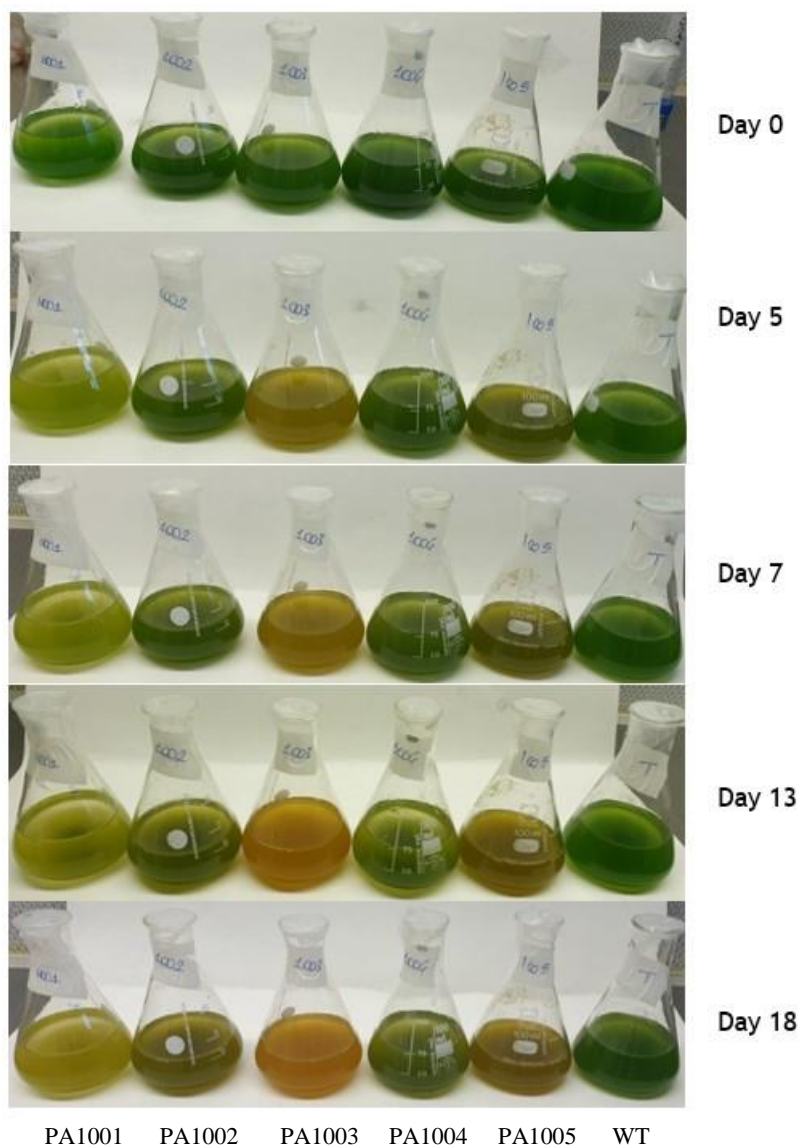
Figure 45: Mutant strains cultures and WT stressed with NaCl

The amount of extracted ASX (**Figure 46**), following the protocol described in section 7.9, reflected the morphological/colours trends observed in figure 45. PA1004 after 10 days produced only about 3 ng / μl, followed by the WT, which, instead, produced about 6.5 ng / μl. The behaviour of the different genotypes showed how selective pressure influenced the ability to perceive and respond to stress. However, analysing these data, it is not clear in what sense this change has occurred. PA1002 and PA1004 may fail to produce astaxanthin or the stress induced by incubation with salt was not sufficient to stimulate its production.
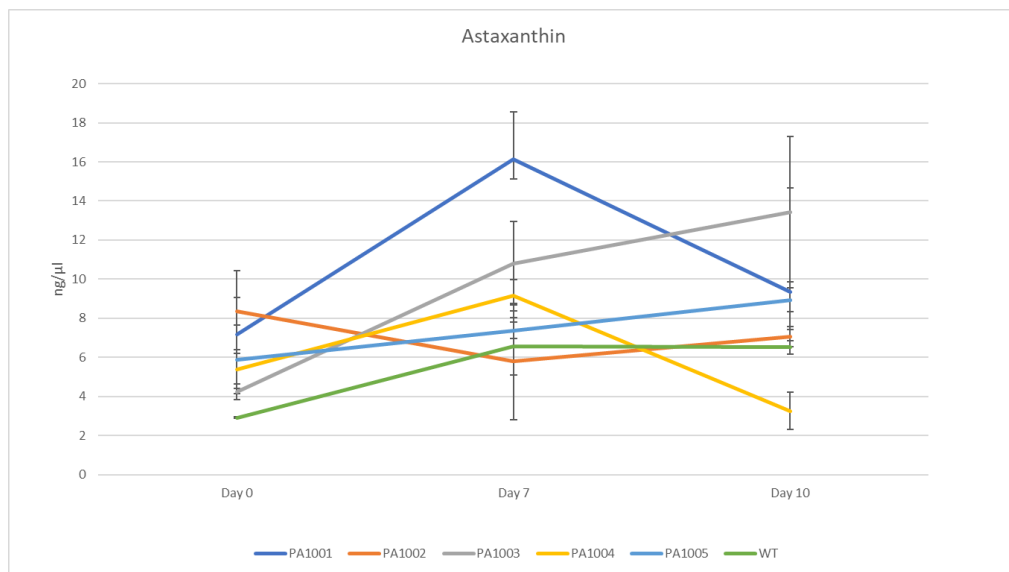
Figure 46: Mutant strains astaxanthin production (ng μl⁻¹) (Means with SEM)

8.5 Transcriptomic analysis

The spectrophotometric measurement with the Nanodrop allowed to determine the concentration of RNA extracted for the various mutant strains, which resulted in a concentration of about 950-1000 ng/µl, with good absorbance ratios 260/280 and 230/280, confirming that the extracted RNA was free from contamination by phenols and carbohydrates or by proteins. As described in section 7.6, different primers were used to highlight changes in transcriptional profiles of the five mutant strains compared to the WT. **Figure 47** shows how the amplification profiles for only one of the set of primers used changed markedly between the samples under analysis. These results support the hypothesis that differential transcription occurred following selective pressure, as also demonstrated in the following dendrogram. Using the Population Genetic Analysis program, as described in section 7.8, it was possible to obtain a dendrogram that allowed highlighting the differences between the five mutant strains and the WT, i.e. *H. pluvialis* before the treatment with crude oil (**Figure 48**). The genetic distances were calculated using UPGMA (Unweighted Pair Group Method with Arithmetic mean) method.
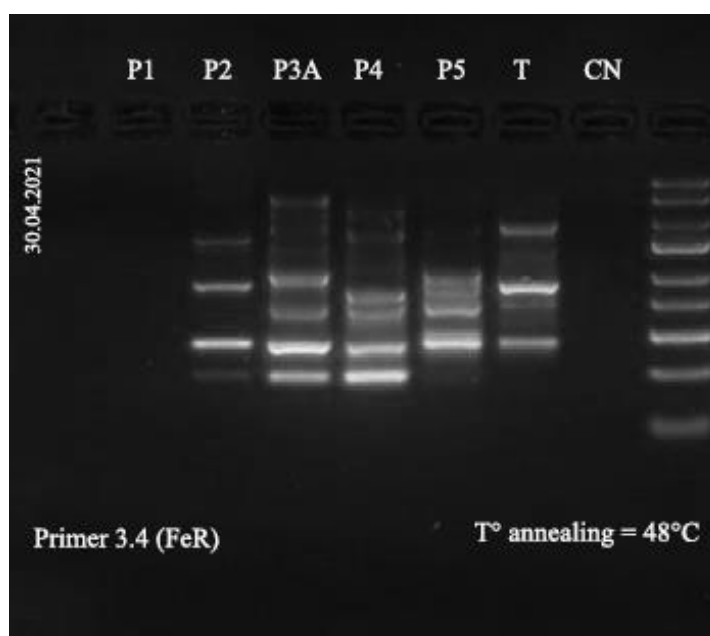

Figure 47: *RAPD-PCR with primer 3.4 (P1: PA1001; P2: PA1002; P3A: PA1003; P4: PA1004; P5: PA1005; T: WT; CN: Negative control)*
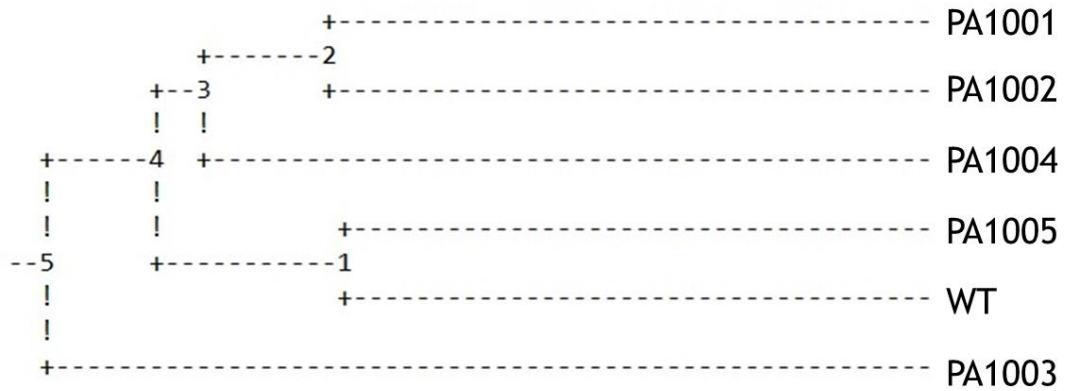
```
                      +------------------------------------ PA1001
        +-------2
    +--3            +------------------------------------ PA1002
    ! !
+------4    +------------------------------------ PA1004
! !        !
! !        !          +------------------------------------ PA1005
--5    +----------1
!          +------------------------------------ WT
!
+----------------------------------------- PA1003
```

Figure 48: Dendrogram of the different species of H. pluvialis before treatment with crude oil

The dendrogram divided the 6 strains into two main clusters. PA1001, PA1002 and PA1004 were grouped in Cluster 1, while PA1005 and WT constituted Cluster 2. The mutant strain PA1003 was separated from the other species under analysis. From the dendrogram, it was possible to see how the mutant strains generated were divided into 5 groups. Compared to the WT, mutant strain PA1005 was the one with a lower genetic distance D = 0.4532. The second group was formed by PA1001 and PA1002 which have a genetic distance equal to D = 0.4666. The two clusters have a genetic distance equal to D = 0.5824. The mutant strain PA1003, as previously mentioned, resulted to be the one farthest away genetically with a D = 0.6333 with respect to cluster 1 (PA1001, PA1002, PA1004) and from Cluster 2 D = 0.6003.

8.6 Bioremediation: morphological analysis

Different crude oil concentrations and different solubilisation methods were tested, in the first instance. For these reasons, different experiments were conducted.

8.6.1 Experiment 1

In the first experiment, two concentrations of crude oil (0.01% - 1%) were compared, using it directly inside the medium (not sonicated **Figure 49**). Growth was followed for 21 days to assess *H. pluvialis* survival and tolerance rate.
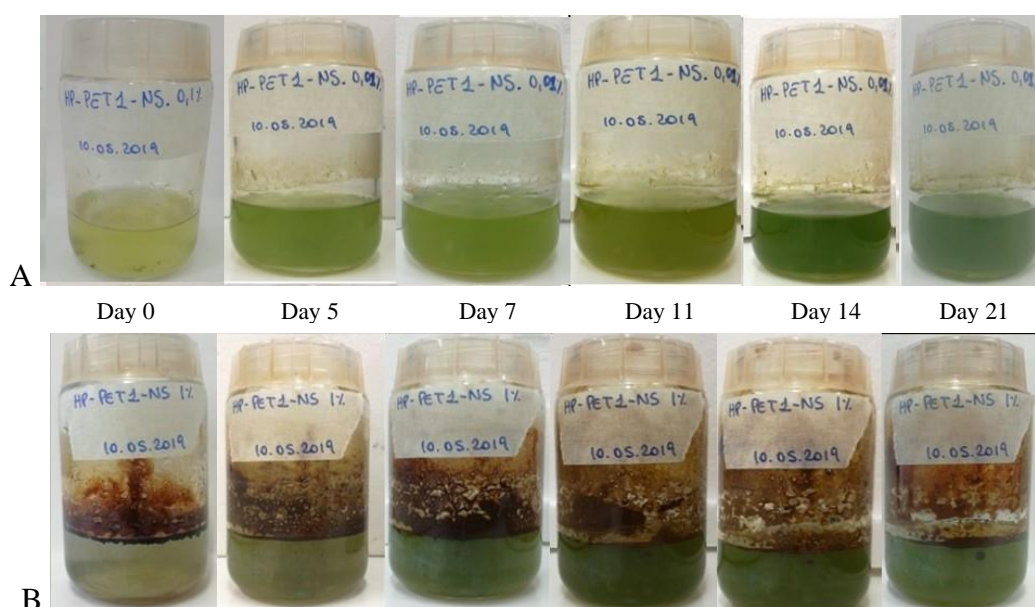

Figure 49: Microalgal growth in not sonicated petroleum. A) 0.01 %; B) 1 %

At macroscopic level, both cultures grew optimally compared with not stressed culture. The culture with 0.01% crude oil reached an optimal colorimetric concentration on day 14, whereas the culture with 1% crude oil reached such concentration already on day 11. It was immediately evident that. in both cases, but especially in the presence of higher concentrations, the crude oil had heavily soiled the container, mixing little with the microalgae which therefore had little contact with the pollutant.

8.6.2 Experiment 2

Given the poor success of the first experiment, it was decided to favour the contact of the algae with the crude oil by sonicating the crude oil in the culture medium before inoculating the microalgae, keeping the previous concentrations constant (0.01% and 1%) (**Figure 50**). In this case, the greater availability of crude oil within the medium allowed the crop containing 1% of crude oil to grow earlier. On the seventh day, optimal growth was already evident. In contrast to the un-sonicated counterpart, the culture containing 0.01% petroleum grew more slowly, reaching optimal growth only between day 14 and day 21.


| Day 0 | Day 5 | Day 7 | Day 11 | Day 14 | Day 21 |
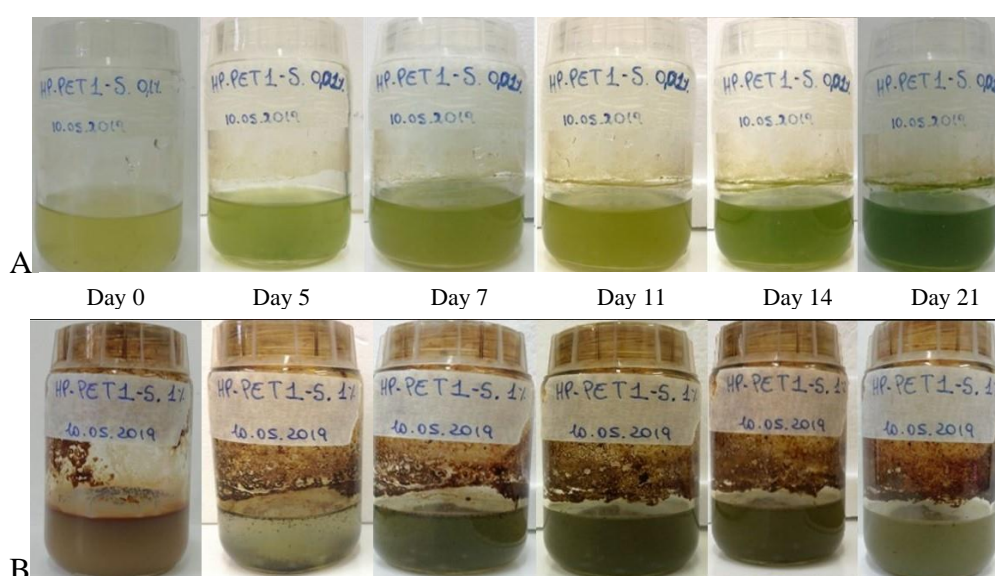
Figure 50: Microalgal growth in sonicated petroleum. A) 0.01 %; B) 1 %

8.6.3 Experiment 3

Experiment 2 was repeated by varying the crude oil concentrations, using 2% and 5%. However, using very high concentration, the level of adhesion with the container was extremely high, making it impossible to visualize the growth and, above all, hindering the passage of light, thus creating a variable that could affect cells growth and give erroneous results. For this reason, 1% of crude oil was found to be the optimal concentration. In experiment 3, all genotypes were tested. Volumes were increased and 5 ml of crude oil were sonicated in 500 ml of the standard growth medium, and subsequently, 25 ml of stock culture, containing approximately 1.5×10^{7} cells/ml, were inoculated.

The experiment was conducted in anaerobic conditions and duplicate. Growth was observed at 40, 97 and 240 days (**Figure 51** and **Figure 52**). On day 0, the cultures were similar, with a brownish colour and a thick oily layer on the surface (**Figure 51A**). After 40 days, however, the behaviour of the mutant strains began to differentiate. The WT showed an oily layer on the container walls whereas PA1001, PA1002 and PA1005. PA1003 and PA1004 showed cleaner walls. Colour of the suspension also indicated differential behaviour: while PA1001, PA1003, PA1005 and WT were green, PA1002 and PA1004 exhibited an unhealthy, brownish colour (**Figure 51B**).

A
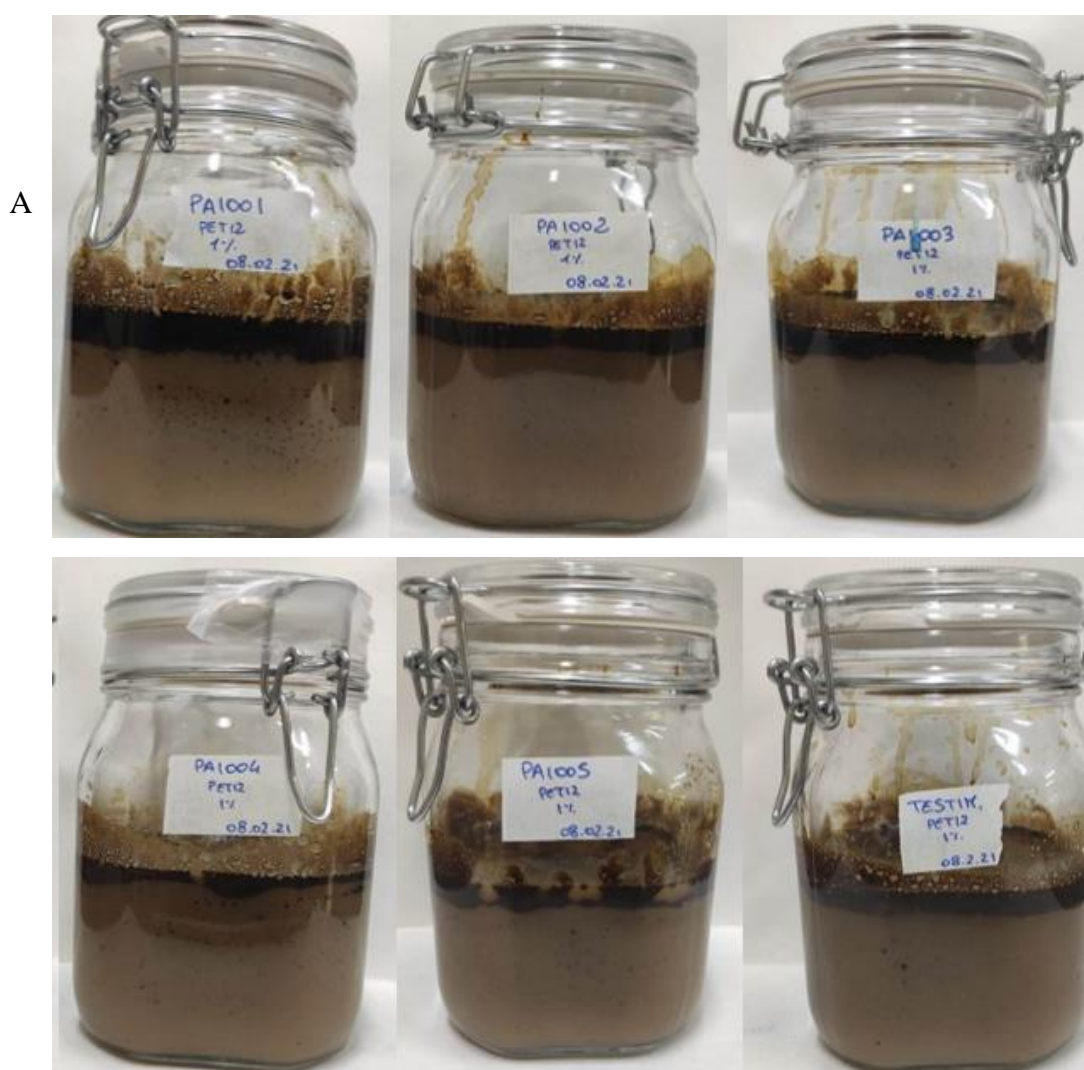
Figure 51: Experiment 3 growth. A= day 0; B = day 40

After 97 days, however, the situation was extremely different. All containers of the mutant strains were clean and free of oily residues (except for PA1002 whose container still had some halo). Algae growth was optimal in WT, where the bright green colour indicated healthy cell growth. PA1005 had an intense colour, but on the bottom, some spheres tended to deposit. Similarly, PA1001 and PA1003 had a bright colour with residues on the bottom. Unlike the other mutant strains, PA1002 appeared to have a higher growth range despite the oily residues on the walls, while PA1004 retained a brownish tint usually attributable to a dead culture.
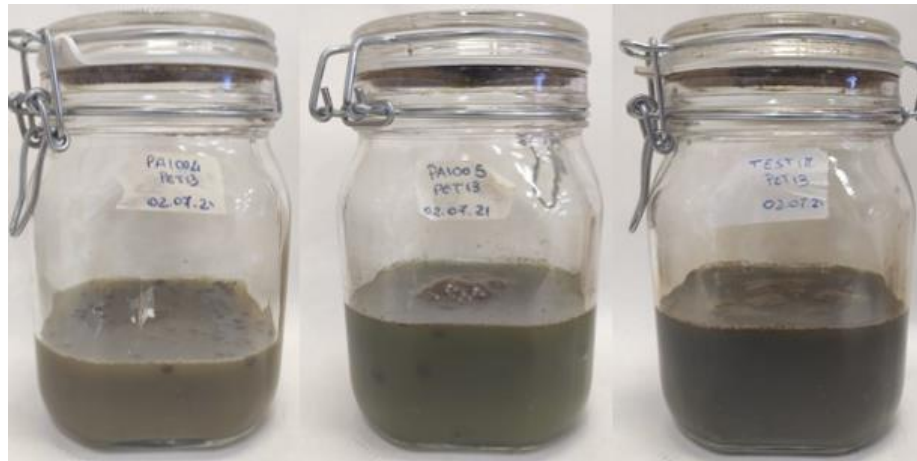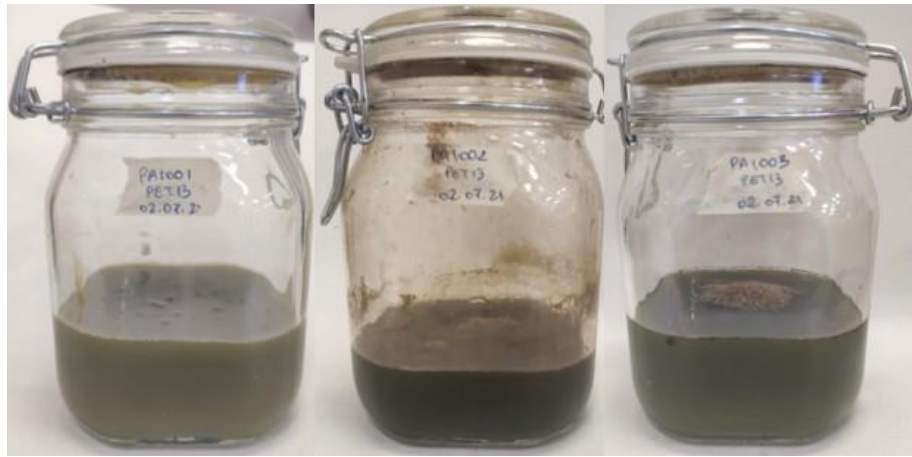
*Figure 52*: *Experiment 3 growth. A= 97 days; B=240 Day*

It was decided to extend the experiment to 240 days, at the end of which all the mutant strains showed different characteristics. PA1001 and PA1003 showed standard colour, attributable to good cell growth, with few residues on the walls and no type of agglomerate on the bottom. PA1005 and WT, on the other hand, although they showed good staining and optimal cell growth, had a considerable amount of residues on the walls. However, PA1002 and PA1004, despite the colour, showed extreme cleanliness of the container, making it impossible to find any trace of the inoculated crude oil. The PA1002, but especially PA1004, showed a particular characteristic: a foamy layer on the surface, capable of lasting over time, especially it was still present following agitation. The presence of this foamy layer supports the hypothesis of the possible production of saponins by the mutant strains that have helped to remove any oily traces from the container, which were found to be the cleanest ever.
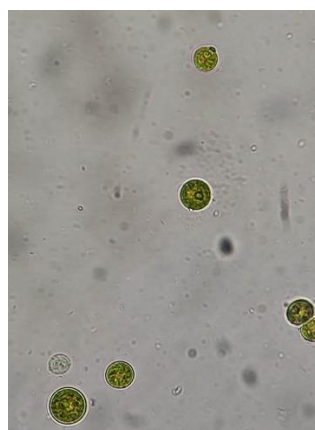
8.7 Microscopically observation

All mutant strains were observed by electron microscope as described in section 7.1 both before the crude oil treatment and after 150 days (each image below was acquired at 40x magnification).
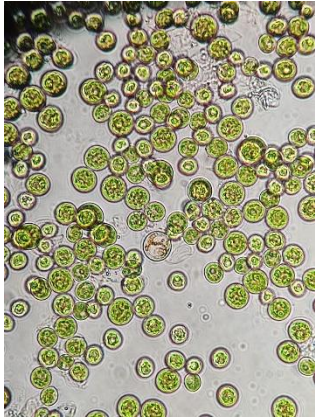
PA1001

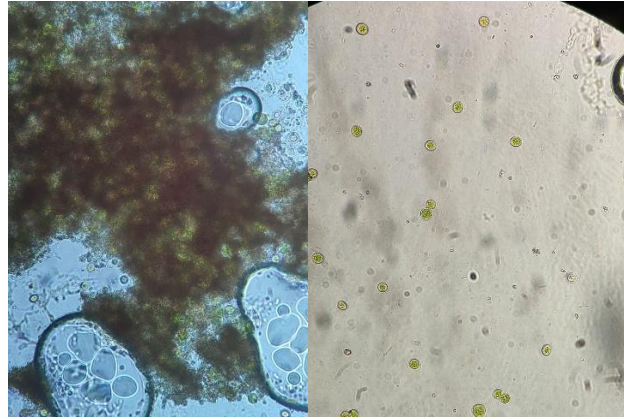No stressed   Post-petroleum
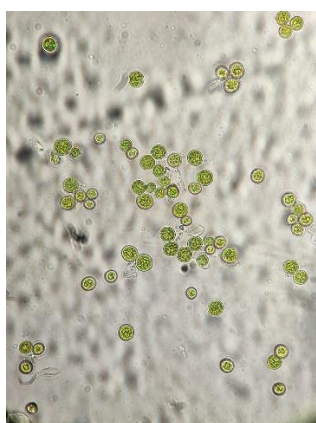
In not stressed culture, PA1001 cells were green, healthy and in divisions. In post-petroleum cells were bigger, alive and with a pyrenoid in the centre.

PA1002

No stressed   Post-petroleum

In not stressed culture, PA1002 cells were green, healthy and very aggregate, in fact, the cells of the liquid culture did not remain suspended but immediately settled to the bottom. In post-petroleum culture, cells were smaller and less green. Many crude oil droplets were present, with many cells attached.

PA1003
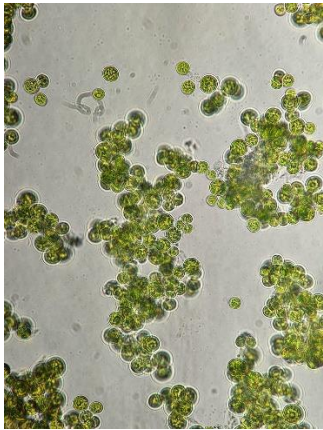
No stressed   Post-petroleum
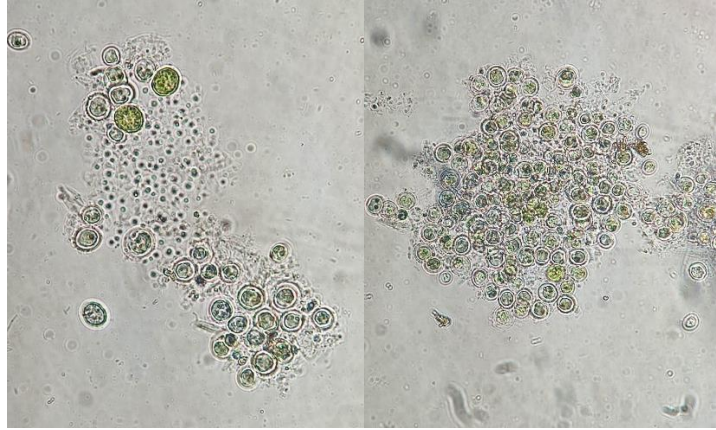

In not stressed culture, PA1003 cells were green, healthy. No particular signs present. In post-petroleum culture, cells were green and normal. Present crude oil in the slide, not blotchy like 1002, but very oily medium.

PA1004

No stressed   Post-petroleum

In not stressed culture, PA1004 cells were very green, healthy and numerous. In post-petroleum culture, cells were clear and uncoloured. The liquid culture had a brownish colour suggesting a state of ill health. Despite this, many cells were dividing.
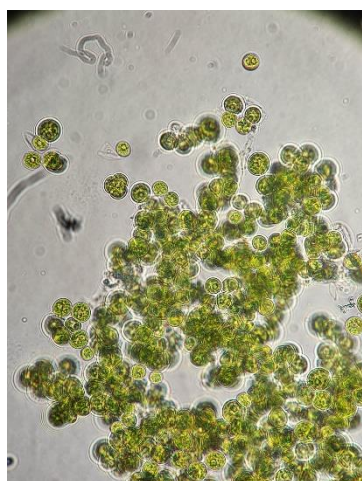
PA1005
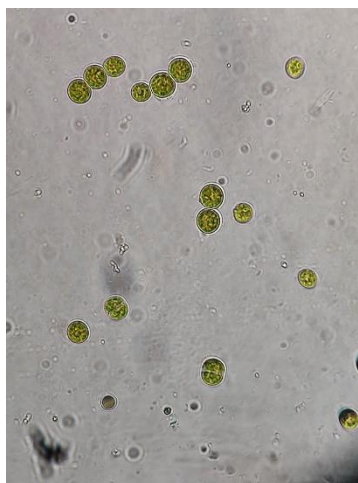
No stressed   Post-petroleum

In not stressed culture, PA1005 cells were green, healthy. No particular signs present. In post-petroleum culture, cells had a typical coloration of astaxanthin production; as for PA1003, very oily medium.

WILD TYPE

No stressed   Post-petroleum

In not stressed culture, WT cells were green, healthy following *H. pluvialis* characteristics. In post-petroleum culture, instead, cells were bigger and in the division, but as for PA1005, cells had reddish colouration.

8.7.1 PA1004

As seen above, the cells of the PA1004 strain were free of chlorophylls and were colourless. One ml of the stressed culture was re-inoculated in 20 ml of standard medium, without crude oil, restoring optimal conditions to assess whether this strange attitude was attributable to the presence of crude oil inside the medium (**Figure 53a**). After 20 days, the culture was green and viable and the cells, viewed under the microscope, were all pigmented, green and healthy, with only sporadic unstained cells (**Figure 53b**). This result highlighted how the cells activated an adaptive mechanism that led to a silencing of the production of pigments and, probably, chlorophylls. It is hypothesized that this could have happened because the culture changed its metabolism from autotrophic to a mixotrophic one, mainly using the organic carbon provided by the crude oil instead of the missing carbon dioxide.
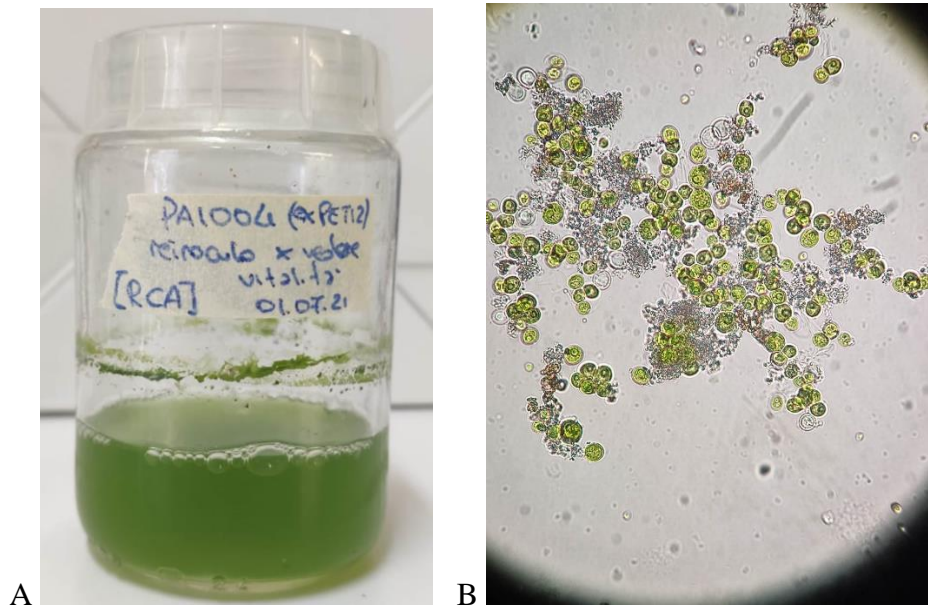
Figure 53: A) PA1004 re-inoculated in fresh standard media; B) Cells at 40x magnification

8.8 Post petroleum transcriptomic analysis

After 120 days of treatment with petroleum, the RNA was extracted again to evaluate possible changes in the transcriptomic level induced by petroleum. Also in this case, the spectrophotometric determination with the Nanodrop allowed determining the concentration of RNA extracted for the various mutant strains, which resulted in about 950-1000 ng/µl, with good absorbance ratios 260/280 and 230/280, confirming that the extracted RNA is free from contamination by phenols and carbohydrates or by proteins. The same primer set described in section 7.6, were used. **Figure 54** shows how the amplification profiles for only one of the set of primers used changed markedly between the samples under analysis. These results support the hypothesis of differentiation that occurred following the selective pressure, and petroleum treatment, as finally demonstrated also in the following dendrogram. Using the Population Genetic Analysis program, as described in section 7.8, it was possible to obtain a dendrogram that allowed highlighting the differences between the five mutant strains and the wild type (T), after the treatment with crude oil (**Figure 55**). The genetic distances were calculated using UPGMA (Unweighted Pair Group Method with Arithmetic mean) method.
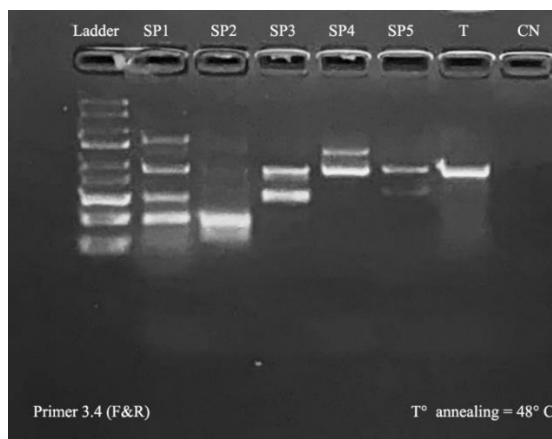
Figure 54: Post Petroleum treatment RAPD-PCR with primer 3.4 (SP1: PA1001;SP2: PA1002; SP3: PA1003; SP4: PA1004; SP5: PA1005; T: WT; CN: Negative control)
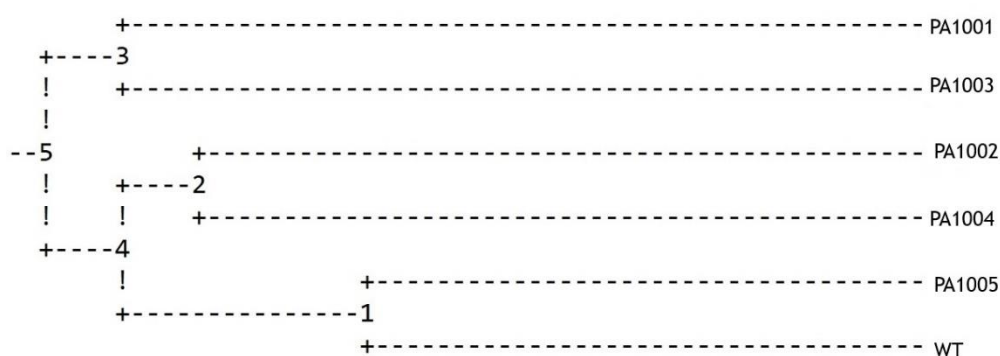

Figure 55: Dendrogram of the different species of H. pluvialis after treatment with crude oil

After 120 days of treatment with crude oil, the dendrogram showed a different division between the mutant strains if compared with the situation shown in **Figure 48**. The dendrogram generated five groups. From these 5, it's possible to identify two main subgroups, the first one composed of 2 different clusters. Cluster 1 (PA1005 and WT) and Cluster 2 (PA1002 and PA1004); the second one included cluster 3 (PA1001 and PA1003). Cluster 1 formed by mutant strain PA1005 and WT had a genetic distance D = 0.3761. Cluster 2 formed by mutant strains PA1002 and PA1004 had a genetic distance D = 0.4911. Therefore, cluster 1 and cluster 2 were separated by a genetic distance of D = 0.5835. The second group with cluster 3 presented a genetic distance of D=0.5411, and the calculated distance between the two main groups was D = 0.6871.

8.9 Analytical analysis

8.9.1 Preliminary analysis

After ten days of stress, the preliminary results were obtained by S.C.A. Lab, showing how in the water, nitrites, which initially were 58 mg / l, were totally absent after ten days in all genotypes, including WT, and the amount of organic carbon (TOC) has almost doubled. At day zero, 22.8 mg/l of TOC were in the aqueous phase, whereas after only 10 days, the value almost doubled for all genotypes. The PA1002 genotype increased the value by 2.15 times, reaching 49 mg/l, while PA1004 increased by only 1.8 times, reaching 42 mg/l (

Figure 56).

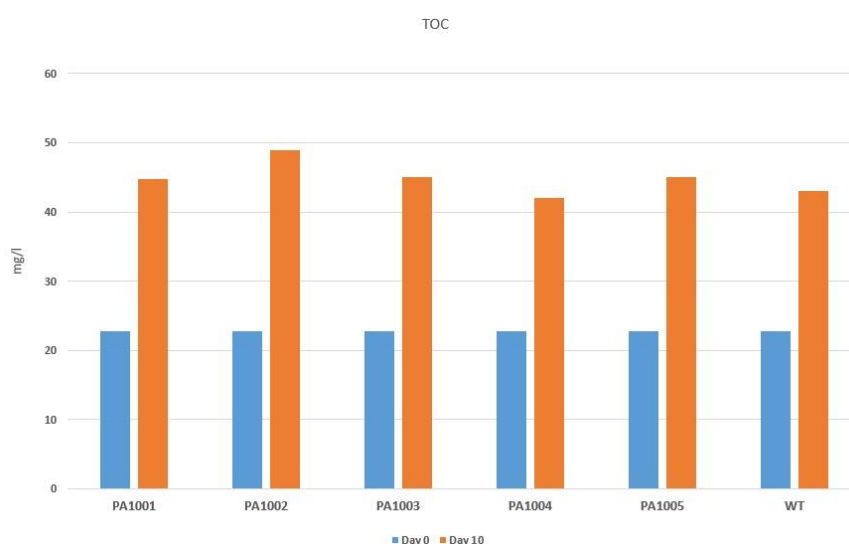**Figure 56:** Total Organic Carbon in water after 10 days of petroleum stress

The analyses of the components illustrated in section 7.3 showed differential trends both between the various genotypes and between them compared with the WT. The concentration of chlorides in the aqueous medium on day zero was equal to 10.5 mg/l, and after 10 days, the values increased by about 3%, reaching maximum values of 13 mg/l (**Figure 57**).
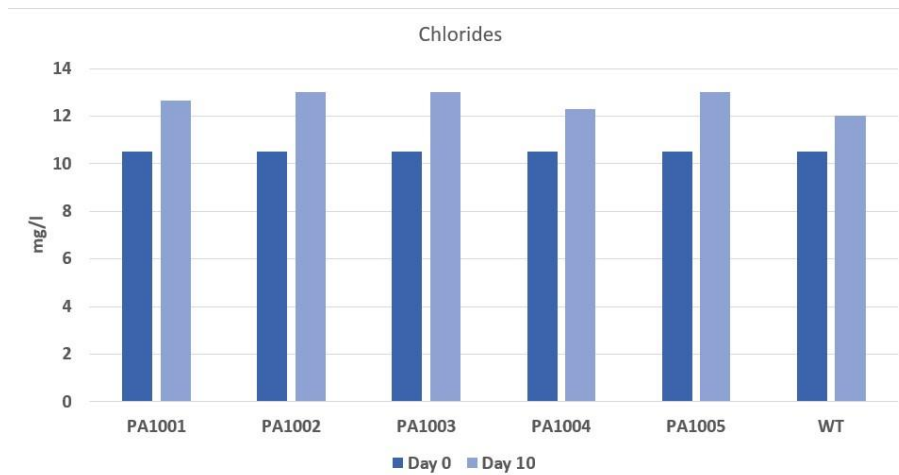
Figure 57: Chlorides in water after 10 days of petroleum stress

Conversely, nitrates and fluorides decreased after stress. The nitrates were initially equal to 0.7 mg/l, and after ten days, the reduction was higher of 70% in WT, PA1002 and PA1003, reaching 0.2 mg/l. However, PA1004 increased the nitrate values in the middle by 1.68 times, reaching 1.17 mg/l. PA1004 activated a different metabolic mechanism after ten days, comparing only these three values (TOC, chlorides and nitrates). The fluorides, which initially amounted to 0.2 mg/l, were similarly halved by all genotypes except for PA1005, which did not act on this element. (**Figure 58**).
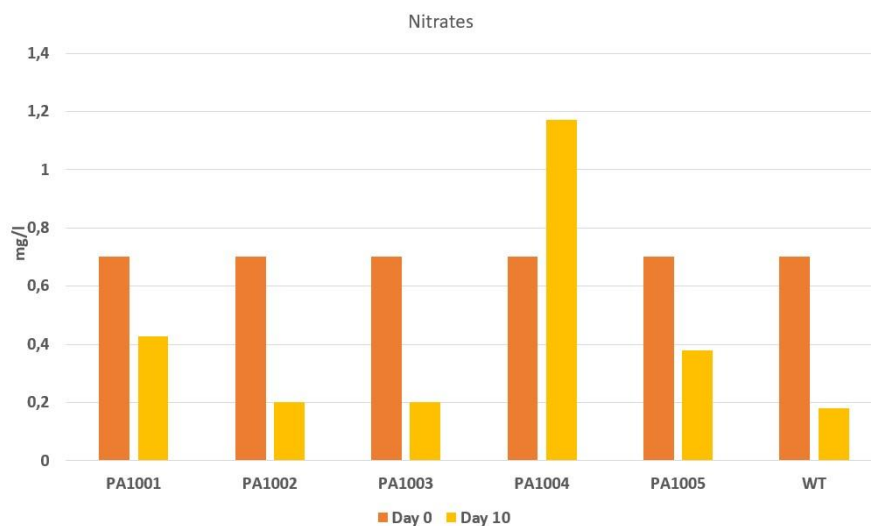
a
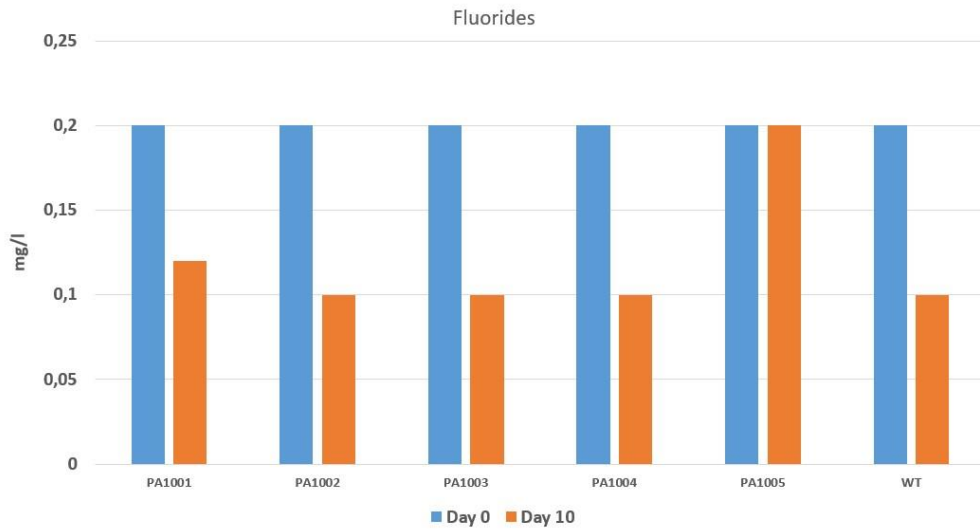
b

Figure 58: a) Nitrates and b) Fluorides in water after 10 days of petroleum stress

Sulphates and phosphates have undergone a minimal reduction by all mutant strains even when compared with the WT, which in these cases seems to have been the most performing, reducing the sulphates from 10 mg/l to 7.8 mg/l and phosphates from 68.4 mg/l to 52 mg/l (**Figure 59**).

a

Figure 59: a) Sulphate and b) Phosphates in water after 10 days of petroleum stress

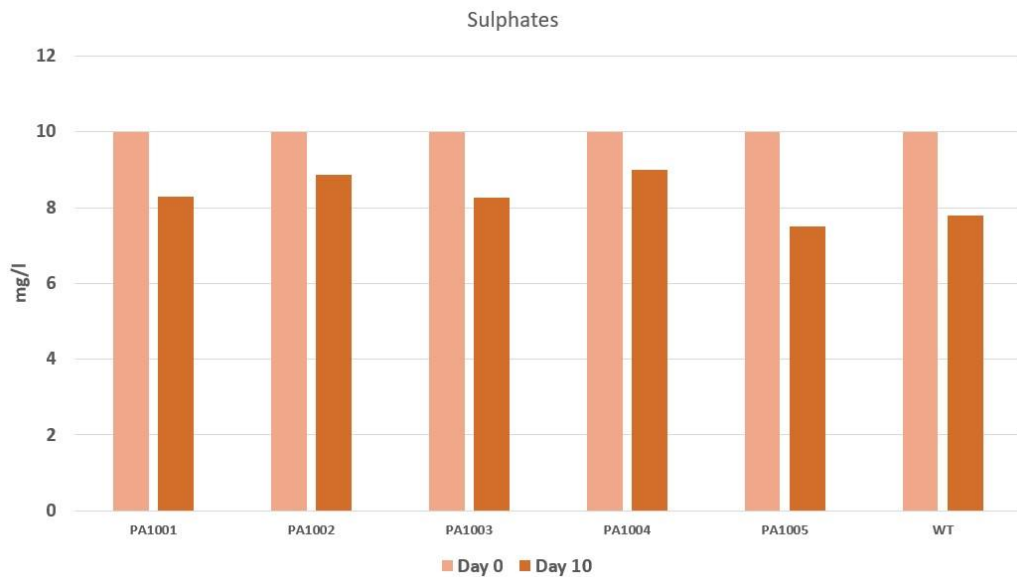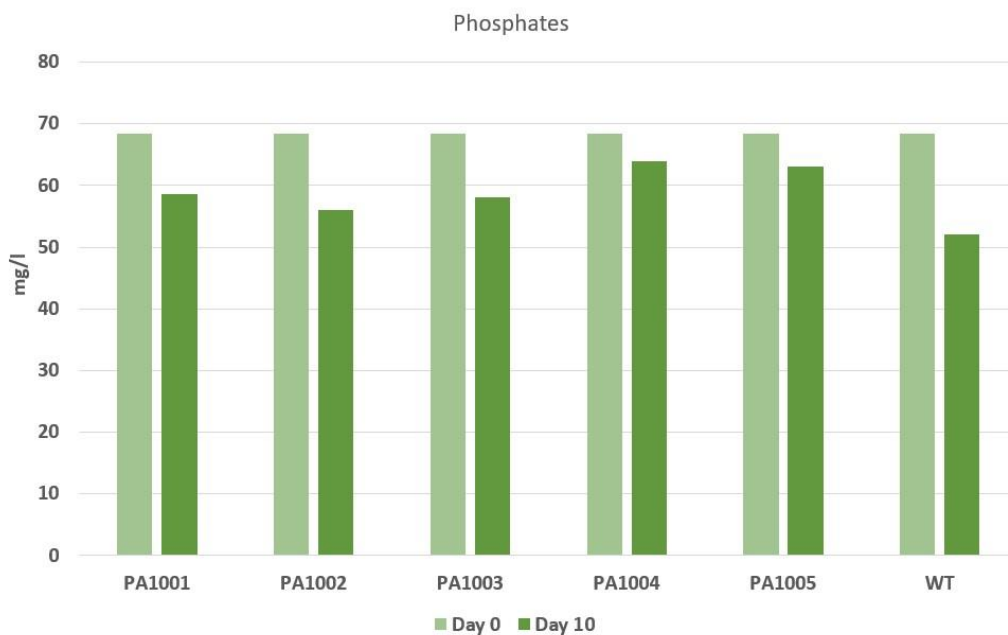These preliminary results showed that, already after 10 days of stress, something was activated inside the cultures. The increase in the amount of TOC showed how a degradative activity was taking place that released organic carbon into the medium, resulting, presumably from the carbon contained within the petroleum hydrocarbons.

8.9.2 GC-MS and GC-FID analysis after 40 days

The results obtained through GC-MS and GC-FID have provided an idea of the oily substances within the aqueous phase and the algae. The GC-MS-TQ-FS spectra, (**Figure 60**-**Figure 61**-**Figure 62**-**Figure 63**) showed the concentration of hydrocarbons and PAHs both in the aqueous phase and in the microalgal biomass. For the mutant strains PA1001 and PA1003, the spectra were not appreciable and therefore were not reported. In the GC-FID spectra of the mutant strains and the WT (**Figure 64**-**Figure 65**-**Figure 66**) it was possible to note that, after 40 days, the oily substances in the water were very high in all genotypes, unlike hydrocarbons which are present in smaller quantities just only 40 days. However, from these spectra, it was not possible to make a comparison between the peak ratios.

Therefore, it was not possible to identify the individual classes of hydrocarbons present. However, it was evident that, in a medium that was initially free of oily substances, following the biological action of the microalgae, these were released within the aqueous phase. As we will see later, these will be significantly reduced over time.
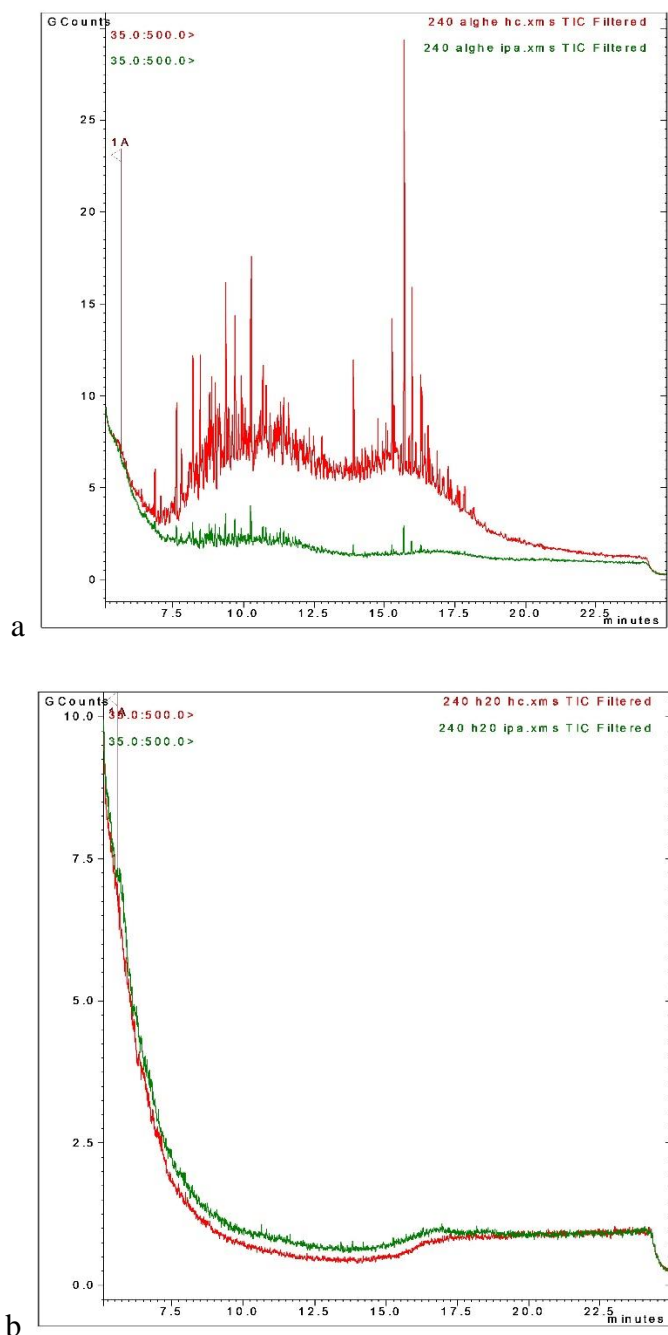
Figure 60*: GC-MS (TQ-FS) PA1002. a) Hydrocarbons (red) and IPA (blue) in the microalgal biomass b) Hydrocarbons (red) and IPA (blue) in aqueous phase.*
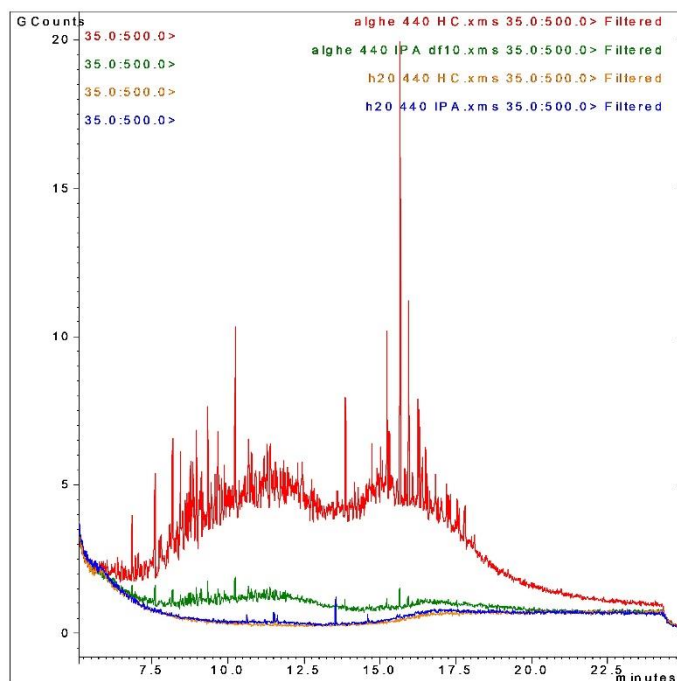
Figure 61: GC-MS (TQ-FS) PA1004. Hydrocarbons in microalgal biomass (red), IPA in microalgal biomass diluted 10 times (green), hydrocarbons in aqueous phase (orange), IPA in aqueous phase (blue)
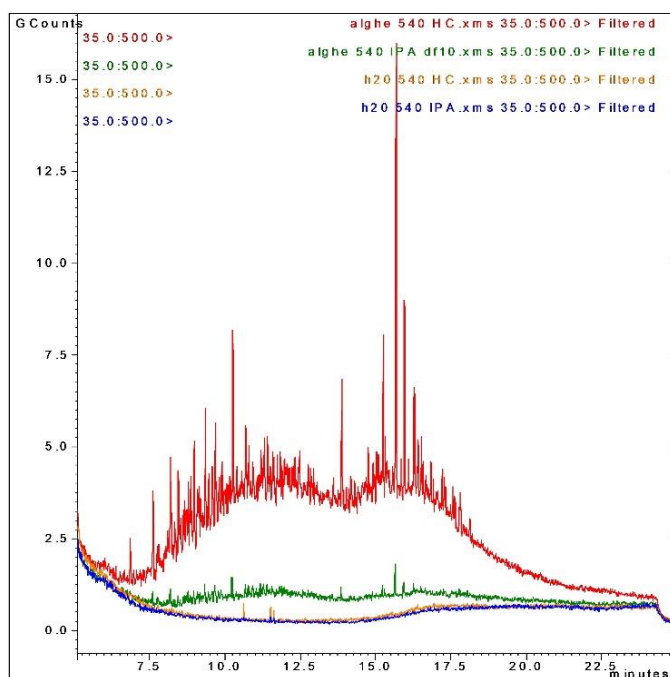
Figure 62: GC-MS (TQ-FS) PA1005. Hydrocarbons in microalgal biomass (red), IPA in microalgal biomass diluted 10 times (green), hydrocarbons in aqueous phase (orange), IPA in aqueous phase (blue)
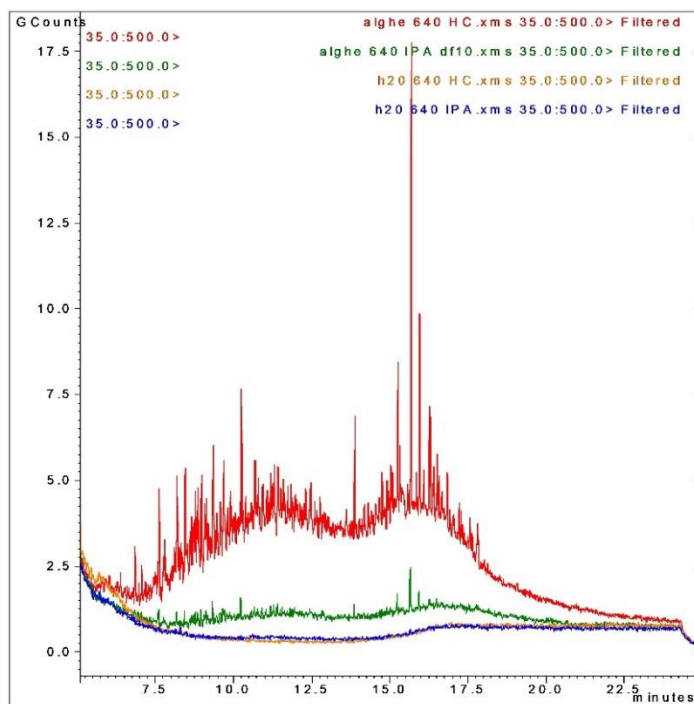
Figure 63: GC-MS (TQ-FS) WT. Hydrocarbons in microalgal biomass (red), IPA in microalgal biomass diluted 10 times (green), hydrocarbons in aqueous phase (orange), IPA in aqueous phase (blue)
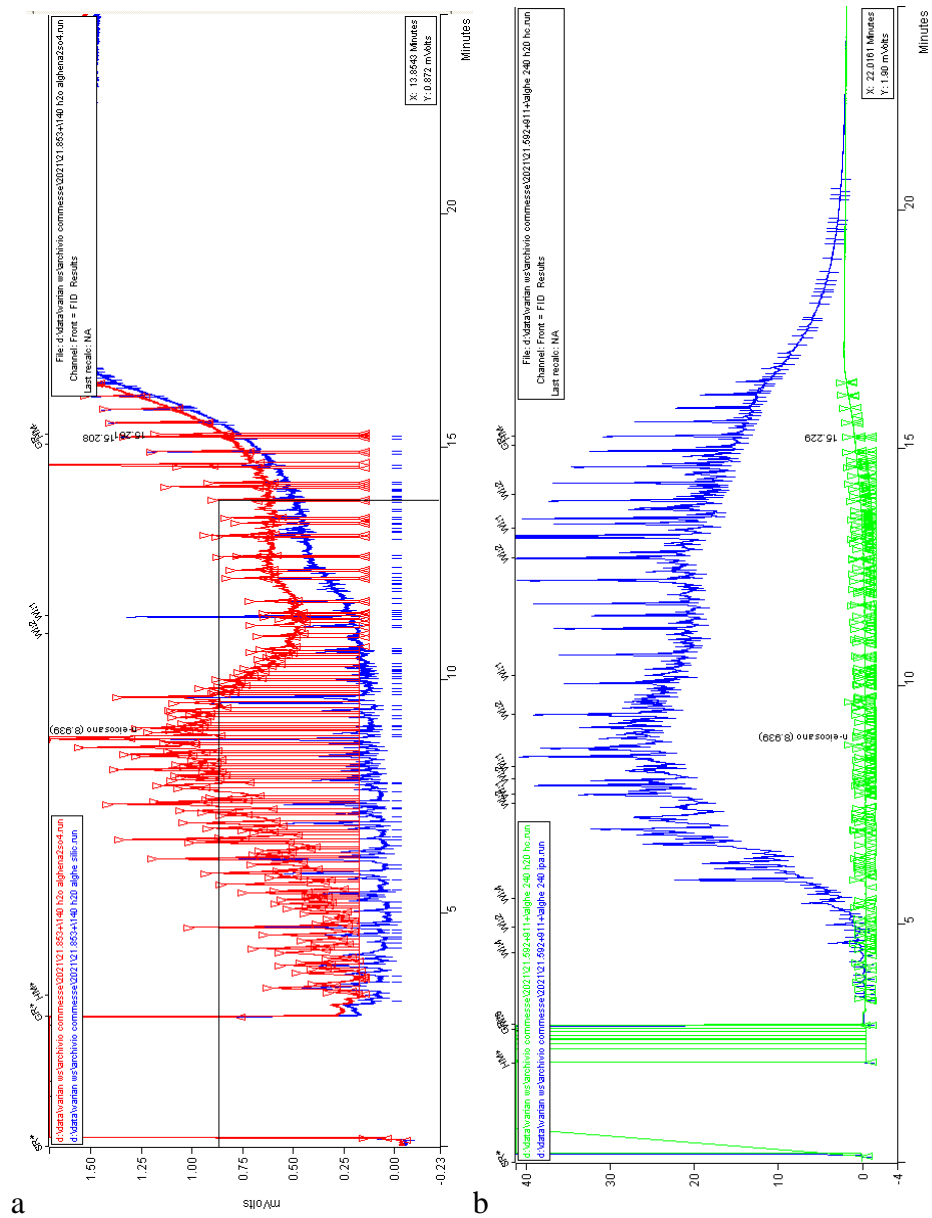
Figure 64: GC-FID spectra of a) PA1001 - red= oily substances; blue= hydrocarbons; b) PA1002 – blue = oily substances diluted 10 times; green =hydrocarbons
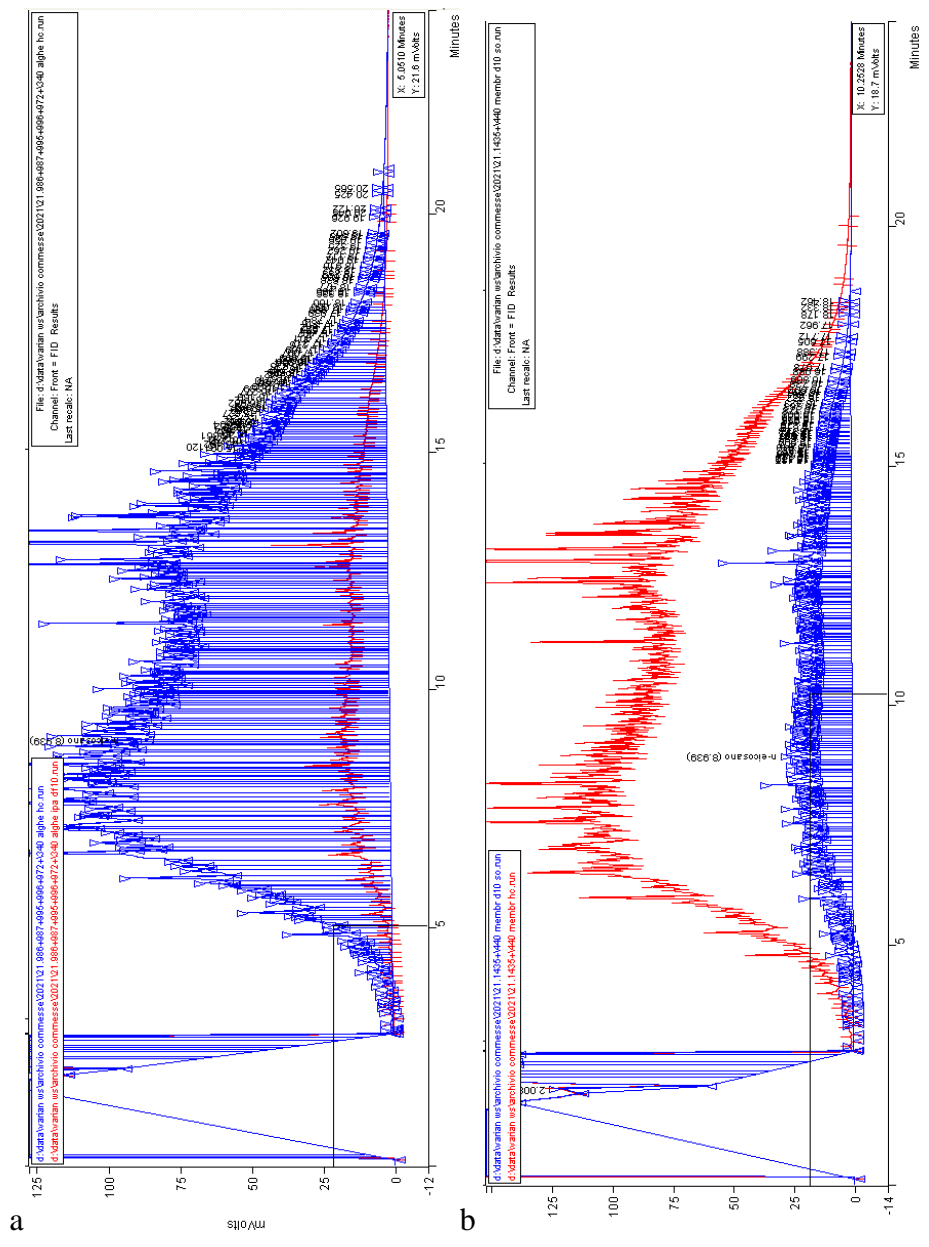
Figure 65: GC-FID spectra of a) PA1003 - red= oily substances diluted 10 times; blue= hydrocarbons; b) PA1004 – blue = oily substances diluted 10 times; red =hydrocarbons
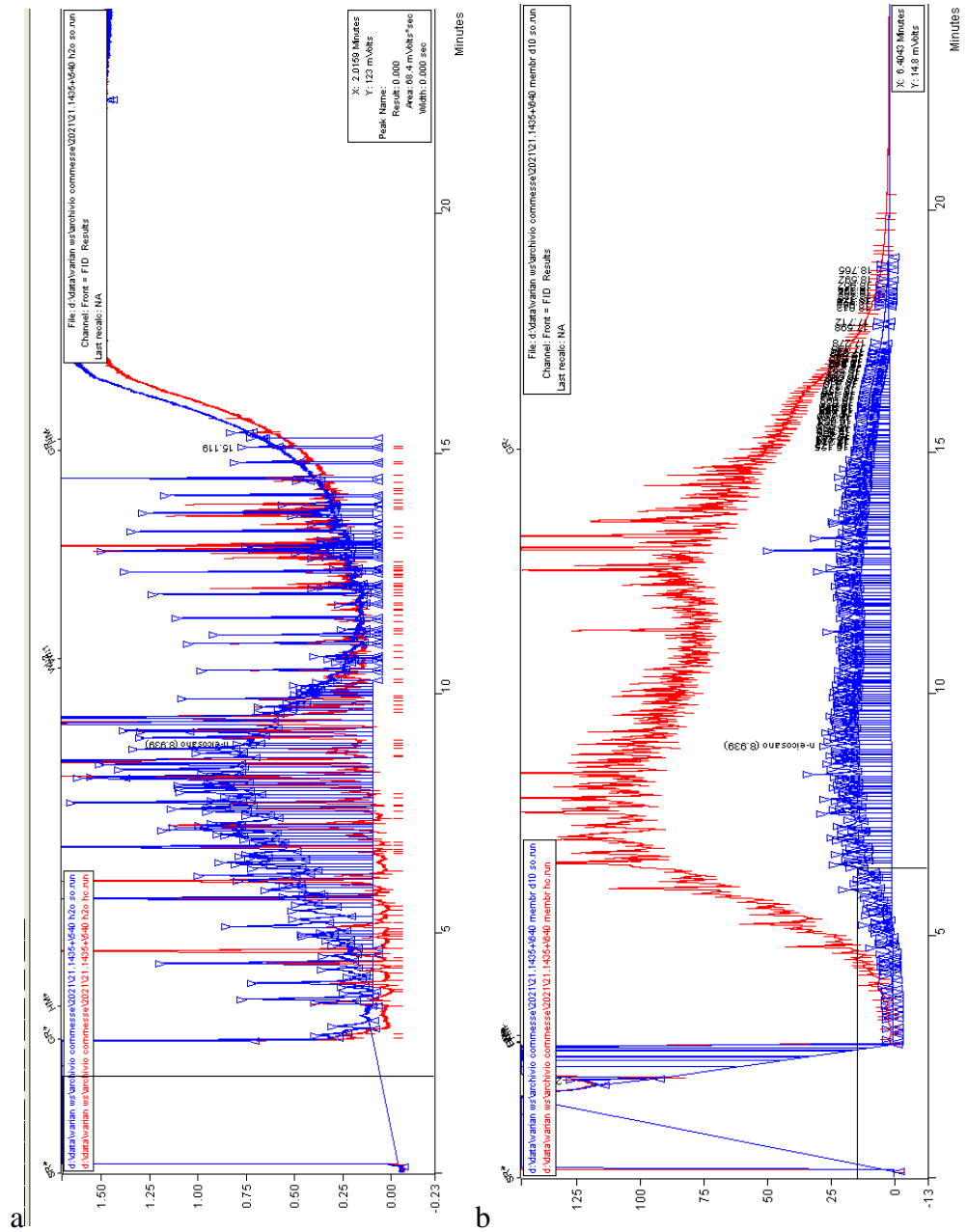
Figure 66: GC-FID spectra of a) PA1005 - blue= oily substances; red= hydrocarbons; b) WT – blue = oily substances diluted 10 times; red =hydrocarbons

8.9.3. Quantitative analysis after 20 and 160 days

The quantitative analyses carried out after 20 and 160 days, on the other hand, showed how the hydrocarbons were reduced both in the aqueous phase (**Figure 67**) and in the microalgal biomass (**Figure 68**).

Figure 67 shows how in the culture water after 160 days of treatment, the quantities of hydrocarbons present were significantly lower than those present after 20 days of treatment. However, the behaviour of the genotypes was different. Specific concentrations are shown in the table below (**Table 6**). Not all genotypes effectively removed hydrocarbons from the aqueous phase. In these conditions and in the long term, the WT was the worst because it only reduced the concentration of hydrocarbons by 32%, followed by PA1005, which reduced them by about 36%. PA1003 reduced the initial value by about 55% while PA1002 by 70%. The best performer was PA1004 which reduced the concentration of hydrocarbons by 95.5%, making the water almost free from them.
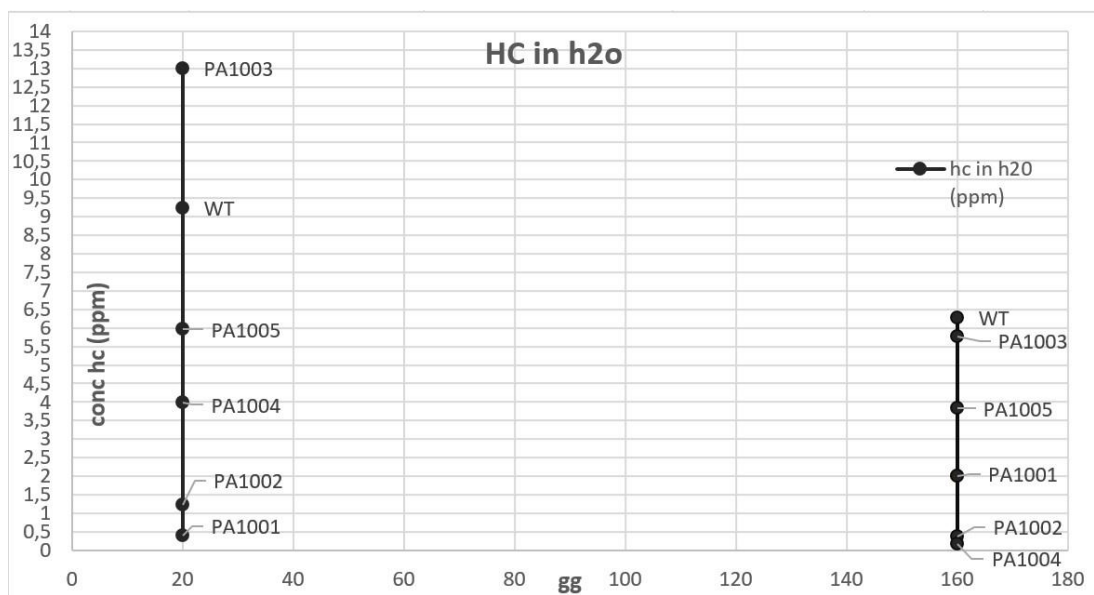
Figure 67: *Hydrocarbons concentration (ppm) in water after 20 and 160 days.*

Genotypes	HC in water after 20 days (ppm)	HC in water after 160 days (ppm)
PA1001	0.39	2
PA1002	1.23	0.37
PA1003	13	5.78
PA1004	4	0.18
PA1005	5.96	3.83
WT	9.24	6.28

Figure 68, on the other hand, shows the quantities of hydrocarbons within the microalgae biomass. Specific concentrations are shown in the table below (**Table 7**). The values, reported in mg per kg of biomass recovered, indicated that even within the microalgae, the concentrations of hydrocarbons were reduced. PA1001, which had even released hydrocarbons in the water, reduced these quantities by about 31% in the biomass, while PA1005 only by 22%. PA1003 and WT decreased the concentrations by 74 and 80%, respectively. However, PA1002 and PA1004 reduced concentrations by 98% and 96%, being the genotypes containing the least.
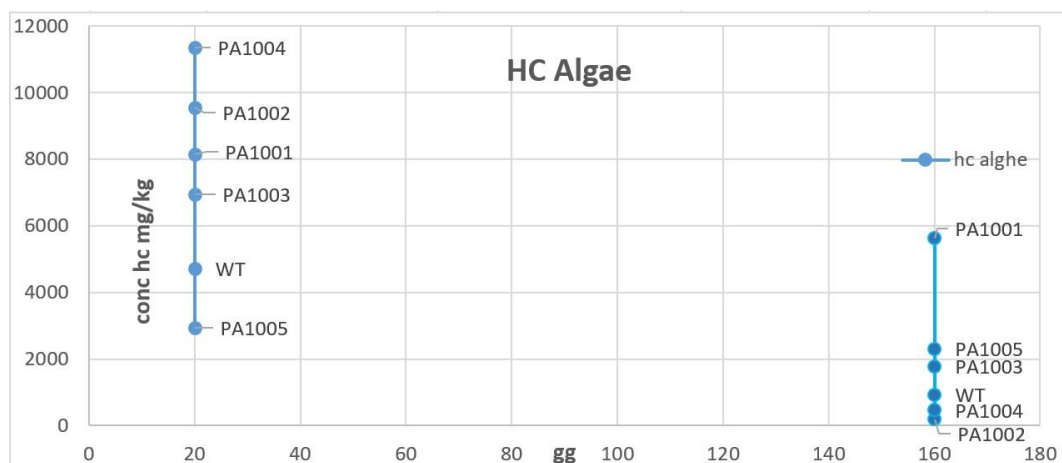
Figure 68: Hydrocarbons concentration (mg/kg) in algae after 20 and 160 days

- 134 -

Table 7: Hydrocarbon concentration in algae (mg/Kg)

Genotypes	HC in algae after 20 days (mg/kg)	HC in algae after 160 days (mg/kg)
PA1001	8142	5620
PA1002	9553	190
PA1003	6945	1781
PA1004	11344	462
PA1005	2941	2304
WT	4725	933

These quantitative results are extremely important because they suggest that a genuine degradation of hydrocarbons occurs within the mutant strains, especially in the PA1004 genotype, which did not release any hydrocarbons into the water and did not contain any within the biomass. This confirms the hypothesis of enzymatic degradation by the mutant strains that has completely used the organic carbon (released after 10 days less than the other genotypes and the WT (see **Figure 56**)) supplied by the crude oil, which is not even physically present at all inside the container (**Figure 52B**).

8.9.4. Qualitative analysis after 20 and 160 days

The quantitative data reported above are also supported by graphs obtained through GC-FID. Preliminarily, the graphs indicate a qualitative analysis of the classes of hydrocarbons most affected. In **Figure 69a**, regarding mutant strain PA1001, it is possible to note how in water, the C6-C7 hydrocarbons on the twentieth day were very high (blue), while after 160 days, these were drastically reduced (red), while they were increased all the others. In **Figure 69b**, the same trend is found within the algal biomass, where, however, the quantities are reduced after 160 days (red)

Figure 69: <u>PA1001</u>. GC-FID spectra. a) water hydrocarbons; b) microalgal biomass hydrocarbons (blue = day 20; red = day 160)

For the mutant strain PA1002, however, it is clear that both in the water (**Figure 70a**) and in the microalgal biomass (**Figure 70b**), after 160 days of treatment (red), the hydrocarbons were reduced. While a long-chain C16-C20 fraction remained in the water, in the microalgal biomass, any amount of all hydrocarbons was present.

Figure 70*: _PA1002_. GC-FID spectra. a) water hydrocarbons; b) microalgal biomass hydrocarbons (blue = day 20; red = day 160)*

For PA1003, both water and microalgae biomass (**Figure 71a** and **Figure 71b**), after 160 days of treatment (red), show a quantitative but not qualitative decrease in hydrocarbons.

Figure 71 *PA1003. GC-FID spectra. a) water hydrocarbons; b) microalgal biomass hydrocarbons (blue = day 20; red = day 160)*

The trend of the mutant strain PA1004 fully reflects the quantitative results obtained. As can be seen from **Figure 72a** and **Figure 72b**, after 160 days of treatment, the spectrum is flat for both water and microalgae biomass. This result indicates the removal of short-chain light hydrocarbons than heavier, long-chain hydrocarbons known to be the most resistant to bioremediation actions.

Figure 72: <u>*PA1004*</u>. *GC-FID spectra. a) water hydrocarbons; b) microalgal biomass hydrocarbons (blue = day 20; red = day 160)*

On the contrary, the mutant strain PA1005, after 160 days, reduces the concentration of hydrocarbons in the water (**Figure 73a**) but has no action on the classes involved. In biomass (**Figure 73b**), on the other hand, it is possible to note that after 160 days, the long-chain classes of hydrocarbons have increased, although the total quantities are still lower.

Figure 73: <u>PA1005</u>. *GC-FID spectra. a) water hydrocarbons; b) microalgal biomass hydrocarbons (blue = day 20; red = day 160)*

Finally, the WT demonstrates a quantitative but not qualitative reduction in the water (**Figure 74a**), while in the microalgal biomass (**Figure 74b**), the C6-C12 fraction was significantly reduced compared to day 20.

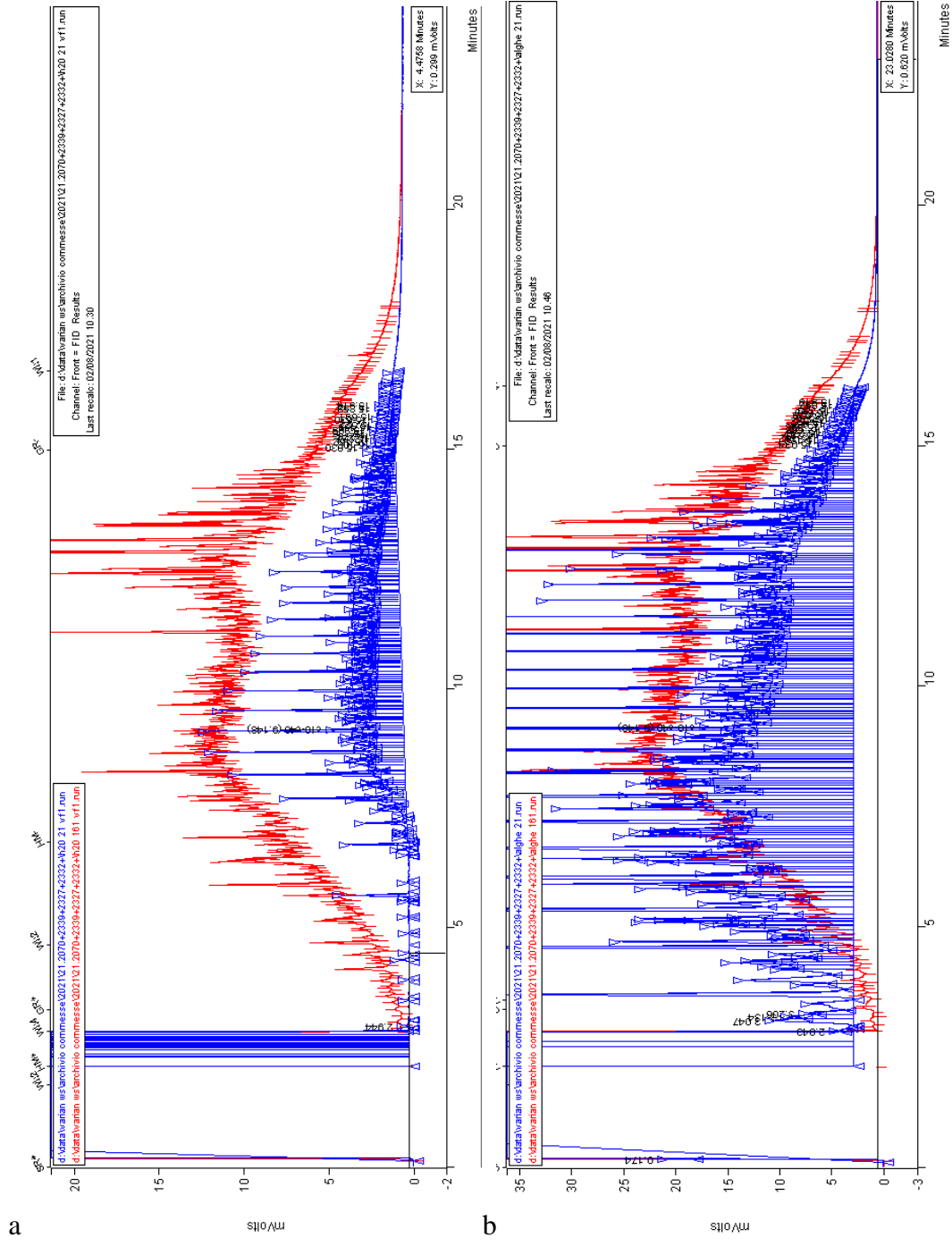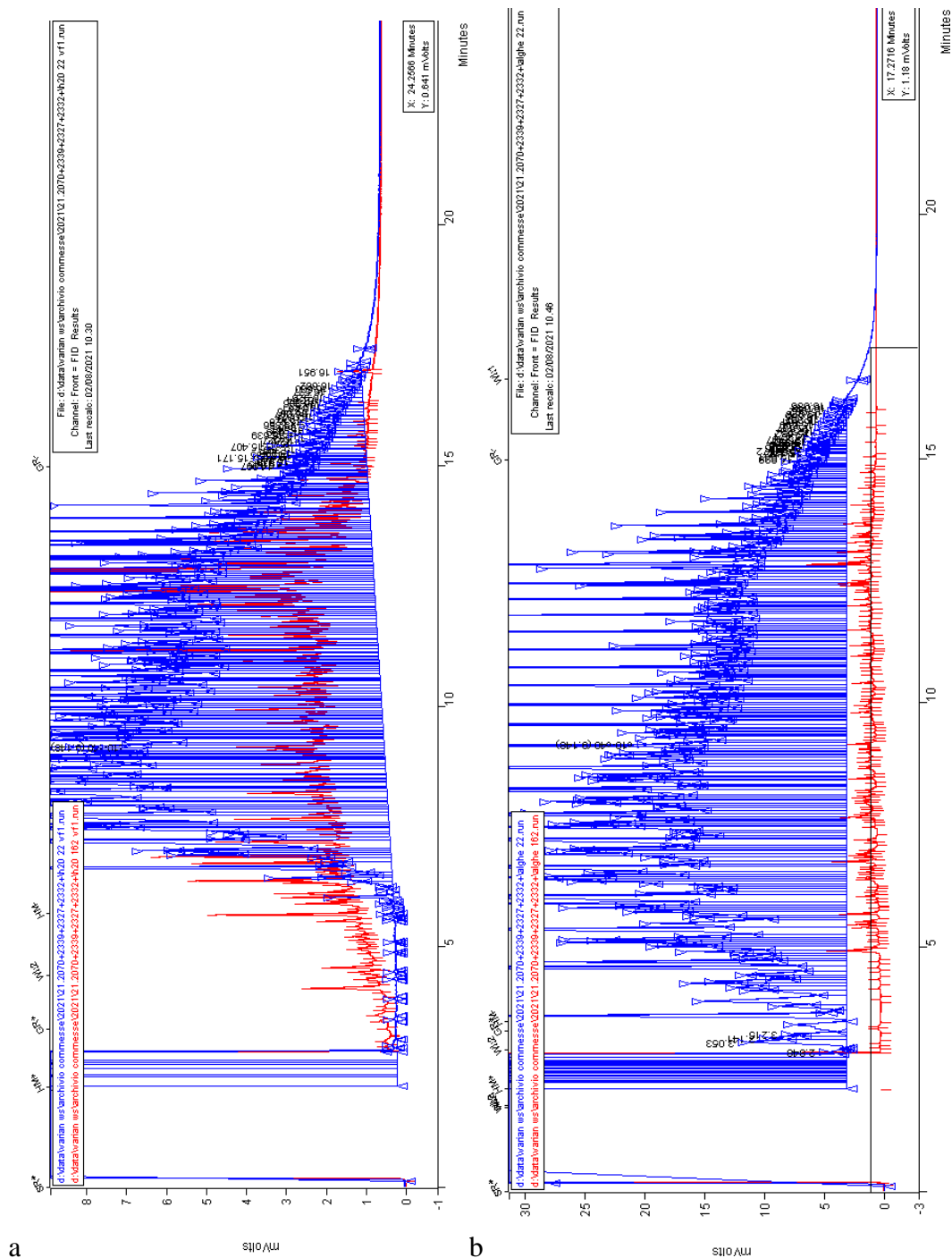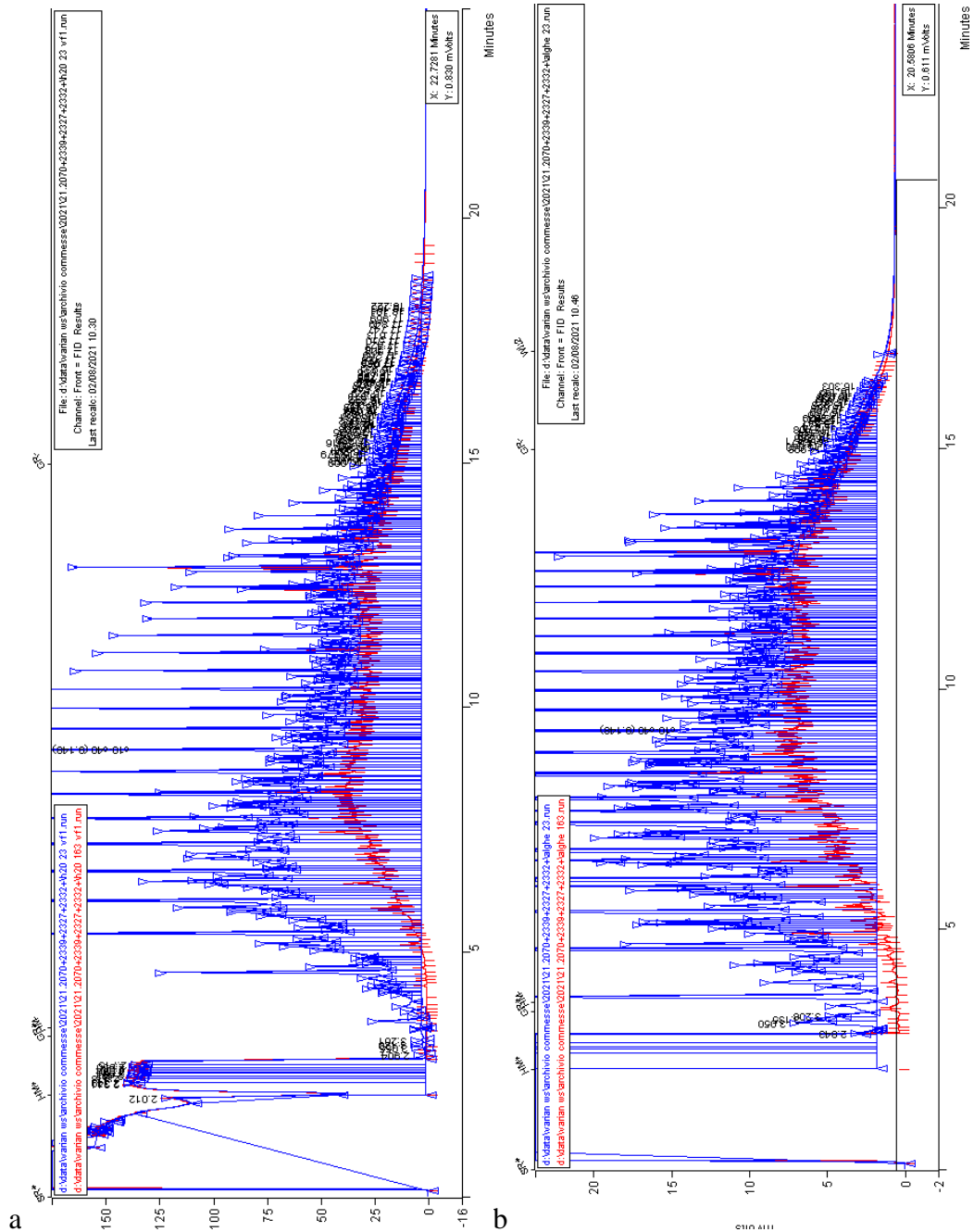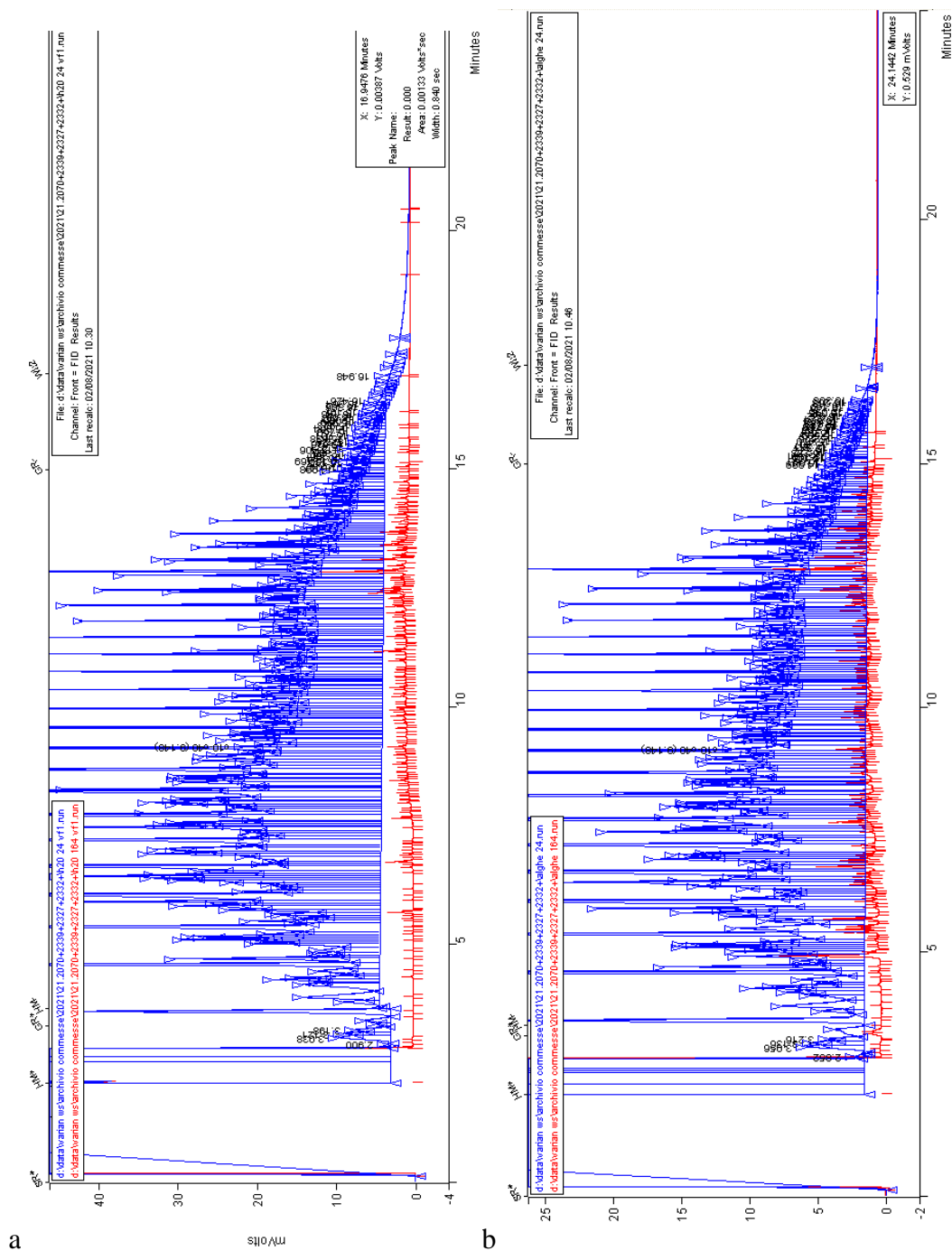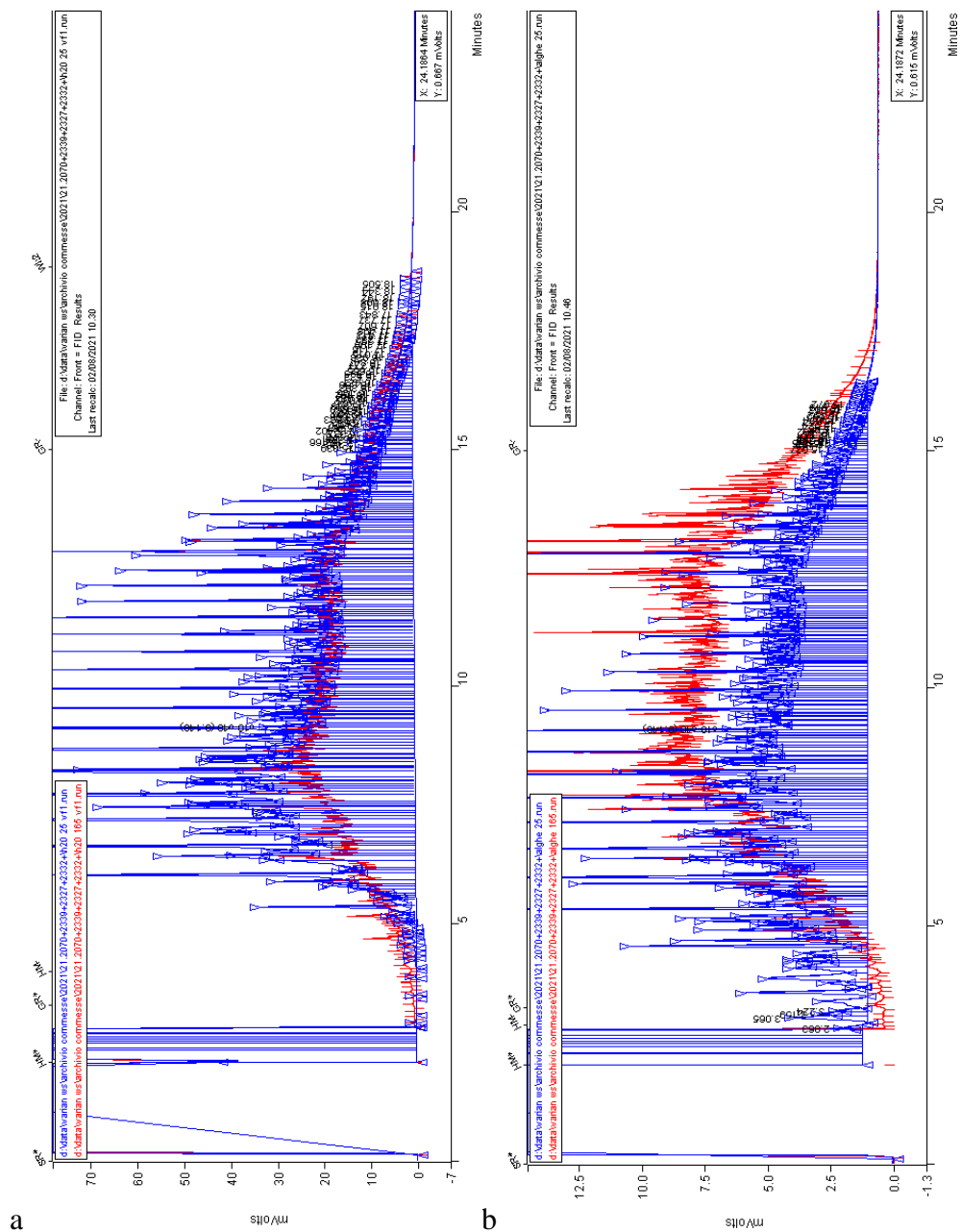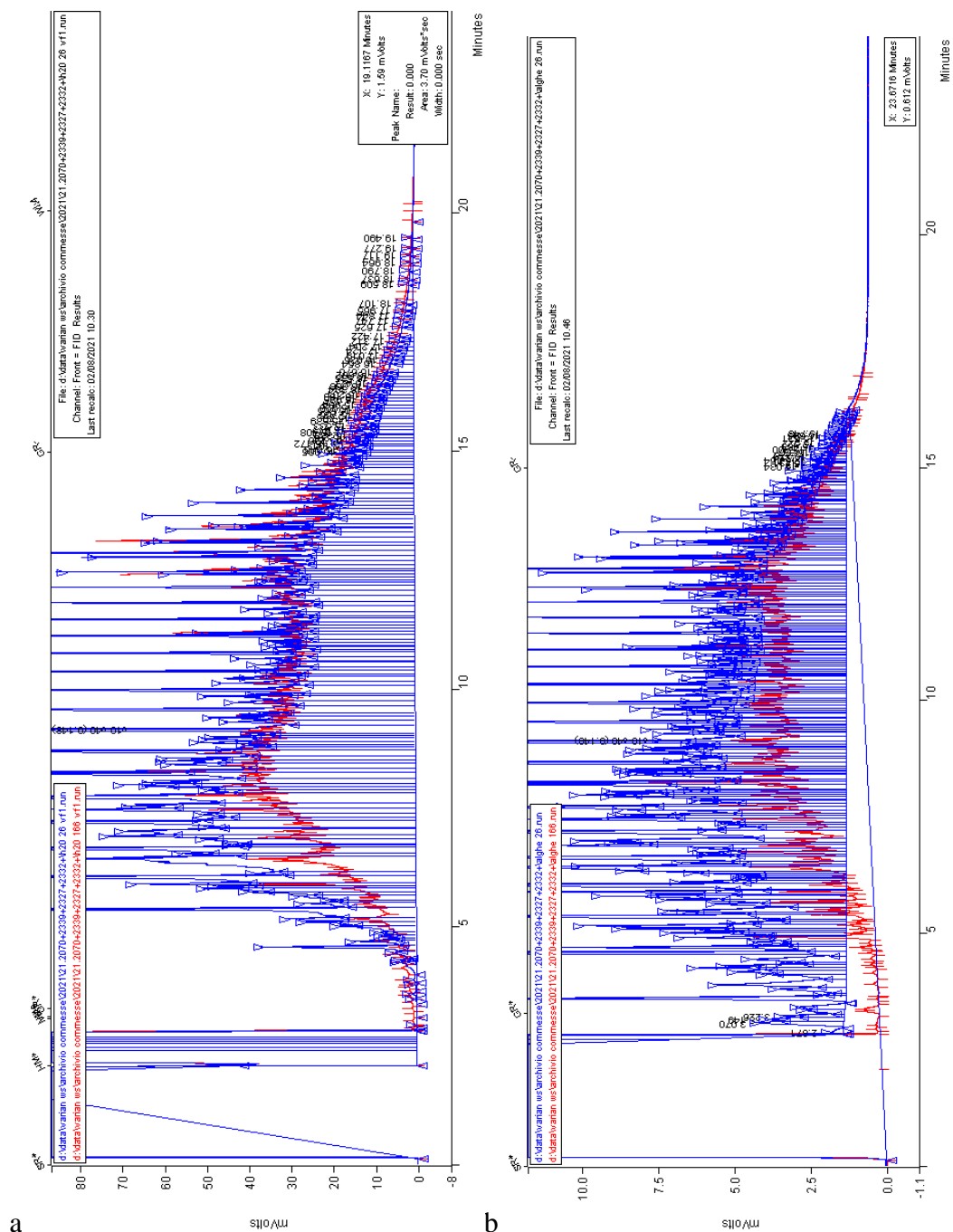**Figure 74**: <u>PA1005</u>. *GC-FID spectra. a) water hydrocarbons; b) microalgal biomass hydrocarbons (blue = day 20; red = day 160)*

CHAPTER 9: CONCLUSION

Concerning the objectives planned and pursued in this PhD project, it is possible to state that *H. pluvialis* is able of generating mutant strains capable of surviving in the presence of hydrocarbons, known as cytotoxic compounds. Specifically, starting from the WT genotype, it was possible to generate by exerting a high selective pressure, new genotypes with modified genomic structure. Initially, the changes induced by selective pressure were observed at the morphological and bio-functional level by analysing the growth of mutant strains in standard media and astaxanthin production compared with the WT genotype. The different growth curves, albeit with different kinetics, showed how the modifications directly involved the genome, overcoming a possible adaptive mechanism. This result was also confirmed after the treatment with hydrocarbons because the obtained mutant strains were able to use the hydrocarbons as a potential source of carbon for the performance of vegetative-reproductive functions. Furthermore, the mutant strains, grown in the presence of crude oil, if re-inoculated in fresh medium, after several multiplication cycles restored a growth curve identical to that originally recorded. This bio-physiological behaviour leads us to consider that the structural modifications generated in the mutant strains selected are stable over time. The genomic and transcriptomic analysis confirms what emerged from the macroscopic analysis. Analysing the genomic cDNA obtained starting from extracted transcripts (RNA), in the same phenological phase, in all mutant strains and the WT, it was shown that the differences were demonstrated both at a structural and functional level.

This result was highlighted by the analysis of the dendrograms reported and discussed previously. For example, **Figure 48** shows the degree of relationship of all genotypes studied on a transcriptomic basis generated by cluster analysis starting from a matrix obtained on a differential basis from the analysis of the investigated cDNA with a specific set of primers. The dendrogram shows how the genetic improvement scheme, directed by the high selective pressure exerted, made it possible to obtain new genotypes. Having highlighted different degrees of similarity between genotypes on a transcriptomic basis indicates that the selective pressure exerted to generate them has induced structural changes that have affected diverse portions of the genome. The analysis of the dendrogram shown in **Figure 55**

highlights how the presence of hydrocarbons induced a different transcriptomic change in the distinct mutant strains. In substance, it is plausible to hypothesize that the different genotypes have implemented different bio-functional strategies (different pathways, different enzyme sets) to degrade the crude oil. This aspect is further supported by the data deriving from the chemical analysis of the medium and the microalgal biomass obtained in the presence of crude oil for the different genotypes under study. After only ten days of treatment, some components, such as nitrites and nitrates, had been significantly reduced, while the amount of carbon in the medium (TOC) was increased. Following a sort of biodegradative kinetics, the results obtained after 40 days showed that, in the medium, there were oily substances, initially absent, and hydrocarbons, which after 160 days, for some mutant strains, had been removed.

These data lead to two reflections, one related to the continuation of the studies and one of an applicative type. The one on the continuation and deepening of the research activities leads us to direct future efforts on better understanding the structural and functional bases underlying the degradation processes mediated by the different genotypes (identification of genes with specific action, characterization of the pathways involved). The application type is based precisely on the assumption, previously highlighted, that the differences on a transcriptomic basis identified and highlighted in graphic form in the dendrogram 17 are based on stable structural changes, and therefore determine a genotype-specific function. The different genotypes attack and degrade crude oil in different ways, for example, by acting specifically on specific classes of hydrocarbons. PA1004, which turned out to be the "best performer" in terms of degradation, and production of oily substances attributable to saponins, makes the applicability of the project even more interesting, as it highlights how different by-products could be obtained following the biodegradation of a pollutant that would lead not only to economic revenue but to the closure of a green recycling economy.

Another reflection that must be developed is how these genotypes are used/applied. Microalgae could represent a technology capable of purifying water contaminated by hydrocarbons (processing water, wastewater), especially in an area as important for extraction as Basilicata, thus putting an otherwise unused industrial by-product back into circulation. Even the biomass of microalgae itself would become a reusable by-product both in the production of biofuels and in the extraction of

secondary metabolites that can be used in the pet-food industry. Furthermore, given the diversity of function, this could be exploited to generate a multi genotypic biodegradation strategy involving a combined population of the different genotypes to stimulate biofunctional synergies to improve and optimize the biodegradation of the different types of mixtures of hydrocarbons.

The structural diversity highlighted by the different genotypes, compared to the WT, leads to the hypothesis that they may be characterized by differentiated fitness, so their application in an open environment could involve a selective pressure such as to radically modify the structure of the natural algal populations belonging to the species under study. In this regard, the application of newly selected genotypes should be conducted in a controlled environment where containment measures must necessarily be applied to avoid potential escapes that can have an impact on the environment.

In conclusion, it can be said that the results observed up to now are of great scientific value and that the strategy applied for the development and obtaining of tools capable of implementing bioremediation in the presence of crude oil has been performing, allowing to obtain genetically improved genotypes for the required function. At the same time, the transcriptomic-based data obtained led to further investigation of the genetic basis that characterize the different genotypes concerning the crude oil degradation processes to better understand and characterize the metabolic pathways directly and indirectly involved in the biodegradation process.

REFERENCES

[1]   Energia, fonti di in "Dizionario di Storia," (n.d.). https://www.treccani.it/enciclopedia/fonti-di-energia_(Dizionario-di-Storia)/ (accessed February 10, 2021).

[2]   H. Schobert, Chemistry of fossil fuels and biofuels, 2010. https://doi.org/10.1017/CBO9780511844188.

[3]   R.A. Berner, The long-term carbon cycle, fossil fuels and atmospheric composition, Nature. 426 (2003) 323–326. https://doi.org/10.1038/nature02131.

[4]   H. Riebeek, The Carbon Cycle, NASA, Earth Obs. (2011). https://earthobservatory.nasa.gov/features/CarbonCycle (accessed March 13, 2021).

[5]   G.J. Retallack, J.J. Veevers, R. Morante, Global coal gap between Permian-Triassic extinction and Middle Triassic recovery of peat-forming plants, Bull. Geol. Soc. Am. 108 (1996) 195–207. https://doi.org/10.1130/0016-7606(1996)108<0195:GCGBPT>2.3.CO;2.

[6]   E. Taylor, T. Taylor, M. Kring, Paleobotany: The Biology and Evolution of Fossil Plants, 2nd Editio, 2008.

[7]   W. Boerjian, J. Ralph, M. Baucher, Lignin Biosynthesis, Annu. Rev. Plant Biol. 54 (2003) 519–546. https://doi.org/10.1146/annurev.arplant.54.031902.134938.

[8]   Anthracitic Coal, Kentucky Geol. Surv. (n.d.). http://www.uky.edu/KGS/coal/coal-anthracite.php (accessed March 15, 2021).

[9]   E.A. Wrigley, Continuity, Chance and Change: The Character of the Industrial Revolution in England, Cambridge Univ. Press. 10 (1988) 121–121. https://doi.org/https://doi.org/10.1177/027046769001000236.

[10]   R. Elsen, M. Fleischmann, Neurath F and G set newbenchmarks, 2008. https://www.alstom.com/press-releases-news/2015/11/alstom-refocused-on-rail-transport-with-strong-leadership-positions (accessed March 16, 2021).

[11]   N.E.T.L. NETL, 10.6. Direct liquefaction processes, (n.d.). http://www.netl.doe.gov/research/coal/energy-

systems/gasification/gasifipedia/direct-liquefaction (accessed March 20, 2021).

[12] CarbonBrief, Mapped: The world's coal power plants in 2020, (2020). https://www.carbonbrief.org/mapped-worlds-coal-power-plants (accessed March 16, 2021).

[13] P.J. Crutzen, J. Lelieveld, Human impacts on atmospheric chemisty, Annu. Rev. Earth Planet. Sci. 29 (2001) 17–45. https://doi.org/10.1146/annurev.earth.29.1.17.

[14] P. Room, C. Us, How much carbon dioxide (CO 2) is produced when different fuels are burned ?, (2013). https://www.eia.gov/tools/faqs/faq.php?id=73&t=11 (accessed March 20, 2021).

[15] BP, Statistical Review of World Energy analyses data on world energy markets from the prior year, (2020) 66. https://www.bp.com/content/dam/bp/business-sites/en/global/corporate/pdfs/energy-economics/statistical-review/bp-stats-review-2020-full-report.pdf.

[16] Statistical Review of World Energy - Coal, n.d.

[17] I.E. Agency, Coal 2020 - Analysis and forecast to 2025, 2020. https://www.iea.org/news/a-rebound-in-global-coal-demand-in-2021-is-set-to-be-short-lived-but-no-immediate-decline-in-sight (accessed March 29, 2021).

[18] C.F.R. Gargiulo, A. Cimenti, S.T.V.E. Cimenti, Gli idrati di metano: fonte energetica del futuro?, 2006.

[19] Gas Naturale | Sorgenia, (n.d.). https://www.sorgenia.it/guida-energia/gas-naturale (accessed March 29, 2021).

[20] EIA, Natural gas explained, U.S. Energy Inf. Adm. (2020). https://www.eia.gov/energyexplained/natural-gas/ (accessed March 29, 2021).

[21] Treccani, Gas non convenzionali, Encicl. Degli Idrocarb. III (1991) 57–84.

[22] M.. Beychok, Coal gasification and the Phenosolvan process (Conference) | OSTI.GOV, Am. Chem. Soc., Div. Fuel Chem., Prepr.; (United States). (1974). https://www.osti.gov/biblio/7362109 (accessed March 29, 2021).

[23] N. Scarlat, J.F. Dallemand, F. Fahl, Biogas: Developments and perspectives in Europe, Renew. Energy. 129 (2018) 457–472.

https://doi.org/10.1016/j.renene.2018.03.006.

[24]   American Public Gas Association (APGA), A Brief History of Natural Gas - American Public Gas Association, (n.d.). https://www.apga.org/apgamainsite/aboutus/facts/history-of-natural-gas (accessed March 29, 2021).

[25]   GasNaturali 3C, (n.d.). https://it.padlet.com/cc331/y00vy4zwmlsf (accessed March 30, 2021).

[26]   Energy Information Administration, Natural Gas Processing : The Crucial Link Between Natural Gas Production and Its Transportation to Market, (2006) 1–11.

[27]   A. Rivera-Alvarez, J.D. Osorio, L. Montoya-Duque, J. Fontalvo, E. Botero, A. Escudero-Atehortua, Comparative analysis of natural gas cogeneration incentives on electricity production in Latin America, Energy Policy. 142 (2020) 111466. https://doi.org/10.1016/j.enpol.2020.111466.

[28]   S.Y. Kan, B. Chen, X.F. Wu, Z.M. Chen, G.Q. Chen, Natural gas overview for world economy: From primary supply to final demand via global supply chains, Energy Policy. 124 (2019) 215–225. https://doi.org/10.1016/j.enpol.2018.10.002.

[29]   V.A. Likhanov, A. V. Rossokhin, Optimization of environmental performance of a car diesel engine running on natural gas by reducing carbon black in the exhaust gas, in: IOP Conf. Ser. Mater. Sci. Eng., Institute of Physics Publishing, 2020: p. 062046. https://doi.org/10.1088/1757-899X/862/6/062046.

[30]   Natural gas - Statistical Review of World Energy, 2020.

[31]   G. Methane Initiative, Global Methane Emissions and Mitigation Opportunities, 2020. www.globalmethane.org/oil-gas (accessed April 9, 2021).

[32]   D.D. Chiras, Environmental Science, ninth edit, 2012.

[33]   L. Zhu, Z. Li, E. Hiltunen, Microalgae Chlorella vulgaris biomass harvesting by natural flocculant: Effects on biomass sedimentation, spent medium recycling and lipid extraction, Biotechnol. Biofuels. 11 (2018) 1–10. https://doi.org/10.1186/s13068-018-1183-z.

[34]   H. Abraham, Asphalts and Allied Substances: Raw materials and manufactured products - Herbert Abraham - Google Libri, New York, 1945.

[35]   G. Agricola, De natura fossilium (Textbook of mineralogy) - Translated from

the first Latin edition of 1546 by Bandy Mark Chance and Bandy Jean A., Dover Publications, Mineola, N.Y., 2004.

[36] J.G. Speight, The Chemistry and Technology of Petroleum, Chem. Technol. Pet. (2014). https://doi.org/10.1201/b16559.

[37] A. Urciuoli, Note di storia del petrolio in Italia, Rass. Del Bitume. (2007) 53–56.

[38] ENI, La storia della ricerca del petrolio in Italia, (n.d.). https://www.eni.com/it-IT/chi-siamo/storia-ricerca-petrolifera-italia.html (accessed April 29, 2021).

[39] L.J. White, A. Sampson, The Seven Sisters: The Great Oil Companies and the World They Shaped., Polit. Sci. Q. 91 (1976) 364. https://doi.org/10.2307/2148435.

[40] M. Boldrini, Prospettive e problemi della produzione degli idrocarburi in Italia, G. Degli Econ. e Ann. Di Econ. Anno 9 (1950) 258–267.

[41] N. Santocchi, IL MARE - Supplemento al Bollettino ufficiale degli idrocarburi e delle georisorse - Anno LVII N. 2 - 28 Febbraio 2013, 2013. http://unmig.sviluppoeconomico.gov.it (accessed April 29, 2021).

[42] A. Amati, Elementi di geografia dell'Italia: Con cenni storici e statistici, Milano, 1890.

[43] J.. Van Dijk, V. Affinito, R. Atena, A. Caputi, A. Cestari, S. D'Elia, N. Giancipoli, M. Lanzellotti, M. Lazzari, N. Oriolo, S. Picone, Cento Anni di Ricerca Petrolifera: l'Alta Val d'Agri (Basilicata, Italia meridionale), in: Congr. Dell'Ordine Dei Geol. Di Basilicata,"Ricerca, Svilupp. Ed Util. Delle Fonti Foss. Ruolo Del Geol., 2012.

[44] Storia - Osservatorio Val d'Agri, (n.d.). http://www.osservatoriovaldagri.it/web/guest/storia (accessed May 4, 2021).

[45] In Val d'Agri con le attività Upstream, (n.d.). https://www.eni.com/it-IT/attivita/italia-val-agri-attivita-upstream.html (accessed May 4, 2021).

[46] Il Post, C'è ancora molto petrolio in Basilicata, (2020). https://www.ilpost.it/2020/12/18/petrolio-basilicata-tempa-rossa/ (accessed April 30, 2021).

[47] Total, Il progetto Tempa Rossa, (2017). https://www.it.total.com/it/pagine/attivita/il-progetto-tempa-rossa (accessed May 5, 2021).

[48] Banca di'Italia, Economie regionali L'economia della Basilicata

Aggiornamento congiunturale, 2020. http://www.bancaditalia.it (accessed April 30, 2021).

[49] GaiaMente sulla Terra: Il prezzo del petrolio, (2020). https://gaiamentesullaterra.blogspot.com/2020/04/post-zero.html?_sm_au_=i5V6JsL4Q7vH4VsVML8tvK34L00HF&fbclid=IwAR2SxLPKPcxI4A9eX1NR6yRU447Vt4S1CtrUuMQ3AWYQR9PYtu_iQPgjcmY (accessed May 5, 2021).

[50] N. Manfrinato, Il mercato del petrolio durante la crisi Globale, Università degli studi di Padova, 2020.

[51] EIA, Crude oils have different quality characteristics, Eia. (2012). https://www.eia.gov/todayinenergy/detail.php?id=7110 (accessed May 5, 2021).

[52] P. Szatmari, Petroleum formation by Fischer-Tropsch synthesis in plate teconics, Am. Assoc. Pet. Geol. Bull. 73 (1989) 989–998. https://doi.org/10.1306/44b4a2cb-170a-11d7-8645000102c1865d.

[53] I. Volkova, D. Gura, I. Aksenov, Abiogenic and Biogenic Petroleum Origin: A Common Theory for Geological Surveys, Asian J. Water, Environ. Pollut. 18 (2021) 59–65. https://doi.org/10.3233/AJW210008.

[54] K. McCarthy, K. Rojas, M. Niemann, D. Palrnowski, K. Peters, A. Stankiewicz, Basic petroleum geochemistry for source rock evaluation, Oilf. Rev. 23 (2011) 32–43.

[55] Schlumberge, catagenesis | Oilfield Glossary, (2021). https://glossary.oilfield.slb.com/en/terms/c/catagenesis (accessed May 31, 2021).

[56] C.S. Hsu, P.R. Robinson, Springer Handbook of Petroleum Technology, 2017. https://books.google.it/books?id=mgxEDwAAQBAJ&dq=petroleum+composition&lr=&source=gbs_navlinks_s (accessed June 3, 2021).

[57] Y. V. Kissin, Catagenesis and composition of petroleum: Origin of n-alkanes and isoalkanes in petroleum crudes, Geochim. Cosmochim. Acta. 51 (1987) 2445–2457. https://doi.org/10.1016/0016-7037(87)90296-1.

[58] American Petroleum Institute, API Recommended Practice Standard Procedure for Testing Drilling Fluids, American Petroleum Institute,Dallas, United States, 1997.

[59] ASTM International, ASTM D3238-17a, Standard Test Method for

Calculation of Carbon Distribution and Structural Group Analysis of Petroleum Oils by the n-d-M Method, 05 (2017) 1–2. www.astm.org (accessed June 7, 2021).

[60] N. Press, M. Sella, Prospezioni geologiche, Encicl. Degli Idrocarb. TRECCANI. 1 (2005) 185–195.

[61] A. Diantini, Petrolio e biodiversità in Val D'Agri, 2016. www.mastergiscience.it (accessed June 7, 2021).

[62] M. Gonfalini, Prospezioni geofisiche, Encicl. Degli Idrocarb. TRECCANI. (2005).

[63] Eni SPA, Studio di Impatto Ambientale, Progetto di Sviluppo Val d'Agri. Area Cluster "S. Elia 1 – Cerro Falcone 7," 2012.

[64] P. Mancini, Impianti e tecnologie di perforazione, Encicl. Degli Idrocarb. I (2003) 303–336.

[65] E. Tzimas, A. Georgakaki, C. Garcia Cortes, S.D. Peteves, Enhanced oil recovery using carbon dioxide in the European energy system, 2005. http://ie.jrc.cec.eu.int/ (accessed June 7, 2021).

[66] M.E. Tennyson, Growth history of oil reserves in major California oil fields during the twentieth century, 2005.

[67] BC Oil and Gas Commission, Flaring and Venting Reduction Guideline Version 5.2, Victoria, 2021.

[68] J. Pereira, I. Velasquez, R. Blanco, M. Sanchez, C. Pernalete, C. Canelón, Crude Oil Desalting Process, in: Adv. Petrochemicals, InTech, 2015. https://doi.org/10.5772/61274.

[69] I. Dincer, M.A. Rosen, Exergy analyses of crude oil distillation systems, in: Exergy, Elsevier, 2021: pp. 439–457. https://doi.org/10.1016/b978-0-12-824372-5.00016-6.

[70] K. Kolmetz, W.K. Ng, S.H. Lee, T.Y. Lim, D.R. Summers, C.A. Soyza, Optimize distillation column design for improved reliability in operation and maintenance, Asia-Pacific J. Chem. Eng. 2 (2007) 294–307. https://doi.org/10.1002/apj.23.

[71] G. Alonso-Ramírez, F. Sánchez-Minero, J. Ramírez, R. Cuevas-Garcia, N. Moreno-Montiel, Analysis of the thermal hydrocracking of heavy fuel oil, Pet. Sci. Technol. 36 (2018) 507–513. https://doi.org/10.1080/10916466.2018.1428627.

[72] A. Safari, M. Vesali-Naseh, Design and optimization of hydrodesulfurization

process for liquefied petroleum gases, J. Clean. Prod. 220 (2019) 1255–1264. https://doi.org/10.1016/j.jclepro.2019.02.226.

[73] R.S. Kraus, Petroleum Refining Process, Encycl. Occup. Heal. Saf. (2011). http://www.ilocis.org/documents/chpt78e.htm (accessed June 9, 2021).

[74] A. Corma, A. V. Orchillés, Current views on the mechanism of catalytic cracking, Microporous Mesoporous Mater. 35–36 (2000) 21–30. https://doi.org/10.1016/S1387-1811(99)00205-X.

[75] J. Weitkamp, Catalytic Hydrocracking-Mechanisms and Versatility of the Process, ChemCatChem. 4 (2012) 292–306. https://doi.org/10.1002/cctc.201100315.

[76] coke | Oilfield Glossary, (n.d.). https://glossary.oilfield.slb.com/en/terms/c/coke (accessed June 9, 2021).

[77] M.S. Masnadi, H.M. El-Houjeiri, D. Schunack, Y. Li, S.O. Roberts, S. Przesmitzki, A.R. Brandt, M. Wang, Well-to-refinery emissions and net-energy analysis of China's crude-oil supply, Nat. Energy. 3 (2018) 220–226. https://doi.org/10.1038/s41560-018-0090-7.

[78] The Lakeview Gusher, (2021). http://www.sjvgeology.org/history/lakeview.html (accessed June 10, 2021).

[79] Z. Nixon, J. Michel, A Review of distribution and quantity of lingering subsurface oil from the Exxon Valdez Oil Spill, Deep. Res. Part II Top. Stud. Oceanogr. 147 (2018) 20–26. https://doi.org/10.1016/j.dsr2.2017.07.009.

[80] A.G. Kostianoy, A. Carpenter, History, sources and volumes of oil pollution in the mediterranean sea, in: Handb. Environ. Chem., Springer Verlag, 2018: pp. 9–31. https://doi.org/10.1007/698_2018_369.

[81] J. Beyer, H.C. Trannum, T. Bakke, P. V. Hodson, T.K. Collier, Environmental effects of the Deepwater Horizon oil spill: A review, Mar. Pollut. Bull. 110 (2016) 28–51. https://doi.org/10.1016/j.marpolbul.2016.06.027.

[82] T.B. Ryerson, R. Camilli, J.D. Kessler, E.B. Kujawinski, C.M. Reddy, D.L. Valentine, E. Atlas, D.R. Blake, J. De Gouw, S. Meinardi, D.D. Parrish, J. Peischl, J.S. Seewald, C. Warneke, Chemical data quantify Deepwater Horizon hydrocarbon flow rate and environmental distribution, Proc. Natl. Acad. Sci. U. S. A. 109 (2012) 20246–20253. https://doi.org/10.1073/pnas.1110564109.

[83] J.L. Ramseur, CRS Report for Congress Deepwater Horizon Oil Spill: The

Fate of the Oil, 2010. www.crs.gov (accessed June 11, 2021).

[84] P.W. Sammarco, S.R. Kolian, R.A.F. Warby, J.L. Bouldin, W.A. Subra, S.A. Porter, Distribution and concentrations of petroleum hydrocarbons associated with the BP/Deepwater Horizon Oil Spill, Gulf of Mexico, Mar. Pollut. Bull. 73 (2013) 129–143. https://doi.org/10.1016/j.marpolbul.2013.05.029.

[85] Z. Liu, J. Liu, W.S. Gardner, G.C. Shank, N.E. Ostrom, The impact of Deepwater Horizon oil spill on petroleum hydrocarbons in surface waters of the northern Gulf of Mexico, Deep. Res. Part II Top. Stud. Oceanogr. 129 (2016) 292–300. https://doi.org/10.1016/j.dsr2.2014.01.013.

[86] M. Escobar, G. Márquez, S. Inciarte, J. Rojas, I. Esteves, G. Malandrino, The organic geochemistry of oil seeps from the Sierra de Perijá eastern foothills, Lake Maracaibo Basin, Venezuela, Org. Geochem. 42 (2011) 727–738. https://doi.org/10.1016/j.orggeochem.2011.06.005.

[87] V. Mulabagal, F. Yin, G.F. John, J.S. Hayworth, T.P. Clement, Chemical fingerprinting of petroleum biomarkers in Deepwater Horizon oil spill samples collected from Alabama shoreline, Mar. Pollut. Bull. 70 (2013) 147–154. https://doi.org/10.1016/j.marpolbul.2013.02.026.

[88] A.J. Smith, P.B. Flemings, P.M. Fulton, Hydrocarbon flux from natural deepwater Gulf of Mexico vents, Earth Planet. Sci. Lett. 395 (2014) 241–253. https://doi.org/10.1016/j.epsl.2014.03.055.

[89] J.L. Gray, L.K. Kanagy, E.T. Furlong, C.J. Kanagy, J.W. McCoy, A. Mason, G. Lauenstein, Presence of the Corexit component dioctyl sodium sulfosuccinate in Gulf of Mexico waters after the 2010 Deepwater Horizon oil spill, Chemosphere. 95 (2014) 124–130. https://doi.org/10.1016/j.chemosphere.2013.08.049.

[90] J.P. Lewis, J.H. Tarnecki, S.B. Garner, D.D. Chagaris, W.F. Patterson, Changes in Reef Fish Community Structure Following the Deepwater Horizon Oil Spill, Sci. Rep. 10 (2020) 1–13. https://doi.org/10.1038/s41598-020-62574-y.

[91] F. Girard, C.R. Fisher, Long-term impact of the Deepwater Horizon oil spill on deep-sea corals detected after seven years of monitoring, Biol. Conserv. 225 (2018) 117–127. https://doi.org/10.1016/j.biocon.2018.06.028.

[92] J.W. Anderson, S.L. Kiesser, D.L. McQuerry, G.W. Fellingham, Effects of oil and chemically dispersed oil in sediments on clams, in: 2005 Int. Oil Spill

Conf. IOSC 2005, 2005: p. 2327. https://doi.org/10.7901/2169-3358-1985-1-349.

[93]   M. Hussein, M. Jin, J.W. Weaver, Development and verification of a screening model for surface spreading of petroleum, J. Contam. Hydrol. 57 (2002) 281–302. https://doi.org/10.1016/S0169-7722(01)00220-0.

[94]   M. Fingas, Oil and Petroleum Evaporation, in: Handb. Oil Spill Sci. Technol., wiley, 2015: pp. 205–223. https://doi.org/10.1002/9781118989982.ch7.

[95]   S.I. Andersen, J.M. Del Rio, D. Khvostitchenko, S. Shakir, C. Lira-Galeana, Interaction and solubilization of water by petroleum asphaltenes in organic solution, Langmuir. 17 (2001) 307–313. https://doi.org/10.1021/la000871m.

[96]   The International Tanker Owners Pollution Federation Limited, Weathering - ITOPF, (2018). https://www.itopf.org/knowledge-resources/documents-guides/fate-of-oil-spills/weathering/ (accessed June 24, 2021).

[97]   ISPRA, Sversamenti di prodotti petroliferi: sicurezza e controllo del trasporto marittimo, 2011.

[98]   R.C. Prince, A. Gramain, T.J. McGenity, Prokaryotic Hydrocarbon Degraders, in: Handb. Hydrocarb. Lipid Microbiol., Springer Berlin Heidelberg, 2010: pp. 1669–1692. https://doi.org/10.1007/978-3-540-77587-4_118.

[99]   M. Teramoto, M. Suzuki, F. Okazaki, A. Hatmanti, S. Harayama, Oceanobacter-related bacteria are important for the degradation of petroleum aliphatic hydrocarbons in the tropical marine environment, Microbiology. 155 (2009) 3362–3370. https://doi.org/10.1099/mic.0.030411-0.

[100] T.J. Mcgenity, B.D. Folwell, B.A. Mckew, G.O. Sanni, Marine crude-oil biodegradation A central role for interspecies interactions, Saline Systems. 8 (2012) 1–19. https://doi.org/10.1186/2046-9063-8-10.

[101] C. Liu, W. Wang, Y. Wu, Z. Zhou, Q. Lai, Z. Shao, Multiple alkane hydroxylase systems in a marine alkane degrader, Alcanivorax dieselolei B-5, Environ. Microbiol. 13 (2011) 1168–1178. https://doi.org/10.1111/j.1462-2920.2010.02416.x.

[102] M. Niepceron, F. Portet-Koltalo, C. Merlin, A. Motelay-Massei, S. Barray, J. Bodilis, Both Cycloclasticus spp. and Pseudomonas spp. as PAH-degrading bacteria in the Seine estuary (France), FEMS Microbiol. Ecol. 71 (2010) 137–147. https://doi.org/10.1111/j.1574-6941.2009.00788.x.

[103] E.A. Dubinsky, M.E. Conrad, R. Chakraborty, M. Bill, S.E. Borglin, J.T. Hollibaugh, O.U. Mason, Y. M. Piceno, F.C. Reid, W.T. Stringfellow, L.M. Tom, T.C. Hazen, G.L. Andersen, Succession of hydrocarbon-degrading bacteria in the aftermath of the deepwater horizon oil spill in the gulf of Mexico, Environ. Sci. Technol. 47 (2013) 10860–10867. https://doi.org/10.1021/es401676y.

[104] D.L. Valentine, J.D. Kessler, M.C. Redmond, S.D. Mendes, M.B. Heintz, C. Farwell, L. Hu, F.S. Kinnaman, S. Yvon-Lewis, M. Du, E.W. Chan, F.G. Tigreros, C.J. Villanueva, Propane respiration jump-starts microbial response to a deep oil spill, Science (80-.). 330 (2010) 208–211. https://doi.org/10.1126/science.1196830.

[105] T. Gutierrez, D. Berry, T. Yang, S. Mishamandani, L. McKay, A. Teske, M.D. Aitken, Role of Bacterial Exopolysaccharides (EPS) in the Fate of the Oil Released during the Deepwater Horizon Oil Spill, PLoS One. 8 (2013) e67717. https://doi.org/10.1371/journal.pone.0067717.

[106] O.U. Mason, T.C. Hazen, S. Borglin, P.S.G. Chain, E.A. Dubinsky, J.L. Fortney, J. Han, H.Y.N. Holman, J. Hultman, R. Lamendella, R. MacKelprang, S. Malfatti, L.M. Tom, S.G. Tringe, T. Woyke, J. Zhou, E.M. Rubin, J.K. Jansson, Metagenome, metatranscriptome and single-cell sequencing reveal microbial response to Deepwater Horizon oil spill, ISME J. 6 (2012) 1715–1727. https://doi.org/10.1038/ismej.2012.59.

[107] P.H. Pritchard, J.G. Mueller, J.C. Rogers, F. V Kremer, J.A. Glaser, Oil spill bioremediation: experiences, lessons and results from the Exxon Valdez oil spill in Alaska, Biodegradation. 3 (1992) 315–335. https://doi.org/10.1007/BF00129091.

[108] Total, Scheda Dati di Sciurezza in conformità con il Regolamento (CE) N PETROLIO GREGGIO (Tempa Rossa), 2018. www.it.total.com (accessed July 5, 2021).

[109] M.I. Ramirez, A.P. Arevalo, S. Sotomayor, N. Bailon-Moscoso, Contamination by oil crude extraction – Refinement and their effects on human health, Environ. Pollut. 231 (2017) 415–425. https://doi.org/10.1016/j.envpol.2017.08.017.

[110] Y. Mustafa Salih, A. Rahim Karim, I. Khorshid, Estimation the time of spill crude oil in deep soil by the detection of volatile organic compounds (VOCs), Pet. Sci. Technol. 36 (2018) 1497–1502.

https://doi.org/10.1080/10916466.2018.1479423.

[111] M.A. D'Andrea, G.K. Reddy, Health risks associated with crude oil spill exposure, Am. J. Med. 127 (2014) 886.e9-886.e13. https://doi.org/10.1016/j.amjmed.2014.04.035.

[112] H. Rajabi, M. Hadi Mosleh, P. Mandal, A. Lea-Langton, M. Sedighi, Emissions of volatile organic compounds from crude oil processing - Global emission inventory and environmental release, Sci. Total Environ. 727 (2020) 138654. https://doi.org/10.1016/j.scitotenv.2020.138654.

[113] M. Stark, I. O'Gara, An Introduction to Photosynthetic Microalgae, Disruptive Sci. Technol. 1 (2012) 65–67. https://doi.org/10.1089/dst.2012.0017.

[114] A.M.N. Caruana, Z. Amzil, Microalgae and toxins, Elsevier Inc., 2018. https://doi.org/10.1016/B978-0-12-811405-6.00013-X.

[115] M.R. Tredici, Colture massive di microalghe: calamità o risorsa?, (2006).

[116] I.A. Levine, Algae: A way of life and health, Elsevier Inc., 2018. https://doi.org/10.1016/B978-0-12-811405-6.00001-3.

[117] R.E. Lee, Phycology, 2008.

[118] W.W. Carmichael, Cyanobacteria secondary metabolites—the cyanotoxins, J. Appl. Bacteriol. 72 (1992) 445–459. https://doi.org/10.1111/j.1365-2672.1992.tb01858.x.

[119] S. Mishra, D.R. Mishra, Z. Lee, C.S. Tucker, Quantifying cyanobacterial phycocyanin concentration in turbid productive waters: A quasi-analytical approach, Remote Sens. Environ. 133 (2013) 141–151. https://doi.org/10.1016/j.rse.2013.02.004.

[120] Cyanobacterium - User:Kelvin13 - Wikimedia Commons, (n.d.). https://commons.wikimedia.org/wiki/User:Kelvin13#/media/File:Cyanobac terium.svg (accessed September 6, 2021).

[121] D. Kumar, P. Kaštánek, S.P. Adhikary, Exopolysaccharides from cyanobacteria and microalgae and their commercial application, Curr. Sci. 115 (2018) 234–241. https://doi.org/10.18520/cs/v115/i2/234-241.

[122] M.R. Badger, D. Hanson, G.D. Price, Evolution and diversity of CO2 concentrating mechanisms in cyanobacteria, in: Funct. Plant Biol., CSIRO, 2002: pp. 161–173. https://doi.org/10.1071/pp01213.

[123] M. Iino, H. Hashimoto, Intermediate features of cyanelle division of Cyanophora paradoxa (Glaucocystophyta) between cyanobacterial and

plastid division, J. Phycol. 39 (2003) 561–569. https://doi.org/10.1046/j.1529-8817.2003.02132.x.

[124] J.P. Sexton, M.W. Lomas, Microalgal systematics, Elsevier Inc., 2018. https://doi.org/10.1016/B978-0-12-811405-6.00004-9.

[125] M.A. Borowitzka, Biology of microalgae, Elsevier Inc., 2018. https://doi.org/10.1016/B978-0-12-811405-6.00003-7.

[126] A.W. Larkum, Photosynthesis and Light Harvesting in Algae, in: Physiol. Microalgae, Springer International Publishing, 2016: pp. 67–87. https://doi.org/10.1007/978-3-319-24945-2_3.

[127] H.J. Shin, J.H. Im, H.C. Jeong, O.M. Lee, Nine taxa of newly recorded species of chlorophytes (Chlorophyceae and trebouxiophyceae, chlorophyta) in Korea, J. Ecol. Environ. 38 (2015) 637–646. https://doi.org/10.5141/ecoenv.2015.064.

[128] O. Pulz, W. Gross, Valuable products from biotechnology of microalgae, Appl. Microbiol. Biotechnol. 65 (2004) 635–648. https://doi.org/10.1007/s00253-004-1647-x.

[129] A. Lehmuskero, M. Skogen Chauton, T. Boström, Light and photosynthetic microalgae: A review of cellular- and molecular-scale optical processes, Prog. Oceanogr. 168 (2018) 43–56. https://doi.org/10.1016/j.pocean.2018.09.002.

[130] M. Aranda, Y. Li, Y.J. Liew, S. Baumgarten, O. Simakov, M.C. Wilson, J. Piel, H. Ashoor, S. Bougouffa, V.B. Bajic, T. Ryu, T. Ravasi, T. Bayer, G. Micklem, H. Kim, J. Bhak, T.C. LaJeunesse, C.R. Voolstra, Genomes of coral dinoflagellate symbionts highlight evolutionary adaptations conducive to a symbiotic lifestyle, Sci. Rep. 6 (2016). https://doi.org/10.1038/srep39734.

[131] C.F. Delwiche, R.A. Andersen, D. Bhattacharya, B.D. Mishler, R.M. McCourt, Algal evolution and the early radiation of green plants, Assem. Tree Life. (2004) 121–137.

[132] bioluminescence | National Geographic Society, (n.d.). https://www.nationalgeographic.org/encyclopedia/bioluminescence/ (accessed July 13, 2021).

[133] A. Richmond, Handbook of microalgal mass culture, Taylor & Francis Group, 1986.

[134] P. Hegemann, P. Berthold, Sensory Photoreceptors and Light Control of

Flagellar Activity, in: Chlamydomonas Sourceb. 3-Vol Set, Elsevier Inc., 2009: pp. 395–429. https://doi.org/10.1016/B978-0-12-370873-1.00050-2.

[135] A. Synytsya, J. Copíková, W.J. Kim, Y.I. Park, Cell wall polysaccharides of marine algae, in: Springer Handb. Mar. Biotechnol., Springer, Berlin, Heidelberg, 2015: pp. 543–590. https://doi.org/10.1007/978-3-642-53971-8_22.

[136] A.A. Arnold, B. Genard, F. Zito, R. Tremblay, D.E. Warschawski, I. Marcotte, Identification of lipid and saccharide constituents of whole microalgal cells by 13C solid-state NMR, Biochim. Biophys. Acta - Biomembr. 1848 (2015) 369–377. https://doi.org/10.1016/j.bbamem.2014.07.017.

[137] lvaro Torres, F. G., B. Rincn, J. Bartacek, R. Borja, D. Jeiso, Challenges for Cost-Effective Microalgae Anaerobic Digestion, in: Biodegrad. - Eng. Technol., IntechOpen, 2013. https://doi.org/10.5772/55975.

[138] R. Praveenkumar, K. Lee, J. Lee, Y.K. Oh, Breaking dormancy: An energy-efficient means of recovering astaxanthin from microalgae, Green Chem. 17 (2015) 1226–1234. https://doi.org/10.1039/c4gc01413h.

[139] D.Y. Kim, D. Vijayan, R. Praveenkumar, J.I. Han, K. Lee, J.Y. Park, W.S. Chang, J.S. Lee, Y.K. Oh, Cell-wall disruption and lipid/astaxanthin extraction from microalgae: Chlorella and Haematococcus, Bioresour. Technol. 199 (2016) 300–310. https://doi.org/10.1016/j.biortech.2015.08.107.

[140] A.J. Simpson, X. Zang, R. Kramer, P.G. Hatcher, New insights on the structure of algaenan from Botryoccocus braunii race A and its hexane insoluble botryals based on multidimensional NMR spectroscopy and electrospray-mass spectrometry techniques, Phytochemistry. 62 (2003) 783–796. https://doi.org/10.1016/S0031-9422(02)00628-3.

[141] H.G. Gerken, B. Donohoe, E.P. Knoshaug, Enzymatic cell wall degradation of Chlorella vulgaris and other microalgae for biofuels production, Planta. 237 (2013) 239–253. https://doi.org/10.1007/s00425-012-1765-0.

[142] H.M. Zabed, S. Akter, J. Yun, G. Zhang, F.N. Awad, X. Qi, J.N. Sahu, Recent advances in biological pretreatment of microalgae and lignocellulosic biomass for biofuel production, Renew. Sustain. Energy Rev. 105 (2019) 105–128. https://doi.org/10.1016/j.rser.2019.01.048.

[143] B. Becker, Function and Evolution of the Vacuolar Compartment in Green

Algae and Land Plants (Viridiplantae), Int. Rev. Cytol. 264 (2007) 1–24. https://doi.org/10.1016/S0074-7696(07)64001-7.

[144] M. Turmel, C. Lemieux, Evolution of the Plastid Genome in Green Algae, in: Adv. Bot. Res., Academic Press, 2018: pp. 157–193. https://doi.org/10.1016/bs.abr.2017.11.010.

[145] R.R. Wise, The Diversity of Plastid Form and Function, in: R.R. Wise, J.K. Hoober (Eds.), Springer Netherlands, 2007: pp. 3–26. https://doi.org/10.1007/978-1-4020-4061-0_1.

[146] M.A. Borowitzka, J. Beardall, J.A. Raven, The Physiology of Microalgae, 1st ed., Springer International Publishing, 2016. https://doi.org/10.1007/978-3-319-24945-2.

[147] Y. Zhan, C.H. Marchand, A. Maes, A. Mauries, Y. Sun, J.S. Dhaliwal, J. Uniacke, S. Arragain, H. Jiang, N.D. Gold, V.J.J. Martin, S.D. Lemaire, W. Zerges, Pyrenoid functions revealed by proteomics in Chlamydomonas reinhardtii, PLoS One. 13 (2018). https://doi.org/10.1371/journal.pone.0185039.

[148] M.T. Meyer, C. Whittaker, H. Griffiths, The algal pyrenoid: Key unanswered questions, J. Exp. Bot. 68 (2017) 3739–3749. https://doi.org/10.1093/jxb/erx178.

[149] P.G. Falkowski, J.A. Raven, Aquatic photosynthesis. 2nd Edition., Princet. Univ. Press. (2007) 484. https://press.princeton.edu/titles/8337.html (accessed July 15, 2021).

[150] O. Perez-Garcia, F.M.E. Escalante, L.E. De-Bashan, Y. Bashan, Heterotrophic cultures of microalgae: Metabolism and potential products, Water Res. 45 (2011) 11–36. https://doi.org/10.1016/j.watres.2010.08.037.

[151] J. Lowrey, M.S. Brooks, P.J. McGinn, Heterotrophic and mixotrophic cultivation of microalgae for biodiesel production in agricultural wastewaters and associated challenges—a critical review, J. Appl. Phycol. 27 (2015) 1485–1498. https://doi.org/10.1007/s10811-014-0459-3.

[152] K. Chojnacka, A. Noworyta, Evaluation of Spirulina sp. growth in photoautotrophic, heterotrophic and mixotrophic cultures, Enzyme Microb. Technol. 34 (2004) 461–465. https://doi.org/10.1016/j.enzmictec.2003.12.002.

[153] J. Masojídek, M. Koblízek, G. Torzillo, Photosynthesis in Microalgae, Handb. Microalgal Cult. Biotechnol. Appl. Phycol. (2004) 20–39.

[154] D.I. Arnon, The light reactions of photosynthesis., Proc. Natl. Acad. Sci. U. S. A. 68 (1971) 2883–2892. https://doi.org/10.1073/pnas.68.11.2883.

[155] Somepics/Wikimedia Commons/CC Attribution-Share alike 4.0 International, File:Thylakoid membrane, (n.d.). https://commons.wikimedia.org/wiki/File:Thylakoid_membrane_3.svg (accessed July 19, 2021).

[156] S. X, W. A, L. A, K. E, S. C, M. K, S. D, M. J, L. Z, Structural insight into light harvesting for photosystem II in green algae, Nat. Plants. 5 (2019) 1320–1330. https://doi.org/10.1038/S41477-019-0543-4.

[157] A. Zouni, H.T. Witt, J. Kern, P. Fromme, N. Krauss, W. Saenger, P. Orth, Crystal structure of photosystem II from Synechococcus elongatus at 3.8 Å resolution, Nature. 409 (2001) 739–743. https://doi.org/10.1038/35055589.

[158] S. Caffarri, T. Tibiletti, R.C. Jennings, S. Santabarbara, A Comparison Between Plant Photosystem I and Photosystem II Architec-ture and Functioning, Curr. Protein Pept. Sci. 15 (2014) 296–331.

[159] C.S. Reynolds, The ecology of phytoplankton, Cambridge University Press, 2006. https://doi.org/10.1017/CBO9780511542145.

[160] A. Richmond, Q. Hu, Handbook of Microalgal Culture: Applied Phycology and Biotechnology: Second Edition, WILEY Blackwell, 2013. https://doi.org/10.1002/9781118567166.

[161] J.C.G. Canedo, G.L.L. Lizarraga, eds., Photosynthesis - From Its Evolution to Future Improvements in Photosynthetic Efficiency Using Nanomaterials, InTech, 2018. https://doi.org/10.5772/intechopen.71794.

[162] Mike Jones/Wikimedia Commons/CC BY-SA 3.0, File: Calvin-cycle4.svg, (n.d.). https://commons.wikimedia.org/wiki/File:Calvin-cycle4.svg (accessed July 19, 2021).

[163] K.S. Rowan, Photosynthetic Pigments of Algae, Science, 1989. https://books.google.it/books?hl=en&lr=&id=aZNOAAAAIAAJ&oi=fnd&pg=PR11&dq=algae+pigments&ots=YjNFLI7Arl&sig=QORA4leXX_a3BHwGn0NKsypza3I&redir_esc=y#v=onepage&q=algae pigments&f=false (accessed July 19, 2021).

[164] E. Gantt, F.X. Cunningham, Algal Pigments, in: Encycl. Life Sci., American Cancer Society, 2001. https://doi.org/10.1038/npg.els.0000323.

[165] M. Morançais, J.L. Mouget, J. Dumay, Proteins and pigments, Elsevier Inc., 2018. https://doi.org/10.1016/B978-0-12-811405-6.00007-4.

[166] M.N. Rammuni, T.U. Ariyadasa, P.H.V. Nimarshana, R.A. Attalage, Comparative assessment on the extraction of carotenoids from microalgal sources: Astaxanthin from H. pluvialis and β-carotene from D. salina, Food Chem. 277 (2019) 128–134. https://doi.org/10.1016/j.foodchem.2018.10.066.

[167] S.M. Rivera, R. Canela-Garayoa, Analytical tools for the analysis of carotenoids in diverse materials, J. Chromatogr. A. 1224 (2012) 1–10. https://doi.org/10.1016/j.chroma.2011.12.025.

[168] J. Eonseon, J.E. Polle, H.K. Lee, S.M. Hyun, M. Chang, Xanthophylls in Microalgae: from Biosynthesis to Biotechnological Mass Production and Application, J. Microbiol. Biotechnol. 13 (2003) 165–174.

[169] P. Tandon, Q. Jin, L. Huang, A promising approach to enhance microalgae productivity by exogenous supply of vitamins, Microb. Cell Fact. 16 (2017) 1–13. https://doi.org/10.1186/s12934-017-0834-2.

[170] M. De Luca, I. Pappalardo, A.R. Limongi, E. Viviano, R.P. Radice, S. Todisco, G. Martelli, V. Infantino, A. Vassallo, Lipids from Microalgae for Cosmetic Applications, Cosmetics. 8 (2021) 52. https://doi.org/10.3390/cosmetics8020052.

[171] M.A. Borowitzka, N.R. Moheimani, Algae for biofuels and energy, Algae for Biofuels and Energy. (2013) 1–288. https://doi.org/10.1007/978-94-007-5479-9.

[172] V. Mimouni, A. Couzinet-Mossion, L. Ulmann, G. Wielgosz-Collin, Lipids from microalgae, Elsevier Inc., 2018. https://doi.org/10.1016/B978-0-12-811405-6.00005-0.

[173] N. Mizusawa, H. Wada, The role of lipids in photosystem II, Biochim. Biophys. Acta - Bioenerg. 1817 (2012) 194–208. https://doi.org/10.1016/j.bbabio.2011.04.008.

[174] J.K. Volkman, Sterols in microorganisms, Appl. Microbiol. Biotechnol. 60 (2003) 495–506. https://doi.org/10.1007/s00253-002-1172-8.

[175] D. Liestianty, I. Rodianawati, R.A. Arfah, A. Assa, Patimah, Sundari, Muliadi, Nutritional analysis of spirulina sp to promote as superfood candidate, IOP Conf. Ser. Mater. Sci. Eng. 509 (2019). https://doi.org/10.1088/1757-899X/509/1/012031.

[176] B. Ramesh Kumar, G. Deviram, T. Mathimani, P.A. Duc, A. Pugazhendhi, Microalgae as rich source of polyunsaturated fatty acids, Biocatal. Agric.

Biotechnol. 17 (2019) 583–588. https://doi.org/10.1016/j.bcab.2019.01.017.

[177] L. Hooper, Lipid biochemistry, J. Hum. Nutr. Diet. 15 (2002) 469–469. https://doi.org/10.1046/j.1365-277x.2002.00394.x.

[178] Y. Yao, Y. Lu, K.T. Peng, T. Huang, Y.F. Niu, W.H. Xie, W.D. Yang, J.S. Liu, H.Y. Li, Glycerol and neutral lipid production in the oleaginous marine diatom Phaeodactylum tricornutum promoted by overexpression of glycerol-3-phosphate dehydrogenase, Biotechnol. Biofuels. 7 (2014) 1–9. https://doi.org/10.1186/1754-6834-7-110.

[179] A.R. Burch, A.K. Franz, Combined nitrogen limitation and hydrogen peroxide treatment enhances neutral lipid accumulation in the marine diatom Phaeodactylum tricornutum, Bioresour. Technol. 219 (2016) 559–565. https://doi.org/10.1016/j.biortech.2016.08.010.

[180] K. Zienkiewicz, Z.Y. Du, W. Ma, K. Vollheyde, C. Benning, Stress-induced neutral lipid biosynthesis in microalgae — Molecular, cellular and physiological insights, Biochim. Biophys. Acta - Mol. Cell Biol. Lipids. 1861 (2016) 1269–1281. https://doi.org/10.1016/j.bbalip.2016.02.008.

[181] M. V. Busi, J. Barchiesi, M. Martín, D.F. Gomez-Casati, Starch metabolism in green algae, Starch/Staerke. 66 (2014) 28–40. https://doi.org/10.1002/star.201200211.

[182] M.L. Julius, Carbohydrate diversity in microalgae: A phylogenetically arranged presentation, Elsevier Inc., 2018. https://doi.org/10.1016/B978-0-12-811405-6.00006-2.

[183] D. Chaudhuri, N.B. Ghate, S. Deb, S. Panja, R. Sarkar, J. Rout, N. Mandal, Assessment of the phytochemical constituents and antioxidant activity of a bloom forming microalgae Euglena tuba, Biol. Res. 47 (2014) 1–11. https://doi.org/10.1186/0717-6287-47-24.

[184] K. Manivannan, P. Anantharaman, T. Balasubramanian, Evaluation of antioxidant properties of marine microalga Chlorella marina (Butcher, 1952), Asian Pac. J. Trop. Biomed. 2 (2012) S342–S346. https://doi.org/10.1016/S2221-1691(12)60185-3.

[185] P. Cos, L. Ying, M. Calomme, J.P. Hu, K. Cimanga, B. Van Poel, L. Pieters, A.J. Vlietinck, D. Vanden Berghe, Structure-activity relationship and classification of flavonoids as inhibitors of xanthine oxidase and superoxide scavengers, J. Nat. Prod. 61 (1998) 71–76. https://doi.org/10.1021/np970237h.

[186] L. Machu, L. Misurcova, J.V. Ambrozova, J. Orsavova, J. Mlcek, J. Sochor, T. Jurikova, Phenolic content and antioxidant capacity in algal food products, Molecules. 20 (2015) 1118–1133. https://doi.org/10.3390/molecules20011118.

[187] A. Kanazawa, S.I. Teshima, M. Sakamoto, Effects of dietary lipids, fatty acids, and phospholipids on growth and survival of prawn (Penaeus japonicus) larvae, Aquaculture. 50 (1985) 39–49. https://doi.org/10.1016/0044-8486(85)90151-6.

[188] H. Karan, C. Funk, M. Grabert, M. Oey, B. Hankamer, Green Bioplastics as Part of a Circular Bioeconomy, Trends Plant Sci. 24 (2019) 237–249. https://doi.org/10.1016/j.tplants.2018.11.010.

[189] G. Coppola, M.T. Gaudio, C.G. Lopresto, V. Calabro, S. Curcio, S. Chakraborty, Bioplastic from Renewable Biomass: A Facile Solution for a Greener Environment, Earth Syst. Environ. 5 (2021) 231–251. https://doi.org/10.1007/s41748-021-00208-7.

[190] L. Gouveia, S. Graça, C. Sousa, L. Ambrosano, B. Ribeiro, E.P. Botrel, P.C. Neto, A.F. Ferreira, C.M. Silva, Microalgae biomass production using wastewater: Treatment and costs. Scale-up considerations., Algal Res. 16 (2016) 167–176. https://doi.org/10.1016/j.algal.2016.03.010.

[191] J. Coppens, O. Grunert, S. Van Den Hende, I. Vanhoutte, N. Boon, G. Haesaert, L. De Gelder, The use of microalgae as a high-value organic slow-release fertilizer results in tomatoes with increased carotenoid and sugar levels, J. Appl. Phycol. 28 (2016) 2367–2377. https://doi.org/10.1007/S10811-015-0775-2.

[192] E.S.D. F. Barbato, C.A. Campiotti, G. Giagnacovo, V. Pignatelli, D. Tumminelli, C. Viola, Sfruttamento delle microalghe: tra realtà e prospettive, 26 (2012) 20–28. https://doi.org/10.1088/1742-6596/738/1/012025.

[193] A. Muller-Feuga, J. Moal, R. Kaas, The Microalgae of Aquaculture, Live Feed. Mar. Aquac. (2007) 206–252. https://doi.org/10.1002/9780470995143.ch6.

[194] J.L. García, M. de Vicente, B. Galán, Microalgae, old sustainable food and fashion nutraceuticals, Microb. Biotechnol. 10 (2017) 1017–1024. https://doi.org/10.1111/1751-7915.12800.

[195] M.G. De Morais, B.D.S. Vaz, E.G. De Morais, J.A.V. Costa, Biologically Active Metabolites Synthesized by Microalgae, Biomed Res. Int. 2015

(2015). https://doi.org/10.1155/2015/835761.

[196] W. M. Bishop, H. M. Zubeck, Evaluation of Microalgae for use as Nutraceuticals and Nutritional Supplements, J. Nutr. Food Sci. 02 (2012). https://doi.org/10.4172/2155-9600.1000147.

[197] A.W. Armstrong, S. V. Voyles, E.J. Armstrong, E.N. Fuller, J.C. Rutledge, Angiogenesis and oxidative stress: Common mechanisms linking psoriasis with atherosclerosis, J. Dermatol. Sci. 63 (2011) 1–9. https://doi.org/10.1016/j.jdermsci.2011.04.007.

[198] T. Sugawara, K. Matsubara, R. Akagi, M. Mori, T. Hirata, Antiangiogenic activity of brown algae fucoxanthin and its deacetylated product, fucoxanthinol, J. Agric. Food Chem. 54 (2006) 9805–9810. https://doi.org/10.1021/jf062204q.

[199] S.J. Heo, Y.J. Jeon, Protective effect of fucoxanthin isolated from Sargassum siliquastrum on UV-B induced cell damage, J. Photochem. Photobiol. B Biol. 95 (2009) 101–107. https://doi.org/10.1016/j.jphotobiol.2008.11.011.

[200] R.B. Volk, F.H. Furkert, Antialgal, antibacterial and antifungal activity of two metabolites produced and excreted by cyanobacteria during growth, Microbiol. Res. 161 (2006) 180–186. https://doi.org/10.1016/j.micres.2005.08.005.

[201] J.A. Mendiola, S. Santoyo, A. Cifuentes, G. Reglero, E. Ibáñez, F. Javier Señoráns, Antimicrobial activity of sub- and supercritical CO2 extracts of the green alga Dunaliella salina, J. Food Prot. 71 (2008) 2138–2143. https://doi.org/10.4315/0362-028X-71.10.2138.

[202] M.L. Mourelle, C.P. Gómez, J.L. Legido, The potential use of marine microalgae and cyanobacteria in cosmetics and thalassotherapy, Cosmetics. 4 (2017) 46. https://doi.org/10.3390/cosmetics4040046.

[203] S.N. Naik, V. V. Goud, P.K. Rout, A.K. Dalai, S.N. Naik, V. V. Goud, P.K. Rout, A.K. Dalai, Production of first and second generation biofuels: A comprehensive review, Renew. Sustain. Energy Rev. 14 (2010) 578–597. https://econpapers.repec.org/RePEc:eee:rensus:v:14:y:2010:i:2:p:578-597 (accessed July 30, 2021).

[204] J.R.. P.P. Benemann, Biofissazione di CO 2 fossile mediante microalghe per l'abbattimento dei gas serra 9.4.1, Encicl. Degli Idrocarb. TRECCANI. III (2003) 837–862.

[205] P.M. Schenk, S.R. Thomas-Hall, E. Stephens, U.C. Marx, J.H. Mussgnug,

C. Posten, O. Kruse, B. Hankamer, Second Generation Biofuels: High-Efficiency Microalgae for Biodiesel Production, BioEnergy Res. 1 (2008) 20–43. https://doi.org/10.1007/s12155-008-9008-8.

[206] Y.A. Ugya, D.B. Hasan, S.M. Tahir, T.S. Imam, H.A. Ari, X. Hua, Microalgae biofilm cultured in nutrient-rich water as a tool for the phycoremediation of petroleum-contaminated water, Int. J. Phytoremediation. (2021) 1–9. https://doi.org/10.1080/15226514.2021.1882934.

[207] M.S. Kuttiyathil, M.M. Mohamed, S. Al-Zuhair, Using microalgae for remediation of crude petroleum oil-water emulsion, Biotechnol. Prog. (2020). https://doi.org/10.1002/btpr.3098.

[208] K. Özhan, S.M. Miles, H. Gao, S. Bargu, Relative Phytoplankton growth responses to physically and chemically dispersed South Louisiana sweet crude oil, Environ. Monit. Assess. 186 (2014) 3941–3956. https://doi.org/10.1007/s10661-014-3670-4.

[209] H. Znad, A.M.D. Al Ketife, S. Judd, F. AlMomani, H.B. Vuthaluru, Bioremediation and nutrient removal from wastewater by Chlorella vulgaris, Ecol. Eng. 110 (2018) 1–7. https://doi.org/10.1016/j.ecoleng.2017.10.008.

[210] K. Ramadass, M. Megharaj, K. Venkateswarlu, R. Naidu, Toxicity of diesel water accommodated fraction toward microalgae, Pseudokirchneriella subcapitata and Chlorella sp. MM3, Ecotoxicol. Environ. Saf. 142 (2017) 538–543. https://doi.org/10.1016/j.ecoenv.2017.04.052.

[211] A. Xaaldi Kalhor, A. Movafeghi, A.D. Mohammadi-Nassab, E. Abedi, A. Bahrami, Potential of the green alga Chlorella vulgaris for biodegradation of crude oil hydrocarbons, Mar. Pollut. Bull. 123 (2017) 286–290. https://doi.org/10.1016/j.marpolbul.2017.08.045.

[212] A. Xaaldi Kalhor, A.D. Mohammadi Nassab, E. Abedi, A. Bahrami, A. Movafeghi, Biodiesel production in crude oil contaminated environment using Chlorella vulgaris, Bioresour. Technol. 222 (2016) 190–194. https://doi.org/10.1016/j.biortech.2016.09.110.

[213] R.A.E.F. Hamouda, N.M. Sorour, D.S. Yeheia, Biodegradation of crude oil by Anabaena oryzae, Chlorella kessleri and its consortium under mixotrophic conditions, Int. Biodeterior. Biodegrad. 112 (2016) 128–134. https://doi.org/10.1016/j.ibiod.2016.05.001.

[214] M.M. El-Sheekh, R.A. Hamouda, A.A. Nizam, Biodegradation of crude oil

by Scenedesmus obliquus and Chlorella vulgaris growing under heterotrophic conditions, Int. Biodeterior. Biodegrad. 82 (2013) 67–72. https://doi.org/10.1016/j.ibiod.2012.12.015.

[215] P. Das, M. AbdulQuadir, M. Thaher, S. Khan, A.K. Chaudhary, G. Alghasal, H.M.S.J. Al-Jabri, Microalgal bioremediation of petroleum-derived low salinity and low pH produced water, J. Appl. Phycol. 31 (2019) 435–444. https://doi.org/10.1007/s10811-018-1571-6.

[216] H.X. Sun, Y. Xie, Y.P. Ye, Advances in saponin-based adjuvants, Vaccine. 27 (2009) 1787–1796. https://doi.org/10.1016/j.vaccine.2009.01.091.

[217] Sakshi, A.K. Haritash, A comprehensive review of metabolic and genomic aspects of PAH-degradation, Arch. Microbiol. 2020 2028. 202 (2020) 2033–2058. https://doi.org/10.1007/S00203-020-01929-5.

[218] M. Ghodrati, M. Kosari-Nasab, G. Zarrini, A. Movafeghi, Crude oil contamination enhances the lipoxygenase gene expression in the green microalga scenedesmus dimorphus, Biointerface Res. Appl. Chem. 11 (2021) 11431–11439. https://doi.org/10.33263/BRIAC114.1143111439.

[219] P. SureshKumar, J. Thomas, V. Poornima, Structural insights on bioremediation of polycyclic aromatic hydrocarbons using microalgae: a modelling-based computational study, Environ. Monit. Assess. 190 (2018). https://doi.org/10.1007/s10661-017-6459-4.

[220] A.R.D. Stebbing, Hormesis - The stimulation of growth by low levels of inhibitors, Sci. Total Environ. 22 (1982) 213–234. https://doi.org/10.1016/0048-9697(82)90066-3.

[221] A.R. Rao, A.H. Reddy, S.M. Aradhya, Antibacterial properties of Spirulina platensis, Haematococcus pluvialis, Botryococcus braunii micro algal extracts, Curr. Trends Biotechnol. Pharm. 4 (2010) 809–819.

[222] V.C. Liyanaarachchi, G.K.S.H. Nishshanka, R.G.M.M. Premaratne, T.U. Ariyadasa, P.H.V. Nimarshana, A. Malik, Astaxanthin accumulation in the green microalga Haematococcus pluvialis: Effect of initial phosphate concentration and stepwise/continuous light stress, Biotechnol. Reports. 28 (2020) e00538. https://doi.org/10.1016/j.btre.2020.e00538.

[223] M.M.R. Shah, Y. Liang, J.J. Cheng, M. Daroch, Astaxanthin-Producing Green Microalga Haematococcus pluvialis: From Single Cell to High Value Commercial Products, Front. Plant Sci. 7 (2016). https://doi.org/10.3389/fpls.2016.00531.

[224] L. Pan, S. Zhang, K. Gu, N. Zhang, Preparation Of astaxanthin-loaded liposomes: Characterization, storage stability and antioxidant activity, CYTA - J. Food. 16 (2018) 607–618. https://doi.org/10.1080/19476337.2018.1437080.

[225] S. Davinelli, M.E. Nielsen, G. Scapagnini, Astaxanthin in skin health, repair, and disease: A comprehensive review, Nutrients. 10 (2018). https://doi.org/10.3390/nu10040522.

[226] J. Matos, C. Cardoso, N.M. Bandarra, C. Afonso, Microalgae as healthy ingredients for functional food: A review, Food Funct. 8 (2017) 2672–2685. https://doi.org/10.1039/c7fo00409e.

[227] M. Guerin, M.E. Huntley, M. Olaizola, Haematococcus astaxanthin: Applications for human health and nutrition, Trends Biotechnol. 21 (2003) 210–216. https://doi.org/10.1016/S0167-7799(03)00078-7.

[228] Y. Lemoine, B. Schoefs, Secondary ketocarotenoid astaxanthin biosynthesis in algae: A multifunctional response to stress, Photosynth. Res. 106 (2010) 155–177. https://doi.org/10.1007/s11120-010-9583-3.

[229] R. Sarada, R. Vidhyavathi, D. Usha, G.A. Ravishankar, An efficient method for extraction of astaxanthin from green alga Haematococcus pluvialis, J. Agric. Food Chem. 54 (2006) 7585–7588. https://doi.org/10.1021/jf060737t.

[230] S. Boussiba, A. Vonshak, Astaxanthin accumulation in the green alga haematococcus pluvialis, Plant Cell Physiol. 32 (1991) 1077–1082. https://doi.org/10.1093/oxfordjournals.pcp.a078171.

[231] R. Vidhyavathi, L. Venkatachalam, R. Sarada, G. Aswathanarayana Ravishankar, Regulation of carotenoid biosynthetic genes expression and carotenoid accumulation in the green alga Haematococcus pluvialis under nutrient stress conditions, J. Exp. Bot. 59 (2008) 1409–1418. https://doi.org/10.1093/jxb/ern048.

[232] M. Kobayashi, Y. Kurimura, T. Kakizono, N. Nishio, Y. Tsuji, Morphological changes in the life cycle of the green alga Haematococcus pluvialis, J. Ferment. Bioeng. 84 (1997) 94–97. https://doi.org/10.1016/S0922-338X(97)82794-8.

[233] M. Wayama, S. Ota, H. Matsuura, N. Nango, A. Hirata, Three-Dimensional Ultrastructural Study of Oil and Astaxanthin Accumulation during Encystment in the Green Alga Haematococcuspluvialis, PLoS One. 8 (2013) 53618. https://doi.org/10.1371/journal.pone.0053618.

[234] A. Triki, P. Maillard, C. Gudin, Gametogenesis in Haematococcus pluvialis Flotow (Volvocales, Chlorophyta), Phycologia. 36 (2010) 190–194. https://doi.org/10.2216/i0031-8884-36-3-190.1.

[235] S. Ota, A. Morita, S. Ohnuki, A. Hirata, S. Sekida, K. Okuda, Y. Ohya, S. Kawano, Carotenoid dynamics and lipid droplet containing astaxanthin in response to light in the green alga Haematococcus pluvialis, Sci. Rep. 8 (2018) 1–10. https://doi.org/10.1038/s41598-018-23854-w.

[236] C.B. Grewe, C. Griehl, The carotenoid astaxanthin from Haematococcus pluvialis, Microalgal Biotechnol. Integr. Econ. (2013). https://doi.org/10.1515/9783110298321.129/HTML.

[237] C. Hagen, S. Siegmund, W. Braune, Ultrastructural and chemical changes in the cell wall of Haematococcus pluvialis (Volvocales, Chlorophyta) during aplanospore formation, Eur. J. Phycol. 37 (2002) 217–226. https://doi.org/10.1017/S0967026202003669.

[238] R.P. Radice, R. Fiorentino, M. De Luca, A.R. Limongi, E. Viviano, G. Bermano, G. Martelli, An innovative protocol to select the best growth phase for astaxanthin biosynthesis in H. pluvialis., Biotechnol. Reports. 31 (2021) e00655. https://doi.org/10.1016/j.btre.2021.e00655.

[239] S.W. Hwang, H. Il Choi, S.J. Sim, Acidic cultivation of Haematococcus pluvialis for improved astaxanthin production in the presence of a lethal fungus, Bioresour. Technol. 278 (2019) 138–144. https://doi.org/10.1016/j.biortech.2019.01.080.

[240] S.A. Choi, Y.K. Oh, J. Lee, S.J. Sim, M.E. Hong, J.Y. Park, M.S. Kim, S.W. Kim, J.S. Lee, High-efficiency cell disruption and astaxanthin recovery from Haematococcus pluvialis cyst cells using room-temperature imidazolium-based ionic liquid/water mixtures, Bioresour. Technol. 274 (2019) 120–126. https://doi.org/10.1016/j.biortech.2018.11.082.

[241] A.A. Martínez-Delgado, S. Khandual, S.J. Villanueva–Rodríguez, Chemical stability of astaxanthin integrated into a food matrix: Effects of food processing and methods for preservation, Food Chem. 225 (2017) 23–30. https://doi.org/10.1016/j.foodchem.2016.11.092.

[242] M. Østerlie, B. Bjerkeng, S. Liaaen-Jensen, Plasma appearance and distribution of astaxanthin E/Z and R/S isomers in plasma lipoproteins of men after single dose administration of astaxanthin, J. Nutr. Biochem. 11 (2000) 482–490. https://doi.org/10.1016/S0955-2863(00)00104-2.

[243] R.P. Radice, A.R. Limongi, E. Viviano, M.C. Padula, G. Martelli, G. Bermano, Effects of astaxanthin in animal models of obesity-associated diseases: A systematic review and meta-analysis., Free Radic. Biol. Med. 171 (2021) 156–168. https://doi.org/10.1016/j.freeradbiomed.2021.05.008.

[244] Y. Ni, M. Nagashimada, F. Zhuge, L. Zhan, N. Nagata, A. Tsutsui, Y. Nakanuma, S. Kaneko, T. Ota, Astaxanthin prevents and reverses diet-induced insulin resistance and steatohepatitis in mice: A comparison with Vitamin E, Sci. Rep. 5 (2015) 1–15. https://doi.org/10.1038/srep17192.

[245] J.R. Jones, C. Barrick, K.-A. Kim, J. Lindner, B. Blondeau, Y. Fujimoto, M. Shiota, R.A. Kesterson, B.B. Kahn, M.A. Magnuson, Deletion of PPAR in adipose tissues of mice protects against high fat diet-induced obesity and insulin resistance, 2005. www.pnas.orgcgidoi10.1073pnas.0306743102 (accessed November 26, 2020).

[246] M. Kimura, M. Iida, H. Yamauchi, M. Suzuki, T. Shibasaki, Y. Saito, H. Saito, Astaxanthin supplementation effects on adipocyte size and lipid profile in OLETF rats with hyperphagia and visceral fat accumulation, J. Funct. Foods. 11 (2014) 114–120. https://doi.org/10.1016/j.jff.2014.08.001.

[247] K. Uchiyama, Y. Naito, G. Hasegawa, N. Nakamura, J. Takahashi, T. Yoshikawa, Astaxanthin protects β-cells against glucose toxicity in diabetic db/db mice, Redox Rep. 7 (2002) 290–293. https://doi.org/10.1179/135100002125000811.

[248] B. Kim, C. Farruggia, C.S. Ku, T.X. Pham, Y. Yang, M. Bae, C.J. Wegner, N.J. Farrell, E. Harness, Y.K. Park, S.I. Koo, J.Y. Lee, Astaxanthin inhibits inflammation and fibrosis in the liver and adipose tissue of mouse models of diet-induced obesity and nonalcoholic steatohepatitis, J. Nutr. Biochem. 43 (2017) 27–35. https://doi.org/10.1016/j.jnutbio.2016.01.006.

[249] M. Kobori, Y. Takahashi, M. Sakurai, Y. Ni, G. Chen, M. Nagashimada, S. Kaneko, T. Ota, Hepatic transcriptome profiles of mice with diet-induced nonalcoholic steatohepatitis treated with astaxanthin and vitamin E, Int. J. Mol. Sci. 18 (2017) 7–9. https://doi.org/10.3390/ijms18030593.

[250] Y. Jia, C. Wu, J. Kim, B. Kim, S.J. Lee, Astaxanthin reduces hepatic lipid accumulations in high-fat-fed C57BL/6J mice via activation of peroxisome proliferator-activated receptor (PPAR) alpha and inhibition of PPAR gamma and Akt, J. Nutr. Biochem. 28 (2016) 9–18. https://doi.org/10.1016/j.jnutbio.2015.09.015.

[251] Y. Yang, T.X. Pham, C.J. Wegner, B. Kim, C.S. Ku, Y.K. Park, J.Y. Lee, Astaxanthin lowers plasma TAG concentrations and increases hepatic antioxidant gene expression in diet-induced obesity mice, Br. J. Nutr. 112 (2014) 1797–1804. https://doi.org/10.1017/S0007114514002554.

[252] Z. Gao, C. Meng, X. Zhang, D. Xu, X. Miao, Y. Wang, L. Yang, H. Lv, L. Chen, N. Ye, Induction of salicylic acid (SA) on transcriptional expression of eight carotenoid genes and astaxanthin accumulation in Haematococcus pluvialis, Enzyme Microb. Technol. 51 (2012) 225–230. https://doi.org/10.1016/j.enzmictec.2012.07.001.

[253] M. Rohmer, The discovery of a mevalonate-independent pathway for isoprenoid biosynthesis in bacteria, algae and higher plants†, Nat. Prod. Rep. 16 (1999) 565–574. https://doi.org/10.1039/A709175C.

[254] F. Bai, C. Gusbeth, W. Frey, P. Nick, Nanosecond pulsed electric fields modulate the expression of the astaxanthin biosynthesis genes psy, crtR-b and bkt 1 in Haematococcus pluvialis, Sci. Rep. 10 (2020) 1–15. https://doi.org/10.1038/s41598-020-72479-5.

[255] A.R. Wellburn, The Spectral Determination of Chlorophylls a and b, as well as Total Carotenoids, Using Various Solvents with Spectrophotometers of Different Resolution, J. Plant Physiol. 144 (1994) 307–313. https://doi.org/10.1016/S0176-1617(11)81192-2.

[256] F. Li, M. Cai, M. Lin, X. Huang, J. Wang, X. Zheng, S. Wu, Y. An, Accumulation of Astaxanthin Was Improved by the Nonmotile Cells of Haematococcus pluvialis, Biomed Res. Int. 2019 (2019). https://doi.org/10.1155/2019/8101762.

APPENDIX 1: PUBLICATIONS

Review

Lipids from Microalgae for Cosmetic Applications

Maria De Luca [1,2,†], Ilaria Pappalardo [1,3,†], Antonina Rita Limongi [1,4], Emanuele Viviano [1,5], Rosa Paola Radice [1,4], Simona Todisco [1], Giuseppe Martelli [1], Vittoria Infantino [1] and Antonio Vassallo [1,6,*]

[1] Department of Science, University of Basilicata, Viale dell'Ateneo Lucano 10, 85100 Potenza, Italy; maria.deluca@unibas.it (M.D.L.); ilaria.pappalardo@unibas.it (I.P.); antonina.limongi92@gmail.com (A.R.L.); emanueleviviano@gmail.com (E.V.); rosapaolaradice@gmail.com (R.P.R.); simona.todisco@unibas.it (S.T.); giuseppe.martelli@unibas.it (G.M.); vittoria.infantino@unibas.it (V.I.)
[2] ALMACABIO Srl, C/so Italia 27, 39100 Bolzano, Italy
[3] KAMABIO Srl, Via Al Boschetto 4/B, 39100 Bolzano, Italy
[4] Bioinnova s.r.l.s., Via Ponte 9 Luci, 22, 85100 Potenza, Italy
[5] Thema Informatik s.r.l., Via Ressel 2/F, 39100 Bolzano, Italy
[6] Spinoff TNcKILLERS s.r.l., Viale dell'Ateneo Lucano 10, 85100 Potenza, Italy
* Correspondence: antonio.vassallo@unibas.it
† These authors contributed equally to this work.

Abstract: In recent years, there has been considerable interest in using microalgal lipids in the food, chemical, pharmaceutical, and cosmetic industries. Several microalgal species can accumulate appreciable lipid quantities and therefore are characterized as oleaginous. In cosmetic formulations, lipids and their derivatives are one of the main ingredients. Different lipid classes are great moisturizing, emollient, and softening agents, work as surfactants and emulsifiers, give consistence to products, are color and fragrance carriers, act as preservatives to maintain products integrity, and can be part of the molecules delivery system. In the past, chemicals have been widely used but today's market and customers' demands are oriented towards natural products. Microalgae are an extraordinary source of lipids and other many bioactive molecules. Scientists' attention to microalgae cultivation for their industrial application is increasing. For the high costs associated, commercialization of microalgae and their products is still not very widespread. The possibility to use biomass for various industrial purposes could make microalgae more economically competitive.

Keywords: lipids; microalgae; cosmetic products; new ingredients

---

Review

Biohydrogen from Microalgae: Production and Applications

Antonina Rita Limongi [1,2], Emanuele Viviano [1,3,*], Maria De Luca [1,4], Rosa Paola Radice [1,2], Giuliana Bianco [1] and Giuseppe Martelli [1]

[1] Department of Science, University of Basilicata, 10, 85100 Potenza, Italy; antonina.limongi92@gmail.com (A.R.L.); mariadeluca92.mdl@gmail.com (M.D.L.); rosapaolaradice@gmail.com (R.P.R.); giuliana.bianco@unibas.it (G.B.); giuseppe.martelli@unibas.it (G.M.)
[2] Bioinnova s.r.l.s., Via Ponte 9 luci, 22, 85100 Potenza, Italy
[3] Thema Informatik s.r.l., Via Ressel 2/F, 39100 Bolzano, Italy
[4] Almacabio s.r.l., Via Ressel 2/F, 39100 Bolzano, Italy
* Correspondence: emanueleviviano@gmail.com

Abstract: The need to safeguard our planet by reducing carbon dioxide emissions has led to a significant development of research in the field of alternative energy sources. Hydrogen has proved to be the most promising molecule, as a fuel, due to its low environmental impact. Even if various methods already exist for producing hydrogen, most of them are not sustainable. Thus, research focuses on the biological sector, studying microalgae, and other microorganisms' ability to produce this precious molecule in a natural way. In this review, we provide a description of the biochemical and molecular processes for the production of biohydrogen and give a general overview of one of the most interesting technologies in which hydrogen finds application for electricity production: fuel cells.

Keywords: green fuel; biohydrogen; microalgae; *Chlamydomonas reinhardtii;* hydrogenase; fuel cell

Contents lists available at ScienceDirect

Biotechnology Reports

An innovative protocol to select the best growth phase for astaxanthin biosynthesis in *H. pluvialis*.

Rosa Paola Radice [a,b,f,*], Rocco Fiorentino [a], Maria De Luca [a,d], Antonina Rita Limongi [a,b], Emanuele Viviano [a,e], Giovanna Bermano [c], Giuseppe Martelli [a,*]

[a] University of Basilicata, Viale dell'AteneoLucano, 1 85100 Potenza (Pz), Italy
[b] Bioinnova s.r.l.s, via Ponte Nove Luci 9, 85100 Potenza (Pz), Italy
[c] Centre for Obesity Research and Education (CORE), School of Pharmacy and Life Sciences, Robert Gordon University, Aberdeen United Kingdom
[d] ALMACABIO Srl, C/so Italia 27, 39100 Bolzano, Italy
[e] Thema Informatik s.r.l., Via Ressel 2/F, 39100 Bolzano, Italy
[f] Department of science, University of Basilicata, via dell'ateneo lucano 10

ARTICLE INFO

ABSTRACT

H. pluvialis is a green unicellular microalgae and it is the first producer of natural astaxanthin in the world if subjected to stress conditions such as high light, high salinity and nutrient starvation. Astaxanthin is a powerful antioxidant used in many fields, such as aquaculture, pharmaceutical, food supplements and cosmetic. To obtain a large amount of astaxanthin, researcher focused on the optimisation of *H. pluvialis* growth. *H. pluvialis* has four different size growth stage (macrozooids, microzooids, palmelloid and "red non-motile astaxanthin accumulated encysted"), and astaxanthin production occur in the last phase. Recent studies shown that non-motile cells can produce more astaxanthin than motile cells if subjected to light stress. For these reasons, the aim of this study is to find a new and innovative methodology to select and recovery *H. pluvialis* in his last growth phase thanks to an electrophoretic run, and optimize, in this way, astaxanthin production.

Contents lists available at ScienceDirect

Free Radical Biology and Medicine

Original article

Effects of astaxanthin in animal models of obesity-associated diseases: A systematic review and meta-analysis

Rosa Paola Radice [a,b], Antonina Rita Limongi [a,b], Emanuele Viviano [a], Maria Carmela Padula [a,c], Giuseppe Martelli [a], Giovanna Bermano [d,*]

[a] Department of Sciences, University of Basilicata, Potenza, Italy
[b] Bioinnova s.r.l.s., Via Ponte Nove Luci, Potenza, Italy
[c] Rheumatology Department of Lucania, Rheumatology Institute of Lucania (IReL), San Carlo Hospital of Potenza and Madonna delle Grazie Hospital of Matera, Potenza, Italy
[d] Centre for Obesity Research and Education (CORE), School of Pharmacy and Life Sciences, Robert Gordon University, Aberdeen, UK

ARTICLE INFO

ABSTRACT

Background and aim: Obesity is a major risk factor for several diseases, including metabolic syndrome (MetS), non-alcoholic fatty liver disease (NAFLD) and type 2 diabetes (T2D). The use of natural products, such as astaxanthin (ASX), a potent antioxidant compound produced by the freshwater green microalga *Haematococcus pluvialis*, has gained particular interest to reduce oxidative stress and inflammation, and to improve redox status, often associated with obesity. A systematic review and meta-analysis was performed to comprehensively examine the effects of ASX in animal models of diet induced obesity-associated diseases in order to inform the design of future human clinical studies for ASX use as supplement or nutraceutical.
Methods: Cinahl, Cochraine, MEDLINE, Scopus and Web of Science were searched for English-language manuscripts published between January 2000 and April 2020 using the following key words: astaxanthin, obesity, non-alcoholic fatty liver disease, diabetes mellitus type 2, NAFLD and metabolic.
Results: Seventeen eligible articles, corresponding to 21 animal studies, were included in the final quantitative analysis. ASX, at different concentrations and administered for different length of time, induced a significant reduction in adipose tissue weight (P = 0.05) and systolic blood pressure (P < 0.0001) in control animals. In animal models of T2D, ASX significantly reduced serum glucose levels (P = 0.04); whereas it improved several disease biomarkers in the blood (e.g. cholesterol, triglycerides, ALT and AST, P < 0.10), and reduced liver (P = 0.0002) and body weight (P = 0.11), in animal models of NAFLD.
Conclusions: Supplementation of ASX in the diet has positive effects on symptoms associated with obesity related diseases in animals, by having lipid-lowering, hypo-insulin and hypoglycaemic capacity, protecting organs from oxidative stress and mitigating the immune system, as suggested in this review.

ACKNOWLEDGMENT

Non sembra vero che siano già trascorsi tre anni dall'inizio di questo percorso di dottorato, eppure ancora una volta (e si spera sia l'ultima) è doveroso da parte mia ringraziare tutti coloro che hanno reso questo percorso possibile.

Vorrei ringraziare, prima di tutto, il Professor Martelli, per aver creduto in me e per avermi dato la possibilità di dimostrare cosa posso fare, e dove posso arrivare utilizzando lo studio, l'impegno, la passione, la costanza e, perché no anche un pizzico di follia. Non sempre si trovano persone disposte ad investire nei giovani, e di questo ne sarò sempre riconoscente.

Ringrazio la Dott.ssa Giovanna Bermano, non solo per essersi resa disponibile ad accogliermi e a fornirmi i mezzi per ampliare la mia mente e le mie conoscenze, ma per aver dedicato tempo, pazienza e gentilezza nel seguirmi in tutto il percorso formativo.

Vorrei ringraziare Pietro Sabia, e Bioinnova tutta, per aver contribuito alla realizzazione di questo progetto di ricerca.

Vorrei ringraziare Luigi Pariti per essere stato un ascoltatore gentile e lo spirito allegro di questi anni.

Vorrei ringraziare i miei colleghi Antonina, Maria ed Emanuele per aver condiviso con me quest'esperienza che mi ha insegnato tanto.

Vorrei ringraziare le due donne della mia vita mia mamma e mia sorella Giulia, per esserci sempre state, per avermi infuso coraggio, avermi ascoltato ogni singolo giorno anche quando quello di cui ti parlavo sembrava arabo antico. Il vostro amore, è ciò che non mi fa mai sentire sola, e insieme al nostro angelo mi sento sempre amata e protetta.

Vorrei dedicare questo traguardo l'amore della mia vita, il mio migliore amico e la persona che più mi conosce. In questi 10 anni siamo cresciuti insieme, siamo maturati e abbiamo progettato un futuro insieme che piano piano si sta realizzando. Sei l'unico che riesce a vedere oltre il mio scudo di forza e sfacciataggine, riuscendo a cogliere le mie insicurezze e a farle tue. Stare al tuo fianco mi ha reso una persona migliore. Grazie per amarmi senza pretese.

Doveroso ringraziare i miei piccoli cuccioli, Carmine, Andrea, Rocco Manuel e Marilù. Siete la mia gioia e vi vorrò per sempre bene.

Grazie a tutta la mia famiglia, nonni, zii, cugini, i miei suoceri, i miei cognati, dal primo all'ultimo…essere parte di una grande famiglia unita è un privilegio che ogni giorno ringrazio di avere…spero di avervi resi orgogliosi di me.
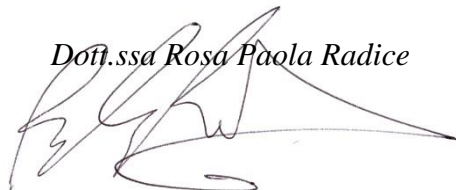
Grazie ai miei amici, per le migliori serate passate a ridere, scherzare e soprattutto a mangiare.

Forse in maniera scontata, ringrazio coloro che non hanno mai creduto in me e che mi hanno sempre sottovalutato…così facendo mi avete spronato a dimostrare il mio valore.

Se incontrassi la me stessa bambina, o la me stessa di dieci anni fa, gli direi di non mollare mai, di lottare e di credere sempre nell'amore per la scienza, nonostante le difficoltà che la vita le porrà davanti.

"La variabile del cambiamento è l'unica costante nell'arco della vita"

Dott.ssa Rosa Paola Radice